ICS 21.200
CCS J 17

中华人民共和国国家标准

GB/T 10095.1—2022/ISO 1328-1:2013
代替 GB/T 10095.1—2008

圆柱齿轮　ISO 齿面公差分级制
第 1 部分:齿面偏差的定义和允许值

Cylindrical gears—ISO system of flank tolerance classification—
Part 1:Definitions and allowable values of deviations relevant to flanks of gear teeth

(ISO 1328-1:2013,IDT)

2022-10-12 发布　　2022-10-12 实施

国家市场监督管理总局
国家标准化管理委员会　发布

目　次

前言 …… Ⅰ

引言 …… Ⅱ

1　范围 …… 1

2　规范性引用文件 …… 1

3　术语、定义和符号 …… 2

　3.1　基本术语和符号 …… 2

　3.2　通用参数 …… 7

　3.3　齿距偏差 …… 8

　3.4　齿廓偏差 …… 9

　3.5　螺旋线偏差 …… 13

4　ISO 齿面公差分级制的应用 …… 15

　4.1　通则 …… 15

　4.2　需要验证的几何参数 …… 15

　4.3　检测仪器的认证和不确定性 …… 17

　4.4　单项偏差测量的注意事项 …… 17

　4.5　齿面公差要求的规范 …… 21

　4.6　验收及评定标准 …… 22

　4.7　数据展示 …… 22

5　公差值 …… 22

　5.1　通则 …… 22

　5.2　公式的使用 …… 22

　5.3　公差公式 …… 23

附录 A（规范性）　分段公差评价 …… 25

附录 B（规范性）　采用二阶分析法评价齿廓和螺旋线偏差 …… 28

附录 C（资料性）　齿廓和螺旋线数据滤波 …… 31

附录 D（资料性）　齿距累积偏差 …… 33

附录 E（规范性）　径向跳动的允许值 …… 35

附录 F（资料性）　单面啮合综合测量 …… 37

附录 G（资料性）　相邻齿距差 f_u …… 41

参考文献 …… 42

前　言

本文件按照GB/T 1.1—2020《标准化工作导则　第1部分:标准化文件的结构和起草规则》的规定起草。

本文件是GB/T 10095《圆柱齿轮　ISO齿面公差分级制》的第1部分。GB/T 10095已经发布了以下部分:

——第1部分:齿面偏差的定义和允许值;

——第2部分:径向综合偏差与径向跳动的定义和允许值。

本文件代替GB/T 10095.1—2008《圆柱齿轮　精度制　第1部分:轮齿同侧齿面偏差的定义和允许值》,与GB/T 10095.1—2008相比,除结构调整和编辑性改动外,主要技术变化如下:

a) 更改了适用范围(见第1章,2008年版的第1章);

b) 更改了确定齿面公差的公式(见5.3,2008年版的第6章);

c) 增加了修形齿廓和螺旋线的分析方法(见附录A和附录B);

d) 增加了径向跳动的允许值计算(见附录E)。

本文件等同采用ISO 1328-1:2013《圆柱齿轮　ISO齿面公差分级制　第1部分:齿面偏差的定义和允许值》。

请注意本文件的某些内容可能涉及专利。本文件的发布机构不承担识别专利的责任。

本文件由全国齿轮标准化技术委员会(SAC/TC 52)提出并归口。

本文件起草单位:郑州机械研究所有限公司、北京工业大学、宁波中大力德智能传动股份有限公司、浙江双环传动机械股份有限公司、南京高精齿轮集团有限公司、西安法士特汽车传动有限公司、江苏国茂减速机股份有限公司、浙江丰立智能科技股份有限公司、深圳市兆威机电股份有限公司、浙江夏厦精密制造股份有限公司、河南科技大学、重庆大学、郑州天时海洋石油装备有限公司、哈尔滨精达测量仪器有限公司、湖南磐钴传动科技有限公司、东莞市星火齿轮有限公司、中铁工程服务有限公司。

本文件主要起草人:石照耀、王志刚、于渤、王伟、范瑞丽、岑国建、吴长鸿、汪正兵、严鉴铂、黄晓英、李清、王友利、辛栋、谢桂平、王笑一、周广才、徐家科、敬代云、童爱军、寇植达、陈永洪、王建敏、周长江、李海霞、纪谢茹、任继华、庄元顺、赵凤霞、徐珂。

本文件及其所代替文件的历次版本发布情况为:

——1988年首次发布GB/T 10095—1988;

——2001年第一次修订时分为部分出版,本文件对应GB/T 10095.1—2001《渐开线圆柱齿轮　精度　第1部分:轮齿同侧齿面偏差的定义和允许值》;2008年第二次修订;

——本次为第三次修订。

引　言

GB/T 10095《圆柱齿轮　ISO齿面公差分级制》在我国齿轮行业广泛使用，完善了我国的齿轮标准体系，促进了我国齿轮产品与国际接轨。

依据测量原理、测量装备和评价方法的不同，GB/T 10095《圆柱齿轮　ISO齿面公差分级制》拟由两个部分构成：

——第1部分：齿面偏差的定义和允许值；

——第2部分：双侧齿面径向综合偏差的定义和允许值。

本文件主要说明对于单个齿轮齿面的基本偏差(齿距偏差、齿廓偏差、螺旋线偏差和径向跳动)的各个精度等级的公差计算方法；精度等级定为11级，从高到低为1级到11级；测量方法基于单个圆柱齿轮单侧齿面的坐标式测量，使用坐标类测量仪。

圆柱齿轮　ISO 齿面公差分级制　第 1 部分:齿面偏差的定义和允许值

重要提示:强烈建议本文件的使用者均应非常熟悉 ISO/TR 10064-1 所描述的方法和步骤。在本文件的限制范围内,不宜使用 ISO/TR 10064-1 以外的技术。

警告:使用齿面公差等级来判定齿轮的性能,判定者应在特定工况条件下具有丰富的实践经验。本文件的使用者应注意,不应直接根据尚未装配(散件)齿轮的公差值来判断装配后齿轮的使用性能。

1　范围

本文件规定了单个渐开线圆柱齿轮齿面的制造和合格判定的公差分级制,还规定了各项齿面公差的术语、齿面公差分级制的结构和允许值。

本文件提供了齿轮供需双方参考的公差值。按照公差值由小到大的顺序,定义了 11 个齿面公差等级,从 1 级到 11 级。5.3 提供了公差值计算公式,应用范围如下:

——$5 \leqslant z \leqslant 1\ 000$;

——$5\ \text{mm} \leqslant d \leqslant 15\ 000\ \text{mm}$;

——$0.5\ \text{mm} \leqslant m_n \leqslant 70\ \text{mm}$;

——$4\ \text{mm} \leqslant b \leqslant 1\ 200\ \text{mm}$;

——$\beta \leqslant 45^\circ$。

其中:

z ——齿数;

d ——分度圆直径;

m_n——法向模数;

b ——齿宽(轴向);

β ——螺旋角。

本文件必需和可选的测量方法,见第 4 章。

本文件不包括齿轮设计。

本文件不涉及齿面纹理。关于齿面结构的其他信息,见 ISO/TR 10064-4。

2　规范性引用文件

下列文件中的内容通过文中的规范性引用而构成本文件必不可少的条款。其中,注日期的引用文件,仅该日期对应的版本适用于本文件;不注日期的引用文件,其最新版本(包括所有的修改单)适用于本文件。

ISO 701　齿轮几何要素代号(International gear notation—Symbols for geometrical data)

注:GB/T 2821—2003　齿轮几何要素代号(ISO 701:1998,IDT)

ISO 1122-1　齿轮术语和定义　第 1 部分:几何学定义(Vocabulary of gear terms—Part 1:Definitions related to geometry)

注:GB/T 3374.1—2010[1)]　齿轮　术语和定义　第 1 部分:几何学定义(ISO 1122-1:1998,IDT)

1)　不含 ISO 1122-1:1998/Cor.1:1999 和 ISO 1122-1:1998/Cor.2:2009。

ISO 1328-2 圆柱齿轮 精度制 第2部分:径向综合偏差与径向跳动的定义和允许值(Cylindrical gears—ISO system of accuracy—Part 2:Definitions and allowable values of deviations relevant to radial composite deviations and runout information)

注:GB/T 10095.2—2008 圆柱齿轮 精度制 第2部分:径向综合偏差与径向跳动的定义和允许值(ISO 1328-2:1997,IDT)

ISO/TR 10064-1 检验实施规范 第1部分:轮齿同侧齿面的检验(Code of inspection practice—Part 1:Inspection of corresponding flanks of gear teeth)

注:GB/Z 18620.1—2008 圆柱齿轮 检验实施规范 第1部分:轮齿同侧齿面的检验(ISO/TR 10064-1:1992,IDT)

ISO/TS 16610-1 产品几何技术规范(GPS) 滤波 第1部分:概述和基本概念[Geometrical product specifications(GPS)—Filtration—Part 1:Overview and basic concepts]

注:GB/Z 26958.1—2011 产品几何技术规范(GPS) 滤波 第1部分:概述和基本概念(ISO/TS 16610-1:2006,IDT)

ISO 16610-21 产品几何技术规范(GPS) 滤波 第21部分:线性轮廓滤波器 高斯滤波器[Geometrical product specifications(GPS)—Filtration—Part 21:Linear profile filters:Gaussian filters]

注:GB/T 26958.21—2020 产品几何技术规范(GPS) 滤波 第21部分:线性轮廓滤波器 高斯滤波器(ISO 16610-21:2011,IDT)

ISO 21771 齿轮 渐开线圆柱齿轮和齿轮副概念和几何学(Gears—Cylindrical involute gears and gear pairs—Concepts and geometry)

3 术语、定义和符号

下列术语、定义和符号适用于本文件。

3.1 基本术语和符号

注1:关于齿轮几何术语的其他定义,见 ISO 701、ISO 1122-1 和 ISO 21771。

注2:本文件中的一些符号和术语可能与其他文件和国际标准中的符号和术语不相同。

注3:本文件使用的术语和符号分两个表按字母顺序排列。按术语的英文对应词字母顺序排列见表1,按符号的字母顺序排列见表2。表1中的术语经文字整理后构成逻辑性的术语组。角标"T"应用于公差值符号。

表1 按术语的英文对应词字母顺序排列的术语和符号

术语	符号	单位
有效齿顶圆直径	d_{Na}	mm
有效齿顶点(有效齿顶圆与啮合线的交点)	N_a	—
相邻齿距差	f_u	μm
相邻齿距差的公差	f_{uT}	μm
任一相邻齿距差	f_{ui}	μm
修根量(齿根)	C_{af}	μm
修缘量(齿顶)	C_{aa}	μm
基圆直径	d_b	mm
接触斑点评价	c_p	—
啮合线与基圆相切的点	T	—

表 1 按术语的英文对应词字母顺序排列的术语和符号（续）

术语	符号	单位
任一齿距累积偏差(任一分度偏差)	F_{pi}	μm
齿距累积总偏差(总分度偏差)	F_{p}	μm
齿距(分度)累积总公差	F_{pT}	μm
齿宽(轴向)	b	mm
齿面公差等级	A	—
螺旋角	β	(°)
螺旋线总偏差	F_{β}	μm
螺旋线计值长度	L_{β}	mm
螺旋线形状偏差	$f_{f\beta}$	μm
螺旋线形状滤波器截止波长	λ_{β}	mm
螺旋线形状公差	$f_{f\beta T}$	μm
螺旋线倾斜偏差	$f_{H\beta}$	μm
螺旋线倾斜公差	$f_{H\beta T}$	μm
螺旋线总公差	$F_{\beta T}$	μm
任一径向测量距离	r_{i}	μm
啮合线长度	g_{α}	mm
最大修缘长度	$L_{Ca\alpha,max}$	mm
最大修根长度	$L_{Cf\alpha,max}$	mm
测量圆直径	d_{M}	mm
齿廓中部区域	$L_{\alpha m}$	—
最小修缘长度	$L_{Ca\alpha,min}$	mm
最小修根长度	$L_{Cf\alpha,min}$	mm
法向模数	m_{n}	mm
齿数	z	—
扇形区内齿距数	k	—
测量圆上的端面齿距	p_{tM}	mm
节点	C	—
齿距跨度偏差	F_{pSk}	μm
齿廓控制圆直径	d_{Cf}	mm
齿廓总偏差	F_{α}	μm
齿廓计值长度	L_{α}	mm
齿廓形状偏差	$f_{f\alpha}$	μm
齿廓形状滤波器截止波长	λ_{α}	mm
齿廓形状公差	$f_{f\alpha T}$	μm

表 1　按术语的英文对应词字母顺序排列的术语和符号（续）

术语	符号	单位
齿廓倾斜偏差	$f_{H\alpha}$	μm
齿廓倾斜公差	$f_{H\alpha T}$	μm
齿廓总公差	$F_{\alpha T}$	μm
一齿径向综合偏差[a]	f_{id}	μm
径向综合总偏差[a]	F_{id}	μm
分度圆直径	d	mm
齿根成形圆直径	d_{Ff}	mm
修根区域	L_{Caf}	—
径向跳动	F_{r}	μm
k 个齿距累积偏差	F_{pk}	μm
k 个齿距累积公差	F_{pkT}	μm
切向综合总偏差	F_{is}	μm
切向综合总公差	F_{isT}	μm
一齿切向综合偏差	f_{is}	μm
一齿切向综合公差	f_{isT}	μm
单个齿距偏差	f_{p}	μm
任一单个齿距偏差	f_{pi}	μm
单个齿距公差	f_{pT}	μm
有效齿根圆直径	d_{Nf}	mm
有效齿根点(有效齿根圆与啮合线的交点)	$\mathrm{N_f}$	—
齿顶倒角	h_{k}	mm
齿顶圆直径	d_{a}	mm
齿顶成形圆直径	d_{Fa}	mm
修缘区域	L_{Caa}	—
齿厚	s	mm
节圆直径	d_{w}	mm
端面啮合角	α_{wt}	(°)

[a] 在 ISO 1328-2 中给出。

表 2　按符号的字母顺序排列的符号和术语

符号	术语	单位
A	齿面公差等级	—
b	齿宽(轴向)	mm

表 2 按符号的字母顺序排列的符号和术语(续)

符号	术语	单位
C	节点	—
$C_{\alpha a}$	修缘量(齿顶)	μm
$C_{\alpha f}$	修根量(齿根)	μm
c_p	接触斑点评价	—
d	分度圆直径	mm
d_a	齿顶圆直径	mm
d_b	基圆直径	mm
d_{Cf}	齿廓控制圆直径	mm
d_{Fa}	齿顶成形圆直径	mm
d_{Ff}	齿根成形圆直径	mm
d_M	测量圆直径	mm
d_{Na}	有效齿顶圆直径	mm
d_{Nf}	有效齿根圆直径	mm
d_w	节圆直径	mm
F_{id}	径向综合总偏差[a]	μm
F_{is}	切向综合总偏差	μm
F_{isT}	切向综合总公差	μm
F_p	齿距累积总偏差(总分度偏差)	μm
F_{pi}	任一齿距累积偏差(任一分度偏差)	μm
F_{pk}	k 个齿距累积偏差	μm
F_{pkT}	k 个齿距累积公差	μm
F_{pT}	齿距(分度)累积总公差	μm
F_{pSk}	齿距跨度偏差	μm
F_r	径向跳动	μm
F_α	齿廓总偏差	μm
$F_{\alpha T}$	齿廓总公差	μm
F_β	螺旋线总偏差	μm
$F_{\beta T}$	螺旋线总公差	μm
$f_{f\alpha}$	齿廓形状偏差	μm
$f_{f\alpha T}$	齿廓形状公差	μm
$f_{f\beta}$	螺旋线形状偏差	μm
$f_{f\beta T}$	螺旋线形状公差	μm
$f_{H\alpha}$	齿廓倾斜偏差	μm
$f_{H\alpha T}$	齿廓倾斜公差	μm

表 2 按符号的字母顺序排列的符号和术语(续)

符号	术语	单位
$f_{H\beta}$	螺旋线倾斜偏差	μm
$f_{H\beta T}$	螺旋线倾斜公差	μm
f_{id}	一齿径向综合偏差[a]	μm
f_{is}	一齿切向综合偏差	μm
f_{isT}	一齿切向综合公差	μm
f_{p}	单个齿距偏差	μm
f_{pi}	任一单个齿距偏差	μm
f_{pT}	单个齿距公差	μm
f_{u}	相邻齿距差	μm
f_{ui}	任一相邻齿距差	μm
f_{uT}	相邻齿距差的公差	μm
g_{α}	啮合线长度	mm
h_{k}	齿顶倒角	mm
k	扇形区内齿距数	—
$L_{\alpha m}$	齿廓中部区域	—
$L_{C\alpha a}$	修缘区域	—
$L_{C\alpha f}$	修根区域	—
$L_{C\alpha a,max}$	最大修缘长度	mm
$L_{C\alpha a,min}$	最小修缘长度	mm
$L_{C\alpha f,max}$	最大修根长度	mm
$L_{C\alpha f,min}$	最小修根长度	mm
L_{α}	齿廓计值长度	mm
L_{β}	螺旋线计值长度	mm
m_{n}	法向模数	mm
$\mathrm{N_a}$	有效齿顶点(有效齿顶圆与啮合线的交点)	—
$\mathrm{N_f}$	有效齿根点(有效齿根圆与啮合线的交点)	—
p_{tM}	测量圆上的端面齿距	mm
r_{i}	任一径向测量距离	μm
s	齿厚	mm
T	啮合线与基圆相切的点	—
z	齿数	—
α_{wt}	端面啮合角	(°)
β	螺旋角	(°)
λ_{α}	齿廓形状滤波器截止波长	mm
λ_{β}	螺旋线形状滤波器截止波长	mm

[a] 在 ISO 1328-2 中给出。

3.2 通用参数

3.2.1

分度圆直径　reference diameter

d

齿轮分度圆的直径。

注 1：分度圆直径用于计算公差值。

注 2：见 ISO 21771:2007 中 4.2.4。

3.2.2

测量圆直径　measurement diameter

d_M

在测量螺旋线、齿距和齿厚偏差时，测头与齿面接触处所在圆的直径，该圆与基准轴线(3.2.7)同心。

注 1：测量圆通常靠近齿面的中部。

注 2：见 ISO/TR 10064-3。

3.2.3

齿廓形状滤波器截止波长　profile form filter cutoff

λ_α

设定的渐开线齿廓测量数据波幅值的 50％可通过高斯低通滤波器、只输出包含较长波偏差的波长。

注：见 4.4.6 和附录 C。

3.2.4

螺旋线形状滤波器截止波长　helix form filter cutoff

λ_β

设定的螺旋线测量数据波幅值的 50％可通过高斯低通滤波器、只输出包含较长波偏差的波长。

注：见 4.4.6 和附录 C。

3.2.5

展开长度　roll path length;length of roll

端平面内，从基圆切点到渐开线齿廓上给定点沿基圆切线的直线距离。

注 1：展开长度可替代展开角，规定被选定的渐开线齿廓上的直径位置。

注 2：见图 1 和 ISO 21771:2007 中的 4.3.8。

3.2.6

啮合线长度　length of path of contact

g_α

从有效齿根点 N_f 到齿顶成形点 F_a，或到由于配对齿轮根切导致啮合终止的位置点(有效齿顶点 N_a)的展开长度(3.2.5)。

3.2.7

基准轴线　datum axis

用来定义齿轮偏差项目(特别是齿距、齿廓和螺旋线偏差)的轴线。

注 1：齿轮的基准轴线由基准面决定。

注 2：见 ISO/TR 10064-3。

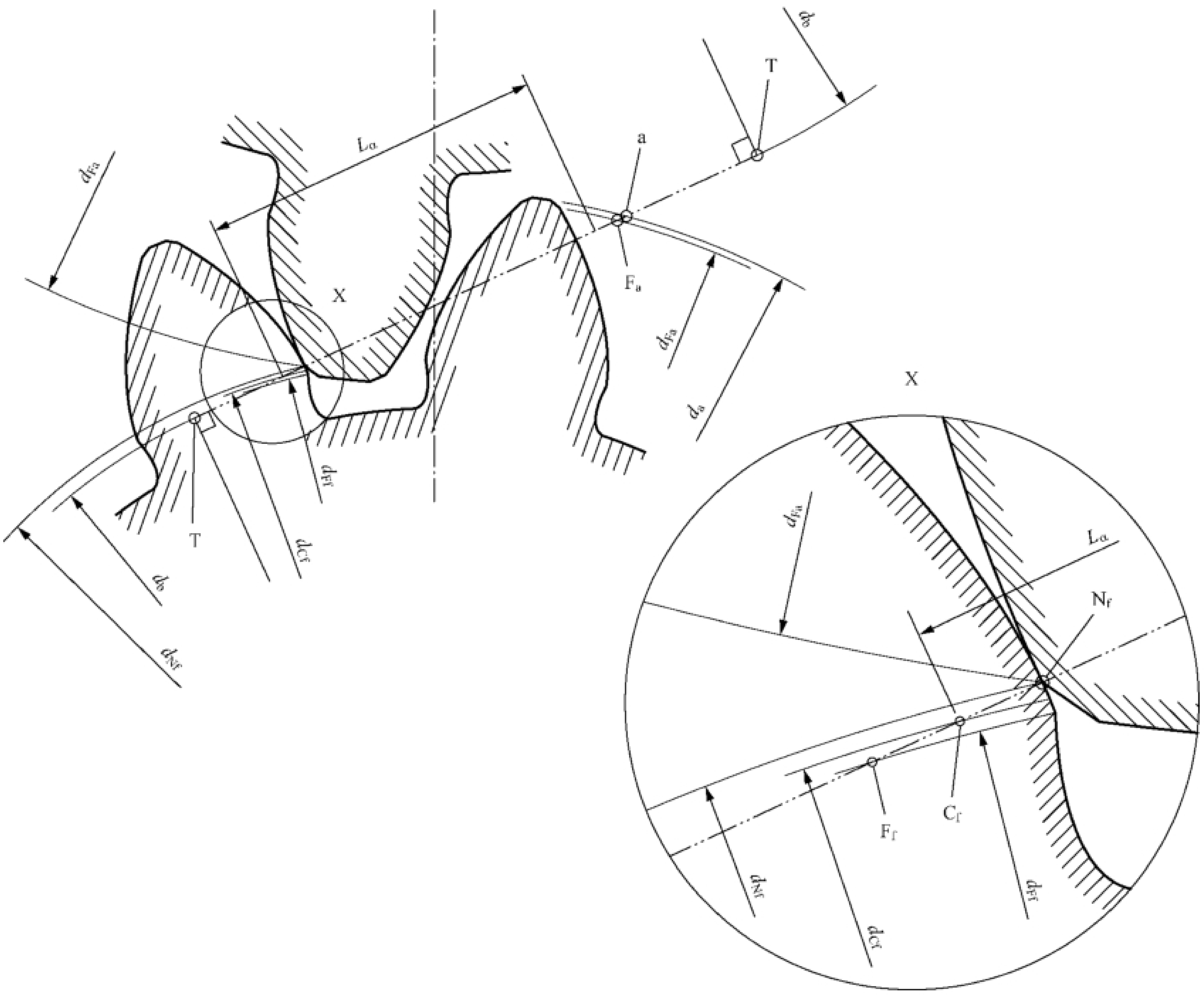

标引符号说明：

L_{α}——齿廓计值长度。

啮合线上的点：

a ——齿顶点；

C_f ——齿廓控制点；

F_a ——齿顶成形点；

F_f ——齿根成形点；

N_f ——有效齿根点；

T ——基圆切点。

—·-——·-— 啮合线。

直径：

d_a ——齿顶圆直径；

d_b ——基圆直径；

d_{Cf} ——齿廓控制圆直径；

d_{Fa} ——齿顶成形圆直径(齿顶渐开线端点直径)；

d_{Ff} ——齿根成形圆直径(齿根渐开线端点直径)；

d_{Nf} ——有效齿根圆直径。

注：对于配对齿轮，直径有相同的符号，但数值不同。

图 1 外啮合齿轮副的直径和展开长度

3.3 齿距偏差

3.3.1

任一单个齿距偏差 individual single pitch deviation

f_{pi}

在齿轮的端平面内、测量圆上，实际齿距与理论齿距的代数差。

注 1：该偏差是任一齿面相对于相邻同侧齿面偏离其理论位置的位移量。

注 2：左侧齿面及右侧齿面的 f_{pi} 值的个数均等于齿数。

注 3：见图 2。

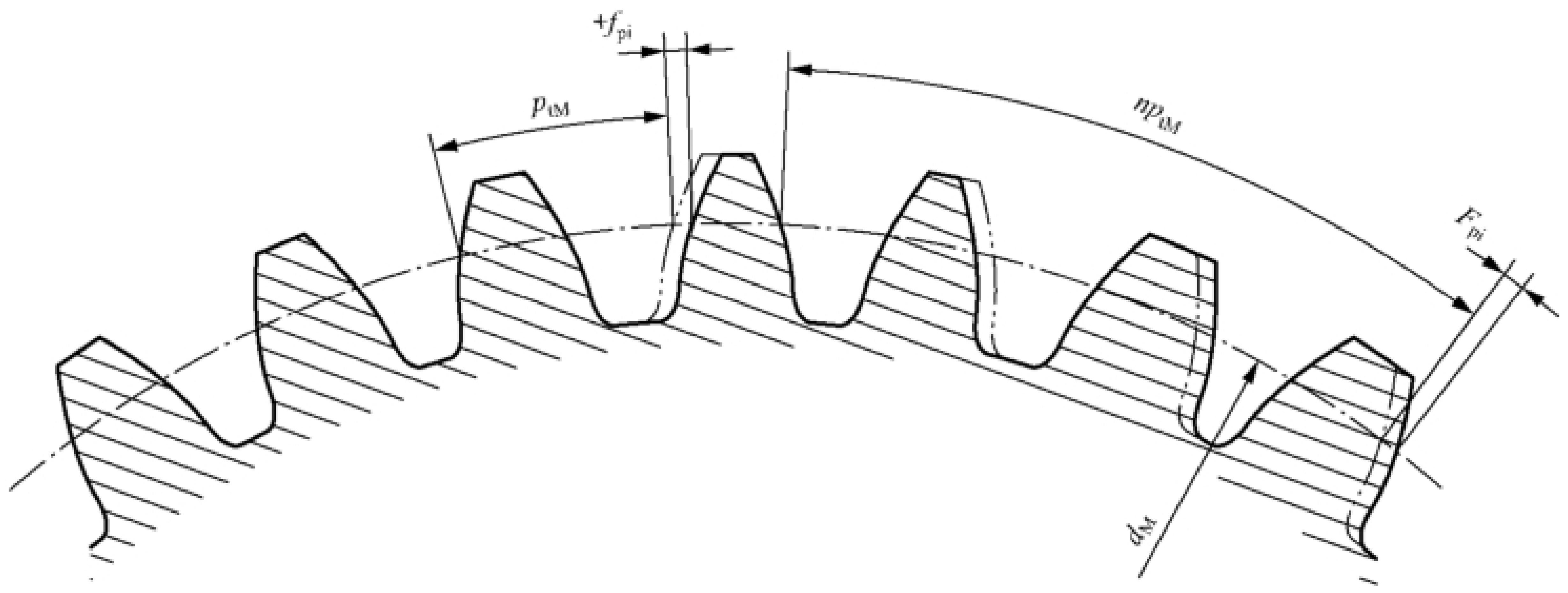

说明：

—··——··— 理论的；

———— 实际的。

注：$p_{tM}=\pi d_M/z$。

图 2 齿距偏差

3.3.2

单个齿距偏差 single pitch deviation

f_p

所有任一单个齿距偏差(3.3.1)的最大绝对值。

注：$f_p=\max|f_{pi}|$。

3.3.3

任一齿距累积偏差 individual cumulative pitch deviation

任一分度偏差 individual index deviation

F_{pi}

n 个相邻齿距的弧长与理论弧长的代数差。

注 1：n 的范围从 1 到 z，左侧齿面和右侧齿面 F_{pi} 值的个数均等于齿数。

注 2：理论上 F_{pi} 等于这 n 个齿距的任一单个齿距偏差(3.3.1)的代数和；是相对于一个基准轮齿齿面，任意轮齿齿面偏离其理论位置的位移量。

注 3：见图 2 和附录 D。

3.3.4

齿距累积总偏差 total cumulative pitch deviation

总分度偏差 total index deviation

F_p

齿轮所有齿的指定齿面的任一齿距累积偏差(3.3.3)的最大代数差。

注：$F_p=F_{pi,\max}-F_{pi,\min}$。

3.4 齿廓偏差

3.4.1 齿廓偏差概述

3.4.1.1

齿廓控制圆直径 profile control diameter

齿廓评价起点圆直径 start of profile evaluation diameter

d_{Cf}

齿廓控制点 C_f 所在圆的直径，超过该直径的齿廓部分与设计齿廓(3.4.2.1)一致。

注 1：如果未指定d_{Cf}，有效齿根圆直径d_{Nf}可作为齿廓控制圆直径，见 4.5 最后一段。

注 2：见图 1 和图 3。

3.4.1.2

齿顶成形圆直径　tip form diameter

d_{Fa}

除非另有规定，齿顶成形圆直径等于齿顶圆直径减去两倍的齿顶圆角半径或齿顶倒角高度。

注 1：修顶(齿顶倒角或倒圆)位置，对于外齿轮为最小指定直径处，对于内齿轮为最大指定直径处。

注 2：当名义渐开螺旋面和齿顶外圆柱面直接相交时，齿顶圆角半径为 0，齿顶成形圆直径等于齿顶圆直径。

注 3：见图 1 和图 3。

3.4.1.3

被测齿廓　measured profile

齿廓测量时，测头沿齿面走过的齿廓部分，包含从齿廓控制圆直径d_{Cf}(3.4.1.1)到齿顶成形圆直径d_{Fa}(3.4.1.2)在内的部分。

注：见图 3。

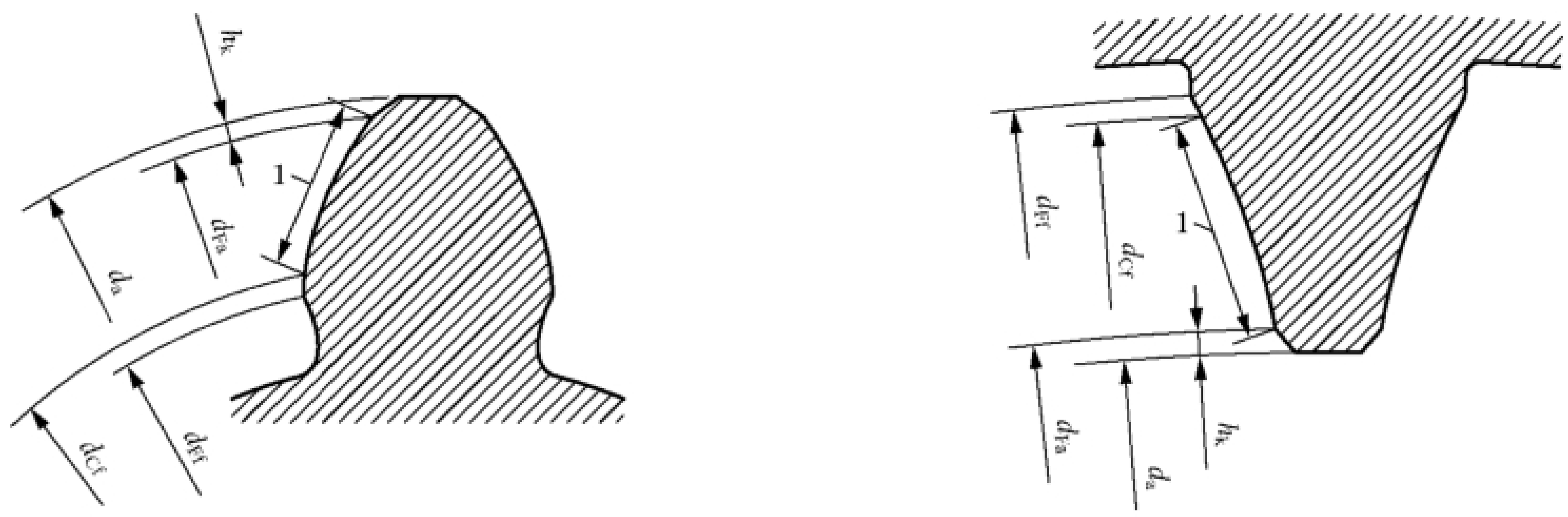

a)　外齿轮　　　　b)　内齿轮

标引序号说明：

1——被测齿廓。

图 3　被测齿廓

3.4.1.4

齿廓计值范围　profile evaluation range

对于被测齿廓(3.4.1.3)，从齿廓控制圆直径d_{Cf}(3.4.1.1)到齿顶成形圆直径d_{Fa}(3.4.1.2)范围的95%(从d_{Cf}算起)。另有规定时除外。

注：见图 4～图 8、4.4.8 和 ISO 21771。

3.4.1.5

齿廓计值长度　profile evaluation length

L_α

端平面上，齿廓计值范围(3.4.1.4)对应的展开长度(3.2.5)。

注：见图 1。

3.4.1.6

齿廓偏差　profile deviation

被测齿廓(3.4.1.3)偏离设计齿廓(3.4.2.1)的量。

注：见图 4～图 8。

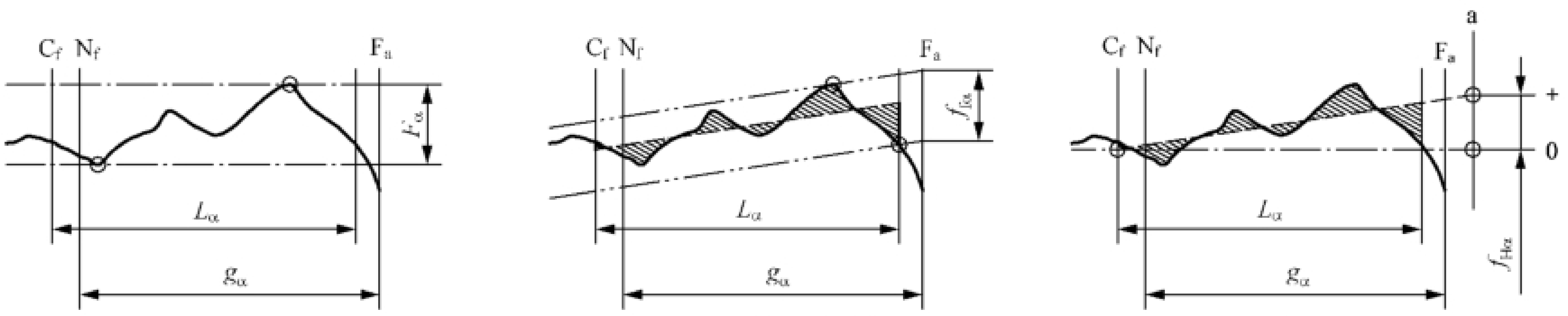

a) 齿廓总偏差　　b) 齿廓形状偏差　　c) 齿廓倾斜偏差

说明：

——————	被测齿廓；	啮合线上的点：	
—·—·—·—	设计齿廓平行线；	C_f	——齿廓控制点；
— — — —	平均齿廓线；	N_f	——有效齿根点；
—··—··—	平均齿廓线平行线。	F_a	——齿顶成形点(修顶起始处)；
		a	——齿顶点。

图 4　渐开线未修形的齿廓偏差

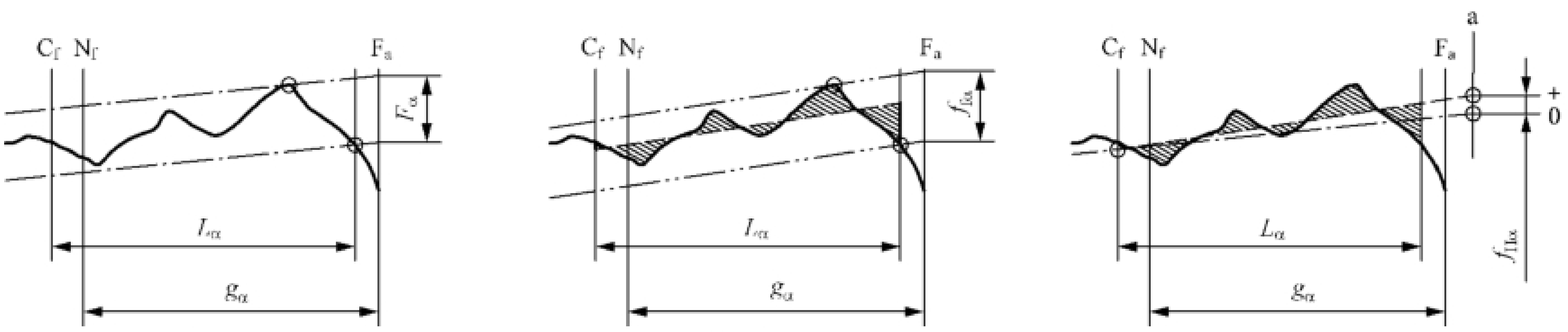

a) 齿廓总偏差　　b) 齿廓形状偏差　　c) 齿廓倾斜偏差

说明见图 4。

图 5　压力角修形的齿廓偏差

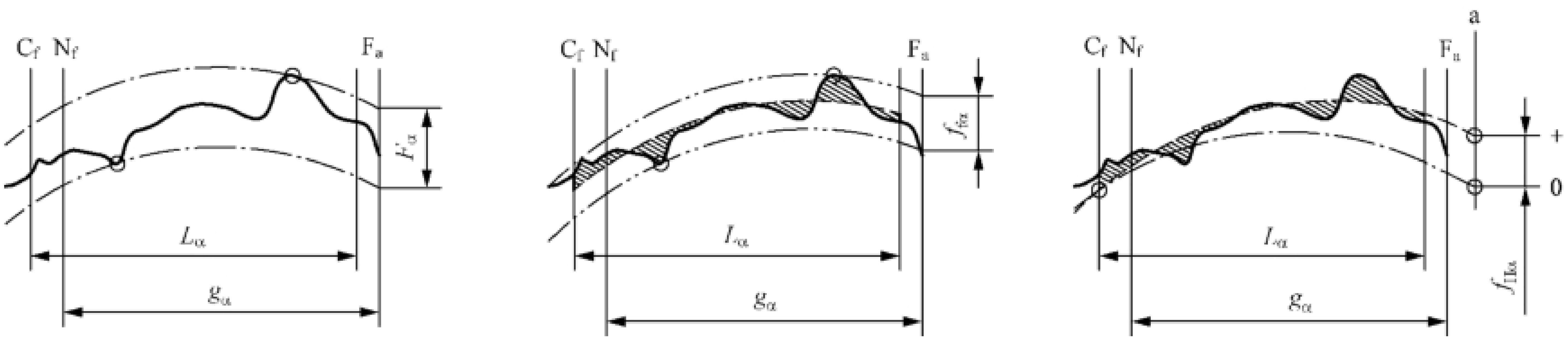

a) 齿廓总偏差　　b) 齿廓形状偏差　　c) 齿廓倾斜偏差

说明见图 4。

图 6　齿廓鼓形修形的齿廓偏差

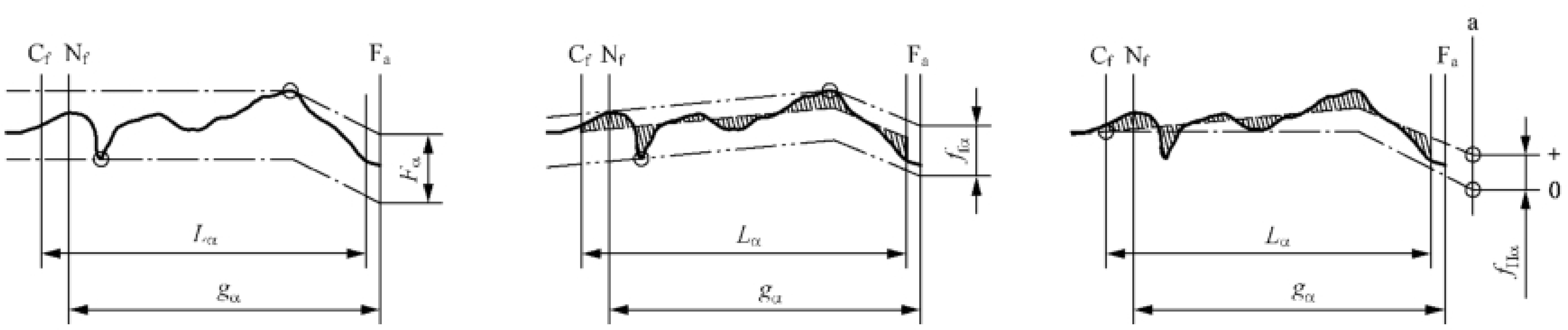

a) 齿廓总偏差　　b) 齿廓形状偏差　　c) 齿廓倾斜偏差

说明见图 4。

图 7　齿顶修缘的齿廓偏差

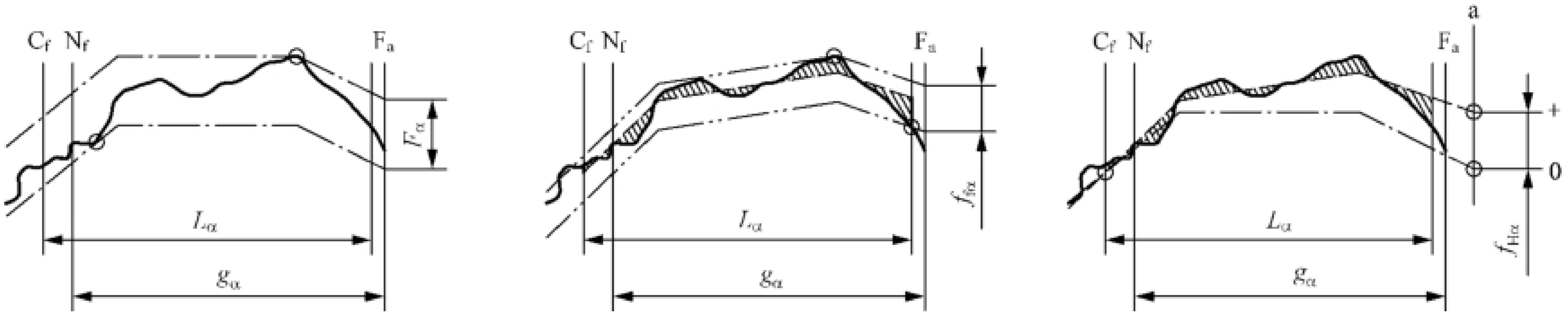

a) 齿廓总偏差　　b) 齿廓形状偏差　　c) 齿廓倾斜偏差

说明见图 4。

图 8　修缘与修根的齿廓偏差

3.4.2　齿廓偏差分析

3.4.2.1

设计齿廓　design profile

由设计者给定的齿廓。在展开图中，竖向代表对理论渐开线进行修正，横向代表沿基圆切线方向上的展开长度。

注 1：未说明时，设计齿廓就是一条未修形的渐开线，在图 4～图 8 中呈现为直线(以点划线表示)。

注 2：见图 4～图 8。

3.4.2.2

平均齿廓线　mean profile line

与在齿廓计值范围(3.4.1.4)内测得迹线相匹配的、表达设计齿廓(3.4.2.1)总体趋势的直线(或曲线)。

注：生成方法见 4.4.8.2。

3.4.2.3

齿廓总偏差　total profile deviation

F_α

在齿廓计值范围内(3.4.1.4)，包容被测齿廓(3.4.1.3)的两条设计齿廓(3.4.2.1)平行线之间的距离。

注 1：设计齿廓平行线与设计齿廓平行。

注 2：见图 4～图 8 和 4.4.8.2。

3.4.2.4

齿廓形状偏差　profile form deviation

$f_{f\alpha}$

在齿廓计值范围内(3.4.1.4)，包容被测齿廓(3.4.1.3)的两条平均齿廓线(3.4.2.2)平行线之间的距离。

注 1：平均齿廓线平行线与平均齿廓线平行。

注 2：见图 4～图 8 和 4.4.8.2。

3.4.2.5

齿廓倾斜偏差　profile slope deviation

$f_{H\alpha}$

以齿廓控制圆直径 d_{Cf} 为起点，以平均齿廓线(3.4.2.2)的延长线与齿顶圆直径 d_a 的交点为终点，与这两点相交的两条设计齿廓(3.4.2.1)平行线间的距离。

注 1：设计齿廓平行线与设计齿廓保持平行。

注 2：见图 4～图 8。

3.5 螺旋线偏差

3.5.1 螺旋线偏差概述

3.5.1.1

被测螺旋线 measured helix

测量螺旋线时，两端面之间的齿面全长与测头接触的部分。如存在倒角、圆角及其他类型的修角，即为修角起始点间的部分。

3.5.1.2

螺旋线计值范围 helix evaluation range

两端面之间的齿面区域。如存在倒角、圆角及其他类型的修角，则为修角起始点间的齿面区域。在满足使用要求的前提下，除另有规定外，该区域沿轴线两端各减去5％的齿宽或一个模数的长度这两个数值中较小的一个。

注 1：齿轮设计者有责任使螺旋线计值范围满足使用要求。

注 2：见4.4.8.4。

3.5.1.3

螺旋线计值长度 helix evaluation length

L_β

螺旋线计值范围(3.5.1.2)的轴向长度。

3.5.1.4

螺旋线偏差 helix deviation

被测螺旋线(3.5.1.1)偏离设计螺旋线(3.5.2.1)的量。

注：见图9～图13。

3.5.2 螺旋线偏差分析

3.5.2.1

设计螺旋线 design helix

由设计者给定的螺旋线，在展开图中，竖向代表对理论螺旋线进行的修正，横向代表齿宽。

注 1：未给定时，设计螺旋线是无修形的螺旋线。

注 2：见图9～图13。

3.5.2.2

平均螺旋线 mean helix line

与测得迹线相匹配的、表达设计螺旋线(3.5.2.1)总体趋势的直线(或曲线)。

注：使用方法见4.4.8.4。

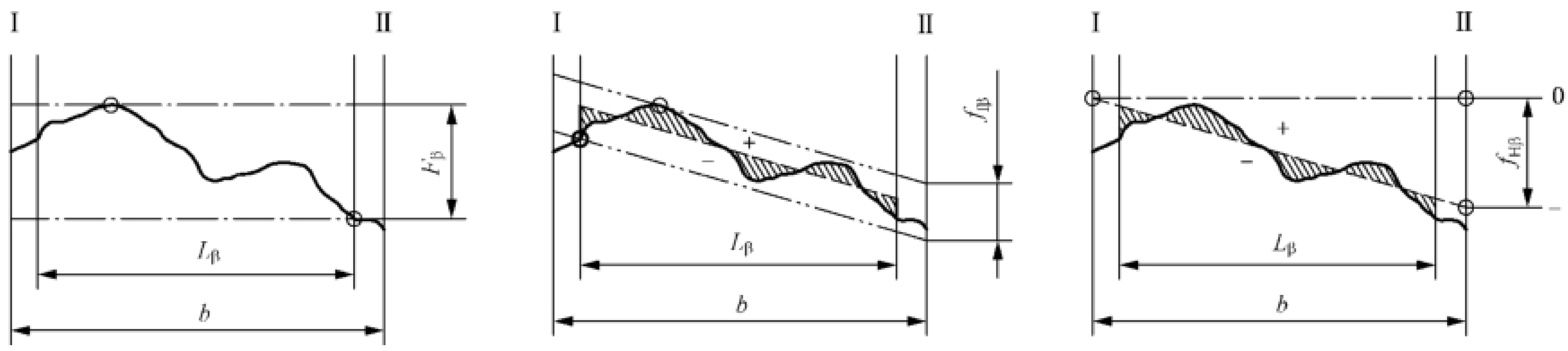

a) 螺旋线总偏差　　b) 螺旋线形状偏差　　c) 螺旋线倾斜偏差

说明：

——— 被测螺旋线；

－－－－ 平均螺旋线；

—·—·— 设计螺旋线平行线；

—··—··— 平均螺旋线平行线。

图9 螺旋线未修形的螺旋线偏差

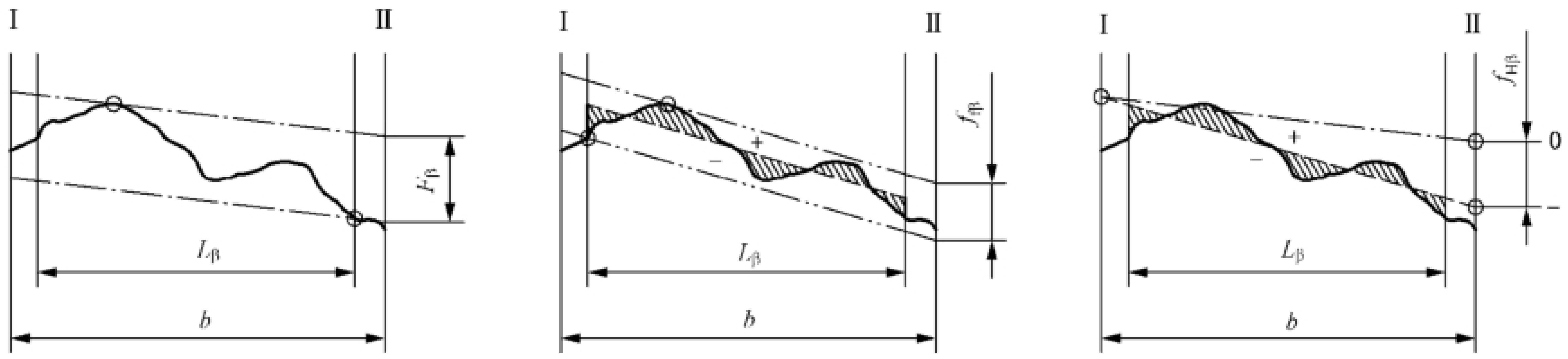

a）　螺旋线总偏差　　b）　螺旋线形状偏差　　c）　螺旋线倾斜偏差

说明见图 9。

图 10　螺旋角修形的螺旋线偏差

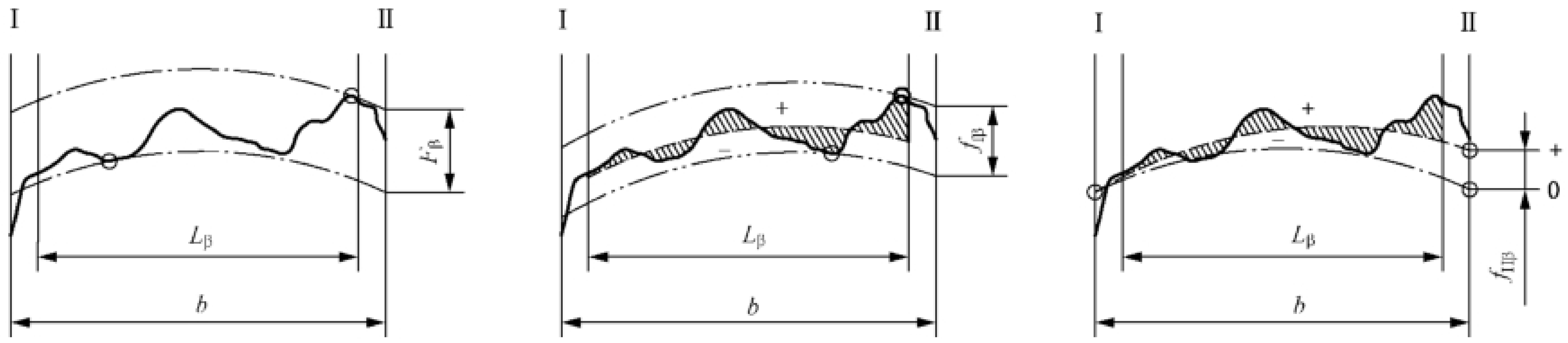

a）　螺旋线总偏差　　b）　螺旋线形状偏差　　c）　螺旋线倾斜偏差

说明见图 9。

图 11　螺旋线鼓形修形的螺旋线偏差

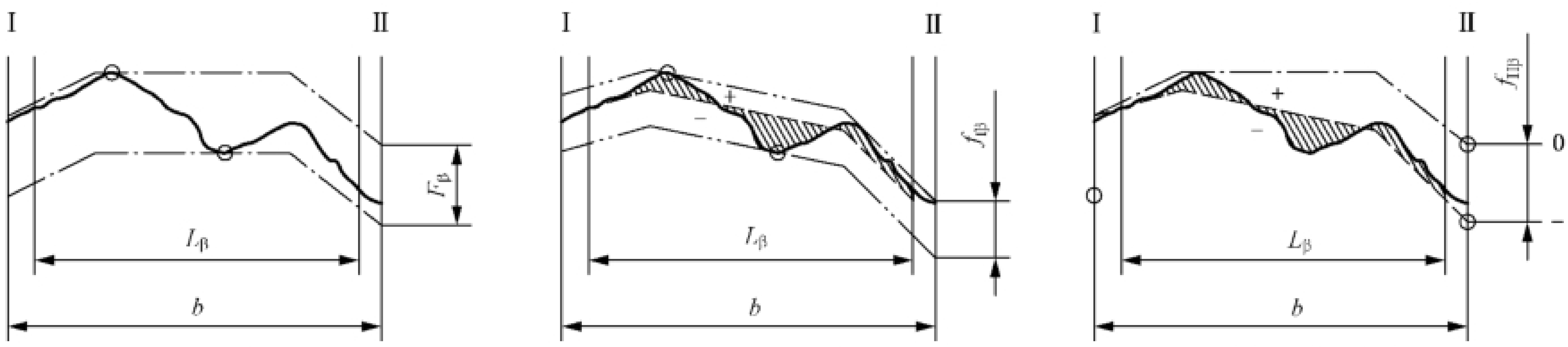

a）　螺旋线总偏差　　b）　螺旋线形状偏差　　c）　螺旋线倾斜偏差

说明见图 9。

图 12　螺旋线齿端修薄的螺旋线偏差

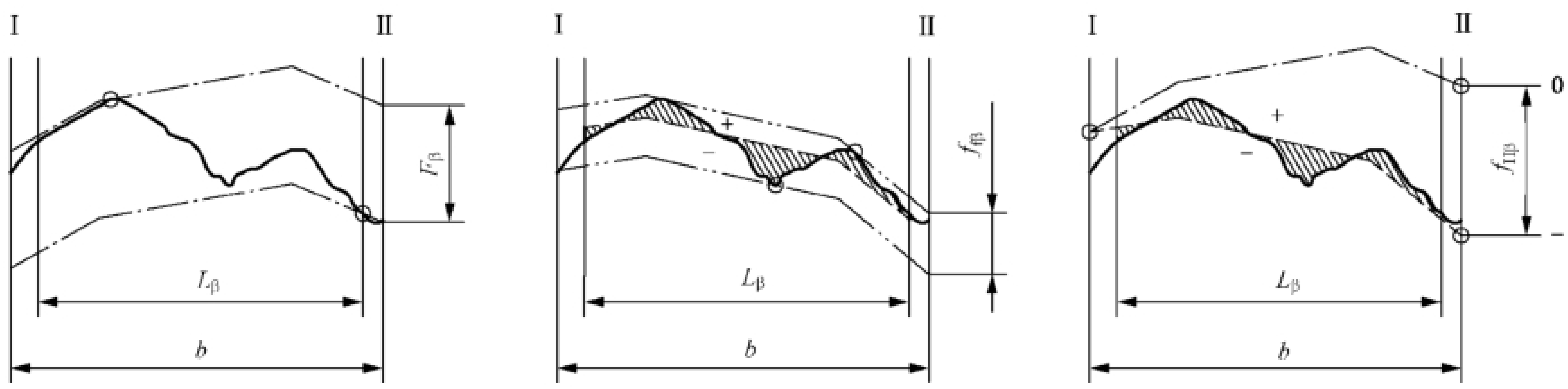

a）　螺旋线总偏差　　b）　螺旋线形状偏差　　c）　螺旋线倾斜偏差

说明见图 9。

图 13　螺旋角修形与齿端修薄的螺旋线偏差

3.5.2.3

螺旋线总偏差　total helix deviation

F_{β}

在螺旋线计值范围内(3.5.1.2),包容被测螺旋线(3.5.1.1)的两条设计螺旋线(3.5.2.1)平行线之间的距离。

注 1:设计螺旋线平行线与设计螺旋线平行。

注 2:见图 9～图 13 和 4.4.8.4。

3.5.2.4

螺旋线形状偏差　helix form deviation

$f_{f\beta}$

在螺旋线计值范围内(3.5.1.2),包容被测螺旋线(3.5.1.1)的两条平均螺旋线(3.5.2.2)平行线之间的距离。

注 1:平均螺旋线平行线与平均螺旋线平行。

注 2:见图 9～图 13 和 4.4.8.4。

3.5.2.5

螺旋线倾斜偏差　helix slope deviation

$f_{H\beta}$

在齿轮全齿宽 b 内,通过平均螺旋线(3.5.2.2)的延长线和两端面的交点的、两条设计螺旋线(3.5.2.1)平行线之间的距离。

注 1:设计螺旋线平行线与设计螺旋线平行。

注 2:见图 9～图 13。

注 3:使用方法见 4.4.8.4。

4　ISO 齿面公差分级制的应用

4.1　通则

本文件提供了齿面精度分级公差,并推荐了未装配齿轮的测量要求。

某些能够保证测量效果的设计和应用,或在制造工艺中未描述的内容,应在合同文件中加以说明。

除非供需双方有特别的约定,具体的测量方法或文件不做强制规定。当某些情况超出了本文件的限定范围,则相应的测量方法应在加工齿轮前做好协商。

当按照本文件来规定齿面公差等级时,应使用 4.6.1 规定的标识。因为对照以前的版本,同一齿面公差等级对应不同的公差值。

4.2　需要验证的几何参数

表 3 中给出齿轮的几何特征可通过多种方法来测量。具体测量方法取决于公差的等级、相关的测量不确定度、齿轮的尺寸、生产数量、可用设备、齿坯精度和测量成本。直齿轮和斜齿轮的测量方法与检验实施在 ISO/TR 10064-1 中有说明。

表 3 参数 定义和公差所在的位置

参数符号	测量描述	公差所在位置	定义所在位置
要素:			
F_p	齿距累积总偏差	5.3.2	3.3.4
f_p	单个齿距偏差	5.3.1	3.3.2
F_α	齿廓总偏差	5.3.3.3	3.4.2.3
$f_{f\alpha}$	齿廓形状偏差	5.3.3.2	3.4.2.4
$f_{H\alpha}$	齿廓倾斜偏差	5.3.3.1	3.4.2.5
F_β	螺旋线总偏差	5.3.4.3	3.5.2.3
$f_{f\beta}$	螺旋线形状偏差	5.3.4.2	3.5.2.4
$f_{H\beta}$	螺旋线倾斜偏差	5.3.4.1	3.5.2.5
F_r	径向跳动	E.4	E.3
F_{pk}	k 个齿距累积偏差	D.5	D.2
f_u	相邻齿距差	G.2	G.1.2
综合:			
F_{is}	切向综合总偏差	F.1.6	附录 F
f_{is}	一齿切向综合偏差	F.1.5	F.1.5
c_p	接触斑点评价(见 ISO/TR 10064-4)	—	
尺寸:			
s	齿厚(按 ISO 21771 规定)	—	

符合 ISO 齿面公差等级规定的齿轮应满足表 4 和表 5 中给出的适用于指定齿面公差等级和尺寸的所有单个偏差要求。

表 4 中列出了符合本文件要求应进行测量的最少参数。当供需双方同意时,可用备选参数表替代默认参数表。选择默认参数表还是备选参数表取决于可用的测量设备。评价齿轮时可使用更高精度的齿面公差等级的参数列表。

通常,轮齿两侧采用相同的公差。在某些情况下,承载齿面可比非承载齿面或轻承载齿面规定更高的精度等级。此时,应在齿轮工程图上说明,并注明承载齿面。

表 4 被测量参数表

直径 mm	齿面公差等级	最少可接受参数	
		默认参数表	备选参数表
$d \leqslant 4\ 000$	10～11	$F_p, f_p, s, F_\alpha, F_\beta$	s, c_p, F_{id}[a], f_{id}[a]
	7～9	$F_p, f_p, s, F_\alpha, F_\beta$	s, c_p[b], F_{is}, f_{is}
	1～6	F_p, f_p, s $F_\alpha, f_{f\alpha}, f_{H\alpha}$ $F_\beta, f_{f\beta}, f_{H\beta}$	s, c_p[b], F_{is}, f_{is}
$d > 4\ 000$	7～11	$F_p, f_p, s, F_\alpha, F_\beta$	F_p, f_p, s, ($f_{f\beta}$或c_p[b])

[a] 根据 ISO 1328-2,仅限于齿轮尺寸不受限制时。

[b] 接触斑点的验收标准和测量方法未包含在本文件中,如需采用,应经供需双方同意。

表 5 典型测量方法及最少测量齿数

检查项目	典型测量方法	最少测量齿数
要素： F_p：齿距累积总偏差	 双测头 单测头	 全齿 全齿
f_p：单个齿距偏差	双测头 单测头	全齿 全齿
F_α：齿廓总偏差 $f_{f\alpha}$：齿廓形状偏差 $f_{H\alpha}$：齿廓倾斜偏差	齿廓测量	3 齿
F_β：螺旋线总偏差 $f_{f\beta}$：螺旋线形状偏差 $f_{H\beta}$：螺旋线倾斜偏差	螺旋线测量	3 齿
综合： F_{is}：切向综合总偏差	 —	 全齿
f_{is}：一齿切向综合偏差	—	全齿
c_p：接触斑点评价	—	3 处
尺寸： s：齿厚	 齿厚卡尺 跨棒距或棒间距 跨齿测量距 综合测量	 3 齿 2 处 2 处 全齿

除非另有规定，制造商应选择：

——采用的测量方法来自 ISO/TR 10064-1 中相关的描述和表 5 的说明；

——与测量方法相关的测量设备被正确地校准；

——齿轮测量时按照表 5 中规定的方法及最少测量齿数进行，且被测轮齿近似等距。

4.3 检测仪器的认证和不确定性

为了确保可追溯性，用来测量齿轮的设备应根据标准校准程序定期认证，例如 ISO 18653 的要求。应明确测量过程中的不确定性。

4.4 单项偏差测量的注意事项

4.4.1 简述

在把单项偏差测量值与公差值进行对比前，应了解测量方法的操作细节，包括：

——基准轴线；

——测量的方向；

——公差的方向；

——测量圆直径；

——数据滤波；

——数据密度；

——所需的测量规程。

通常情况下，测量仪器应满足默认的最低使用要求。其他情况下，应了解引起测量误差的原因，并对此进行补偿。

单项偏差测量应重视区分测量位置(测量圆直径)、测量方向和公差方向。

4.4.2 基准轴线

确定设计齿廓、设计螺旋线和齿距，应定义一个合适的基准回转轴线，称为基准轴线。通过确定基准面来定义基准轴线，见 ISO/TR 10064-3。

轮齿几何参数由基准轴线确定，基准轴线是测量及对应公差的基础，测量圆的位置和方向由基准轴线决定。

4.4.3 测量方向

任意表面的形状或位置的测量，可沿该表面的法向，或在倾斜某个角度的方向，或在沿给定圆的圆弧方向上进行。

常见测量规程是沿被测表面的法线进行测量。齿轮齿面上任意点，其法向向量与齿轮基圆柱面相切，并且相对于端平面倾斜角度为基圆螺旋角。

重要的是，应了解齿轮测量仪可能存在不同的测量方法，或沿法线测量，或沿其他方向测量。

4.4.4 公差方向

在本文件中，公差方向由偏差项目决定。如果实际测量方向和该公差方向不一致，应对原始测量数值进行补偿。符号惯例与数值报告见 4.4.8.2、4.4.8.4 和 4.4.8.6。

齿距偏差规定的公差方向是在端平面内沿直径为d_M的测量圆的圆弧方向。

齿廓偏差和螺旋线偏差规定的公差方向是在端平面内沿基圆切线的方向。

4.4.5 测量圆直径

本文件中规定的测量圆直径d_M在 3.2.2 中定义为测量螺旋线和齿距时的位置(见 4.4.3 和 4.4.4)。测量圆直径应记录在检测报告中。由于公差值是根据分度圆直径计算，当测量圆直径发生改变时，公差值仍保持不变。

当测量圆直径未指定时，按公式(1)和公式(2)计算：

对于外齿轮：

$$d_M = d_a - 2m_n \qquad (1)$$

对于内齿轮：

$$d_M = d_a + 2m_n \qquad (2)$$

式中：

d_M ——测量圆直径，单位为毫米(mm)；

d_a ——齿顶圆直径，单位为毫米(mm)；

m_n ——法向模数，单位为毫米(mm)。

4.4.6 测量数据滤波

任何齿面均可从加工好的齿廓形状中提取不同频率的偏差，包括长周期误差(如大范围的凹陷)和

短周期误差(如齿面粗糙度)。

本文件要求在分析和对比公差之前,应对用于渐开线和螺旋线评价的原始测量数据进行修正,使其仅包含长周期误差,即低通滤波。这样可最大程度地减少或排除短于滤波器截止波长的误差影响。本文件规定的滤波器截止波长是齿轮形状滤波器截止波长λ_α和λ_β,定义分别见3.2.3和3.2.4。齿廓形状滤波器截止波长λ_α应采用展开长度表示,螺旋线形状滤波器截止波长λ_β应采用齿宽表示。推荐的滤波器截止波长按公式(3)和公式(4)计算。大于该计算值,不应作为形状滤波器截止波长。

$$\lambda_\alpha = \frac{L_\alpha}{30} \qquad \cdots\cdots (3)$$

而$\lambda_\alpha \geqslant 0.25$ mm;

$$\lambda_\beta = \frac{b}{30} \qquad \cdots\cdots (4)$$

而$\lambda_\beta \geqslant \lambda_\alpha$。

式中:

λ_α——齿廓形状滤波器截止波长,单位为毫米(mm);

λ_β——螺旋线形状滤波器截止波长,单位为毫米(mm)。

应在检测报告中注明实际滤波类型和形状滤波器截止波长λ_α和λ_β(连同测头直径)。应使用有50%传输特性的高斯滤波器,其定义在ISO/TS 16610-1和ISO 16610-21中。

警告:某些情况下,以公式(3)和公式(4)计算的形状滤波器截止波长进行滤波可能会掩盖与齿轮性能有关的形状偏差。介于形状滤波器截止波长与表面粗糙度滤波器截止波长之间的形状偏差有时候称为波纹度。当有具体要求时,应选择比公式(3)和公式(4)计算的形状滤波器截止波长较短的波长来评价这些形状偏差。

更多信息见附录C。

4.4.7 测量数据密度

数据采样率局限了表面不规则形貌的波长的观测,因此测量数据密度和测量数据滤波密切相关。计值长度内的数据点数应在检测报告中注明。渐开线齿廓测量数据应至少包含150个点,这些点应沿展开长度方向大致等距分布。螺旋线测量数据应包含至少$5\times b/\lambda_\beta$个点。如果检查波纹度,那么数据应至少包含300个点或每毫米内5个点(取两者中的较大值)。

4.4.8 测量和评价规程

4.4.8.1 齿廓测量

测头应扫过整个齿廓长度。起始于齿廓控制圆之下,连续划过齿面,并经过修顶的实际起始点。

4.4.8.2 齿廓分析

在齿廓计值范围内,将被测齿廓迹线对比给定的设计齿廓得到的偏差应用最小二乘法,确定齿廓测量结果的斜率线。评价一般从齿廓控制点C_f开始。在接近齿顶的超过齿廓计值范围的区域,由实体材料增加(凸起)引起的偏差应计入齿廓形状偏差$f_{f\alpha}$和齿廓总偏差F_α,由实体材料减少(凹陷)引起的偏差可忽略不计(见图14)。

说明：

—————— 测量齿廓；	啮合线上的点：
—·—·—·— 设计齿廓平行线；	C_f ——齿廓控制点；
— — — — — 平均齿廓线；	N_f ——有效齿廓起始点；
—··—··—·· 平均齿廓线平行线。	F_a ——齿顶成形点（修顶起始处）。

图 14　齿廓偏差的评价

平均齿廓线由齿廓偏差的斜率线纵坐标叠加设计齿廓的纵坐标而成。平均齿廓线用来决定$f_{f\alpha}$［见图 4 b）、图 5 b）、图 6 b）、图 7 b）、图 8 b）和图 14 b）］和$f_{H\alpha}$［见图 4 c）、图 5 c）、图 6 c）、图 7 c）和图 8 c）］。

对于内齿轮和外齿轮，对比设计齿廓，当平均齿廓线显示在齿顶位置材料是增加（凸起）时，齿廓倾斜偏差$f_{H\alpha}$定义为正值，其对应的压力角偏差定义为负值。

齿廓在齿廓计值范围内进行评价，而齿廓倾斜偏差的确定应延伸至齿顶圆。

4.4.8.3　螺旋线测量

测头应走过整个齿宽，即从轮齿的一个端面到另一个端面。如果存在倒角、圆角及其他类型的修角，则从修角起始点开始。

4.4.8.4　螺旋线分析

在螺旋线计值范围内，对根据给定的设计螺旋线得到的被测螺旋线迹线的偏差应用最小二乘法，确定螺旋线测量结果的斜率线。在螺旋线计值范围以外的区域，由材料增加（凸起）引起的偏差应计入螺旋线形状偏差$f_{f\beta}$和螺旋线总偏差F_β，由材料减少（凹陷）引起的偏差可忽略不计（见图 15）。

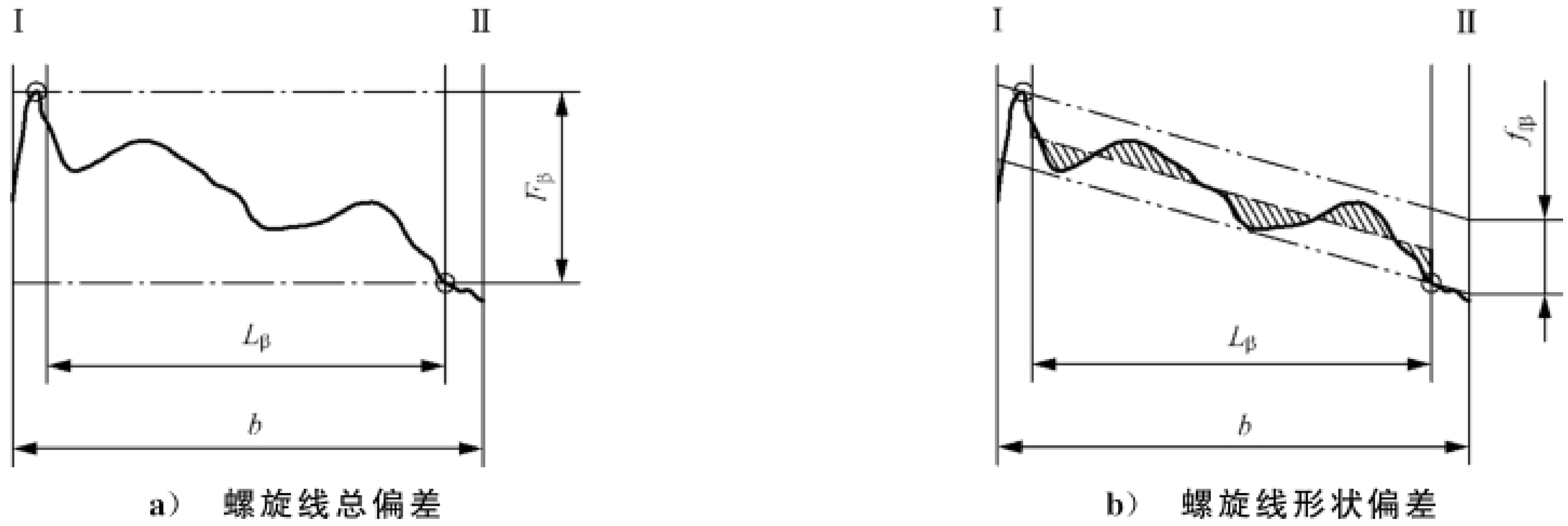

图 15　螺旋线偏差的评价

平均螺旋线由螺旋线偏差的斜率线的纵坐标叠加设计螺旋线的纵坐标而成。平均螺旋线用来决定$f_{f\beta}$［见图 9 b）、图 10 b）、图 11 b）、图 12 b）、图 13 b）和图 15 b）］和$f_{H\beta}$［见图 9 c）、图 10 c）、图 11 c）、图 12 c）和图 13 c）］。

当螺旋角的绝对值大于设计螺旋角时，螺旋线倾斜偏差定义为正值；当螺旋角的绝对值小于设计螺

旋角时,螺旋线倾斜偏差定义为负值。直齿轮的螺旋线倾斜偏差右旋为正,左旋为负。

4.4.8.5 测量位置

螺旋线应在测量圆上测量。齿距也应在测量圆上测量,除非齿距测量是用来评价齿厚。此时,齿距测量应根据选定的评价方法[跨棒(球)距/棒(球)间距,或弦齿厚,或圆弧齿厚]取适当的接触位置。根据第 5 章,公差值的计算应使用分度圆直径 d,而不使用测量圆直径 d_M。

4.4.8.6 齿距偏差值报告

4.4.8.6.1 任一单个齿距偏差

该值应区别正、负号。实际轮齿齿面位置相对于理论位置靠近前一个轮齿齿面定义为负值。实际轮齿齿面位置相对于理论位置远离前一个轮齿齿面定义为正值。

4.4.8.6.2 单个齿距偏差的值

该值无正、负号。左、右齿面的偏差值应分别注明在检测报告中。

4.4.8.6.3 任一齿距累积偏差

该值有测量方向和正、负号的区别。在规定的测量方向(顺时针或逆时针),实际轮齿齿面位置相对于理论位置靠近基准轮齿齿面定义为负值,反之为正值。

4.4.8.6.4 齿距累积总偏差

该值无测量方向和正、负号。如果需要区别,可在构成齿距累积总偏差的两齿之间随意指定一个方向(顺时针或逆时针)。左、右齿面的偏差值应分别注明在检测报告中。

4.5 齿面公差要求的规范

在工程图纸或齿轮计算书中规定的齿轮齿面公差要求应包括但不限于以下内容:

——本文件的引用,如 GB/T 10095.1—2022;

——各个偏差项目的齿面公差等级(各偏差项目的公差等级可不相同)和公差值(根据本文件给出的公差公式进行计算),单位为微米(μm);

——用于测量的基准轴线(最佳工作基准轴线,见 ISO/TR 10064-3);

——工作基准轴线(用于评价);

——测量圆直径如果与 4.4.5 规定的不相同,则应指明测量圆直径;

——最少检查齿数如果与表 5 规定的不相同,则应指明最少检查齿数;

——如果需要,指明齿廓或螺旋线修形的设计形状;

——齿廓和螺旋线测量的计值范围;

——齿廓控制圆直径(表述为直径、展开长度或展开角);

——其他测量要求,如齿厚(表述为分度圆齿厚、跨齿距或跨球距)、齿顶圆直径和齿根圆直径、齿根圆角轮廓、齿面的表面粗糙度。

通常以上要求可用参数表给出。

设计者可在齿根成形点 F_f 和有效齿根点 N_f 之间选择任意位置作为齿廓控制点 C_f。齿根成形点 F_f 取决于根切直径、齿根圆角的切点,或基圆直径(离齿顶圆更近的圆)。如果齿廓控制圆直径 d_{Cf} 未作具体规定,有效齿根圆直径 d_{Nf} 用来替代齿廓控制圆直径 d_{Cf}。当一个齿轮和多个齿轮啮合时,选择控制直径时应考虑每个齿轮的有效齿根圆直径 d_{Nf}。

4.6 验收及评定标准

4.6.1 齿面公差等级的标识

齿面公差等级的标识或规定应按下述格式表示：

GB/T 10095.1—2022,等级 A

A 表示设计齿面公差等级。

注：如果未列出出版年代,则使用最新版本的 GB/T 10095.1。

4.6.2 不同的齿面公差等级

对于给定的具体齿轮,各偏差项目可使用不同的齿面公差等级。

4.6.3 公差

指定齿面公差等级的齿轮的各项公差值可根据第 5 章的公式计算。

4.6.4 评定标准

除非供需双方另有约定,应以本文件中规定的公差、方法和定义为准。测量不确定度和指定公差的使用见 ISO 18653、ISO/TR 10064-5 和 ISO 14253-1。

4.6.5 齿面公差等级评价

齿轮总的公差等级应由本文件规定的所有偏差项目中最大公差等级数来确定。

4.6.6 附加特性

在某些应用中,为取得令人满意的性能,可对齿轮提出额外的特性并指明其公差。例如,齿厚尺寸或表面粗糙度公差在具体应用中为了确保令人满意的性能,该尺寸或公差应体现在工程图上或采购协议中。这些特性的检测方法见 ISO/TR 10064-1 和附录 D～附录 G。

4.7 数据展示

本文件中所有图形显示了设计齿廓、被测齿廓偏离理论渐开线(给定设计压力角)的程度,或设计螺旋线、被测螺旋线偏离理论螺旋线(给定设计螺旋角)的程度。这些图形一般使用水平线显示齿廓或螺旋线,不用指明是左侧齿面还是右侧齿面,或是内齿轮还是外齿轮。大部分测量仪显示齿廓和螺旋线使用竖图,其实显示图是水平的或竖直的并不重要。

5 公差值

5.1 通则

公差值按 5.3 中的公式(5)～公式(12)计算,单位为微米(μm)。

5.2 公式的使用

5.2.1 使用范围

使用范围在第 1 章已规定,5.3 中的公式(5)～公式(12)不应超出这些限制。如果需要超出,齿轮的公差值应由供需双方协商。

5.2.2 级间公比

两相邻公差等级的级间公比是$\sqrt{2}$，本公差级数值乘以(或除以)$\sqrt{2}$可得到相邻较大(或较小)一级的数值。5级精度的未圆整的计算值乘以$\sqrt{2}^{A-5}$即可得任一齿面公差等级的待求值，其中A为指定齿面公差等级。

5.2.3 圆整规则

公式(5)～公式(12)的计算值应按下述规则圆整：

——如果计算值大于10 μm，圆整到最接近的整数值；

——如果计算值不大于10 μm，且不小于5 μm，圆整到最接近的尾数为0.5 μm的值；

——如果计算值小于5 μm，圆整到最接近的尾数为0.1 μm的值。

如果测量仪器采用(英制)英寸(in)，5.3中公式(5)～公式(12)的计算值应转换成万分之一英寸，然后根据圆整规则用微米(μm)进行圆整(例如，用“万分之一英寸”替代上述规则中的“微米”)。公式(5)～公式(12)中的参数应以毫米为单位代入。

5.3 公差公式

5.3.1 单个齿距公差f_{pT}

按公式(5)计算：

$$f_{pT}=(0.001d+0.4m_n+5)\sqrt{2}^{A-5} \tag{5}$$

5.3.2 齿距(分度)累积总公差F_{pT}

按公式(6)计算：

$$F_{pT}=(0.002d+0.55\sqrt{d}+0.7m_n+12)\sqrt{2}^{A-5} \tag{6}$$

5.3.3 齿廓公差

5.3.3.1 齿廓倾斜公差$f_{H\alpha T}$

按公式(7)计算，此公差应加上正、负号(±)。

$$f_{H\alpha T}=(0.4m_n+0.001d+4)\sqrt{2}^{A-5} \tag{7}$$

5.3.3.2 齿廓形状公差$f_{f\alpha T}$

按公式(8)计算：

$$f_{f\alpha T}=(0.55m_n+5)\sqrt{2}^{A-5} \tag{8}$$

5.3.3.3 齿廓总公差$F_{\alpha T}$

按公式(9)计算，其中齿廓倾斜公差和齿廓形状公差使用未圆整的公差值。

$$F_{\alpha T}=\sqrt{f_{H\alpha T}^2+f_{f\alpha T}^2} \tag{9}$$

5.3.4 螺旋线公差

5.3.4.1 螺旋线倾斜公差$f_{H\beta T}$

按公式(10)计算，此公差应该加上正、负号(±)。

$$f_{\mathrm{H\beta T}}=(0.05\sqrt{d}+0.35\sqrt{b}+4)\sqrt{2}^{A-5} \qquad \cdots\cdots (10)$$

5.3.4.2 螺旋线形状公差 $f_{\mathrm{f\beta T}}$

按公式(11)计算：

$$f_{\mathrm{f\beta T}}=(0.07\sqrt{d}+0.45\sqrt{b}+4)\sqrt{2}^{A-5} \qquad \cdots\cdots (11)$$

5.3.4.3 螺旋线总公差 $F_{\mathrm{\beta T}}$

按公式(12)计算，其中螺旋线倾斜公差 $f_{\mathrm{H\beta T}}$ 和螺旋线形状公差 $f_{\mathrm{f\beta T}}$ 使用未圆整的公差值。

$$F_{\mathrm{\beta T}}=\sqrt{f_{\mathrm{H\beta T}}^{2}+f_{\mathrm{f\beta T}}^{2}} \qquad \cdots\cdots (12)$$

附　录　A
（规范性）
分段公差评价

A.1　概述

本附录阐述了针对两个或两个以上区域采用分段或区域评价的策略。例如，齿轮齿廓可划分为齿顶区域、中部区域和齿根区域。相邻区域分开计算，并且可有不同的公差等级。

A.2　分段齿廓公差评价

回归计算对于确定倾斜和形状偏差是非常必要的。在齿顶和齿根修形的情况下，每个区域可单独评价（见图 A.1）。回归线计算仅针对区域$L_{\alpha a}$、$L_{\alpha m}$和$L_{\alpha f}$，在评价形状和总偏差时，夹在以上区域之间的过渡范围只考虑实体增加材料（凸起）的情况。过渡范围的长度应明确且不能为零（除非该范围是圆滑过渡）。设计齿廓的偏差的归化计算使用最小二乘（高斯）法。多数情况下，使用线性回归。

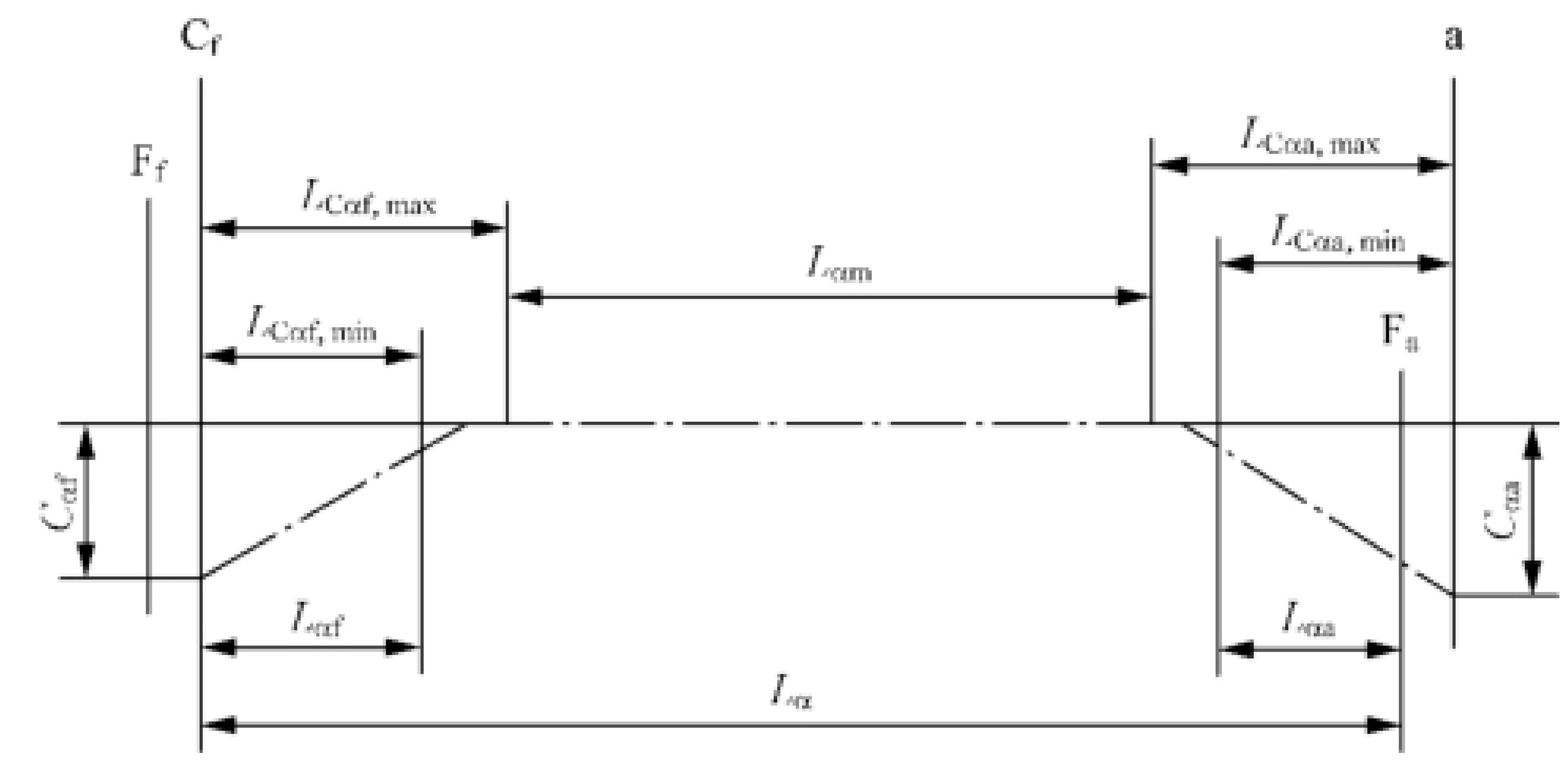

说明：

$C_{\alpha a}$ ——修缘量（齿顶）；
$C_{\alpha f}$ ——修根量（齿根）；
$L_{C\alpha a,\max}$ ——最大修缘长度；
$L_{C\alpha a,\min}$ ——最小修缘长度；
$L_{C\alpha f,\max}$ ——最大修根长度；
$L_{C\alpha f,\min}$ ——最小修根长度；
$L_{\alpha a}$ ——修缘区域；
$L_{\alpha m}$ ——齿廓中部区域；
$L_{\alpha f}$ ——修根区域。

啮合线上的点：
a ——齿顶点；
C_f ——齿廓控制点；
F_a ——齿顶成形点；
F_f ——齿根成形点。

图 A.1　齿顶和齿根修形齿廓的回归区

A.2.1　齿廓倾斜偏差$f_{H\alpha}$

对于齿廓倾斜偏差$f_{H\alpha}$，齿廓中部区域的回归线应延长，包括齿廓控制点到齿顶圆之间的区域［见图 A.2c)］。

A.2.2　齿廓形状偏差$f_{f\alpha}$

齿廓形状偏差$f_{f\alpha}$是在某个区域内包容被测齿廓的回归线的两条平行线之间的距离。对于每个区域，其形状偏差应独立确定。对于修顶以上的区域，实体增加材料（凸起）的情况包含在相邻区域［见图 A.2b)］。

注：回归线平行线与回归线保持平行。

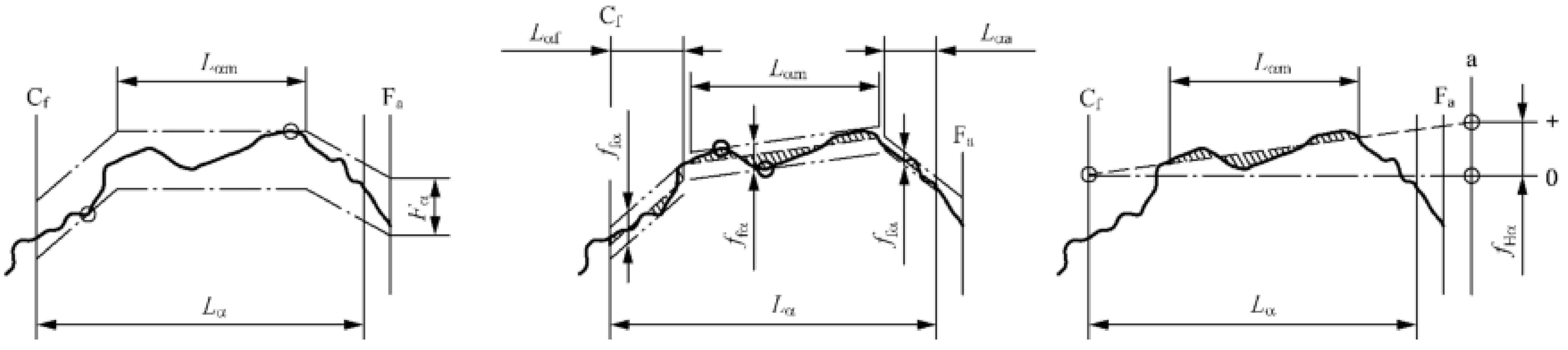

a） 齿廓总偏差　　b） 齿廓形状偏差　　c） 齿廓倾斜偏差

说明：

被测齿廓；　　啮合线上的点：

设计齿廓平行线；　　C_f ——齿廓控制点；

平均齿廓线；　　F_a ——齿顶成形点；

平均齿廓线平行线。　　a ——齿顶点。

图 A.2　齿顶和齿根修形齿廓的分段评价

A.2.3　齿廓总偏差F_α

齿廓总偏差F_α是包容被测齿廓的两条设计齿廓平行线之间的距离[见图 A.2a)]。在接近齿顶的超过齿廓计值范围的区域，实体增加材料（凸起）的情况应加以考虑。

注 1：设计齿廓平行线与设计齿廓保持平行。

注 2：通常的做法是将评价限制在中部区域或完全省略F_α。

A.3　分段螺旋线公差评价

回归计算对于确定倾斜和形状偏差是非常必要的。在齿端修薄的情况下，每个区域可单独评价。在接近端面的位置用Ⅰ和Ⅱ标记（见图 A.3）。

回归线计算仅针对区域$L_{\beta Ⅰ}$、$L_{\beta m}$和$L_{\beta Ⅱ}$，在评价形状和总偏差时，夹在以上区域之间的过渡范围只考虑实体增加材料（凸起）的情况。过渡区域的长度应明确且不能为零（除非该范围是圆滑过渡）。基于设计螺旋线的偏差的回归计算使用最小二乘（高斯）法。在大多数情况下，采用线性回归。

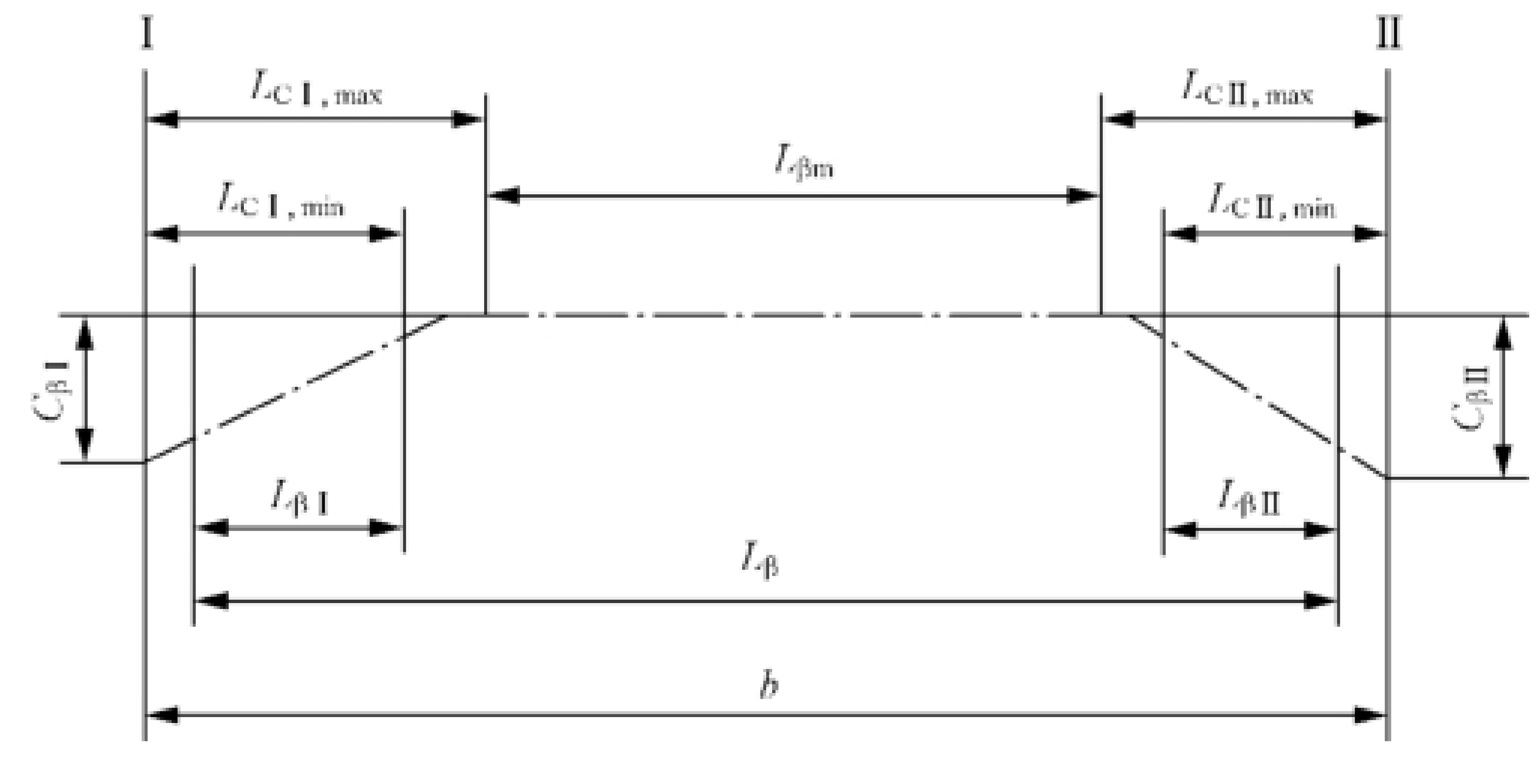

说明：

Ⅰ　——基准面；

Ⅱ　——非基准面；

$C_{\beta Ⅰ}$　——齿端修薄量；

$C_{\beta Ⅱ}$　——齿端修薄量；

$L_{CⅠ,max}$——最大齿端修薄长度；

$L_{CⅠ,min}$——最小齿端修薄长度；

$L_{CⅡ,max}$——最大齿端修薄长度；

$L_{CⅡ,min}$——最小齿端修薄长度；

$L_{\beta Ⅰ}$　——齿端修薄区域；

$L_{\beta m}$　——螺旋线中部区域；

$L_{\beta Ⅱ}$　——齿端修薄区域。

图 A.3　两端齿端修薄的螺旋线的回归区

A.3.1 螺旋线倾斜偏差 $f_{H\beta}$

对于螺旋线倾斜偏差 $f_{H\beta}$，中部区域的回归线应扩展到整个齿宽 b[见图 A.4 c)]所示。

A.3.2 螺旋线形状偏差 $f_{f\beta}$

螺旋线形状偏差 $f_{f\beta}$ 是在区域内包容被测螺旋线的回归线的两条平行线之间的距离。对于每个分段区域，其形状偏差应独立确定[见图 A.4b)]。对于以上区域之间的过渡范围和端部，在分析时任何实体增加材料(凸起)的情况应给予考虑。

注：回归线平行线与回归线保持平行。

A.3.3 螺旋线总偏差 F_β

螺旋线总偏差 F_β 是包容被测螺旋线的两条设计螺旋线平行线之间的距离[见图 A.4a)]所示。齿端超出计值范围 L_β 的部分，实体增加材料(凸起)的情况应给予考虑。

注 1：设计螺旋线平行线与设计螺旋线保持平行。

注 2：通常的做法是将评价限制在中部区域或完全省略 F_β。

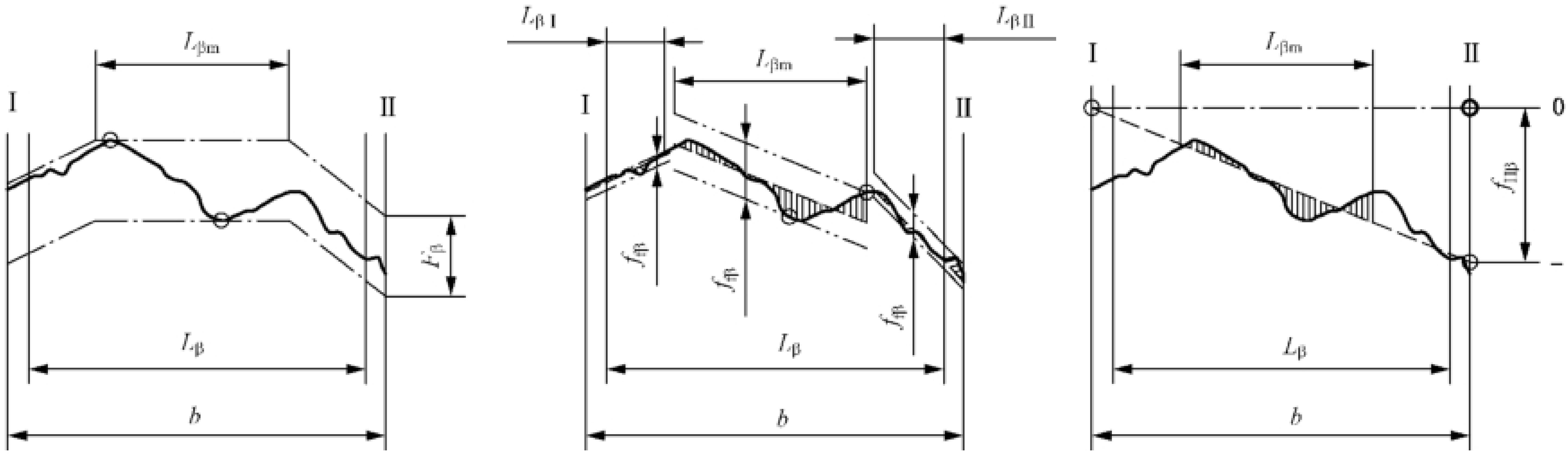

说明：

- ———— 被测螺旋线；
- —·—·— 设计螺旋线平行线；
- - - - - 平均螺旋线；
- —··—··— 平均螺旋线平行线；
- $L_{\beta I}$ ——齿端修薄区域；
- $L_{\beta II}$ ——齿端修薄区域；
- $L_{\beta m}$ ——螺旋线中部区域。

图 A.4 齿端修形螺旋线的分段评价

附 录 B
（规范性）
采用二阶分析法评价齿廓和螺旋线偏差

B.1 目的

本附录适用于齿廓鼓形修形（有时称为“桶形”）或螺旋线鼓形修形的齿轮，或两种修形均有的齿轮。采用二阶最优拟合法处理相对于未修形齿廓或未修形螺旋线的偏差。第5章中的标准齿面公差等级可使用该分析方法。

注：对第3章和第4章中设计齿廓和设计螺旋线偏差使用线性分析方法，而不是使用二阶拟合。线性分析的结果被称为平均齿廓线（或平均螺旋线），即使它与设计齿廓（或螺旋线）具有相同的形状（可能为曲线）。本附录给出的二阶分析结果始终称为曲线。

B.2 二阶齿廓分析

在某些应用情况下，齿廓鼓形修形是一种常用且有效的齿廓修形方法。通常用单一抛物线定义（见图B.1）。抛物线在齿廓计值长度L_α内计算，但评价$f_{H\alpha}$和C_α时，对于不分段评价，抛物线延伸到齿顶圆，对于分段评价，抛物线延伸到分段的终点处。

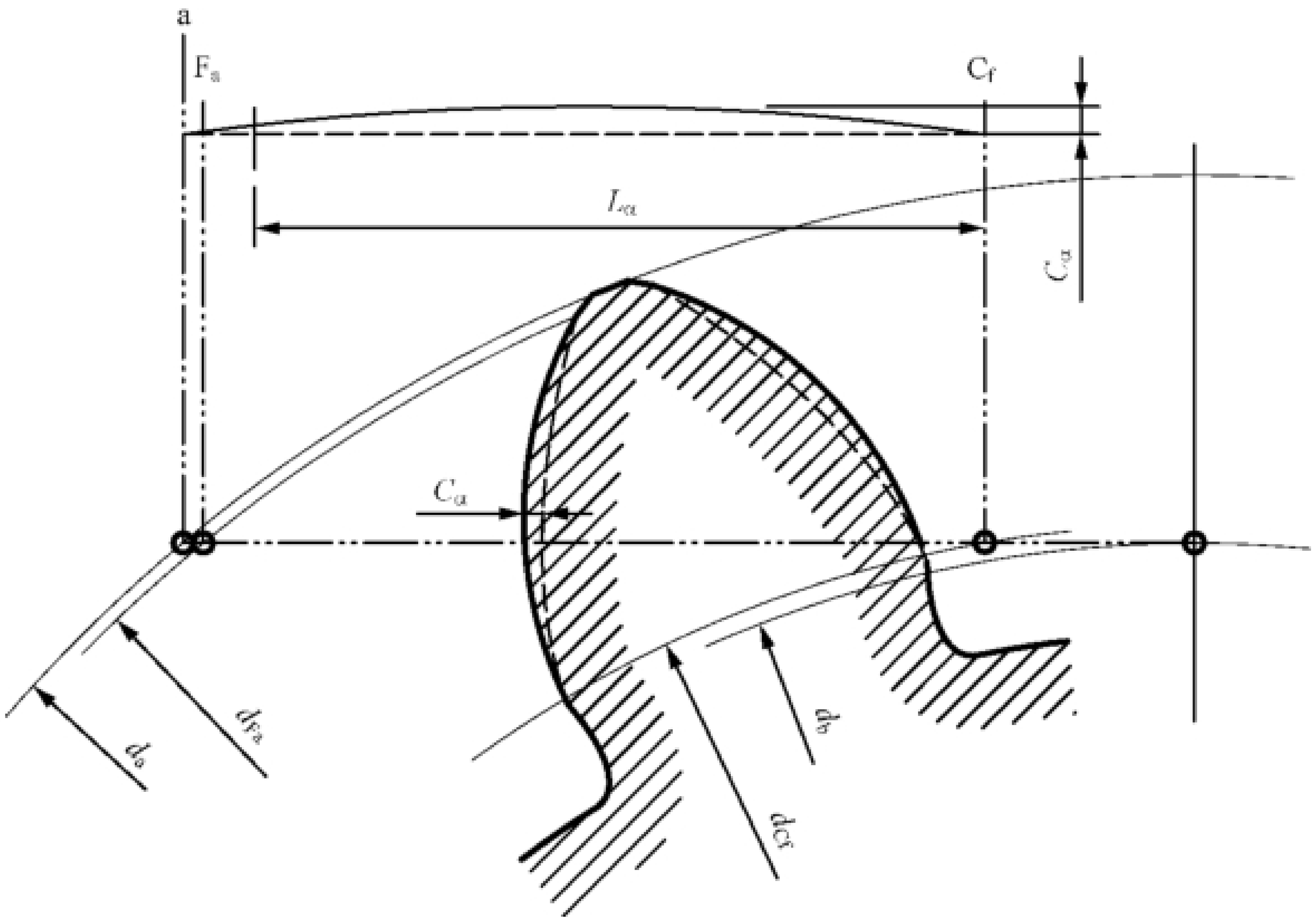

说明：

－－－－－－－ 渐开线；

———— 鼓形齿廓。

图 B.1 齿廓鼓形修形

B.2.1 平均二阶齿廓曲线

平均二阶齿廓曲线是由数学拟合二阶曲线获得的被测齿廓迹线，是在齿廓计值长度L_α内，使用最小二乘法得到的。

注：该曲线是确定$f_{f\alpha}$、$f_{H\alpha}$和C_α的基础。

B.2.2 齿廓形状偏差$f_{f\alpha}$

齿廓形状偏差$f_{f\alpha}$是在齿廓计值长度L_{α}[见3.4.1.4和图B.2 a)]内包容被测齿廓的两条平均二阶齿廓曲线平行线之间的距离，两条平行线与平均二阶齿廓曲线保持恒定的距离。实体材料增加(凸起)的情况见4.4.8.2。

B.2.3 齿廓倾斜偏差$f_{H\alpha}$

齿廓倾斜偏差$f_{H\alpha}$是平均二阶齿廓曲线延长线与齿顶圆的交点相对于该曲线与齿廓控制圆的交点的纵向距离[见图B.2 b)]。

二阶法确定的齿廓倾斜偏差$f_{H\alpha}$的代数符号所遵从的规则与4.4.8.2相同。

如果存在设计齿廓倾斜偏差$C_{H\alpha}$，根据公式(B.1)采用最初计算的$f_{H\alpha C}$来确定齿廓倾斜偏差：

$$f_{H\alpha}=f_{H\alpha C}-C_{H\alpha} \qquad \text{(B.1)}$$

B.2.4 齿廓鼓形C_{α}

齿廓鼓形C_{α}是两条平行直线在记录偏差的方向上的距离，一条是平均二阶齿廓曲线延长线与齿廓控制圆和齿顶圆的交点的连线构成的弦，另一条是与弦平行并与平均二阶齿廓曲线相切的直线[见图B.2c)]。

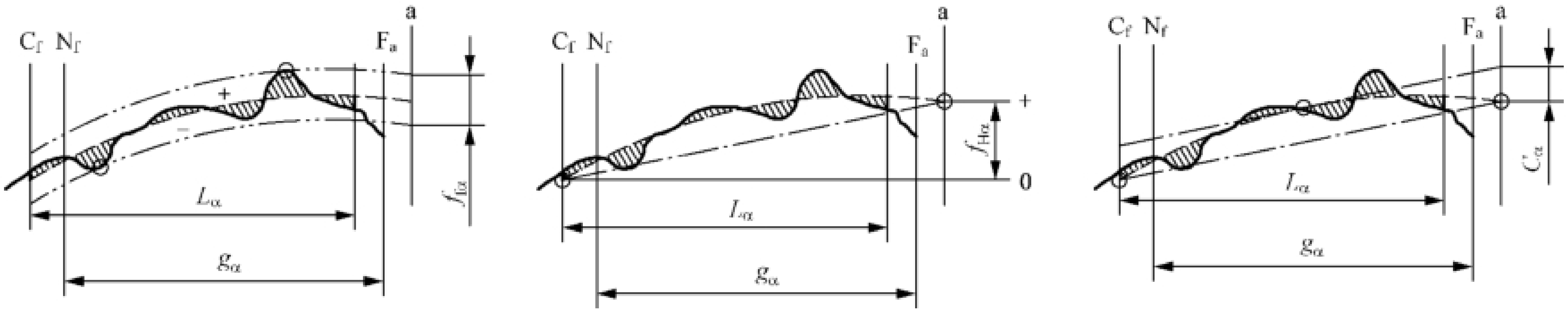

a) 齿廓形状偏差　　b) 齿廓倾斜偏差　　c) 齿廓鼓形

说明：

——————— 被测齿廓；

— — — — — — 平均二阶齿廓曲线；

—··—··— 平均二阶齿廓曲线平行线；

—·—·—·— 平均二阶齿廓曲线的弦。

啮合线上的点：

C_f——齿廓控制点；

N_f——有效齿根点；

F_a——齿顶成形点；

a——齿顶点。

图B.2 二阶齿廓偏差

B.3 二阶螺旋线分析

与齿廓鼓形修形类似，鼓形修形也是一种常用的修形方式。鼓形修形通常用单一抛物线定义，抛物线增加了螺旋线的曲率并且其最高点在螺旋线计值长度L_{β}的中部。抛物线在L_{β}内计算，但评价$f_{H\beta}$和C_{β}时，对于不分段评价，抛物线扩展到整个齿宽b，对于分段评价，抛物线延伸到分段的终点处。

B.3.1 平均二阶螺旋线曲线

平均二阶螺旋线曲线是由数学拟合二阶曲线获得的被测螺旋线迹线，是在螺旋线计值长度L_{β}内，使用最小二乘法得到的。

注：该曲线是确定$f_{f\beta}$、$f_{H\beta}$和C_{β}的基础。

B.3.2 螺旋线形状偏差$f_{f\beta}$

螺旋线形状偏差$f_{f\beta}$是在螺旋线计值长度L_β[见图 B.3 a)]内包容被测螺旋线迹线的两条平均二阶螺旋线曲线平行线之间的距离，两条平行线与平均二阶螺旋线曲线保持恒定的距离。实体材料增加(凸起)的情况见 4.4.8.4。

B.3.3 螺旋线倾斜偏差$f_{H\beta}$

螺旋线倾斜偏差$f_{H\beta}$是一条线的位移，该线通过平均二阶螺旋线曲线延长线分别与齿轮两端面的交点[见图 B.3 b)]。

二阶法确定的螺旋线倾斜偏差$f_{H\beta}$的代数符号所遵从的规则与 4.4.8.4 相同。

如果存在设计螺旋线倾斜偏差$C_{H\beta}$，根据公式(B.2)采用最初计算的$f_{H\beta C}$来确定螺旋线倾斜偏差$f_{H\beta}$：

$$f_{H\beta}=f_{H\beta C}-C_{H\beta} \qquad \text{(B.2)}$$

B.3.4 螺旋线鼓形C_β

螺旋线鼓形C_β是两条平行直线在记录偏差的方向上的距离，一条是平均二阶螺旋线曲线延长线与齿轮两端面的交点的连线构成的弦，另一条是与弦平行并与平均二阶螺旋线曲线相切的直线[见图 B.3c)]。

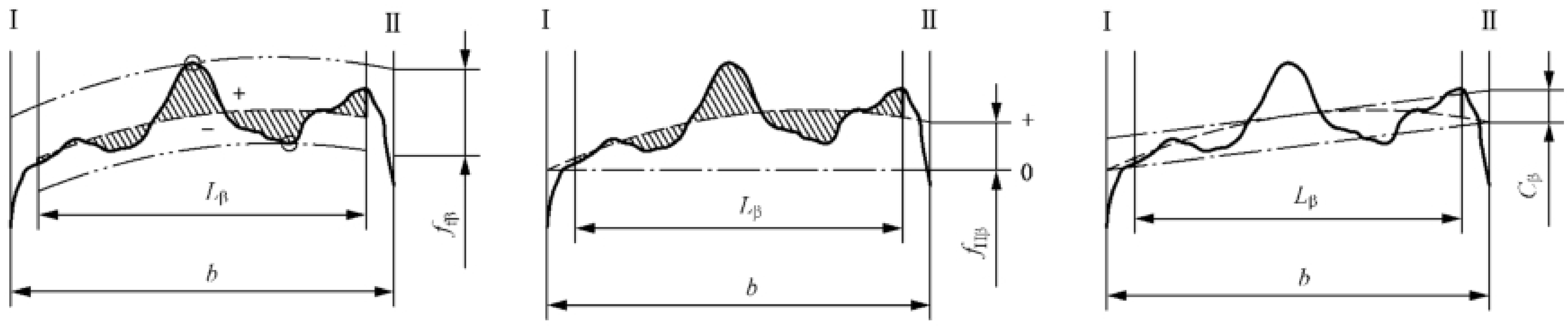

a) 螺旋线形状偏差　　b) 螺旋线倾斜偏差　　c) 螺旋线鼓形

说明：

被测螺旋线；

平均二阶螺旋线曲线；

平均二阶螺旋线曲线平行线；

平均二阶螺旋线曲线的弦。

图 B.3 二阶螺旋线偏差

附　录　C
（资料性）
齿廓和螺旋线数据滤波

C.1　目的

在进行数据分析前,首先对齿廓和螺旋线的测量数据进行低通滤波。所选的滤波方法和截止波长将影响分析结果。本附录提供滤波规程的说明。

C.2　滤波

测量数据包含许多不同波长或频率的成分。滤除测量数据特定成分的频谱称为滤波。滤除较短波长(较高频率)数据的滤波器称为低通滤波器。滤除较长波长(较低频率)数据的滤波器称为高通滤波器。滤除较短波长和较长波长(较高和较低频率),只留下中等波长(中等频率)数据的滤波器称为带通滤波器。在齿轮测量中一般采用低通滤波器,将齿廓和螺旋线总偏差、形状偏差和倾斜偏差的测量数据中的高频表面粗糙度的影响去除。齿轮测量系统中通常存在几种类型的低通滤波。

C.3　机械滤波

机械滤波限制了齿廓和螺旋线测量数据,使其集中在波长较长的波段内,是一个低通滤波器。机械滤波是通过测头几何形状(如测头半径)的桥接作用产生的,因此可抑制较短的波长成分。机械低通滤波另一个相关因素是测头系统的运动部件的惯性质量。

如果要求测量数据包含高频信息,可使用半径较小的测头。因为通常要对齿廓和螺旋线数据进行有目的的低通滤波,故高频信息很少被关注。评价齿面粗糙度最好使用专门的表面粗糙度仪器,而不是使用齿廓和螺旋线测量仪。

C.4　电子滤波

电子滤波限制了测量数据,使其集中在波长较长(频率较低)的波段内,是一个低通滤波器。在电子滤波中,来自测头的数据信号通过电子滤波(RC)电路后,传输到数据分析设备和输出设备。

齿廓和螺旋线测量数据的电子滤波的电路设计目的,是完全消除指定波长(称为截止波长)的高频测量数据。明显高于截止波长的所有频率被消除。接近但不等于截止波长的高频测量数据,根据截止频率与截止波长的接近程度,按比例滤除。

RC 电子滤波有一个副作用,即产生数据的相移,影响测量结果的分析。

旧仪器常用电子滤波,新型仪器已使用数字滤波。电子滤波有局限性,但可以接受。

C.5　数字滤波

数字滤波要求测量数据首先用计算机将模拟信号转为数字信号以便处理。目前有很多种数字滤波器可使用,常见的一种可模拟电子滤波器(包含或不包含 RC 电路的相移特性),另一种采用高斯数字滤波。

相位修正高斯滤波器的传输特性是,当波长等于长波段截止波长时,正弦波振幅的 50%将允许通过。其他频率可通过的数量与它们接近阈值的程度有关。当使用相位修正高斯滤波器时,将减少数据的不规则,并且消除相移。

符合 ISO 标准规定且基于正弦波的振幅传输,使用数字高斯 50%类型滤波器(见 4.4.6)。

数字滤波还有一个优点,即可看到使用不同数字滤波器的测量数据或不使用数字滤波器的测量数据。

C.6 截止波长的选择

标准齿廓和螺旋线数据截止波长的选择应遵照4.4.6。

附 录 D
（资料性）
齿距累积偏差

D.1 目的

本附录提供齿距累积偏差的定义、测量规程、推荐公差和应用指南。

D.2 齿距累积偏差F_{pk}、$F_{pz/8}$

齿距累积偏差F_{pk}是针对指定齿侧面在所有跨k个齿距的扇形区域内，任一齿距累积偏差值（分度偏差）F_{pi}的最大代数差。在特定情况下，k取齿数的八分之一，记为$F_{pz/8}$。

注1：除非另有规定，k不大于齿数的八分之一。对于扇形齿轮，齿数z是完整齿轮的齿数，而不是扇形齿轮的齿数。

注2：当指定了跨测齿数时，这个数显示在符号k的位置。例如，如果是跨4齿的扇形区域，符号记为F_{p4}。

注3：当使用$F_{pz/8}$时，k的计算见公式(D.1)。

$$k \approx \frac{z}{8} \qquad \text{(D.1)}$$

式中：

k ——扇形区域内的齿距数，圆整到最接近的整数；

z ——齿轮的齿数。

k的最小可用值为2。$F_{pz/8}$仅用于齿数大于或等于12的齿轮。

该偏差值有正负的区别。当构成齿距累积偏差F_{pk}的两个轮齿之间的距离小于理论距离时，齿距累积偏差F_{pk}定义为负值；反之为正值。

齿距累积偏差的测量方向是在端平面内沿测量圆d_M的圆弧方向。

D.3 测量规程

通过齿距比较仪（双测头）或分度仪（单测头）收集的轮齿位置数据可用于确定齿距累积偏差。在这两种情况下，先得到任一齿距累积偏差（分度偏差）。

为确定齿距累积偏差F_{pk}，需要先得到每一组k个齿距（$k+1$个相邻轮齿）里任一齿距累积偏差（分度偏差）的最大值和最小值的代数差，如D.2的定义。然后，这些代数差的最大值即为齿距累积偏差F_{pk}。k个齿距的组数和齿轮齿数相同。

D.4 相似参数的对比

理解参数F_{pk}与其他相似参数的不同很重要。例如，齿距跨度偏差F_{pSk}等于k个齿距扇形区域内第一个和最后一个任一齿距累积偏差（分度偏差）的代数差。

以上两种情况均针对k个齿距的扇形区域。对于F_{pk}，针对于跨齿数为k的z个扇形区域，并确定每个扇形区域中所有数值的最大读数减最小读数。

对于F_{pSk}，扇形区域的数目等于z/k的最接近的整数。对于每一个扇形区域，仅第一个和最后一个数值用于相减。

注：F_{pSk}的公差未包含在本文件中。

图D.1给出了区别两种分析方法的实例。图示为齿数35齿的任一齿距累积偏差，对于$F_{pz/8}$而言，k值等于4。在本例中，扇形区域包含4个齿距，齿距累积偏差$F_{pz/8}$的值是4.7，发生在18齿和20齿之间。齿距跨度偏差F_{pS4}的值是4.1，发生在18齿和22齿之间，有4个齿距的间隔。在本例中，$F_{pz/8}$和F_{pS4}出

现在相同的扇形区域,这种情况并不是总会出现。

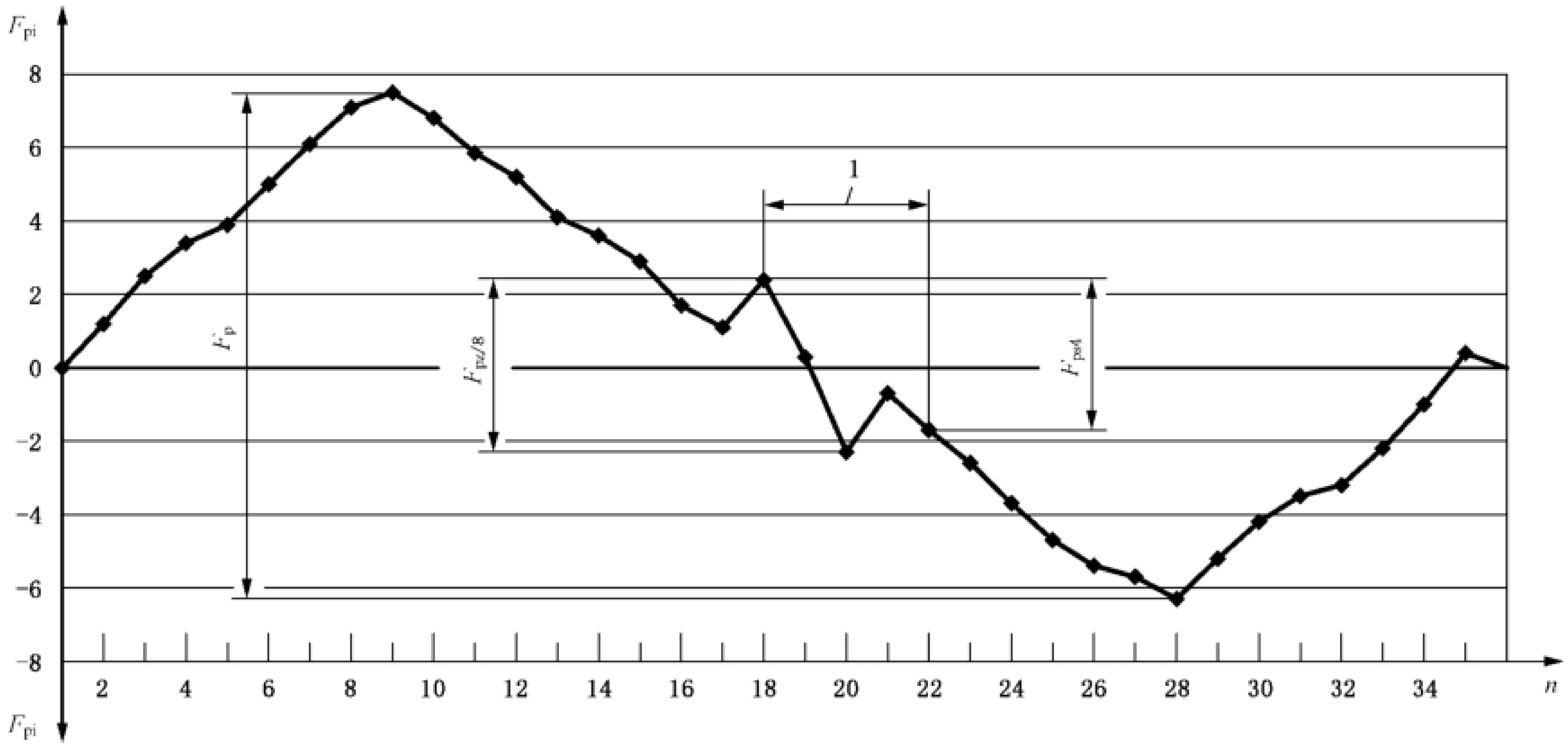

说明:

1 ——最大轮齿偏差所在的4齿距扇形区域;

n ——齿距编号;

F_p ——齿距累积总偏差;

$F_{pz/8}$ ——齿距累积偏差($z/8\approx4$);

F_{pS4} ——4齿的齿距跨度偏差。

图 D.1 扇形区域齿距累积偏差和齿距跨度偏差

D.5 齿距累积公差F_{pkT}

推荐的齿距累积公差用公式(D.2)计算:

$$F_{pkT}=f_{pT}+\frac{4k}{z}(0.001d+0.55\sqrt{d}+0.3m_n+7)\sqrt{2}^{A-5} \quad \cdots\cdots(D.2)$$

式中:

F_{pkT}——齿距累积公差;

f_{pT} ——公差等级为A的单个齿距公差。

齿距累积公差的推荐使用范围与齿距累积总公差F_{pT}一致。

对于$F_{pz/8}$的特殊情况,公式(D.2)可简化为公式(D.3):

$$F_{pz/8T}=\frac{f_{pT}+F_{pT}}{2} \quad \cdots\cdots(D.3)$$

D.6 应用指南

齿距累积偏差的测量不是强制性的,除非另有规定。因此,本附录有关的数据信息未列于正文中。

当供需双方协商一致时,可使用本附录。如果在较少的齿距数上的任一齿距累积偏差过大时,在齿轮实际工作中将产生很大的惯性力,尤其是高速齿轮,动载荷可能相当大。

附 录 E
（规范性）
径向跳动的允许值

E.1 目的

本附录提供径向跳动的公差公式和应用范围。

E.2 任一径向测量距离r_i

r_i为测头（球形、圆柱形或砧形）相继置于每个齿槽内时，齿轮轴线到测头的中心或其他指定位置的径向距离。测量中，测头在近似齿高中部与左右齿面接触。径向跳动也可由齿距测量中获得的点确定（见 E.5 和图 E.2）。

注 1：r_i 的个数与齿槽数相同。

注 2：实际测量的结果与用齿距测量计算的结果有细微的不同。

当指定量球直径进行径向跳动测量时，如果使用齿距的测量数据来计算径向跳动，则齿距测量应在测量球的接触圆上进行，否则应在测量圆上进行。

E.3 径向跳动F_r

齿轮的径向跳动值为任一径向测量距离r_i最大值与最小值的差。图 E.1 给出了径向跳动的示例，图中的偏心量是径向跳动的一部分（见 ISO/TR 10064-2）。

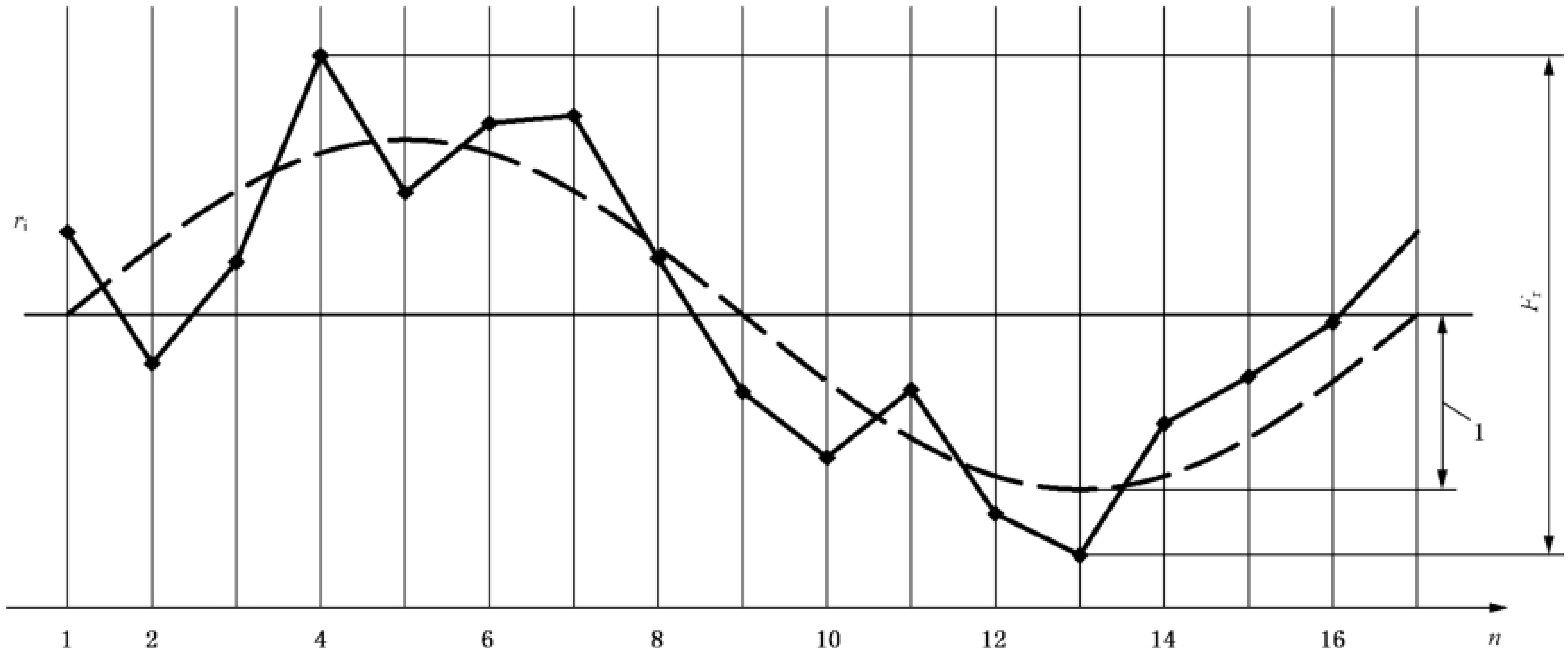

说明：

1 ——偏心量；

n ——齿槽编号。

图 E.1 有 16 个齿齿轮的径向跳动

E.4 径向跳动公差F_{rT}

按公式(E.1)计算：

$$F_{rT}=0.9F_{pT}=0.9(0.002d+0.55\sqrt{d}+0.7m_n+12)\sqrt{2}^{A-5} \quad \cdots\cdots\cdots\cdots\cdots(\text{E.1})$$

应用范围如下：

——公差等级从 1 级到 11 级；

——$5 \leqslant z \leqslant 1\ 000$；

——$5\ \text{mm} \leqslant d \leqslant 15\ 000\ \text{mm}$；

——$0.5\ \text{mm} \leqslant m_{\text{n}} \leqslant 70\ \text{mm}$。

E.5 由齿距测量计算径向跳动

通过测量圆上的测量数据，可知道左右齿面的位置。在端平面内，在齿槽中可构建出两条渐开线，这两条渐开线与对应齿面上被测点间的距离等于量球半径除以基圆螺旋角的余弦。该距离沿基圆切线方向。每个齿槽中构建的两条渐开线的交点给出了径向测量中量球中心的近似径向位置。由于接触位置不同和存在表面误差，由此获得的结果可能与实际使用量球与两齿面接触的测量结果有细微的差距。图 E.2 给出了一个直齿轮的简化示例。

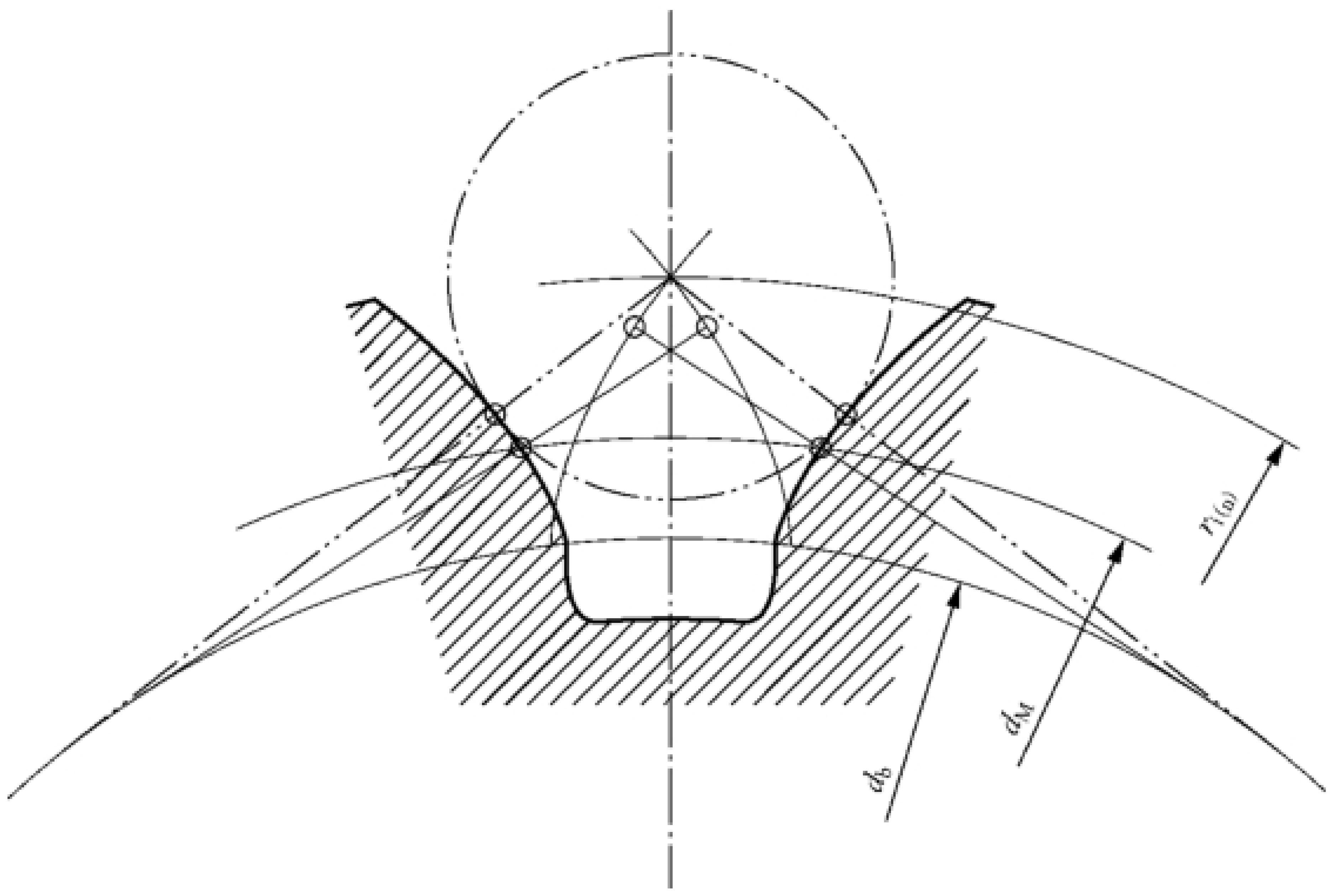

图 E.2 由齿距测量计算径向跳动

E.6 应用指南

径向跳动的测量不是强制性的，除非另有规定。因此，本附录有关的参数信息未列于正文中。当供需双方协商一致时，可使用本附录。

附 录 F
（资料性）
单面啮合综合测量

F.1 目的

F.1.1 概述

本附录讨论齿轮传动误差(偏差)，给出了一齿切向综合偏差的设计值$f_{is(design)}$的公差值。传动误差是从动齿轮的角度位置偏差。对于主动齿轮给定的角度位置，从动齿轮实际位置与理论位置的角度偏差(理论位置是具有完美几何尺寸的齿轮副工作时从动齿轮的位置)。

单面啮合综合测量是测量齿轮传动误差的一种方法。通常是一对产品齿轮在仪器上进行检测，有时也用产品齿轮和测量齿轮配对，来测量单个产品齿轮对传动误差的影响。这些检测一般在轻负载下进行，以避免检测仪器的变形对测量结果产生影响。当要求加载检测时，宜在实际的齿轮箱或刚性好的测试台上进行，但此种情况本附录不做讨论。

单面啮合综合测量中，齿轮需要在给定的中心距上啮合，并确保单侧齿面接触。齿轮副宜有侧隙。因为齿轮单面啮合检测模拟了齿轮的使用状况，其检测结果可用于控制齿轮的使用性能，也可检查划伤、毛刺等缺陷。

单面啮合综合测量给出了空载下的总传动误差和一齿传动误差。一齿传动误差反映齿轮运动平稳性，可用于控制噪声和振动。当考虑空载下的总传动误差的公差时，齿距累积误差是主要的影响因素。当分析一齿传动误差时，啮合轮齿的共轭性(渐开线形状的匹配情况)是主要的影响因素。

当为空载下的一齿传动误差确定公差时，有两组齿轮类型：无修形齿轮和修形齿轮。

F.1.2 无修形齿轮

无修形齿轮应用于很多非常轻载的场合，如家用电器、手持电动工具、汽车配件驱动器等。对于轻载情况，共轭轮齿数越多，运转更平稳，噪声和振动会更小。因此，相对于修形齿轮的检测结果，任何小于公差的检测结果均是可接受的。

F.1.3 修形齿轮

修形齿轮(齿廓鼓形、修缘和齿廓倾斜等)会出现相对较大的一齿传动误差。这是因为检测时采用轻载，而轮齿被设计为在特定的重载环境下才共轭，因此，在轻载检测下齿廓不共轭。一齿传动误差远小于预期的情况并不好。在修形的情况下，宜给出最大公差和最小公差。

有两种可选的方法来确定最大公差和最小公差。

a) 基于实际应用经验。

b) 通过使用轮齿接触分析软件确定齿轮修形，并预测传动误差曲线。这些程序能分析载荷作用下的轮齿形状，并考虑了箱体和轴的变形；能预测不同载荷下的一齿传动误差，其中也能预测轻载下类似单面啮合检测获得的传动误差。

F.1.4 方法 A

设计和制造使用的平均一齿切向综合偏差值及其变化值应通过工作经验或承载能力测试得到，或使用两种方法共同确定所需要的值。这些值和精度等级无关。

F.1.5　方法 B

切向综合偏差的短周期成分(高通滤波)的峰-峰值振幅用来确定一齿切向综合偏差。最大峰-峰值振幅应不大于$f_{isT,max}$,且最小峰-峰值振幅应不小于$f_{isT,min}$。峰-峰值振幅是齿轮副测量的运动曲线中一个齿距内的最高点和最低点的差。

齿轮副的一齿切向综合公差f_{isT}的最大值和最小值的计算见公式(F.1)和公式(F.2),或见公式(F.1)和公式(F.3),单位为微米(μm)。

$$f_{isT,max}=f_{is(design)}+(0.375m_n+5.0)\sqrt{2}^{A-5} \quad \cdots\cdots(F.1)$$

$f_{isT,min}$是公式(F.2)和公式(F.3)计算值的较大值:

$$f_{isT,min}=f_{is(design)}-(0.375m_n+5.0)\sqrt{2}^{A-5} \quad \cdots\cdots(F.2)$$

或

$$f_{isT,min}=0 \quad \cdots\cdots(F.3)$$

f_{isT}的应用范围如下:

——公差等级从 1 级到 11 级;

——1.0 mm≤m_n≤50 mm;

——5≤z≤ 400;

——5 mm≤d≤ 2 500 mm。

如果测量仪器读数以弧度为单位,使用公式(F.4)在分度圆 d 处换算成微米。

$$f_{isT}(\mu rad)=2\ 000\times f_{isT}(\mu m)/d(mm) \quad \cdots\cdots(F.4)$$

公式(F.1)和公式(F.2)中用到的一齿切向综合偏差的设计值$f_{is(design)}$,应通过分析应用设计和检测条件来确定。选择设计值应考虑实际影响,例如,安装误差、轮齿形状误差和工作载荷等。更多信息见F.2。

F.1.6　切向综合总公差F_{isT}

按公式(F.5)计算:

$$F_{isT}=F_{pT}+f_{isT,max} \quad \cdots\cdots(F.5)$$

F_{isT}的应用范围如下:

——公差等级从 1 级到 11 级;

——1.0 mm≤m_n≤50 mm;

——5≤z≤400;

——5 mm≤d≤2 500 mm。

F.2　测量仪器的结构和获得的数据

图 F.1 给出单面啮合测量仪的示意图。转角θ_1和转角θ_2由角度传感器(如置于小齿轮和大齿轮轴上的编码器)测得。齿轮副的传动误差θ_e用公式(F.6)计算:

$$\theta_e=\theta_2-\left(\frac{z_1}{z_2}\right)\theta_1 \quad \cdots\cdots(F.6)$$

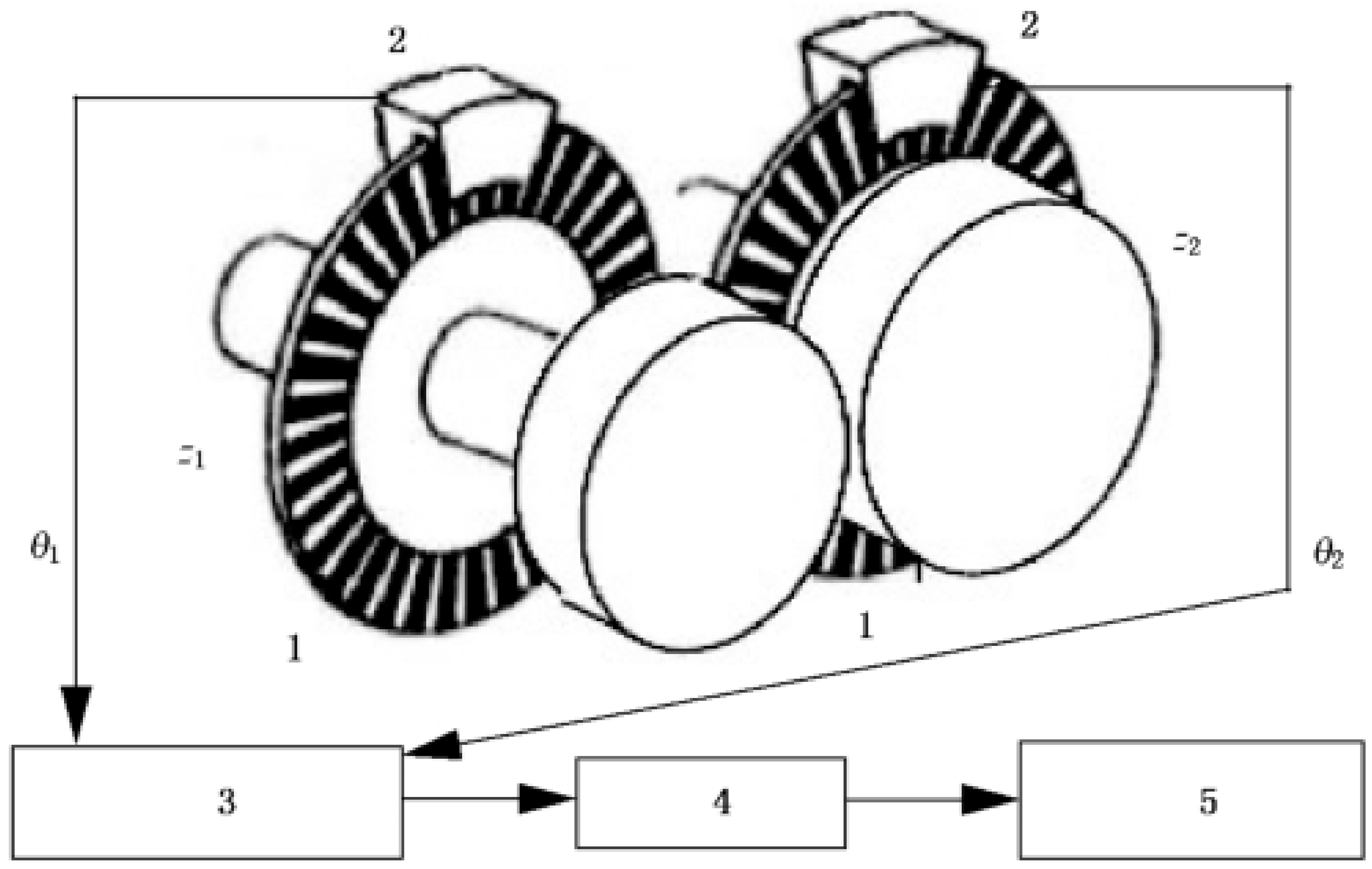

标引序号说明：

1——旋转编码器；

2——读数装置；

3——传动误差计算；

4——滤波器；

5——傅里叶变换。

图 F.1　单面啮合测量仪示意图

推荐的评价单面啮合参数的最少测量点数是每齿 30 个点，并对数据进行滤波和傅里叶变换。图 F.2 是传动波形的示例，显示了由小齿轮和大齿轮的偏差累积造成的复杂波形。

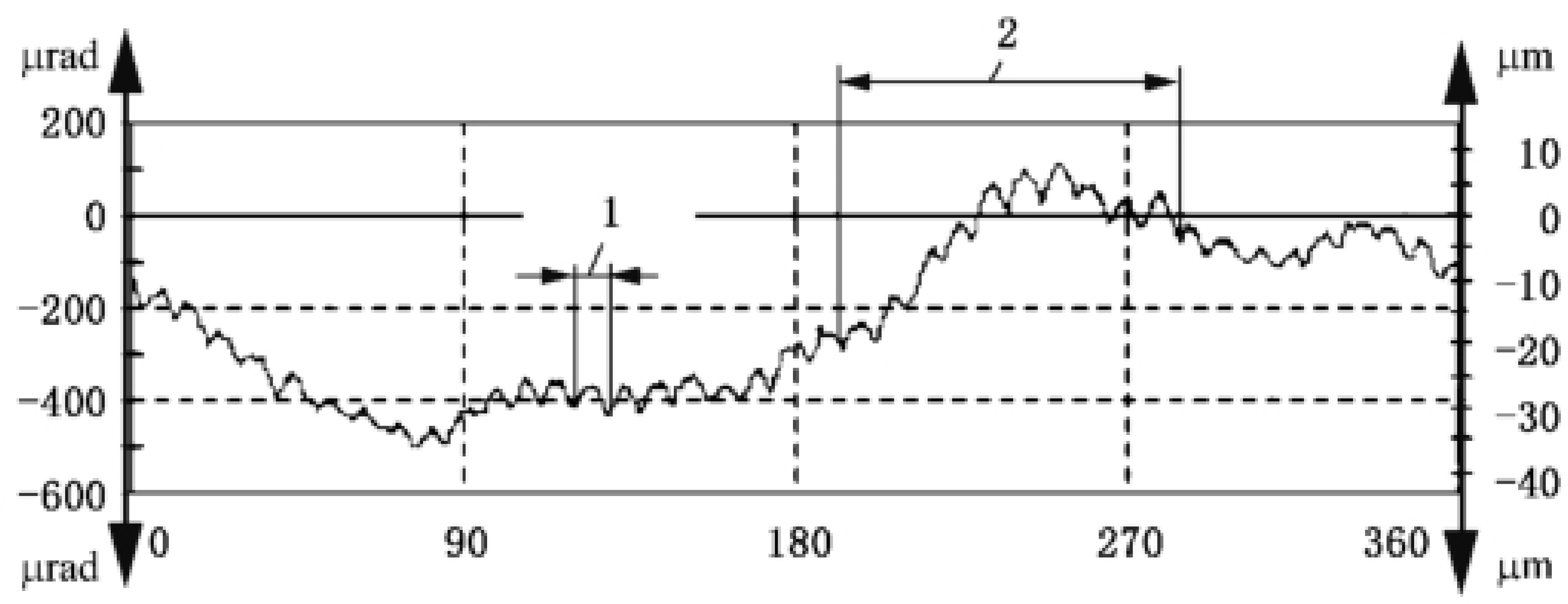

标引序号说明：

1——轮齿齿距；

2——小齿轮旋转一周。

图 F.2　传动误差示例

一个齿距内的小波形是由轮齿形状偏差造成的。图 F.3 显示了一个齿距内与轮齿形状偏差变化量相对应的高通滤波波形。此外，图中显示了一齿切向综合偏差的最小值 $f_{is,min}$ 和最大值 $f_{is,max}$。图 F.4 显示傅里叶变换后的偏差。在啮合频率和二阶啮合频率上可看到波峰。

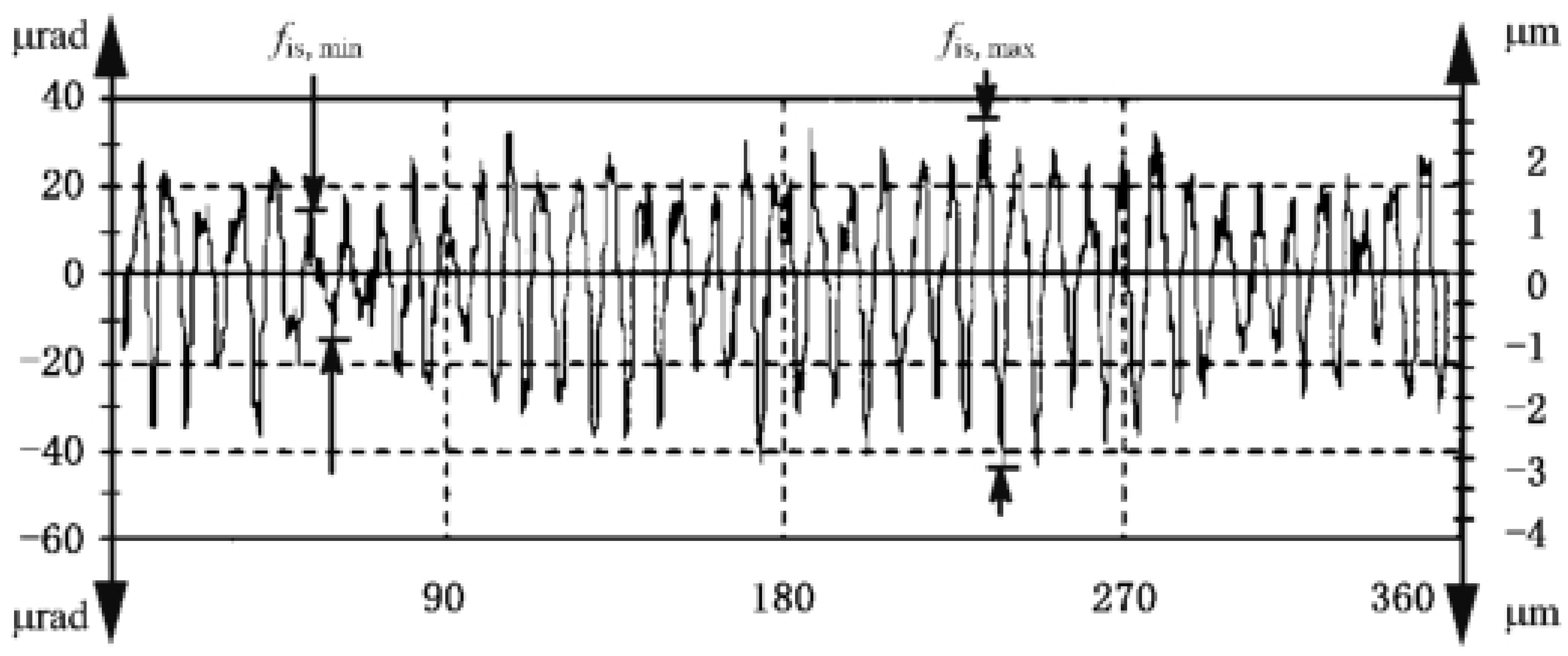

图 F.3　高通滤波后的单面啮合综合偏差

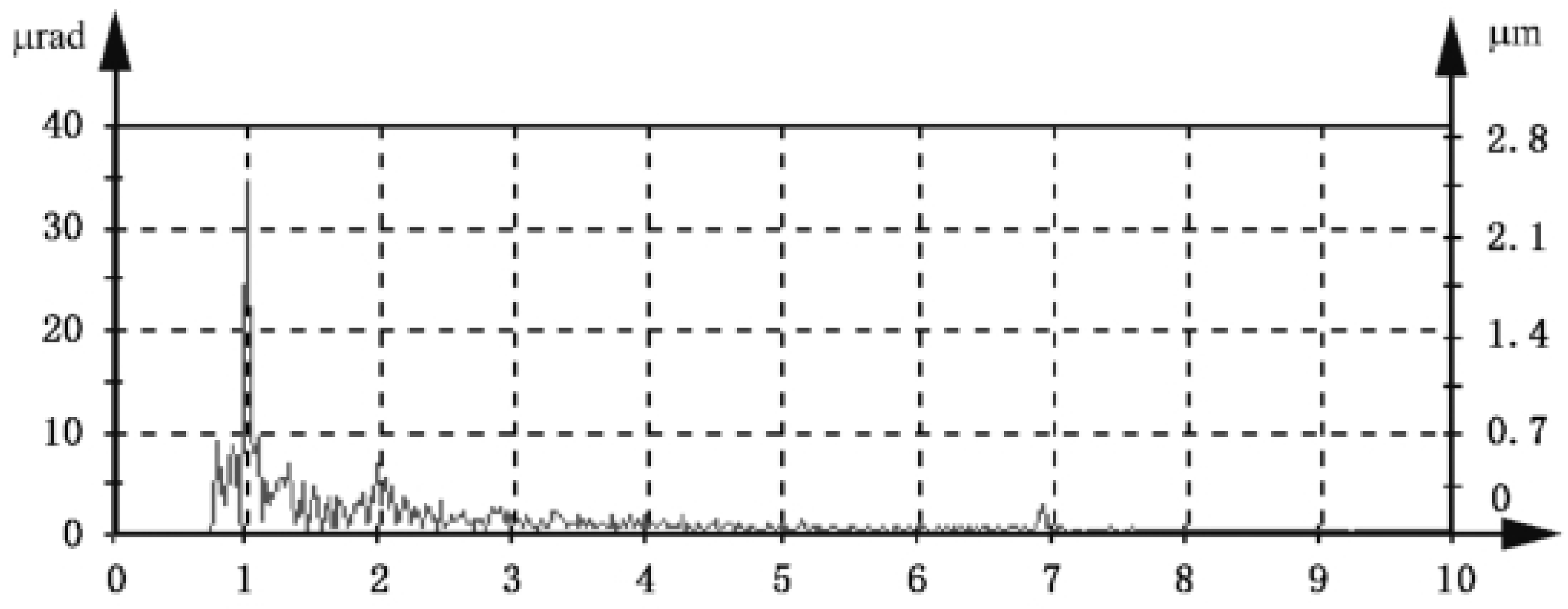

a） 啮合频率的阶次-线性幅值

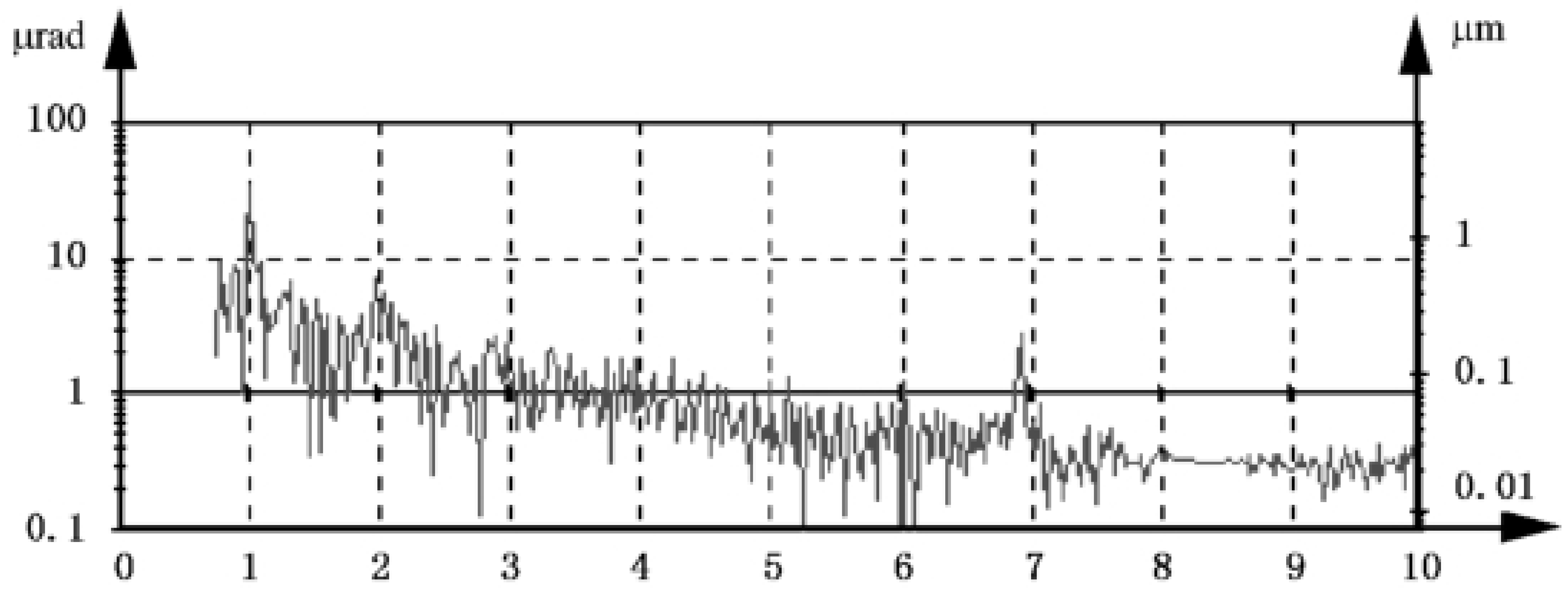

b） 啮合频率的阶次-对数幅值

图 F.4 傅里叶变换后的单面啮合综合偏差

附 录 G
（资料性）
相邻齿距差 f_u

G.1 相邻齿距差定义

G.1.1 任一相邻齿距差 f_{ui}

任一相邻齿距差 f_{ui}（无代数符号）是左侧齿面或右侧齿面两个相邻任一单个齿距偏差实测值的差。它等于两个相邻齿距的任一单个齿距偏差的差（见图 G.1）。

$$f_{ui(n)} = \left| f_{pi(n)} - f_{pi(n-1)} \right| \qquad \cdots\cdots\cdots\cdots\cdots\cdots\cdots\cdots\cdots (G.1)$$

G.1.2 相邻齿距差 f_u

相邻齿距差 f_u是所有任一相邻齿距差 f_{ui}的最大值。

G.2 公差值

相邻齿距差的公差 f_{uT}的计算见公式(G.2)：

$$f_{uT} = \sqrt{2} f_{pT} \qquad \cdots\cdots\cdots\cdots\cdots\cdots\cdots\cdots\cdots (G.2)$$

G.3 应用指南

使用相邻齿距差需经供需双方协商一致。

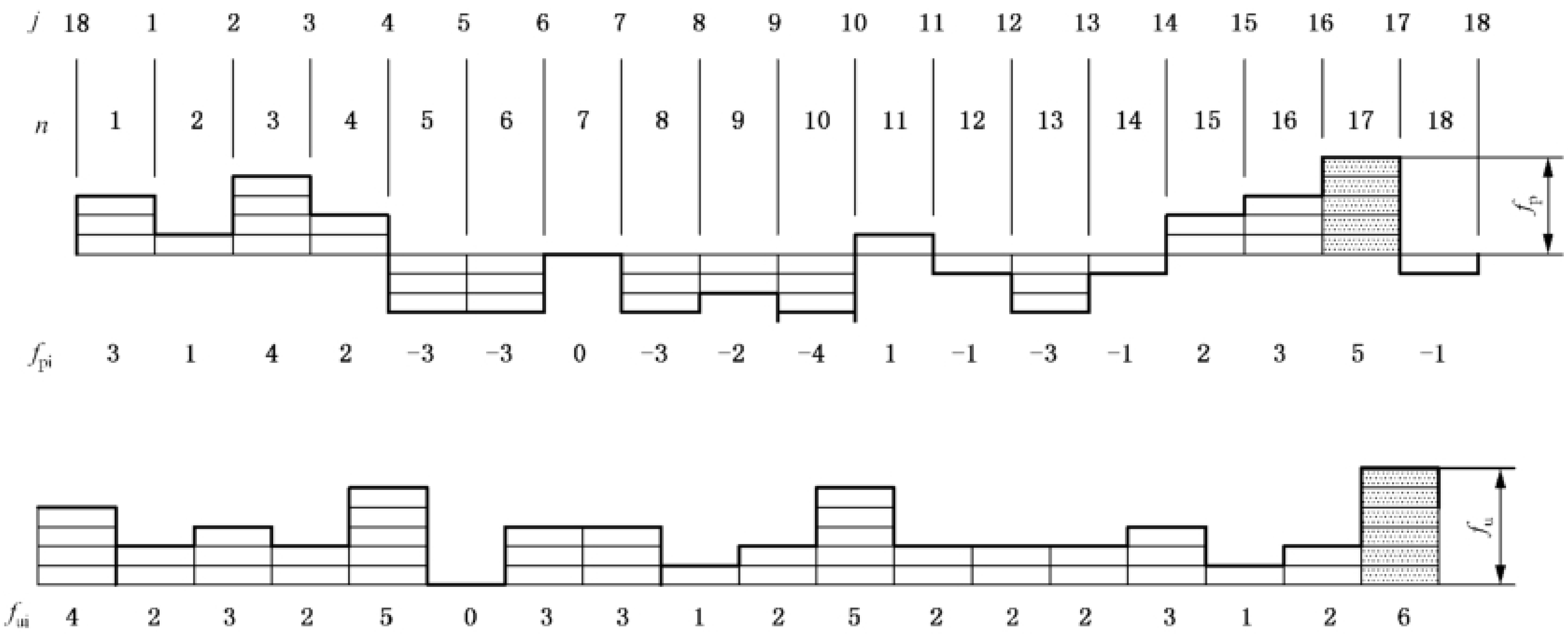

说明：

f_{pi}——任一单个齿距偏差；

f_{ui}——任一相邻齿距差；

j ——齿面编号；

n ——齿距编号。

图 G.1 相邻齿距差

参考文献

[1] ISO/TR 10064-2 Code of inspection practice—Part 2: Inspection related to radial composite deviations, runout, tooth thickness and backlash

[2] ISO/TR 10064-3 Code of inspection practice—Part 3: Recommendations relative to gear blanks, shaft centre distance and parallelism of axes

[3] ISO/TR 10064-4 Code of inspection practice—Part 4: Recommendations relative to surface texture and tooth contact pattern checking

[4] ISO/TR 10064-5 Code of inspection practice—Part 5: Recommendations relative to evaluation of gear measuring instruments

[5] ISO 14253-1 Geometrical product specifications (GPS)—Inspection by measurement of workpieces and measuring equipment—Part 1: Decision rules for proving conformity or nonconformity with specifications

[6] ISO 17485 Bevel gears—ISO system of accuracy

[7] ISO 18653 Gears—Evaluation of instruments for the measurement of individual gears

[8] AGMA 915-1-A02 Inspection Practices—Part 1: Cylindrical Gears—Tangential Measurements

GB/T 10095.1—2022/ISO 1328-1:2013

中 华 人 民 共 和 国

国 家 标 准

圆柱齿轮　ISO 齿面公差分级制

第 1 部分:齿面偏差的定义和允许值

GB/T 10095.1—2022/ISO 1328-1:2013

*

中 国 标 准 出 版 社 出 版 发 行

北京市朝阳区和平里西街甲 2 号(100029)

北京市西城区三里河北街 16 号(100045)

网址:www.spc.org.cn

服务热线:400-168-0010

2022 年 10 月第一版

*

书号:155066·1-71165

GB/T 10095.1-2022

ICS 21.200
CCS J 17

中华人民共和国国家标准

GB/T 10095.2—2023/ISO 1328-2:2020
代替 GB/T 10095.2—2008

圆柱齿轮　ISO 齿面公差分级制
第 2 部分:径向综合偏差的定义和允许值

Cylindrical gears—ISO system of flank tolerance classification—
Part 2:Definitions and allowable values of double flank radial composite deviations

(ISO 1328-2:2020, IDT)

2023-08-06 发布　　　　2024-03-01 实施

国家市场监督管理总局
国家标准化管理委员会　发布

目　次

前言 …… Ⅲ
引言 …… Ⅳ
1 范围 …… 1
2 规范性引用文件 …… 1
3 术语、定义和符号 …… 1
3.1 术语和定义 …… 1
3.2 符号 …… 3
4 ISO 径向综合公差分级制的应用 …… 4
4.1 通则 …… 4
4.2 公差等级 …… 4
4.3 基准面要求 …… 4
4.4 ISO 齿面分级制的应用 …… 4
4.5 验收标准 …… 5
4.6 径向综合偏差与单项偏差的相关性 …… 5
4.7 径向综合公差等级或公差的标注 …… 5
5 公差值 …… 5
5.1 通则 …… 5
5.2 公式的使用 …… 6
5.3 一齿径向综合公差 f_{idT} …… 6
5.4 径向综合总公差 F_{idT} …… 6
附录 A（资料性） 1.0 mm 模数直齿轮的 R34、R44 及 R50 级公差值曲线图 …… 7
附录 B（资料性） k 齿径向综合偏差 …… 8
附录 C（资料性） 改变径向综合公差的原因 …… 10
附录 D（资料性） 径向综合公差的转换 …… 11
附录 E（资料性） 计算示例 …… 12
参考文献 …… 17

前言

本文件按照 GB/T 1.1—2020《标准化工作导则　第1部分:标准化文件的结构和起草规则》的规定起草。

本文件是 GB/T 10095《圆柱齿轮　ISO 齿面公差分级制》的第2部分。GB/T 10095 已经发布了以下部分:

——第1部分:齿面偏差的定义和允许值;

——第2部分:径向综合偏差的定义和允许值。

本文件代替 GB/T 10095.2—2008《圆柱齿轮　精度制　第2部分:径向综合偏差与径向跳动的定义和允许值》,与 GB/T 10095.2—2008 相比,除结构调整和编辑性改动外,主要技术变化如下:

a) 更改了适用范围,包含了扇形齿轮(见第1章,2008年版的第1章);

b) 更改了术语、定义和符号(见第3章,2008年版的第4章和第5章);

c) 更改了齿面公差分级制(见第4章,2008年版的第6章);

d) 更改了径向综合公差的计算公式(见第5章,2008年版的第7章);

e) 删除了径向跳动(见2008年版的附录B)。

本文件等同采用 ISO 1328-2:2020《圆柱齿轮　ISO 齿面公差分级制　第2部分:径向综合偏差的定义和允许值》。

请注意本文件的某些内容可能涉及专利。本文件的发布机构不承担识别专利的责任。

本文件由全国齿轮标准化技术委员会(SAC/TC 52)提出并归口。

本文件起草单位:郑州机械研究所有限公司、北京工业大学、浙江双环传动机械股份有限公司、宁波中大力德智能传动股份有限公司、西安法士特汽车传动有限公司、南京高精齿轮集团有限公司、江苏国茂减速机股份有限公司、哈尔滨精达测量仪器有限公司、浙江丰立智能科技股份有限公司、深圳市兆威机电股份有限公司、浙江夏厦精密制造股份有限公司、河南科技大学、重庆大学、湖南磐钴传动科技有限公司、东莞市星火齿轮有限公司、温岭市明华齿轮有限公司、郑机所(郑州)传动科技有限公司。

本文件主要起草人:石照耀、王志刚、王伟、汤洁、吴长鸿、李海霞、岑国建、寇植达、赵泽方、唐志生、刘丽雪、王友利、范瑞丽、辛栋、谢桂平、王笑一、陈永洪、郭情情、周长江、童爱军、何本益、敬代云、徐家科、金伟锋、魏冰阳、管洪杰、纪谢茹。

本文件及其所代替文件的历次版本发布情况为:

——1988年首次发布为 GB/T 10095—1988;

——2001年第一次修订时分为两个部分出版,本文件对应 GB/T 10095.2—2001《渐开线圆柱齿轮精度　第2部分:径向综合偏差与径向跳动的定义和允许值》;

——2008年第二次修订;

——本次为第三次修订。

引　言

GB/T 10095《圆柱齿轮　ISO 齿面公差分级制》在我国齿轮行业广泛使用，完善了我国的齿轮标准体系，促进了我国齿轮产品与国际接轨。

依据测量原理、测量装备和评价方法的不同，GB/T 10095 由两个部分构成。

——第 1 部分：齿面偏差的定义和允许值。目的在于给出单个齿轮齿面的基本偏差（齿距偏差、齿廓偏差、螺旋线偏差和径向跳动）的定义，以及各个精度等级的公差（从 1 到 11，共分为 11 级）的计算方法；测量方法基于单个圆柱齿轮单侧齿面的坐标式测量；被测齿轮分度圆直径的范围为 5 mm～15 000 mm。

——第 2 部分：径向综合偏差的定义和允许值。目的在于给出单个齿轮径向综合偏差的定义，以及各个精度等级的公差（从 R30 到 R50，共分为 21 级）的计算方法；测量方法基于码特齿轮与产品齿轮双面啮合综合测量；被测齿轮分度圆直径的范围为不大于 600 mm。

以上两个部分共同构成了我国圆柱齿轮精度等级评价体系。但需要说明的是，第 1 部分与第 2 部分的评价体系没有相关性。配套的指导性技术文件 GB/Z 18620 系列给出了具体的检测方法及建议，可以相互结合，一起使用。

另外，GB/T 10095.2—2008 中附录 B（资料性）径向跳动的相关内容移到了 GB/T 10095.1—2022 的附录 E（规范性）中，本文件不再描述。

圆柱齿轮　ISO 齿面公差分级制
第 2 部分:径向综合偏差的定义和允许值

1　范围

本文件确立了单个渐开线圆柱齿轮及扇形齿轮的径向综合偏差的公差分级制,规定了径向综合偏差的定义、公差分级制的结构和偏差允许值,提供了单个产品齿轮与码特齿轮双面啮合时径向综合偏差的公差计算公式,但没有提供公差表。

本文件适用于齿数不小于 3、分度圆直径不大于 600 mm 的齿轮。

本文件不提供齿轮的设计指导,也不推荐齿轮参数的公差。

2　规范性引用文件

下列文件中的内容通过文中的规范性引用而构成本文件必不可少的条款。其中,注日期的引用文件,仅该日期对应的版本适用于本文件;不注日期的引用文件,其最新版本(包括所有的修改单)适用于本文件。

ISO 701　国际齿轮标记法　几何要素代号(International gear notation—Symbols for geometrical data)

注:GB/T 2821—2003　齿轮几何要素代号(ISO 701:1998,IDT)

ISO 1122-1　齿轮术语和定义　第 1 部分:几何学定义(Vocabulary of gear terms — Part 1: Definitions related to geometry)

注:GB/T 3374.1—2010　齿轮　术语和定义　第 1 部分:几何学定义(ISO 1122-1:1998,IDT)

3　术语、定义和符号

3.1　术语和定义

ISO 701 和 ISO 1122-1 界定的以及下列术语和定义适用于本文件。

3.1.1

双面啮合测量　double flank test

码特齿轮(3.1.4)与产品齿轮(3.1.5)在弹力作用下做不脱啮、无侧隙回转啮合运动期间,对中心距的变动量的测量。

3.1.2

单项偏差　elemental deviation

通过单点接触式探头测量得到的偏差,例如齿廓偏差、螺旋线偏差和齿距偏差。

3.1.3

基本方法　elemental method

单项偏差(3.1.2)的测量方法。

注:ISO 1328-1 中对单项偏差和基本方法作了说明。

3.1.4

码特齿轮　master gear

双面啮合测量中，满足精度要求并用来测量产品齿轮(3.1.5)径向综合偏差的齿轮。

3.1.5

产品齿轮　product gear

被测量或被评定的齿轮。

3.1.6

一齿径向综合偏差　tooth-to-tooth radial composite deviation

f_{id}

产品齿轮(3.1.5)的所有轮齿与码特齿轮(3.1.4)双面啮合测量(3.1.1)中，中心距在任一齿距内的最大变动量。

注：见图1。

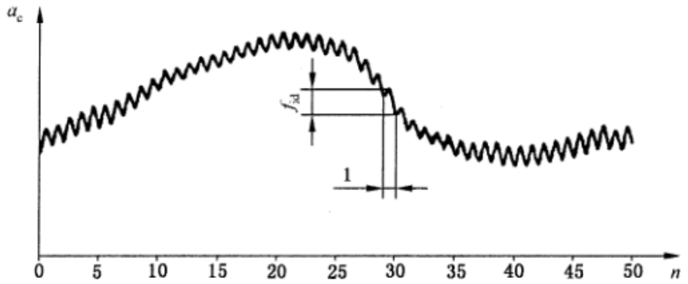

标引说明：

1 ——单个齿距；

n ——齿号；

a_c——双面啮合的中心距。

图1　一齿径向综合偏差

3.1.7

一齿径向综合公差　tooth-to-tooth radial composite tolerance

f_{idT}

一齿径向综合偏差(3.1.6)的最大允许值。

3.1.8

径向综合总偏差　total radial composite deviation

F_{id}

产品齿轮(3.1.5)的所有轮齿与码特齿轮(3.1.4)双面啮合测量(3.1.1)中，中心距的最大值与最小值之差。

注：见图2。

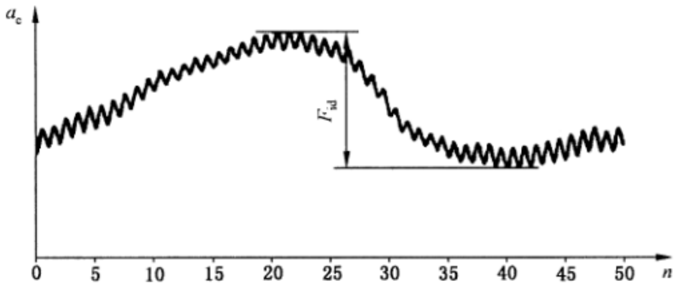

标引符号说明：

n ——齿号；

a_c——双面啮合的中心距。

图 2 径向综合总偏差

3.1.9

径向综合总公差 total radial composite tolerance

F_{idT}

径向综合总偏差(3.1.8)的最大允许值。

3.2 符号

表 1 中的符号适用于本文件。这些符号以 ISO 701 给出的符号为基础。

表 1 符号

符号	术语	单位	第 1 次使用
a_c	双面啮合的中心距	mm	3.1.6
F_{id}	径向综合总偏差	μm	3.1.8
f_{id}	一齿径向综合偏差	μm	3.1.6
F_{idk}	k 齿径向综合偏差	μm	B.3
F_{idkT}	k 齿径向综合公差	μm	B.4
F_{idT}	径向综合总公差	μm	3.1.9
f_{idT}	一齿径向综合公差	μm	3.1.7
k_{max}	测量部分的最大跨齿数	—	B.4
m_n	法向模数	mm	5.3
n	齿号	—	3.1.6
R	公差等级	—	5.3
R_x	基于齿数的公差等级修正系数	—	5.3
z	齿数	—	5.2.1
z_c	计算齿数	—	5.3
z_k	扇形齿轮齿数	—	5.4.2
β	螺旋角	(°)	5.3

4 ISO径向综合公差分级制的应用

4.1 通则

本文件提供未装配齿轮的公差分级及测量方法。

本文件不考虑齿轮表面结构,其相关信息可查看ISO/TR 10064-4。

经供需双方协商一致,本文件的公差可用于圆柱蜗杆、蜗轮、齿条、锥齿轮等其他类型的齿轮零件,但宜修改测量程序及步骤。本文件仅适用于平行轴齿轮,更多信息见ISO/TR 10064-2。

一些设计和应用方案需要的测量或记录可能不属于常见的标准制造工艺,因此具体要求应在合同文件中说明。

其他关于径向综合偏差测量的信息见ISO/TR 10064-2。

注1:根据第5章中的公式计算指定等级的公差。为帮助直观了解公差随齿数的变化规律,附录A提供了3个公差等级的公差数值曲线图。

注2:本文件规定的等级与ISO 1328-1等标准不存在关联性。本文件采用了一套独立的公差等级(即R30至R50)来强调与其他标准中的公差等级不相关(见附录C)。虽然没有相关性,但对于已经按其他标准规定公差的齿轮,仍可通过本文件确定相应的公差等级(见附录D)。

注3:具体测量方法、结果文件、抽检频率和统计方法的使用,通常由供需双方共同商定。

4.2 公差等级

本文件中,径向综合公差等级由径向综合总偏差 F_{id} 和一齿径向综合偏差 f_{id} 的测量来确定。确定一个齿轮的ISO径向综合公差等级时,应同时满足这两个独立的公差要求。

除了径向综合总公差 F_{idT} 和一齿径向综合公差 f_{idT} 外,附录B提供了一个可选用的技术指标,即 k 齿径向综合公差。

注1:提出过高的公差等级或测量标准,可能增加不必要的成本。

注2:双面啮合测量数据(如无侧隙啮合中心距)同时能够用于控制产品齿轮的齿厚及径向综合的整体影响。

本文件允许对径向综合总偏差 F_{id} 和一齿径向综合偏差 f_{id} 提出独立的公差等级要求。

产品齿轮的径向综合公差等级评定应在最终加工工序完成后进行。在制造过程中,任何工序后都可以进行双面啮合测量。

本文件适用于公差等级R30～R50。在特定应用中,可通过公式计算扩展至R30以下或R50以上。在这种情况下,宜给出具体的公差值,而不宜给出R30～R50范围之外的公差等级。

4.3 基准面要求

双面啮合测量时应指定使用的基准面。见ISO/TR 10064-3。

4.4 ISO齿面分级制的应用

4.4.1 测量仪器与码特齿轮

按照本文件测量时,应根据被测产品齿轮选用合适的双面啮合测量设备并进行校准。除非供需双方另有约定,供方可以对双面啮合仪器做出选择。

在径向综合偏差测量过程中应使用码特齿轮。码特齿轮的轮齿设计及公差要求应由产品齿轮的供需双方商定。码特齿轮在使用过程中会有磨损或损坏,宜定期校准。校准数据可溯源到有一定测量不确定度的国家基准。

注:码特齿轮偏差可能会增大或减小产品齿轮偏差的测量值。因此,精度要求高的产品齿轮通常要用更高精度的码特齿轮。使用精度较低的码特齿轮将增加产品齿轮被错误接收或拒收的风险。

产品齿轮与码特齿轮之间不应有啮合干涉。建议检查测量过程中最小中心距处齿顶与齿根过渡曲面之间的干涉。建议检查产品齿轮与码特齿轮之间的最小总重合度，在采用的各公差中该值宜大于1.02。

4.4.2 仪器检定与不确定度

用于产品齿轮测量的仪器宜定期检定。

宜确定测量过程的不确定度，见 ISO 14253-1。

4.4.3 滤波与数据密度

一齿径向综合偏差受径向跳动的影响很大，尤其是齿数较少时。一些双面啮合测量仪器可以选择使用滤波技术，在消除偏心影响后输出一齿径向综合偏差。本文件的公差值适用于不使用滤波功能去除偏心影响的情况。

但是双面啮合测量仪器中移动件的机械动态频率响应，包括齿轮本身质量、移动工作台质量、测量系统摩擦阻力和弹簧等影响，也能发生其他的滤波。在测量过程中，采用较低的转速可降低机械动态响应导致的滤波影响。

当使用电子测量装置时，每个齿距宜采集至少 30 个数据样本。

4.5 验收标准

产品齿轮的径向综合公差等级指本文件规定的各项公差的最大等级。

本文件中的径向综合公差适用于产品齿轮与码特齿轮啮合测量的情况。用于两个产品齿轮互相啮合测量的径向综合公差宜由供需双方协商决定。

4.6 径向综合偏差与单项偏差的相关性

使用本文件的径向综合偏差测量方法确定的公差等级，与使用 ISO 1328-1 中单项偏差测量方法确定的公差等级无关。用户需注意，仅使用本文件中的规范可能无法正确控制在没有径向偏差时仍可能出现的分度偏差或齿距累积总偏差。有关分度偏差的更多信息，见 ISO/TR 10064-1 和 ISO/TR 10064-2。

4.7 径向综合公差等级或公差的标注

本文件规定径向综合公差等级的标注方式为：

GB/T 10095.2—2023，R××级

其中××为设计的径向综合公差等级。

注：如果年份或以前版本限定符都没有列出，则使用最新版本的 GB/T 10095.2。

5 公差值

5.1 通则

公差值由 5.3 和 5.4 中公式进行计算。此外，B.4 中公式可计算 k 齿径向综合公差值。

注：附录 E 提供了公差计算示例。

如果产品齿轮直径或齿数不在第 1 章所列的规定范围内，公差公式应在供需双方协商一致后使用。

径向综合公差体系中将径向综合总偏差和一齿径向综合偏差划分为 21 个公差级，其中 R30 精度最高，R50 精度最低。

5.2 公式的使用

5.2.1 公差计算所用的齿数

对于 200 齿以上的齿轮(扇形齿轮除外),计算齿数应使用默认值 200。

对于扇形齿轮,z 是将扇形扩展到 360°后的当量齿数。

5.2.2 圆整规则

根据公式(1)、公式(4)和公式(5)计算的公差值应圆整到最接近的整数值。如果小数部分为 0.5,应向上圆整到最近的整数值。

如果测量仪器读数以英寸为单位,则根据公式(1)、公式(4)和公式(5)计算的公差值应在圆整前转换为万分之一英寸,然后圆整到最接近的 0.5 万分之一英寸。例如,公差值 11.74 万分之一英寸应圆整为 11.5 万分之一英寸,而公差值 11.75 万分之一英寸则圆整为 12.0 万分之一英寸。

5.3 一齿径向综合公差 f_{idT}

一齿径向综合公差 f_{idT}应通过公式(1)～公式(3)进行计算。

$$f_{idT}=\left(0.08\frac{z_c m_n}{\cos\beta}+64\right)2^{[(R-R_x-44)/4]}=\frac{F_{idT}}{2^{(R_x/4)}} \quad \cdots\cdots(1)$$

$$z_c=\min(|z|,200) \quad \cdots\cdots(2)$$

$$R_x=5\{1-1.12^{[(1-z_c)/1.12]}\} \quad \cdots\cdots(3)$$

5.4 径向综合总公差 F_{idT}

5.4.1 圆柱齿轮径向综合总公差

圆柱齿轮及齿数大于 2/3 整圆齿数的扇形齿轮的径向综合总公差 F_{idT}应按公式(4)进行计算。

$$F_{idT}=\left(0.08\frac{z_c m_n}{\cos\beta}+64\right)2^{[(R-44)/4]} \quad \cdots\cdots(4)$$

5.4.2 扇形齿轮径向综合总公差

本条仅适用于齿数小于或等于 2/3 整圆齿数的扇形齿轮。

当扇形齿轮$|z_k/z|>2/3$ 时,与完整圆柱齿轮一致,应按公式(4)进行径向综合总公差 F_{idT}的计算。

当扇形齿轮$|z_k/z|\leqslant 2/3$ 时,应通过公式(5)进行径向综合总公差 F_{idT}的计算,并对其扇形尺寸进行补偿,其中 R_x通过公式(3)进行计算。

$$F_{idT}=\left(0.08\frac{z_c m_n}{\cos\beta}+64\right)2^{[(R-44)/4]}\left[\left(1-1.5\frac{|z_k|-1}{|z|}\right)2^{\left(\frac{-R_x}{4}\right)}+1.5\frac{|z_k|-1}{|z|}\right] \quad \cdots\cdots(5)$$

附 录 A
(资料性)
1.0 mm 模数直齿轮的 R34、R44 及 R50 级公差值曲线图

图 A.1 描述了模数为 1.0 mm,公差等级分别为 R34、R44 和 R50 的径向综合总公差 F_{idT} 和一齿径向综合公差 f_{idT} 的公差值。这些图根据公式(1)和公式(4)计算并应用 5.2.2 中的规则进行圆整后的数据绘制,以帮助使用者直观了解 ISO 齿面公差分级制的公式特征。

注:图示曲线的阶梯变化是圆整运算的结果。

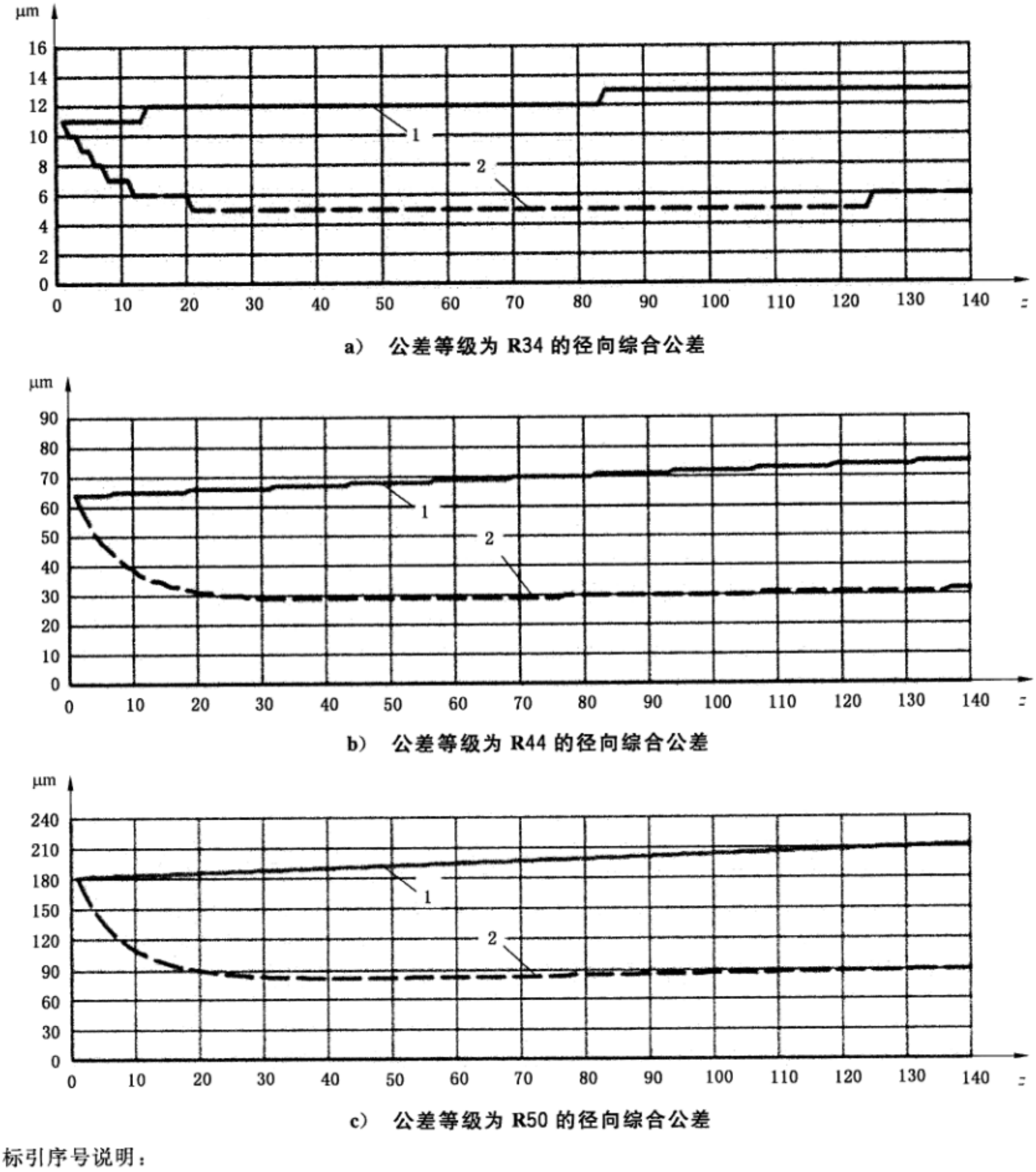

a) 公差等级为 R34 的径向综合公差

b) 公差等级为 R44 的径向综合公差

c) 公差等级为 R50 的径向综合公差

标引序号说明:

1——径向综合总公差,F_{idT};

2——一齿径向综合公差,f_{idT}。

图 A.1 模数为 1.0 mm 的完整直齿轮的径向综合总公差、一齿径向综合公差与齿数的关系

附 录 B
（资料性）
k 齿径向综合偏差

B.1 概述

本附录给出了 k 齿径向综合偏差的定义、测量方法、推荐公差及指导意见，可以作为径向综合总偏差和一齿径向综合偏差的补充规范。

B.2 应用

具有可接受的一齿径向综合偏差和径向综合总偏差的齿轮，如果大部分径向综合偏差仅出现在少数几个齿上，则仍可能存在功能上不可接受的传动误差。在双面啮合接触测量中，对于具有高重合度（啮合重叠范围大）的齿轮，一个轮齿的异常可能会影响到其他多个轮齿。由于较高的重合度，相邻齿上的其他附加缺陷可能会严重影响齿轮的使用效果。跨多个齿距测量径向综合偏差有助于识别此类问题。

B.3 k 齿径向综合偏差 F_{idk}

k 齿径向综合偏差 F_{idk} 是通过双面啮合测量产品齿轮的所有齿后得到的任一 k 个齿距范围内中心距最大变动量。图 B.1 显示了一个跨 4 个齿距的径向综合偏差的具体实例。此例显示了一个产品齿轮，其径向综合偏差的快速变化可能导致运转问题，但无法通过一齿径向综合偏差或径向综合总偏差来检测。

注：指定的跨齿距数在图示中用符号 k 代替。即如果跨 4 个齿距，则符号为 F_{id4}。

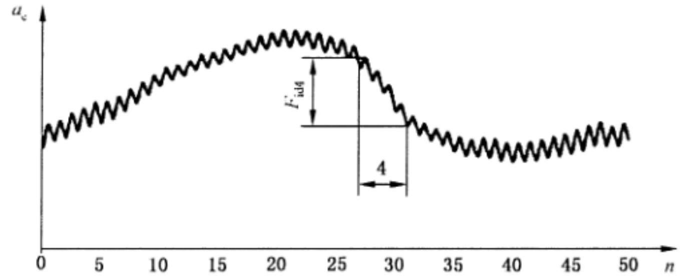

标引符号说明：

n ——齿号；

a_c——双面啮合的中心距。

图 B.1 齿数为 50 跨 4 个齿距的齿轮的径向综合偏差

B.4 k 齿径向综合公差 F_{idkT}

k 齿径向综合公差是跨 k 个齿距的径向综合偏差的最大允许值，按照公式(B.1)计算：

$$F_{idkT}=\left(0.08\frac{z_c m_n}{\cos\beta}+64\right)2^{[(R-44)/4]}\left[\left(1-1.5\frac{k-1}{|z|}\right)2^{\left(\frac{-R_x}{4}\right)}+1.5\frac{k-1}{|z|}\right] \quad \cdots\cdots(B.1)$$

其中 z_c 和 R_x 来自公式(2)和公式(3)。

计算值遵循 5.2.2 中列出的圆整规则。

除扇形齿轮外，其他所有齿轮测量部分的最大跨齿数 k_{max} 为：

$$k_{\max}=\frac{z_{c}}{1.5} \qquad \cdots\cdots\cdots\cdots (B.2)$$

扇形齿轮测量部分的最大齿距数 $k_{\max}$为：

$$k_{\max}=\min\left(\frac{|z|}{1.5},|z_{k}|\right) \qquad \cdots\cdots\cdots\cdots (B.3)$$

k 的选择值超过 $k_{\max}$将导致一齿径向综合公差超过径向综合总公差。通常 k 值范围为 3 至 $z/8$ 个齿距，但并不受此限制。

附 录 C
（资料性）
改变径向综合公差的原因

C.1 概述

新版文件使用了新的公差计算公式。旧版被替代的原因如下：

——随尺寸增大而大幅增加的径向综合总公差和齿轮制造的难度或典型应用的需求不匹配；

——公差较大时，相邻等级公差的公比$\sqrt{2}$过大；

——未规定跨若干齿距的径向综合公差；

——未明确涵盖扇形齿轮；

——旧版公式计算的一齿径向综合公差与径向综合总公差不相适应，尤其齿数较少时。

C.2 扇形齿轮

ISO 1328-2:1997 中的公式不适用于扇形齿轮，尤其是扇形齿轮与整圈齿轮相比齿数较少时。新公式考虑了扇形齿轮，扩大了应用范围。

C.3 一齿径向综合公差

本文件给出的一齿径向综合公差与径向综合总公差相互适应。当斜齿轮齿数为 1 时，新公式计算的径向综合总公差和一齿径向综合公差相等。

C.4 级间公比

对于公差较大的齿轮，在制造的经济性和产品的功能性方面，径向综合公差的级间公比$\sqrt{2}$过大（增加了 41.4%）。这一点对于质量要求不高的齿轮影响很大。

例如，级间公比为$\sqrt{2}$时，某齿轮相邻等级的径向综合总公差为 100 μm 或 141 μm。如果所用工艺具有径向综合总公差 110 μm 的制造能力，则上一等级不能满足，而下一等级公差过大。新的级间公比为 1.19，则下一等级的公差为 119 μm，这是合理的。

C.5 *k* 齿径向综合公差

附录 B 给出了跨 *k* 个齿距的径向综合公差的可选规范。

该规范在概念上类似于 ISO 1328-1:2013 中附录 D 给出的齿距累积偏差的公差。该规范可供设计人员选用，尤其适用于因齿轮局部偏差过大（但未超过径向综合总公差）可能导致使用问题的场合。当应用场景对噪声和振动敏感时常给出该公差。

附 录 D
（资料性）
径向综合公差的转换

D.1 基本方法

要将其他的齿面综合公差等级转换为本文件的公差等级，宜先查询到实际的公差数值。新的公差等级可通过公式(D.1)和公式(D.2)进行转换：

对于径向综合总公差等级：

$$R=4\left[\frac{\ln\dfrac{F_{\mathrm{idT}}}{\left(0.08\dfrac{z_{\mathrm{c}}m_{\mathrm{n}}}{\cos\beta}+64\right)}}{\ln 2}\right]+44 \qquad \text{(D.1)}$$

对于一齿径向公差等级：

$$R=4\left[\frac{\ln\dfrac{f_{\mathrm{idT}}}{\left(0.08\dfrac{z_{\mathrm{c}}m_{\mathrm{n}}}{\cos\beta}+64\right)}}{\ln 2}\right]+44+R_{\mathrm{x}} \qquad \text{(D.2)}$$

式中：

z_{c} ——来自公式(2)；

R_{x}——来自公式(3)。

注 1：在某些现有标准中，径向综合总公差 F_{idT} 使用符号 F''_{i}，而一齿径向综合公差 f_{idT} 使用符号 f''_{i}。

注 2：当采用另一标准的径向综合总公差和一齿径向公差计算公差等级时，设计人员可根据规则圆整，或直接使用该结果。一般情况下不影响最终结果。在 E.6 示例中，结果没有圆整。

D.2 选择

设计人员需要确定选择一个公差等级是否恰当，或者是否为每个公差指定单独的等级。设计人员还需要将计算出的公差等级圆整为最接近的公差等级或下一个较大整数的公差等级。

在某些情况下，只使用新的径向综合总公差等级并接受由此产生的新的一齿径向综合公差等级是合适的。

附　录　E
（资料性）
计算示例

E.1　示例 1——直齿齿轮

齿数为 14、模数 3.0 mm、公差等级 R48 的直齿齿轮。

第一步，根据公式(1)～公式(3)计算一齿径向综合公差：

$$\begin{aligned} z_c &= \min(|z|, 200) \\ &= \min(|14|, 200) \\ &= 14 \end{aligned}$$

$$\begin{aligned} R_x &= 5\{1 - 1.12^{[(1-z_c)/1.12]}\} \\ &= 5\{1 - 1.12^{[(1-14)/1.12]}\} \\ &= 3.658 \end{aligned}$$

$$\begin{aligned} f_{idT} &= \left(0.08\frac{z_c m_n}{\cos\beta} + 64\right) \times 2^{[(R-R_x-44)/4]} \\ &= \left(0.08 \times \frac{14 \times 3}{\cos 0^\circ} + 64\right) \times 2^{[(48-3.658-44)/4]} \\ &= 71.470\ \mu m \end{aligned}$$

根据 5.2.2 的规则圆整到最近的整数值：

$$f_{idT} = 71\ \mu m$$

第二步，根据公式(4)计算径向综合总公差：

$$\begin{aligned} F_{idT} &= \left(0.08\frac{z_c m_n}{\cos\beta} + 64\right) \times 2^{[(R-44)/4]} \\ &= \left(0.08 \times \frac{14 \times 3}{\cos 0^\circ} + 64\right) \times 2^{[(48-44)/4]} \\ &= 134.720\ \mu m \end{aligned}$$

根据 5.2.2 的规则圆整到最近的整数值：

$$F_{idT} = 135\ \mu m$$

E.2　示例 2——斜齿轮（包括 z/8 个齿距）

法向模数 0.7 mm、螺旋角 25°、公差等级 R44、齿数 40 的斜齿轮，计算 $F_{idz/8T}$。

第一步，根据公式(1)～公式(3)计算一齿径向综合公差：

$$\begin{aligned} z_c &= \min(|z|, 200) \\ &= \min(|40|, 200) \\ &= 40 \end{aligned}$$

$$\begin{aligned} R_x &= 5\{1 - 1.12^{[(1-z_c)/1.12]}\} \\ &= 5\{1 - 1.12^{[(1-40)/1.12]}\} \\ &= 4.903 \end{aligned}$$

$$f_{\text{idT}}=\left(0.08\frac{z_{\text{c}}m_{\text{n}}}{\cos\beta}+64\right)\times 2^{[(R-R_{\text{x}}-44)/4]}$$
$$=\left(0.08\times\frac{40\times 0.7}{\cos 25^{\circ}}+64\right)\times 2^{[(44-4.903-44)/4]}$$
$$=28.420\ \mu\text{m}$$

根据 5.2.2 的规则圆整到最近的整数值：

$$f_{\text{idT}}=28\ \mu\text{m}$$

第二步，根据公式(4)计算径向综合总公差：

$$F_{\text{idT}}=\left(0.08\frac{z_{\text{c}}m_{\text{n}}}{\cos\beta}+64\right)\times 2^{[(R-44)/4]}$$
$$=\left(0.08\times\frac{40\times 0.7}{\cos 25^{\circ}}+64\right)\times 2^{[(44-44)/4]}$$
$$=66.472\ \mu\text{m}$$

根据 5.2.2 的规则圆整到最近的整数值：

$$F_{\text{idT}}=66\ \mu\text{m}$$

第三步，计算跨 $z/8$ 个齿距的径向综合公差：

跨齿距数：

$$k=\frac{|z|}{8}=\frac{40}{8}=5$$

根据公式(B.1)计算跨 5 个齿距的径向综合公差：

$$F_{\text{id}k\text{T}}=\left(0.08\frac{z_{\text{c}}m_{\text{n}}}{\cos\beta}+64\right)\times 2^{[(R-44)/4]}\times\left[\left(1-1.5\frac{k-1}{|z|}\right)2^{\left(\frac{-R_{\text{x}}}{4}\right)}+1.5\frac{k-1}{|z|}\right]$$

$$F_{\text{id5T}}=\left(0.08\times\frac{40\times 0.7}{\cos 25^{\circ}}+64\right)\times 2^{[(44-44)/4]}\times\left[\left(1-1.5\times\frac{5-1}{|40|}\right)\times 2^{\left(\frac{-4.903}{4}\right)}+1.5\times\frac{5-1}{|40|}\right]$$
$$=34.128\ \mu\text{m}$$

根据 5.2.2 的规则圆整到最近的整数值：

$$F_{\text{id5T}}=34\ \mu\text{m}$$

E.3 示例 3——200 齿以上的斜齿轮

法向模数 0.8 mm、螺旋角 15°、公差等级 R41、324 个齿的斜齿轮。

由于齿数超过了 5.2.1 中最大齿数 200，因此在所有公式中，公差都是以齿数 200 的齿轮为基础计算的。

第一步，根据公式(1)～公式(3)计算一齿径向综合公差：

$$z_{\text{c}}=\min(|z|,200)$$
$$=\min(|324|,200)$$
$$=200$$

$$R_{\text{x}}=5\{1-1.12^{[(1-z_{\text{c}})/1.12]}\}$$
$$=5\{1-1.12^{[(1-200)/1.12]}\}$$
$$=5.00$$

$$f_{\text{idT}}=\left(0.08\frac{z_{\text{c}}m_{\text{n}}}{\cos\beta}+64\right)\times 2^{[(R-R_{\text{x}}-44)/4]}$$
$$=\left(0.08\times\frac{200\times 0.8}{\cos 15^{\circ}}+64\right)\times 2^{[(41-5-44)/4]}$$
$$=19.313\ \mu\text{m}$$

根据 5.2.2 的规则圆整到最近的整数值：

$$f_{\mathrm{idT}}=19\ \mu\mathrm{m}$$

第二步，根据公式(4)计算径向综合总公差：

$$\begin{aligned}F_{\mathrm{idT}}&=\left(0.08\,\frac{z_{\mathrm{c}}m_{\mathrm{n}}}{\cos\beta}+64\right)\times 2^{[(R-44)/4]}\\&=\left(0.08\times\frac{200\times 0.8}{\cos 15^{\circ}}+64\right)\times 2^{[(41-44)/4]}\\&=45.934\ \mu\mathrm{m}\end{aligned}$$

根据 5.2.2 的规则圆整到最近的整数值。

$$F_{\mathrm{idT}}=46\ \mu\mathrm{m}$$

E.4 示例 4——扇形齿轮

法向模数 1.5 mm、螺旋角 5°、公差等级 R45、齿数 50 的斜齿轮(由 16 个齿组成的扇形齿轮)，计算 $F_{\mathrm{idz/8T}}$。

第一步，根据公式(1)～公式(3)计算一齿径向综合公差：

$$\begin{aligned}z_{\mathrm{c}}&=\min(|z|,200)\\&=\min(|50|,200)\\&=50\end{aligned}$$

$$\begin{aligned}R_{\mathrm{x}}&=5\{1-1.12^{[(1-z_{\mathrm{c}})/1.12]}\}\\&=5\{1-1.12^{[(1-50)/1.12]}\}\\&=4.965\end{aligned}$$

$$\begin{aligned}f_{\mathrm{idT}}&=\left(0.08\,\frac{z_{\mathrm{c}}m_{\mathrm{n}}}{\cos\beta}+64\right)2^{[(R-R_{\mathrm{x}}-44)/4]}\\&=\left(0.08\times\frac{50\times 1.5}{\cos 5^{\circ}}+64\right)\times 2^{[(45-4.965-44)/4]}\\&=35.225\ \mu\mathrm{m}\end{aligned}$$

根据 5.2.2 的规则圆整到最近的整数值：

$$f_{\mathrm{idT}}=35\ \mu\mathrm{m}$$

第二步，计算径向综合总公差：

由于 $\left|\frac{z_{\mathrm{k}}}{z}\right|=\frac{16}{50}=0.32\leqslant\frac{2}{3}$，根据公式(5)计算：

$$\begin{aligned}F_{\mathrm{idT}}&=(0.08\,\frac{z_{\mathrm{c}}m_{\mathrm{n}}}{\cos\beta}+64)\times 2^{[(R-44)/4]}\times\left[(1-1.5\,\frac{z_{\mathrm{k}}-1}{|z|})\times 2^{(\frac{-R_{\mathrm{x}}}{4})}+1.5\times\frac{z_{\mathrm{k}}-1}{|z|}\right]\\&=\left(0.08\times\frac{50\times 1.5}{\cos 5^{\circ}}+64\right)\times 2^{[(45-44)/4]}\times\left[\left(1-1.5\times\frac{16-1}{50}\right)\times 2^{(\frac{-4.965}{4})}+1.5\times\frac{16-1}{50}\right]\\&=56.846\ \mu\mathrm{m}\end{aligned}$$

根据 5.2.2 的规则圆整到最近的整数值：

$$F_{\mathrm{idT}}=57\ \mu\mathrm{m}$$

第三步，计算跨 $z/8$ 个齿的径向综合公差：

跨齿距数：

$$k=\frac{|z|}{8}=\frac{50}{8}=6.25$$

圆整为整数：

$$k=6$$

根据公式(B.1)计算跨 6 个齿的径向综合公差：

$$F_{\mathrm{id}k\mathrm{T}}=\left(0.08\frac{z_{\mathrm{c}}m_{\mathrm{n}}}{\cos\beta}+64\right)\times 2^{[(R-44)]}\times\left[\left(1-1.5\times\frac{k-1}{|z|}\right)\times 2^{\left(\frac{-R_{\mathrm{x}}}{4}\right)}+1.5\times\frac{k-1}{|z|}\right]$$

$$F_{\mathrm{id6T}}=\left(0.08\times\frac{50\times 1.5}{\cos 5^{\circ}}+64\right)\times 2^{[(45-44)/4]}\times\left[\left(1-1.5\times\frac{6-1}{50}\right)\times 2^{\left(\frac{-4.965}{4}\right)}+1.5\times\frac{6-1}{50}\right]$$

$$=42.432\ \mu\mathrm{m}$$

根据 5.2.2 的规则圆整到最近的整数值。

$$F_{\mathrm{id6T}}=42\ \mu\mathrm{m}$$

E.5 示例 5——径节制的斜齿轮

法向径节 12、螺旋角 17°、公差等级为 R48、齿数为 45 的斜齿轮。

第一步，计算法向模数：

$$m_{\mathrm{n}}=\frac{25.4}{12}=2.116\ 7\ \mathrm{mm}$$

第二步，根据公式(1)～公式(3)计算一齿径向综合公差：

$$\begin{aligned}z_{\mathrm{c}}&=\min(|z|,200)\\&=\min(|45|,200)\\&=45\end{aligned}$$

$$\begin{aligned}R_{\mathrm{x}}&=5\{1-1.12^{[(1-z_{\mathrm{c}})/1.12]}\}\\&=5\{1-1.12^{[(1-45)/1.12)]}\}\\&=4.942\end{aligned}$$

$$\begin{aligned}f_{\mathrm{idT}}&=\left(0.08\frac{z_{\mathrm{c}}m_{\mathrm{n}}}{\cos\beta}+64\right)\times 2^{[(R-R_{\mathrm{x}}-44)/4]}\\&=\left(0.08\times\frac{45\times 2.1167}{\cos 17^{\circ}}+64\right)\times 2^{[(48-4.942-44)/4]}\\&=61.132\ \mu\mathrm{m}\end{aligned}$$

基于 5.2.2 的圆整规则，首先将该计算值转换为万分之一英寸。

$$f_{\mathrm{idT}}=24.068\times 10^{-4}\ \mathrm{in}$$

然后圆整到最接近的 0.5 万分之一英寸。

$$f_{\mathrm{idT}}=24\times 10^{-4}\ \mathrm{in}$$

第三步，根据公式(4)计算径向综合总公差：

$$\begin{aligned}F_{\mathrm{idT}}&=\left(0.08\frac{z_{\mathrm{c}}m_{\mathrm{n}}}{\cos\beta}+64\right)\times 2^{[(R-44)/4]}\\&=\left(0.08\times\frac{45\times 2.1167}{\cos 17^{\circ}}+64\right)\times 2^{[(48-44)/4]}\\&=143.937\ \mu\mathrm{m}\end{aligned}$$

根据圆整规则，首先将该计算值转换为万分之一英寸。

$$F_{\mathrm{idT}}=56.667\times 10^{-4}\ \mathrm{in}$$

然后圆整到最接近的 0.5 万分之一英寸。

$$f_{\mathrm{idT}}=56.5\times 10^{-4}\ \mathrm{in}$$

E.6 示例 6——从 GB/T 10095.2—2008 转换为 R 公差等级

齿数 40、法向模数 0.7 mm、螺旋角 25°、GB/T 10095.2—2008 中精度 9 级的斜齿轮。

第一步，计算现有公差：

径向综合公差：

$$d=\frac{|z|m_n}{\cos\beta}=\frac{40\times 0.7}{\cos 25^\circ}=30.894\ 6\ \text{mm}$$

$$\begin{aligned} F''_i &= (3.2m_n+1.01\sqrt{d}+6.4)\,2^{\left(\frac{Q-5}{2}\right)} \\ &= (3.2\times 0.7+1.01\times\sqrt{30.894\ 6}+6.4)\times 2^{\left(\frac{9-5}{2}\right)} \\ &= 57.02\ \mu\text{m} \end{aligned}$$

$$\begin{aligned} f''_i &= (2.96m_n+0.01\sqrt{d}+0.8)\times 2^{\left(\frac{Q-5}{2}\right)} \\ &= (2.96\times 0.7+0.01\times\sqrt{30.8946}+0.8)\times 2^{\left(\frac{9-5}{2}\right)} \\ &= 11.71\ \mu\text{m} \end{aligned}$$

第二步，计算 R 公差等级：

径向综合总公差等级：

$$\begin{aligned} z_c &= \min(|z|,200) \\ &= \min(|40|,200) \\ &= 40 \end{aligned}$$

$$\begin{aligned} R &= 4\left[\frac{\ln\dfrac{F_{\mathrm{idT}}}{\left(0.08\dfrac{z_c m_n}{\cos\beta}+64\right)}}{\ln 2}\right]+44 \\ &= 4\left[\frac{\ln\dfrac{57.02}{(0.08\times 30.894\ 6+64)}}{\ln 2}\right]+44 \\ &= 43.1 \end{aligned}$$

一齿径向综合公差等级：

$$\begin{aligned} R_x &= 5\{1-1.12^{[(1-z_c)/1.12]}\} \\ &= 5\{1-1.12^{[(1-40)/1.12]}\} \\ &= 4.903\ 4 \end{aligned}$$

$$\begin{aligned} R &= 4\times\left[\frac{\ln\dfrac{f_{\mathrm{idT}}}{\left(0.08\dfrac{z_c m_n}{\cos\beta}+64\right)}}{\ln 2}\right]+44+R_x \\ &= 4\times\left[\frac{\ln\dfrac{11.71}{(0.08\times 30.894\ 6+64)}}{\ln 2}\right]+44+4.903\ 4 \\ &= 38.9 \end{aligned}$$

第三步，确定公差等级：

设计人员需要确定是否使用当前版本文件中规定的径向综合总公差 R43 级和一齿径向综合公差 R39 级来修改图纸。如果实际应用中能够接受一齿径向综合公差为 R43 时计算得到的 24 μm，而不是原来旧版中的 12 μm，则可确定该公差等级为 R43。当前生产零件的偏差数据十分有助于确定正确的公差等级。

参 考 文 献

[1] ISO 1328-1:2013 Cylindrical gears—ISO system of flank tolerance classification—Part 1: Definitions and allowable values of deviations relevant to flanks of gear teeth

[2] ISO/TR 10064-1 Code of inspection practice—Part 1: Measurement of cylindrical gear tooth flanks

[3] ISO/TR 10064-2 Code of inspection practice—Part 2: Inspection related to radial composite deviations, runout, tooth thickness and backlash

[4] ISO/TR 10064-3 Code of inspection practice—Part 3: Recommendations relative to gear blanks, shaft centre distance and parallelism of axes

[5] ISO/TR 10064-4:1998 Code of inspection practice—Part 4: Recommendations relative to surface texture and tooth contact pattern checking

[6] ISO 14253-1:2017 Geometrical product specifications (GPS)—Inspection by measurement of workpieces and measuring equipment—Part 1: Decision rules for verifying conformity or nonconformity with specifications

[7] BS 3696-1:1977 Master Gears

中 华 人 民 共 和 国
国 家 标 准
圆柱齿轮 ISO 齿面公差分级制
第 2 部分：径向综合偏差的定义和允许值
GB/T 10095.2—2023/ISO 1328-2:2020
*
中国标准出版社出版发行
北京市朝阳区和平里西街甲 2 号(100029)
北京市西城区三里河北街 16 号(100045)
网址 www.spc.net.cn
总编室：(010)68533533 发行中心：(010)51780238
读者服务部：(010)68523946
中国标准出版社秦皇岛印刷厂印刷
各地新华书店经销
*
开本 880×1230 1/16 印张 1.5 字数 43 千字
2023 年 8 月第一版 2023 年 8 月第一次印刷
*
书号：155066・1-73427 定价 36.00 元

GB/T 10095.2-2023

码上扫一扫 正版服务到

ICS 21.200
J 17

中华人民共和国国家标准化指导性技术文件

GB/Z 18620.2—2008/ISO/TR 10064-2:1996
代替 GB/Z 18620.2—2002

圆柱齿轮　检验实施规范 第2部分:径向综合偏差、径向跳动、齿厚和侧隙的检验

**Cylindrical gears—Code of inspection practice—
Part 2:Inspection related to radial composite deviations, runout,tooth thickness and backlash**

(ISO/TR 10064-2:1996,IDT)

2008-03-31 发布

中华人民共和国国家质量监督检验检疫总局
中国国家标准化管理委员会　发布

目　　次

前言 …………………………………………………………………………………… Ⅲ
ISO 前言 ………………………………………………………………………………… Ⅳ
1　范围 …………………………………………………………………………………… 1
2　规范性引用文件 ……………………………………………………………………… 1
3　符号、相关项目和定义 ……………………………………………………………… 1
4　径向综合偏差的测量 ………………………………………………………………… 5
5　径向跳动的测量、偏心量的确定 …………………………………………………… 7
6　齿厚、公法线长度和跨球(圆柱)尺寸的测量 ……………………………………… 13
7　齿轮的公差和配合 …………………………………………………………………… 20
附录 A(资料性附录)　侧隙和齿厚公差 ……………………………………………… 22
参考文献 ………………………………………………………………………………… 25

前 言

GB/Z 18620《圆柱齿轮 检验实施规范》包括下列四部分：

——第1部分：轮齿同侧齿面的检验；

——第2部分：径向综合偏差、径向跳动、齿厚和侧隙的检验；

——第3部分：齿轮坯、轴中心距和轴线平行度的检验；

——第4部分：表面结构和轮齿接触斑点的检验。

本部分是 GB/Z 18620 的第2部分。

本部分等同采用 ISO/TR 10064-2:1996《圆柱齿轮 检验实施规范 第2部分：径向综合偏差、径向跳动、齿厚和侧隙的检验》(英文版)。

本部分等同翻译 ISO/TR 10064-2:1996。为便于使用，本部分作了下列编辑性修改：

——按照汉语习惯对一些编排格式进行了修改；

——用小数点“.”代替作为小数点的“,”。

——对 ISO/TR 10064-2:1996 引用的其他国际标准中，有被等同采用为我国标准的，用我国标准代替对应的国际标准，未被等同采用为我国标准的直接引用国际标准。

本部分是对 GB/Z 18620.2—2002《圆柱齿轮 检验实施规范 第2部分：径向综合偏差、径向跳动、齿厚和侧隙的检验》的修订。与 GB/Z 18620.2—2002 相比，主要内容修改如下：

——对部分术语作了修改，如“跨距”改为“公法线长度”，“公称齿厚 s_n”改为“法向齿厚 s_n”。

本部分的附录A是资料性附录。

本部分由中国机械工业联合会提出。

本部分由全国齿轮标准化技术委员会归口。

本部分起草单位：郑州机械研究所、机械科学研究总院。

本部分主要起草人：张元国、明翠新、张民安、历始忠、王长路、王琦、杨星原、陈爱闻、林太军、许洪基。

本部分所代替标准的历次版本发布情况为：

——GB/Z 18620.2—2002。

ICS 21.200
J 17

中华人民共和国国家标准

GB/T 11365—2019/ISO 17485:2006
代替 GB/T 11365—1989

锥齿轮　精度制

Bevel gears—ISO system of accuracy

(ISO 17485:2006, IDT)

2019-10-17 发布　　　　2020-05-01 实施

国家市场监督管理总局
中国国家标准化管理委员会　发布

目　次

前言 …… Ⅰ

1　范围 …… 1

2　规范性引用文件 …… 1

3　术语和定义、符号 …… 1

　3.1　术语和定义 …… 1

　3.2　基本术语和符号 …… 4

4　精度等级制的应用 …… 6

　4.1　概述 …… 6

　4.2　精度等级 …… 7

　4.3　公差方向 …… 7

　4.4　附加特性 …… 7

5　公差 …… 7

　5.1　公差值 …… 7

　5.2　分级系数 …… 7

　5.3　圆整规则 …… 8

　5.4　公差公式 …… 8

6　测量方法的使用 …… 9

　6.1　测量方法 …… 9

　6.2　推荐的测量控制方法 …… 10

　6.3　测量数据的滤波 …… 11

　6.4　轮齿接触斑点检验 …… 11

附录A（资料性附录）　公差示例表 …… 12

附录B（资料性附录）　单面啮合综合测量方法 …… 14

附录C（资料性附录）　小模数锥齿轮的精度 …… 18

附录D（资料性附录）　综合数据说明 …… 20

参考文献 …… 26

前　言

本标准按照 GB/T 1.1—2009 给出的规则起草。

本标准代替 GB/T 11365—1989《锥齿轮和准双曲面齿轮　精度》，与 GB/T 11365—1989 相比，主要技术变化如下：

——公差数值原来由表格给出，改为由公式计算得出；

——术语定义由 23 项修订为 10 项，如切向综合误差改为切向综合总偏差，增加了传动误差术语定义，删减了轴交角综合误差、齿形相对误差等；有些术语定义放在资料性附录里，如双面啮合综合偏差等。

本标准使用翻译法等同采用 ISO 17485：2006《锥齿轮　精度制》。

本标准做了下列编辑性修改：

——表 1 和表 2 中 f_{is} 的首次使用处由“3.1.6”改为“3.1.5”；

——表 1 中 R_i 的首次使用处由“图 1”改为“图 2”；

——表 2 中的 f_{is}(design)改为 $f_{is(design)}$；

——5.4 条的公式右边序号“(2)”～“(9)”依次改为“(4)”～“(11)”，段落文字中的公式序号不变。

本标准由全国齿轮标准化技术委员会(SAC/TC 52)提出并归口。

本标准起草单位：河南科技大学、郑州机械研究所有限公司、山东华成中德传动设备有限公司、哈尔滨精达测量仪器有限公司、北京工业大学、江苏中工高端装备研究院有限公司、西北工业大学、北京航空航天大学。

本标准主要起草人：魏冰阳、王志刚、邓效忠、李天兴、鞠国强、周广才、曹雪梅、毛玺、刘世军、吴鲁纪、管洪杰、石照耀、王长路、赵宁、王延忠、陶常彬、张元国。

本标准所代替标准的历次版本发布情况为：

——GB/T 11365—1989。

ICS 21.200
J 17

中华人民共和国国家标准

GB/T 10089—2018
代替 GB/T 10089—1988

圆柱蜗杆、蜗轮精度

Accuracy of cylindrical worm and wormwheel

2018-05-14 发布　　　　2018-12-01 实施

国家市场监督管理总局
中国国家标准化管理委员会　发布

前　言

本标准按照 GB/T 1.1—2009 给出的规则起草。

本标准代替 GB/T 10089—1988《圆柱蜗杆、蜗轮精度》。

本标准与 GB/T 10089—1988 相比,主要变化如下:

——增加了标准的前言;

——修改了标准的适用范围(见第 1 章,1988 年版的第 1 章);

——删除了对 GB/T 1800、GB/T 10086 和 GB/T 10087 的引用,增加引用了 GB/T 3374.2(见第 2 章,1988 年版的第 2 章);

——修改了蜗杆蜗轮轮齿尺寸参数偏差的术语定义和代号,其中删除了蜗杆一转螺旋线偏差、蜗杆轴向齿距累积偏差、蜗轮 k 个齿距累积偏差、蜗轮径向综合偏差、齿厚偏差、蜗杆副的中心距偏差、蜗杆副的中间平面偏移、蜗杆副的轴交角偏差及蜗杆副的侧隙的术语定义和代号,增加了相邻齿距偏差的术语定义和代号(见第 3 章,1988 年版的第 3 章);

——增加了"符号"一章(见第 4 章);

——修改了有关精度制的构成等的要求,其中删除了有关公差组的规定(见第 5 章,1988 年版的第 4 章);

——删除了关于齿坯的要求(1988 年版的第 5 章);

——修改了偏差允许值的计算公式(见第 6 章,1988 年版的附录 A);

——增加了"检验规则"一章(见第 7 章);

——修改了偏差允许值表格中的参数分段及数值(见第 8 章,1988 年版的第 6 章);

——删除了蜗杆副的中心距偏差、蜗杆副的中间平面偏移、蜗杆副的轴交角偏差及蜗杆副的侧隙的要求(见 1988 年版的第 7 章、第 8 章);

——删除了其他说明和图样标注的要求(见 1988 年版的第 9 章、第 10 章)。

请注意本文件的某些内容可能涉及专利。本文件的发布机构不承担识别这些专利的责任。

本标准由全国齿轮标准化技术委员会(SAC/TC 52)提出并归口。

本标准起草单位:重庆机床(集团)有限责任公司、郑州机械研究所有限公司、北京工业大学。

本标准主要起草人:李先广、李毅、喻可斌、张元国、石照耀、张良、隆林、李明玉、谢小卿、李武、黄光荣、王志刚、陆军。

本标准所代替标准的历次版本发布情况为:

——GB/T 10089—1988。

圆柱蜗杆、蜗轮精度

1 范围

本标准规定了圆柱蜗杆蜗轮传动机构的精度。

本标准适用于轴交角$\Sigma=90°$,最大模数 $m=40$ mm 及最大分度圆直径 $d=2\ 500$ mm 的圆柱蜗杆蜗轮传动机构。最大分度圆直径 $d>2\ 500$ mm 的圆柱蜗杆蜗轮传动机构可参照本标准使用。

2 规范性引用文件

下列文件对于本文件的应用是必不可少的。凡是注日期的引用文件,仅注日期的版本适用于本文件。凡是不注日期的引用文件,其最新版本(包括所有的修改单)适用于本文件。

GB/T 3374.2 齿轮术语和定义 第2部分:蜗轮几何学定义

3 术语和定义

GB/T 3374.2 界定的以及下列术语和定义适用于本文件。

3.1 蜗杆偏差

3.1.1

齿廓总偏差 total profile deviation

$F_{\alpha 1}$

在轴向截面的计值范围 $L_{\alpha 1}$(齿廓的工作范围)内,包容实际齿廓迹线的两条设计齿廓迹线间的轴向距离。示例见图1。

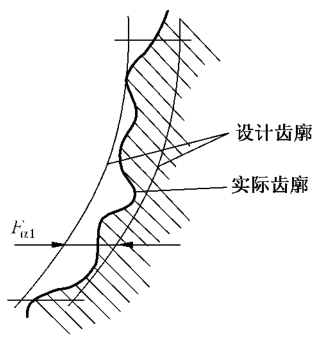

图1 ZC 蜗杆轴向截面内的齿廓总偏差 $F_{\alpha 1}$

在齿廓检验图中(见图2),齿廓总偏差 $F_{\alpha 1}$ 为两个设计齿廓迹线之间的距离(垂直于设计齿廓迹线测量)。

注: 在图2中,设计齿廓和蜗杆的齿面形状 A、N、I、K 及 C 无关并用直线标出,实际齿廓包含在画出的范围内。

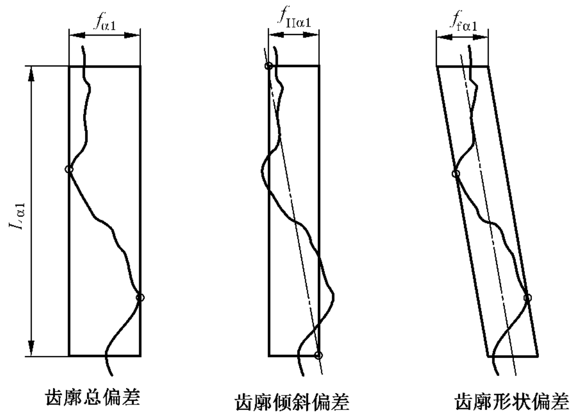

图 2　计值范围 $L_{\alpha1}$ 内的齿廓检验图

3.1.2

齿廓形状偏差　profile form deviation

$f_{f\alpha1}$

在轴向截面的计值范围 $L_{\alpha1}$ 内，包容实际齿廓迹线的，与平均齿廓迹线平行的两条辅助线间的距离（垂直于设计齿廓迹线测量，见图 2）。

注：本标准没有给出齿廓形状偏差 $f_{f\alpha1}$ 的允许值。

3.1.3

齿廓倾斜偏差　profile slope deviation

$f_{H\alpha1}$

在轴向截面的计值范围 $L_{\alpha1}$ 内，与平均齿廓迹线相交的两条平行于设计齿廓迹线的辅助线间的距离（见图 2）。

注：本标准没有给出齿廓倾斜偏差 $f_{H\alpha1}$ 的允许值。

3.1.4

轴向齿距偏差　axial pitch deviation

f_{px}

在蜗杆轴向截面内实际齿距和公称齿距之差。

3.1.5

相邻轴向齿距偏差　adjacent axial pitch deviation

f_{ux}

在蜗杆轴向截面内两相邻齿距之差。

3.1.6

径向跳动偏差　radial run-out deviation

F_{r1}

在蜗杆任意一转范围内，测头在齿槽内与齿高中部的齿面双面接触，其测头相对于蜗杆主导轴线的径向最大变动量。

注：径向跳动偏差是由蜗杆轮齿中点圆柱面的轴线和蜗杆轴承位置决定的蜗杆主导轴线之间的距离和交叉角度造成的。

3.1.7

导程偏差　lead deviation

F_{pz}

蜗杆导程的实际尺寸和公称尺寸之差。

3.2 蜗轮偏差

3.2.1

单个齿距偏差　single pitch deviation

f_{p2}

在蜗轮分度圆上，实际齿距与公称齿距之差。

用相对法测量时，公称齿距是指所有实际齿距的平均值。

注：当实际齿距大于平均值时为正偏差；当实际齿距小于平均值时为负偏差。

3.2.2

齿距累积总偏差　total cumulative pitch deviation

F_{p2}

在蜗轮分度圆上，任意两个同侧齿面间的实际弧长与公称弧长之差的最大绝对值。

3.2.3

相邻齿距偏差　adjacent pitch deviation

f_{u2}

蜗轮右齿面或左齿面两个相邻齿距的实际尺寸之差。

3.2.4

齿廓总偏差　total profile deviation

$F_{\alpha 2}$

在轮齿给定截面的计值范围内，包容实际齿廓迹线的两条设计齿廓迹线间的距离。

3.2.5

径向跳动偏差　radial run-out deviation

F_{r2}

在蜗轮一转范围内，测头在靠近中间平面的齿槽内与齿高中部的齿面双面接触，其测头相对于蜗轮轴线径向距离的最大变动量。

注：径向跳动偏差是由轮齿偏心以及由于右齿面和左齿面的齿距偏差而产生的齿槽宽的不均匀性和轮齿轴线相对于主导轴线的偏移量(偏心量)造成的。

3.3 啮合偏差

3.3.1

单面啮合偏差　single-flank enagement deviation

F_i'

蜗轮实际旋转位置和理论旋转位置的波动。理论旋转位置是由蜗杆的旋转确定的。当旋转方向确定时(左侧齿面啮合或右侧齿面啮合)，单面啮合偏差等于蜗轮旋转一周范围内相对于起始位置的最大偏差之和(见图 3)。

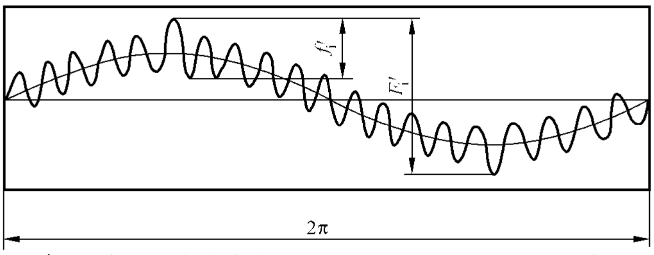

注：单面啮合偏差 F_{i1}' 和 F_{i2}' 是用标准蜗轮或者标准蜗杆测量得到的。如果没有标准蜗轮和标准蜗杆，则使用配对的蜗杆蜗轮副，其单面啮合偏差为 F_{i12}'。

图 3　蜗轮旋转时单面啮合偏差 F_i' 和单面一齿啮合偏差 f_i'

3.3.2

单面一齿啮合偏差　tooth-to-tooth single-flank engagement deviation

f_i'

一个齿啮合过程中旋转位置的偏差(见图3)。

注：单面一齿啮合偏差 f_{i1}' 和 f_{i2}' 是用标准蜗轮或者标准蜗杆测量得到的。如果没有标准蜗轮和标准蜗杆，则使用配对的蜗杆蜗轮副，其单面一齿啮合偏差为 f_{i12}'。

3.3.3

蜗杆副的接触斑点　worm gearing engagement pattern

安装好的蜗杆副中，在轻微力的制动下，蜗杆与蜗轮啮合运转后，在蜗轮齿面上分布的接触痕迹。

注：接触斑点以接触面积大小、形状和分布位置表示(见图4)。

接触面积大小按接触痕迹的百分比计算确定：

沿齿长方向——接触痕迹的长度 b'' 与工作长度 b' 之比的百分数，即 $(b''/b')\times 100\%$(在确定接触痕迹长度 b'' 时，应扣除超过模数值的断开部分)；

沿齿高方向——接触痕迹的平均高度 h'' 与工作高度 h' 之比的百分数，即 $(h''/h')\times 100\%$。

接触形状以齿面接触痕迹总的几何形状的状态确定。

接触位置以接触痕迹离齿面啮入、啮出端或齿顶、齿根的位置确定。

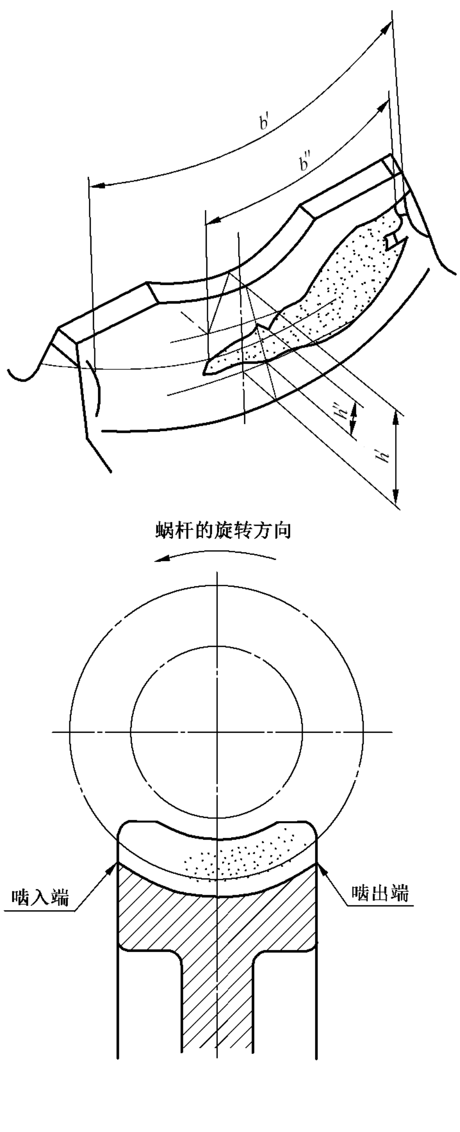

图4　蜗杆副的接触斑点

4 符号

下列符号适用于本文件。

4.1 蜗杆、蜗轮的参数(长度单位:毫米)

a　中心距
b'　蜗杆副接触面的工作长度
b''　蜗杆副接触痕迹的长度
d_1　蜗杆分度圆直径
d_2　蜗轮分度圆直径
h'　蜗杆副接触面的工作高度
h''　蜗杆副接触痕迹的平均高度
l　蜗杆测量长度
m_x　蜗杆轴向模数
m_t　蜗轮端面模数
z_1　蜗杆头数
z_2　蜗轮齿数
L_α　齿廓计值范围
φ　精度等级级间公比
Σ　轴交角

4.2 蜗杆、蜗轮的偏差(单位:微米)

f　单项偏差
$f_{f\alpha}$　齿廓形状偏差
$f_{f\alpha1}$　蜗杆齿廓形状偏差
$f_{f\alpha2}$　蜗轮齿廓形状偏差
$f_{H\alpha}$　齿廓倾斜偏差
$f_{H\alpha1}$　蜗杆齿廓倾斜偏差
$f_{H\alpha2}$　蜗轮齿廓倾斜偏差
f_i'　单面一齿啮合偏差
f_{i1}'　用标准蜗轮测量得到的单面一齿啮合偏差
f_{i2}'　用标准蜗杆测量得到的单面一齿啮合偏差
f_{i12}'　用配对的蜗杆副测量得到的单面一齿啮合偏差
f_p　单个齿距偏差
f_{px}　蜗杆轴向齿距偏差
f_{p2}　蜗轮单个齿距偏差
f_u　相邻齿距偏差
f_{ux}　蜗杆相邻轴向齿距偏差
f_{u2}　蜗轮相邻齿距偏差
F　总偏差
F_i'　单面啮合偏差
F_{i1}'　用标准蜗轮测量得到的单面啮合偏差

F'_{i2} 用标准蜗杆测量得到的单面啮合偏差

F'_{i12} 用配对的蜗杆副测量得到的单面啮合偏差

F_{pz} 蜗杆导程偏差

F_{p2} 蜗轮齿距累积总偏差

F_r 径向跳动偏差

F_{r1} 蜗杆径向跳动偏差

F_{r2} 蜗轮径向跳动偏差

F_α 齿廓总偏差

$F_{\alpha1}$ 蜗杆齿廓总偏差

$F_{\alpha2}$ 蜗轮齿廓总偏差

5 精度制的构成

5.1 总则

为了满足蜗杆蜗轮传动机构的所有性能要求,如传动的平稳性、载荷分布均匀性、传递运动的准确性以及长使用寿命,应保证蜗杆蜗轮的轮齿尺寸参数偏差以及中心距偏差和轴交角偏差在规定的允许值范围内。

注:中心距偏差和轴交角偏差的允许值在本标准中未作规定。

5.2 轮齿尺寸参数的偏差

单项偏差 f 是指蜗杆蜗轮传动机构轮齿单项尺寸参数的偏差,例如齿距偏差等。总偏差 F 包括多个单项偏差的综合影响。蜗杆蜗轮传动机构轮齿尺寸参数偏差的定义在第 3 章中给出。

5.3 精度等级

本标准对蜗杆蜗轮传动机构规定了 12 个精度等级;第 1 级的精度最高,第 12 级的精度最低。

根据使用要求不同,允许选用不同精度等级的偏差组合。

蜗杆和配对蜗轮的精度等级一般取成相同,也允许取成不相同。在硬度高的钢制蜗杆和材质较软的蜗轮组成的传动机构中,可选择比蜗轮精度等级高的蜗杆,在磨合期可使蜗轮的精度提高。例如蜗杆可以选择 8 级精度,蜗轮选择 9 级精度。

5.4 偏差的允许值

把测量出的偏差与表 1～表 12 规定的数值进行比较,以评定蜗杆蜗轮的精度等级。表中的数值是用第 6 章中对 5 级精度规定的公式乘以级间公比 φ 计算出来的。

两相邻精度等级的级间公比 φ 为:$\varphi=1.4$(1～9 级精度);$\varphi=1.6$(9 级精度以下);径向跳动偏差 F_r的级间公比为 $\varphi=1.4$(1～12 级精度)。

例如,计算 7 级精度的偏差允许值时,5 级精度的未修约的计算值乘以 1.4^2,然后再按照 5.5 规定的规则修约。

5.5 修约规则

表 1～表 12 列出的数值是用第 6 章的公式计算并修约后的数值。如果计算值小于 10 μm,修约到最接近的相差小于 0.5 μm 的小数或整数,如果大于 10 μm,修约到最接近的整数。

6 5级精度的蜗杆蜗轮偏差允许值的计算公式

6.1 单个齿距偏差 f_p 的计算公式：

$$f_p = 4 + 0.315 \cdot (m_x + 0.25 \cdot \sqrt{d})$$

6.2 相邻齿距偏差 f_u 的计算公式：

$$f_u = 5 + 0.4 \cdot (m_x + 0.25 \cdot \sqrt{d})$$

6.3 导程偏差 F_{pz} 的计算公式：

$$F_{pz} = 4 + 0.5 \cdot z_1 + 5 \cdot \sqrt[3]{z_1} \cdot (\lg m_x)^2$$

6.4 齿距累积总偏差 F_{p2} 的计算公式：

$$F_{p2} = 7.25 \cdot d_2^{\frac{1}{5}} \cdot m_x^{\frac{1}{7}}$$

6.5 齿廓总偏差 F_α 的计算公式：

$$F_\alpha = \sqrt{(f_{H\alpha})^2 + (f_{f\alpha})^2}$$

6.6 齿廓倾斜偏差 $f_{H\alpha}$ 的计算公式：

$$f_{H\alpha} = 2.5 + 0.25 \cdot (m_x + 3 \cdot \sqrt{m_x})$$

6.7 齿廓形状偏差 $f_{f\alpha}$ 的计算公式：

$$f_{f\alpha} = 1.5 + 0.25 \cdot (m_x + 9 \cdot \sqrt{m_x})$$

6.8 径向跳动偏差 F_r 的计算公式：

$$F_r = 1.68 + 2.18 \cdot \sqrt{m_x} + (2.3 + 1.2\lg m_x) \cdot d^{\frac{1}{4}}$$

6.9 单面啮合偏差 F_i' 的计算公式：

$$F_i' = 5.8 \cdot d^{\frac{1}{5}} \cdot m_x^{\frac{1}{7}} + 0.8 \cdot F_\alpha$$

6.10 单面一齿啮合偏差 f_i' 的计算公式：

$$f_i' = 0.7 \cdot (f_p + F_\alpha)$$

6.11 公式中的参数 m_x、d 和 z_1 的取值为各参数分段界限值的几何平均值；公式中 m_x 和 d 的单位均为 mm，偏差允许值的单位为 μm；公式中的蜗杆头数 $z_1 > 6$ 时取平均数 $z_1 = 8.5$ 计算；公式中蜗杆蜗轮的模数 $m_x = m_t$；计算 F_α、F_i' 和 f_i' 偏差允许值时应取 $f_{H\alpha}$、$f_{f\alpha}$、F_α 和 f_p 计算修约后的数值。

7 检验规则

7.1 径向跳动偏差

蜗轮：应测量蜗轮分度圆的齿宽中间位置。

蜗杆：一般通过间接测量齿距变动得到径向跳动偏差值。

7.2 单个齿距偏差和相邻齿距偏差

蜗轮：应测量蜗轮分度圆的齿宽中间位置。

蜗杆：在分度圆柱面测量轴向齿距偏差。多头蜗杆还要测量其他轴向截面，直到获得蜗杆所有齿的偏差。

7.3 齿距累积总偏差

蜗轮：应测量蜗轮分度圆的齿宽中间位置。

7.4 单面啮合偏差和单面一齿啮合偏差

单面啮合检验反映了蜗杆蜗轮啮合过程中的轮齿单项参数偏差对啮合过程的综合影响。蜗杆和蜗

轮在给定的中心距内啮合，蜗杆右齿面或者左齿面始终与蜗轮配对齿面处于啮合状态，如果没有固定的工作齿面，则必须检测右齿面和左齿面。

使用标准蜗杆蜗轮副检验单面啮合偏差 F_i'和单面一齿啮合偏差 f_i'。一般来说没有标准的蜗杆蜗轮副，在企业中一般使用单面啮合检测仪检验配对蜗杆蜗轮副。如果企业中没有用于单面啮合检验的单面啮合检测仪，也可检验配对蜗杆蜗轮副的接触斑点，其要求见附录 A。

7.5 齿廓总偏差

应在齿根圆和齿顶圆范围内测量齿廓总偏差。在蜗杆轴向截面内测量齿廓总偏差，在蜗轮中间平面内测量齿廓总偏差。

7.6 导程偏差

在蜗杆啮合范围内的测量长度 l 内测量导程偏差。测量长度可参照表 1～表 12 的规定。如果蜗杆实际啮合长度小于规定的测量长度 l，蜗杆导程偏差 F_{pz}要直接按照实际啮合长度测量。

8 轮齿尺寸参数偏差的允许值

蜗杆蜗轮轮齿尺寸参数偏差各精度等级的允许值见表 1～表 12。表中的数值和蜗杆轴向模数 m_x、蜗轮端面模数 m_t、分度圆直径 d 以及蜗杆头数 z_1 有关。测量蜗杆偏差时要用到蜗杆分度圆直径 d_1，测量蜗轮偏差时要用到蜗轮分度圆直径 d_2。

对于蜗杆副的单面啮合偏差 F_i'和单面一齿啮合偏差 f_i'的偏差允许值，其计算公式为：

$$F_i'=\sqrt{(F_{i1}')^2+(F_{i2}')^2}$$

$$f_i'=\sqrt{(f_{i1}')^2+(f_{i2}')^2}$$

表 1 1 级精度轮齿偏差的允许值

单位为微米

模数 $m(m_t,m_x)$/mm	偏差		分度圆直径 d/mm						
	F_α		>10～50	>50～125	>125～280	>280～560	>560～1 000	>1 000～1 600	>1 600～2 500
>0.5～2.0	1.5	f_u	1.5	1.5	2.0	2.0	2.0	2.5	2.5
		f_p	1.0	1.5	1.5	1.5	1.5	2.0	2.0
		F_{pz}	3.5	4.5	5.5	6.0	7.0	8.0	8.5
		F_r	2.5	3.0	3.0	3.5	4.0	4.5	5.0
		F_i'	4.0	4.5	5.5	6.0	7.0	7.5	8.0
		f_i'	2.0	2.0	2.0	2.0	2.0	2.5	2.5
>2.0～3.55	2.0	f_u	1.5	2.0	2.0	2.0	2.5	2.5	3.0
		f_p	1.5	1.5	1.5	1.5	2.0	2.0	2.0
		F_{pz}	4.0	5.0	6.0	7.5	8.0	9.0	10.0
		F_r	3.0	3.5	4.0	4.5	5.0	5.5	6.0
		F_i'	4.5	5.5	6.5	7.5	8.0	9.0	9.5
		f_i'	2.5	2.5	2.5	2.5	2.5	3.0	3.0
>3.55～6.0	2.5	f_u	2.0	2.0	2.0	2.5	2.5	2.5	3.0
		f_p	1.5	1.5	1.5	2.0	2.0	2.0	2.5
		F_{pz}	4.5	5.5	7.0	8.0	9.0	10.0	11.0
		F_r	3.5	4.0	4.5	5.0	6.0	6.5	7.0
		F_i'	5.5	6.5	7.5	8.0	9.0	10.0	11.0
		f_i'	3.0	3.0	3.0	3.0	3.0	3.5	3.5

表 1（续）

单位为微米

模数	偏差		分度圆直径 d/mm						
$m(m_t, m_x)$/mm	F_α		>10 ~50	>50 ~125	>125 ~280	>280 ~560	>560 ~1 000	>1 000 ~1 600	>1 600 ~2 500
>6.0 ~10	3.0	f_u	2.0	2.5	2.5	2.5	3.0	3.0	3.5
		f_p	2.0	2.0	2.0	2.0	2.0	2.5	2.5
		F_{p2}	4.5	6.0	7.5	8.5	9.5	11.0	11.0
		F_r	4.0	4.5	5.0	6.0	6.5	7.5	8.0
		F_i'	6.0	7.5	8.5	9.0	10.0	11.0	12.0
		f_i'	3.5	3.5	3.5	3.5	3.5	4.0	4.0
>10 ~16	4.0	f_u	3.0	3.0	3.0	3.0	3.5	3.5	4.0
		f_p	2.0	2.0	2.5	2.5	2.5	3.0	3.0
		F_{p2}	5.0	6.5	8.0	9.0	10.0	11.0	12.0
		F_r	4.5	5.0	6.0	7.0	7.5	8.0	9.0
		F_i'	7.5	8.5	9.5	10.0	11.0	12.0	13.0
		f_i'	4.5	4.5	4.5	4.5	4.5	5.0	5.0
>16 ~25	5.0	f_u	3.5	3.5	3.5	4.0	4.0	4.5	4.5
		f_p	3.0	3.0	3.0	3.0	3.0	3.5	3.5
		F_{p2}	5.5	7.0	8.5	9.5	11.0	12.0	13.0
		F_r	5.0	6.0	7.0	7.5	8.5	9.0	9.5
		F_i'	8.5	9.5	11.0	12.0	13.0	14.0	15.0
		f_i'	5.5	5.5	5.5	5.5	5.5	6.0	6.0
>25 ~40	7.0	f_u	4.5	5.0	5.0	5.0	5.0	5.5	6.0
		f_p	3.5	4.0	4.0	4.0	4.0	4.5	4.5
		F_{p2}	5.5	7.5	9.0	10.0	12.0	13.0	14.0
		F_r	6.0	7.0	7.5	8.5	9.0	10.0	11.0
		F_i'	10.0	11.0	13.0	14.0	15.0	16.0	17.0
		f_i'	7.5	7.5	7.5	8.0	8.0	8.0	8.0
偏差 F_{pz}									
测量长度/mm			15	25	45	75	125	200	300
轴向模数 m_x/mm			>0.5 ~2	>2 ~3.55	>3.55 ~6	>6 ~10	>10 ~16	>16 ~25	>25 ~40
蜗杆头数 z_1	1		1.0	1.5	1.5	2.0	3.0	3.5	4.0
	2		1.5	1.5	2.0	2.5	3.5	4.0	5.0
	3 和 4		1.5	2.0	2.5	3.0	4.0	5.0	6.0
	5 和 6		1.5	2.0	3.0	3.5	4.5	5.5	7.0
	>6		2.0	2.5	3.5	4.0	5.5	7.0	8.0

表 2　2 级精度轮齿偏差的允许值

单位为微米

模数 $m(m_t,m_x)$/mm	偏差		分度圆直径 d/mm						
	F_α		>10~50	>50~125	>125~280	>280~560	>560~1 000	>1 000~1 600	>1 600~2 500
>0.5~2.0	2.0	f_u	2.0	2.5	2.5	2.5	3.0	3.5	3.5
		f_p	1.5	2.0	2.0	2.0	2.5	2.5	3.0
		F_{p2}	4.5	6.0	7.5	8.5	10.0	11.0	12.0
		F_r	3.5	4.0	4.5	5.0	6.0	6.5	7.0
		F_i'	5.5	6.5	7.5	8.5	9.5	11.0	11.0
		f_i'	2.5	2.5	2.5	3.0	3.0	3.5	3.5
>2.0~3.55	2.5	f_u	2.5	2.5	2.5	3.0	3.5	3.5	4.0
		f_p	2.0	2.0	2.0	2.5	2.5	2.5	3.0
		F_{p2}	6.0	7.5	8.5	10.0	11.0	13.0	14.0
		F_r	4.0	5.0	6.0	6.5	7.5	8.0	8.5
		F_i'	6.5	8.0	9.0	10.0	11.0	12.0	13.0
		f_i'	3.5	3.5	3.5	3.5	3.5	4.0	4.0
>3.55~6.0	3.5	f_u	2.5	2.5	3.0	3.5	3.5	3.5	4.0
		f_p	2.0	2.0	2.5	2.5	2.5	3.0	3.5
		F_{p2}	6.0	8.0	9.5	11.0	12.0	14.0	15.0
		F_r	4.5	6.0	6.5	7.5	8.5	9.0	10.0
		F_i'	7.5	9.0	10.0	11.0	13.0	14.0	15.0
		f_i'	4.0	4.0	4.0	4.5	4.5	4.5	4.5
>6.0~10	4.5	f_u	3.0	3.5	3.5	3.5	4.0	4.5	4.5
		f_p	2.5	2.5	2.5	3.0	3.0	3.5	3.5
		F_{p2}	6.5	8.5	10.0	12.0	13.0	15.0	16.0
		F_r	5.5	6.5	7.5	8.5	9.0	10.0	11.0
		F_i'	8.5	10.0	12.0	13.0	14.0	15.0	16.0
		f_i'	4.5	4.5	5.0	5.0	5.0	5.5	5.5
>10~16	6.0	f_u	4.0	4.0	4.0	4.5	4.5	5.0	5.5
		f_p	3.0	3.0	3.5	3.5	3.5	4.0	4.5
		F_{p2}	7.0	9.0	11.0	12.0	14.0	16.0	17.0
		F_r	6.0	7.5	8.5	9.5	10.0	11.0	12.0
		F_i'	10.0	12.0	13.0	15.0	16.0	17.0	19.0
		f_i'	6.0	6.0	6.5	6.5	6.5	7.0	7.5
>16~25	7.5	f_u	4.5	5.0	5.0	5.5	6.0	6.0	6.0
		f_p	4.0	4.0	4.0	4.5	4.5	4.5	5.0
		F_{p2}	7.5	10.0	12.0	13.0	15.0	17.0	19.0
		F_r	7.5	8.5	9.5	11.0	12.0	12.0	13.0
		F_i'	12.0	13.0	15.0	16.0	18.0	19.0	21.0
		f_i'	8.0	8.0	8.0	8.0	8.0	8.5	8.5
>25~40	10.0	f_u	6.5	7.0	7.0	7.5	7.5	7.5	8.0
		f_p	5.0	5.5	5.5	6.0	6.0	6.0	6.0
		F_{p2}	8.0	10.0	12.0	14.0	16.0	18.0	20.0
		F_r	8.5	9.5	11.0	12.0	13.0	14.0	15.0
		F_i'	14.0	16.0	18.0	19.0	21.0	22.0	24.0
		f_i'	11.0	11.0	11.0	11.0	11.0	11.0	11.0
偏差 F_{pz}									
测量长度/mm			15	25	45	75	125	200	300
轴向模数 m_x/mm			>0.5~2	>2~3.55	>3.55~6	>6~10	>10~16	>16~25	>25~40
蜗杆头数 z_1	1		1.5	2.0	2.5	3.0	4.0	4.5	6.0
	2		2.0	2.0	3.0	3.5	4.5	6.0	7.0
	3 和 4		2.0	2.5	3.5	4.5	5.5	7.0	8.5
	5 和 6		2.5	3.0	4.0	5.0	6.0	8.0	10.0
	>6		3.0	3.5	4.5	6.0	7.5	9.5	11.0

表 3　3 级精度轮齿偏差的允许值

单位为微米

模数 $m(m_t,m_x)$/mm	偏差		分度圆直径 d/mm						
	F_α		>10 ~50	>50 ~125	>125 ~280	>280 ~560	>560 ~1 000	>1 000 ~1 600	>1 600 ~2 500
>0.5 ~2.0	3.0	f_u	3.0	3.5	3.5	4.0	4.0	4.5	5.0
		f_p	2.5	2.5	3.0	3.0	3.5	3.5	4.0
		F_{p2}	6.5	8.5	11.0	12.0	14.0	15.0	17.0
		F_r	4.5	5.5	6.0	7.0	8.0	9.0	9.5
		F_i'	7.5	9.0	11.0	12.0	13.0	15.0	16.0
		f_i'	3.5	4.0	4.0	4.0	4.5	4.5	5.0
>2.0 ~3.55	4.0	f_u	3.5	3.5	4.0	4.0	4.5	5.0	5.5
		f_p	2.5	3.0	3.0	3.5	3.5	4.0	4.5
		F_{p2}	8.0	10.0	12.0	14.0	16.0	18.0	19.0
		F_r	5.5	7.0	8.0	9.0	10.0	11.0	12.0
		F_i'	9.0	11.0	13.0	14.0	16.0	17.0	19.0
		f_i'	4.5	4.5	5.0	5.0	5.0	5.5	5.5
>3.55 ~6.0	5.0	f_u	4.0	4.0	4.0	4.5	5.0	5.0	5.5
		f_p	3.0	3.0	3.5	3.5	4.0	4.5	4.5
		F_{p2}	8.5	11.0	13.0	15.0	17.0	19.0	21.0
		F_r	6.5	8.0	9.0	10.0	12.0	13.0	14.0
		F_i'	11.0	13.0	14.0	16.0	18.0	19.0	21.0
		f_i'	5.5	5.5	5.5	6.0	6.0	6.5	6.5
>6.0 ~10	6.0	f_u	4.5	4.5	5.0	5.0	5.5	6.0	6.5
		f_p	3.5	3.5	4.0	4.0	4.5	4.5	5.0
		F_{p2}	9.0	12.0	14.0	16.0	18.0	21.0	22.0
		F_r	7.5	9.0	10.0	12.0	13.0	14.0	15.0
		F_i'	12.0	14.0	16.0	18.0	20.0	21.0	23.0
		f_i'	6.5	6.5	7.0	7.0	7.0	7.5	7.5
>10 ~16	8.0	f_u	5.5	5.5	5.5	6.0	6.5	7.0	7.5
		f_p	4.5	4.5	4.5	5.0	5.0	5.5	6.0
		F_{p2}	9.5	13.0	15.0	17.0	20.0	22.0	24.0
		F_r	8.5	10.0	12.0	13.0	14.0	16.0	17.0
		F_i'	14.0	17.0	19.0	20.0	22.0	24.0	26.0
		f_i'	8.5	8.5	9.0	9.0	9.0	9.5	10.0
>16 ~25	10.0	f_u	6.5	7.0	7.0	7.5	8.0	8.5	8.5
		f_p	5.5	5.5	5.5	6.0	6.0	6.5	7.0
		F_{p2}	11.0	14.0	16.0	19.0	21.0	23.0	26.0
		F_r	10.0	12.0	13.0	15.0	16.0	17.0	19.0
		F_i'	17.0	19.0	21.0	23.0	25.0	27.0	29.0
		f_i'	11.0	11.0	11.0	11.0	11.0	12.0	12.0
>25 ~40	14.0	f_u	9.0	9.5	9.5	10.0	10.0	11.0	11.0
		f_p	7.0	7.5	7.5	8.0	8.0	8.5	8.5
		F_{p2}	11.0	14.0	17.0	20.0	23.0	26.0	28.0
		F_r	12.0	13.0	15.0	16.0	18.0	19.0	21.0
		F_i'	20.0	22.0	25.0	27.0	29.0	31.0	33.0
		f_i'	15.0	15.0	15.0	15.0	15.0	16.0	16.0
偏差 F_{pz}									
测量长度/mm			15	25	45	75	125	200	300
轴向模数 m_x/mm			>0.5 ~2	>2 ~3.55	>3.55 ~6	>6 ~10	>10 ~16	>16 ~25	>25 ~40
蜗杆头数 z_1	1		2.5	3.0	3.5	4.5	5.5	6.5	8.0
	2		2.5	3.0	4.0	5.0	6.5	8.0	9.5
	3 和 4		3.0	3.5	4.5	6.0	7.5	9.5	12.0
	5 和 6		3.5	4.5	5.5	7.0	8.5	11.0	14.0
	>6		4.5	5.0	6.5	8.0	11.0	13.0	16.0

表 4　4 级精度轮齿偏差的允许值

单位为微米

模数 $m(m_t,m_x)$/mm	偏差		分度圆直径 d/mm						
	F_α		>10～50	>50～125	>125～280	>280～560	>560～1 000	>1 000～1 600	>1 600～2 500
>0.5～2.0	4.0	f_u	4.5	4.5	5.0	5.5	5.5	6.5	7.0
		f_p	3.0	3.5	4.0	4.5	4.5	5.0	5.5
		F_{p2}	9.5	12.0	15.0	17.0	19.0	21.0	24.0
		F_r	6.5	8.0	8.5	10.0	11.0	13.0	14.0
		F_i'	11.0	13.0	15.0	17.0	19.0	21.0	22.0
		f_i'	5.0	5.5	5.5	5.5	6.0	6.5	7.0
>2.0～3.55	5.5	f_u	4.5	5.0	5.5	5.5	6.5	7.0	8.0
		f_p	3.5	4.0	4.5	4.5	5.0	5.5	6.0
		F_{p2}	11.0	14.0	17.0	20.0	22.0	25.0	27.0
		F_r	8.0	10.0	11.0	13.0	14.0	16.0	17.0
		F_i'	13.0	16.0	18.0	20.0	22.0	24.0	26.0
		f_i'	6.5	6.5	7.0	7.0	7.0	8.0	8.0
>3.55～6.0	7.0	f_u	5.5	5.5	5.5	6.5	7.0	7.0	8.0
		f_p	4.5	4.5	4.5	5.0	5.5	6.0	6.5
		F_{p2}	12.0	16.0	19.0	21.0	24.0	27.0	29.0
		F_r	9.5	11.0	13.0	14.0	16.0	18.0	19.0
		F_i'	15.0	18.0	20.0	22.0	25.0	27.0	29.0
		f_i'	8.0	8.0	8.0	8.5	8.5	9.5	9.5
>6.0～10	8.5	f_u	6.0	6.5	7.0	7.0	8.0	8.5	9.5
		f_p	5.0	5.0	5.5	5.5	6.0	6.5	7.0
		F_{p2}	13.0	16.0	20.0	23.0	26.0	29.0	31.0
		F_r	11.0	13.0	14.0	16.0	18.0	20.0	21.0
		F_i'	17.0	20.0	23.0	25.0	28.0	30.0	32.0
		f_i'	9.5	9.5	10.0	10.0	10.0	11.0	11.0
>10～16	11.0	f_u	8.0	8.0	8.0	8.5	9.5	10.0	11.0
		f_p	6.0	6.0	6.5	7.0	7.0	8.0	8.5
		F_{p2}	14.0	18.0	21.0	24.0	28.0	31.0	34.0
		F_r	12.0	14.0	16.0	19.0	20.0	22.0	24.0
		F_i'	20.0	24.0	26.0	29.0	31.0	34.0	36.0
		f_i'	12.0	12.0	13.0	13.0	13.0	14.0	14.0
>16～25	14.0	f_u	9.5	10.0	10.0	11.0	11.0	12.0	12.0
		f_p	8.0	8.0	8.0	8.5	8.5	9.5	10.0
		F_{p2}	15.0	19.0	23.0	26.0	30.0	33.0	36.0
		F_r	14.0	16.0	19.0	21.0	23.0	24.0	26.0
		F_i'	24.0	26.0	29.0	32.0	35.0	38.0	41.0
		f_i'	16.0	16.0	16.0	16.0	16.0	16.0	17.0
>25～40	19.0	f_u	13.0	14.0	14.0	14.0	14.0	15.0	16.0
		f_p	10.0	11.0	11.0	11.0	11.0	12.0	12.0
		F_{p2}	16.0	20.0	24.0	28.0	32.0	36.0	39.0
		F_r	16.0	19.0	21.0	23.0	25.0	27.0	29.0
		F_i'	28.0	31.0	35.0	38.0	41.0	44.0	46.0
		f_i'	21.0	21.0	21.0	21.0	21.0	22.0	22.0
偏差 F_{pz}									
测量长度/mm			15	25	45	75	125	200	300
轴向模数 m_x/mm			>0.5～2	>2～3.55	>3.55～6	>6～10	>10～16	>16～25	>25～40
蜗杆头数 z_1	1		3.0	4.0	4.5	6.0	8.0	9.5	11.0
	2		3.5	4.5	5.5	7.0	9.5	11.0	14.0
	3 和 4		4.0	5.0	6.5	8.5	11.0	14.0	16.0
	5 和 6		4.5	6.0	8.0	10.0	12.0	16.0	19.0
	>6		6.0	7.0	9.5	11.0	15.0	19.0	22.0

表 5　5 级精度轮齿偏差的允许值

单位为微米

模数 $m(m_t,m_x)$/mm	偏差		分度圆直径 d/mm						
	F_α		>10~50	>50~125	>125~280	>280~560	>560~1 000	>1 000~1 600	>1 600~2 500
>0.5~2.0	5.5	f_u	6.0	6.5	7.0	7.5	8.0	9.0	10.0
		f_p	4.5	5.0	5.5	6.0	6.5	7.0	8.0
		F_{p2}	13.0	17.0	21.0	24.0	27.0	30.0	33.0
		F_r	9.0	11.0	12.0	14.0	16.0	18.0	19.0
		F_i'	15.0	18.0	21.0	24.0	26.0	29.0	31.0
		f_i'	7.0	7.5	7.5	8.0	8.5	9.0	9.5
>2.0~3.55	7.5	f_u	6.5	7.0	7.5	8.0	9.0	9.5	11.0
		f_p	5.0	5.5	6.0	6.5	7.0	7.5	8.5
		F_{p2}	16.0	20.0	24.0	28.0	31.0	35.0	38.0
		F_r	11.0	14.0	16.0	18.0	20.0	22.0	24.0
		F_i'	18.0	22.0	25.0	28.0	31.0	34.0	37.0
		f_i'	9.0	9.0	9.5	10.0	10.0	11.0	11.0
>3.55~6.0	9.5	f_u	7.5	7.5	8.0	9.0	9.5	10.0	11.0
		f_p	6.0	6.0	6.5	7.0	7.5	8.5	9.0
		F_{p2}	17.0	22.0	26.0	30.0	34.0	38.0	41.0
		F_r	13.0	16.0	18.0	20.0	23.0	25.0	27.0
		F_i'	21.0	25.0	28.0	31.0	35.0	38.0	41.0
		f_i'	11.0	11.0	11.0	12.0	12.0	13.0	13.0
>6.0~10	12.0	f_u	8.5	9.0	9.5	10.0	11.0	12.0	13.0
		f_p	7.0	7.0	7.5	8.0	8.5	9.0	10.0
		F_{p2}	18.0	23.0	28.0	32.0	36.0	41.0	44.0
		F_r	15.0	18.0	20.0	23.0	25.0	28.0	30.0
		F_i'	24.0	28.0	32.0	35.0	39.0	42.0	45.0
		f_i'	13.0	13.0	14.0	14.0	14.0	15.0	15.0
>10~16	16.0	f_u	11.0	11.0	11.0	12.0	13.0	14.0	15.0
		f_p	8.5	8.5	9.0	9.5	10.0	11.0	12.0
		F_{p2}	19.0	25.0	30.0	34.0	39.0	43.0	48.0
		F_r	17.0	20.0	23.0	26.0	28.0	31.0	34.0
		F_i'	28.0	33.0	37.0	40.0	44.0	48.0	51.0
		f_i'	17.0	17.0	18.0	18.0	18.0	19.0	20.0
>16~25	20.0	f_u	13.0	14.0	14.0	15.0	16.0	17.0	17.0
		f_p	11.0	11.0	11.0	12.0	12.0	13.0	14.0
		F_{p2}	21.0	27.0	32.0	37.0	42.0	46.0	51.0
		F_r	20.0	23.0	26.0	29.0	32.0	34.0	37.0
		F_i'	33.0	37.0	41.0	45.0	49.0	53.0	57.0
		f_i'	22.0	22.0	22.0	22.0	22.0	23.0	24.0
>25~40	27.0	f_u	18.0	19.0	19.0	20.0	20.0	21.0	22.0
		f_p	14.0	15.0	15.0	16.0	16.0	17.0	17.0
		F_{p2}	22.0	28.0	34.0	39.0	45.0	50.0	54.0
		F_r	23.0	26.0	29.0	32.0	35.0	38.0	41.0
		F_i'	39.0	44.0	49.0	53.0	57.0	61.0	65.0
		f_i'	29.0	29.0	29.0	30.0	30.0	31.0	31.0
偏差 F_{pz}									
测量长度/mm			15	25	45	75	125	200	300
轴向模数 m_x/mm			>0.5~2	>2~3.55	>3.55~6	>6~10	>10~16	>16~25	>25~40
蜗杆头数 z_1	1		4.5	5.5	6.5	8.5	11.0	13.0	16.0
	2		5.0	6.0	8.0	10.0	13.0	16.0	19.0
	3 和 4		5.5	7.0	9.0	12.0	15.0	19.0	23.0
	5 和 6		6.5	8.5	11.0	14.0	17.0	22.0	27.0
	>6		8.5	10.0	13.0	16.0	21.0	26.0	31.0

表 6　6 级精度轮齿偏差的允许值

单位为微米

模数 $m(m_t,m_x)$/mm	偏差		分度圆直径 d/mm						
	F_α		>10 ~50	>50 ~125	>125 ~280	>280 ~560	>560 ~1 000	>1 000 ~1 600	>1 600 ~2 500
>0.5 ~2.0	7.5	f_u	8.5	9.0	10.0	11.0	11.0	13.0	14.0
		f_p	6.5	7.0	7.5	8.5	9.0	10.0	11.0
		F_{p2}	18.0	24.0	29.0	34.0	38.0	42.0	46.0
		F_r	13.0	15.0	17.0	20.0	22.0	25.0	27.0
		F_i'	21.0	25.0	29.0	34.0	36.0	41.0	43.0
		f_i'	10.0	11.0	11.0	11.0	12.0	13.0	13.0
>2.0 ~3.55	11.0	f_u	9.0	10.0	11.0	11.0	13.0	13.0	15.0
		f_p	7.0	7.5	8.5	9.0	10.0	11.0	12.0
		F_{p2}	22.0	28.0	34.0	39.0	43.0	49.0	53.0
		F_r	15.0	20.0	22.0	25.0	28.0	31.0	34.0
		F_i'	25.0	31.0	35.0	39.0	43.0	48.0	52.0
		f_i'	13.0	13.0	13.0	14.0	14.0	15.0	15.0
>3.55 ~6.0	13.0	f_u	11.0	11.0	11.0	13.0	13.0	14.0	15.0
		f_p	8.5	8.5	9.0	10.0	11.0	12.0	13.0
		F_{p2}	24.0	31.0	36.0	42.0	48.0	53.0	57.0
		F_r	18.0	22.0	25.0	28.0	32.0	35.0	38.0
		F_i'	29.0	35.0	39.0	43.0	49.0	53.0	57.0
		f_i'	15.0	15.0	15.0	17.0	17.0	18.0	18.0
>6.0 ~10	17.0	f_u	12.0	13.0	13.0	14.0	15.0	17.0	18.0
		f_p	10.0	10.0	11.0	11.0	12.0	13.0	14.0
		F_{p2}	25.0	32.0	39.0	45.0	50.0	57.0	62.0
		F_r	21.0	25.0	28.0	32.0	35.0	39.0	42.0
		F_i'	34.0	39.0	45.0	49.0	55.0	59.0	63.0
		f_i'	18.0	18.0	20.0	20.0	20.0	21.0	21.0
>10 ~16	22.0	f_u	15.0	15.0	15.0	17.0	18.0	20.0	21.0
		f_p	12.0	12.0	13.0	13.0	14.0	15.0	17.0
		F_{p2}	27.0	35.0	42.0	48.0	55.0	60.0	67.0
		F_r	24.0	28.0	32.0	36.0	39.0	43.0	48.0
		F_i'	39.0	46.0	52.0	56.0	62.0	67.0	71.0
		f_i'	24.0	24.0	25.0	25.0	25.0	27.0	28.0
>16 ~25	28.0	f_u	18.0	20.0	20.0	21.0	22.0	24.0	24.0
		f_p	15.0	15.0	15.0	17.0	17.0	18.0	20.0
		F_{p2}	29.0	38.0	45.0	52.0	59.0	64.0	71.0
		F_r	28.0	32.0	36.0	41.0	45.0	48.0	52.0
		F_i'	46.0	52.0	57.0	63.0	69.0	74.0	80.0
		f_i'	31.0	31.0	31.0	31.0	31.0	32.0	34.0
>25 ~40	38.0	f_u	25.0	27.0	27.0	28.0	28.0	29.0	31.0
		f_p	20.0	21.0	21.0	22.0	22.0	24.0	24.0
		F_{p2}	31.0	39.0	48.0	55.0	63.0	70.0	76.0
		F_r	32.0	36.0	41.0	45.0	49.0	53.0	57.0
		F_i'	55.0	62.0	69.0	74.0	80.0	85.0	91.0
		f_i'	41.0	41.0	41.0	42.0	42.0	43.0	43.0
偏差 F_{pz}									
测量长度/mm			15	25	45	75	125	200	300
轴向模数 m_x/mm			>0.5 ~2	>2 ~3.55	>3.55 ~6	>6 ~10	>10 ~16	>16 ~25	>25 ~40
蜗杆头数 z_1	1		6.5	7.5	9.0	12.0	15.0	18.0	22.0
	2		7.0	8.5	11.0	14.0	18.0	22.0	27.0
	3 和 4		7.5	10.0	13.0	17.0	21.0	27.0	32.0
	5 和 6		9.0	12.0	15.0	20.0	24.0	31.0	38.0
	>6		12.0	14.0	18.0	22.0	29.0	36.0	43.0

表7 7级精度轮齿偏差的允许值

单位为微米

模数 $m(m_t, m_x)$/mm	偏差		分度圆直径 d/mm						
	F_α		>10 ~50	>50 ~125	>125 ~280	>280 ~560	>560 ~1 000	>1 000 ~1 600	>1 600 ~2 500
>0.5 ~2.0	11.0	f_u	12.0	13.0	14.0	15.0	16.0	18.0	20.0
		f_p	9.0	10.0	11.0	12.0	13.0	14.0	16.0
		F_{p2}	25.0	33.0	41.0	47.0	53.0	59.0	65.0
		F_r	18.0	22.0	24.0	27.0	31.0	35.0	37.0
		F_i'	29.0	35.0	41.0	47.0	51.0	57.0	61.0
		f_i'	14.0	15.0	15.0	16.0	17.0	18.0	19.0
>2.0 ~3.55	15.0	f_u	13.0	14.0	15.0	16.0	18.0	19.0	22.0
		f_p	10.0	11.0	12.0	13.0	14.0	15.0	17.0
		F_{p2}	31.0	39.0	47.0	55.0	61.0	69.0	74.0
		F_r	22.0	27.0	31.0	35.0	39.0	43.0	47.0
		F_i'	35.0	43.0	49.0	55.0	61.0	67.0	73.0
		f_i'	18.0	18.0	19.0	20.0	20.0	22.0	22.0
>3.55 ~6.0	19.0	f_u	15.0	15.0	16.0	18.0	19.0	20.0	22.0
		f_p	12.0	12.0	13.0	14.0	15.0	17.0	18.0
		F_{p2}	33.0	43.0	51.0	59.0	67.0	74.0	80.0
		F_r	25.0	31.0	35.0	39.0	45.0	49.0	53.0
		F_i'	41.0	49.0	55.0	61.0	69.0	74.0	80.0
		f_i'	22.0	22.0	22.0	24.0	24.0	25.0	25.0
>6.0 ~10	24.0	f_u	17.0	18.0	19.0	20.0	22.0	24.0	25.0
		f_p	14.0	14.0	15.0	16.0	17.0	18.0	20.0
		F_{p2}	35.0	45.0	55.0	63.0	71.0	80.0	86.0
		F_r	29.0	35.0	39.0	45.0	49.0	55.0	59.0
		F_i'	47.0	55.0	63.0	69.0	76.0	82.0	88.0
		f_i'	25.0	25.0	27.0	27.0	27.0	29.0	29.0
>10 ~16	31.0	f_u	22.0	22.0	22.0	24.0	25.0	27.0	29.0
		f_p	17.0	17.0	18.0	19.0	20.0	22.0	24.0
		F_{p2}	37.0	49.0	59.0	67.0	76.0	84.0	94.0
		F_r	33.0	39.0	45.0	51.0	55.0	61.0	67.0
		F_i'	55.0	65.0	73.0	78.0	86.0	94.0	100.0
		f_i'	33.0	33.0	35.0	35.0	35.0	37.0	39.0
>16 ~25	39.0	f_u	25.0	27.0	27.0	29.0	31.0	33.0	33.0
		f_p	22.0	22.0	22.0	24.0	24.0	25.0	27.0
		F_{p2}	41.0	53.0	63.0	73.0	82.0	90.0	100.0
		F_r	39.0	45.0	51.0	57.0	63.0	67.0	73.0
		F_i'	65.0	73.0	80.0	88.0	96.0	104.0	112.0
		f_i'	43.0	43.0	43.0	43.0	43.0	45.0	47.0
>25 ~40	53.0	f_u	35.0	37.0	37.0	39.0	39.0	41.0	43.0
		f_p	27.0	29.0	29.0	31.0	31.0	33.0	33.0
		F_{p2}	43.0	55.0	67.0	76.0	88.0	98.0	106.0
		F_r	45.0	51.0	57.0	63.0	69.0	74.0	80.0
		F_i'	76.0	86.0	96.0	104.0	112.0	120.0	127.0
		f_i'	57.0	57.0	57.0	59.0	59.0	61.0	61.0

偏差 F_{pz}								
测量长度/mm		15	25	45	75	125	200	300
轴向模数 m_x/mm		>0.5 ~2	>2 ~3.55	>3.55 ~6	>6 ~10	>10 ~16	>16 ~25	>25 ~40
蜗杆头数 z_1	1	9.0	11.0	13.0	17.0	22.0	25.0	31.0
	2	10.0	12.0	16.0	20.0	25.0	31.0	37.0
	3 和 4	11.0	14.0	18.0	24.0	29.0	37.0	45.0
	5 和 6	13.0	17.0	22.0	27.0	33.0	43.0	53.0
	>6	17.0	20.0	25.0	31.0	41.0	51.0	61.0

表 8　8 级精度轮齿偏差的允许值

单位为微米

模数 $m(m_t,m_x)$/mm	偏差		分度圆直径 d/mm						
	F_α		＞10～50	＞50～125	＞125～280	＞280～560	＞560～1 000	＞1 000～1 600	＞1 600～2 500
＞0.5～2.0	15.0	f_u	16.0	18.0	19.0	21.0	22.0	25.0	27.0
		f_p	12.0	14.0	15.0	16.0	18.0	19.0	22.0
		F_{p2}	36.0	47.0	58.0	66.0	74.0	82.0	91.0
		F_r	25.0	30.0	33.0	38.0	44.0	49.0	52.0
		F_i'	41.0	49.0	58.0	66.0	71.0	80.0	85.0
		f_i'	19.0	21.0	21.0	22.0	23.0	25.0	26.0
＞2.0～3.55	21.0	f_u	18.0	19.0	21.0	22.0	25.0	26.0	30.0
		f_p	14.0	15.0	16.0	18.0	19.0	21.0	23.0
		F_{p2}	44.0	55.0	66.0	77.0	85.0	96.0	104.0
		F_r	30.0	38.0	44.0	49.0	55.0	60.0	66.0
		F_i'	49.0	60.0	69.0	77.0	85.0	93.0	102.0
		f_i'	25.0	25.0	26.0	27.0	27.0	30.0	30.0
＞3.55～6.0	26.0	f_u	21.0	21.0	22.0	25.0	26.0	27.0	30.0
		f_p	16.0	16.0	18.0	19.0	21.0	23.0	25.0
		F_{p2}	47.0	60.0	71.0	82.0	93.0	104.0	113.0
		F_r	36.0	44.0	49.0	55.0	63.0	69.0	74.0
		F_i'	58.0	69.0	77.0	85.0	96.0	104.0	113.0
		f_i'	30.0	30.0	30.0	33.0	33.0	36.0	36.0
＞6.0～10	33.0	f_u	23.0	25.0	26.0	27.0	30.0	33.0	36.0
		f_p	19.0	19.0	21.0	22.0	23.0	25.0	27.0
		F_{p2}	49.0	63.0	77.0	88.0	99.0	113.0	121.0
		F_r	41.0	49.0	55.0	63.0	69.0	77.0	82.0
		F_i'	66.0	77.0	88.0	96.0	107.0	115.0	123.0
		f_i'	36.0	36.0	38.0	38.0	38.0	41.0	41.0
＞10～16	44.0	f_u	30.0	30.0	30.0	33.0	36.0	38.0	41.0
		f_p	23.0	23.0	25.0	26.0	27.0	30.0	33.0
		F_{p2}	52.0	69.0	82.0	93.0	107.0	118.0	132.0
		F_r	47.0	55.0	63.0	71.0	77.0	85.0	93.0
		F_i'	77.0	91.0	102.0	110.0	121.0	132.0	140.0
		f_i'	47.0	47.0	49.0	49.0	49.0	52.0	55.0
＞16～25	55.0	f_u	36.0	38.0	38.0	41.0	44.0	47.0	47.0
		f_p	30.0	30.0	30.0	33.0	33.0	36.0	38.0
		F_{p2}	58.0	74.0	88.0	102.0	115.0	126.0	140.0
		F_r	55.0	63.0	71.0	80.0	88.0	93.0	102.0
		F_i'	91.0	102.0	113.0	123.0	134.0	145.0	156.0
		f_i'	60.0	60.0	60.0	60.0	60.0	63.0	66.0
＞25～40	74.0	f_u	49.0	52.0	52.0	55.0	55.0	58.0	60.0
		f_p	38.0	41.0	41.0	44.0	44.0	47.0	47.0
		F_{p2}	60.0	77.0	93.0	107.0	123.0	137.0	148.0
		F_r	63.0	71.0	80.0	88.0	96.0	104.0	113.0
		F_i'	107.0	121.0	134.0	145.0	156.0	167.0	178.0
		f_i'	80.0	80.0	80.0	82.0	82.0	85.0	85.0
偏差 F_{pz}									
测量长度/mm			15	25	45	75	125	200	300
轴向模数 m_x/mm			＞0.5～2	＞2～3.55	＞3.55～6	＞6～10	＞10～16	＞16～25	＞25～40
蜗杆头数 z_1	1		12.0	15.0	18.0	23.0	30.0	36.0	44.0
	2		14.0	16.0	22.0	27.0	36.0	44.0	52.0
	3 和 4		15.0	19.0	25.0	33.0	41.0	52.0	63.0
	5 和 6		18.0	23.0	30.0	38.0	47.0	60.0	74.0
	＞6		23.0	27.0	36.0	44.0	58.0	71.0	85.0

表 9　9 级精度轮齿偏差的允许值

单位为微米

模数 $m(m_t, m_x)$/mm	偏差		分度圆直径 d/mm						
	F_α		>10 ~50	>50 ~125	>125 ~280	>280 ~560	>560 ~1 000	>1 000 ~1 600	>1 600 ~2 500
>0.5 ~2.0	21.0	f_u	23.0	25.0	27.0	29.0	31.0	35.0	38.0
		f_p	17.0	19.0	21.0	23.0	25.0	27.0	31.0
		F_{p2}	50.0	65.0	81.0	92.0	104.0	115.0	127.0
		F_r	35.0	42.0	46.0	54.0	61.0	69.0	73.0
		F_i'	58.0	69.0	81.0	92.0	100.0	111.0	119.0
		f_i'	27.0	29.0	29.0	31.0	33.0	35.0	36.0
>2.0 ~3.55	29.0	f_u	25.0	27.0	29.0	31.0	35.0	36.0	42.0
		f_p	19.0	21.0	23.0	25.0	27.0	29.0	33.0
		F_{p2}	61.0	77.0	92.0	108.0	119.0	134.0	146.0
		F_r	42.0	54.0	61.0	69.0	77.0	85.0	92.0
		F_i'	69.0	85.0	96.0	108.0	119.0	131.0	142.0
		f_i'	35.0	35.0	36.0	38.0	38.0	42.0	42.0
>3.55 ~6.0	36.0	f_u	29.0	29.0	31.0	35.0	36.0	38.0	42.0
		f_p	23.0	23.0	25.0	27.0	29.0	33.0	35.0
		F_{p2}	65.0	85.0	100.0	115.0	131.0	146.0	158.0
		F_r	50.0	61.0	69.0	77.0	88.0	96.0	104.0
		F_i'	81.0	96.0	108.0	119.0	134.0	146.0	158.0
		f_i'	42.0	42.0	42.0	46.0	46.0	50.0	50.0
>6.0 ~10	46.0	f_u	33.0	35.0	36.0	38.0	42.0	46.0	50.0
		f_p	27.0	27.0	29.0	31.0	33.0	35.0	38.0
		F_{p2}	69.0	88.0	108.0	123.0	138.0	158.0	169.0
		F_r	58.0	69.0	77.0	88.0	96.0	108.0	115.0
		F_i'	92.0	108.0	123.0	134.0	150.0	161.0	173.0
		f_i'	50.0	50.0	54.0	54.0	54.0	58.0	58.0
>10 ~16	61.0	f_u	42.0	42.0	42.0	46.0	50.0	54.0	58.0
		f_p	33.0	33.0	35.0	36.0	38.0	42.0	46.0
		F_{p2}	73.0	96.0	115.0	131.0	150.0	165.0	184.0
		F_r	65.0	77.0	88.0	100.0	108.0	119.0	131.0
		F_i'	108.0	127.0	142.0	154.0	169.0	184.0	196.0
		f_i'	65.0	65.0	69.0	69.0	69.0	73.0	77.0
>16 ~25	77.0	f_u	50.0	54.0	54.0	58.0	61.0	65.0	65.0
		f_p	42.0	42.0	42.0	46.0	46.0	50.0	54.0
		F_{p2}	81.0	104.0	123.0	142.0	161.0	177.0	196.0
		F_r	77.0	88.0	100.0	111.0	123.0	131.0	142.0
		F_i'	127.0	142.0	158.0	173.0	188.0	204.0	219.0
		f_i'	85.0	85.0	85.0	85.0	85.0	88.0	92.0
>25 ~40	104.0	f_u	69.0	73.0	73.0	77.0	77.0	81.0	85.0
		f_p	54.0	58.0	58.0	61.0	61.0	65.0	65.0
		F_{p2}	85.0	108.0	131.0	150.0	173.0	192.0	207.0
		F_r	88.0	100.0	111.0	123.0	134.0	146.0	158.0
		F_i'	150.0	169.0	188.0	204.0	219.0	234.0	250.0
		f_i'	111.0	111.0	111.0	115.0	115.0	119.0	119.0
偏差 F_{pz}									
测量长度/mm			15	25	45	75	125	200	300
轴向模数 m_x/mm			>0.5 ~2	>2 ~3.55	>3.55 ~6	>6 ~10	>10 ~16	>16 ~25	>25 ~40
蜗杆头数 z_1	1		17.0	21.0	25.0	33.0	42.0	50.0	61.0
	2		19.0	23.0	31.0	38.0	50.0	61.0	73.0
	3 和 4		21.0	27.0	35.0	46.0	58.0	73.0	88.0
	5 和 6		25.0	33.0	42.0	54.0	65.0	85.0	104.0
	>6		33.0	38.0	50.0	61.0	81.0	100.0	119.0

表 10　10 级精度轮齿偏差的允许值

单位为微米

模数 $m(m_t,m_x)$/mm	偏差		分度圆直径 d/mm						
	F_α		＞10～50	＞50～125	＞125～280	＞280～560	＞560～1 000	＞1 000～1 600	＞1 600～2 500
＞0.5～2.0	34.0	f_u	37.0	40.0	43.0	46.0	49.0	55.0	61.0
		f_p	28.0	31.0	34.0	37.0	40.0	43.0	49.0
		F_{p2}	80.0	104.0	129.0	148.0	166.0	184.0	203.0
		F_r	48.0	59.0	65.0	75.0	86.0	97.0	102.0
		F_i'	92.0	111.0	129.0	148.0	160.0	178.0	191.0
		f_i'	43.0	46.0	46.0	49.0	52.0	55.0	58.0
＞2.0～3.55	46.0	f_u	40.0	43.0	46.0	49.0	55.0	58.0	68.0
		f_p	31.0	34.0	37.0	40.0	43.0	46.0	52.0
		F_{p2}	98.0	123.0	148.0	172.0	191.0	215.0	234.0
		F_r	59.0	75.0	86.0	97.0	108.0	118.0	129.0
		F_i'	111.0	135.0	154.0	172.0	191.0	209.0	227.0
		f_i'	55.0	55.0	58.0	61.0	61.0	68.0	68.0
＞3.55～6.0	58.0	f_u	46.0	46.0	49.0	55.0	58.0	61.0	68.0
		f_p	37.0	37.0	40.0	43.0	46.0	52.0	55.0
		F_{p2}	104.0	135.0	160.0	184.0	209.0	234.0	252.0
		F_r	70.0	86.0	97.0	108.0	124.0	134.0	145.0
		F_i'	129.0	154.0	172.0	191.0	215.0	234.0	252.0
		f_i'	68.0	68.0	68.0	74.0	74.0	80.0	80.0
＞6.0～10	74.0	f_u	52.0	55.0	58.0	61.0	68.0	74.0	80.0
		f_p	43.0	43.0	46.0	49.0	52.0	55.0	61.0
		F_{p2}	111.0	141.0	172.0	197.0	221.0	252.0	270.0
		F_r	81.0	97.0	108.0	124.0	134.0	151.0	161.0
		F_i'	148.0	172.0	197.0	215.0	240.0	258.0	277.0
		f_i'	80.0	80.0	86.0	86.0	86.0	92.0	92.0
＞10～16	98.0	f_u	68.0	68.0	68.0	74.0	80.0	86.0	92.0
		f_p	52.0	52.0	55.0	58.0	61.0	68.0	74.0
		F_{p2}	117.0	154.0	184.0	209.0	240.0	264.0	295.0
		F_r	91.0	108.0	124.0	140.0	151.0	167.0	183.0
		F_i'	172.0	203.0	227.0	246.0	270.0	295.0	313.0
		f_i'	104.0	104.0	111.0	111.0	111.0	117.0	123.0
＞16～25	123.0	f_u	80.0	86.0	86.0	92.0	98.0	104.0	104.0
		f_p	68.0	68.0	68.0	74.0	74.0	80.0	86.0
		F_{p2}	129.0	166.0	197.0	227.0	258.0	283.0	313.0
		F_r	108.0	124.0	140.0	156.0	172.0	183.0	199.0
		F_i'	203.0	227.0	252.0	277.0	301.0	326.0	350.0
		f_i'	135.0	135.0	135.0	135.0	135.0	141.0	148.0
＞25～40	166.0	f_u	111.0	117.0	117.0	123.0	123.0	129.0	135.0
		f_p	86.0	92.0	92.0	98.0	98.0	104.0	104.0
		F_{p2}	135.0	172.0	209.0	240.0	277.0	307.0	332.0
		F_r	124.0	140.0	156.0	172.0	188.0	204.0	221.0
		F_i'	240.0	270.0	301.0	326.0	350.0	375.0	400.0
		f_i'	178.0	178.0	178.0	184.0	184.0	191.0	191.0
偏差 F_{pz}									
测量长度/mm			15	25	45	75	125	200	300
轴向模数 m_x/mm			＞0.5～2	＞2～3.55	＞3.55～6	＞6～10	＞10～16	＞16～25	＞25～40
蜗杆头数 z_1	1		28.0	34.0	40.0	52.0	68.0	80.0	98.0
	2		31.0	37.0	49.0	61.0	80.0	98.0	117.0
	3 和 4		34.0	43.0	55.0	74.0	92.0	117.0	141.0
	5 和 6		40.0	52.0	68.0	86.0	104.0	135.0	166.0
	＞6		52.0	61.0	80.0	98.0	129.0	160.0	191.0

表 11　11 级精度轮齿偏差的允许值

单位为微米

模数 $m(m_t,m_x)$/mm	偏差		分度圆直径 d/mm						
	F_α		>10 ~50	>50 ~125	>125 ~280	>280 ~560	>560 ~1 000	>1 000 ~1 600	>1 600 ~2 500
>0.5 ~2.0	54.0	f_u	59.0	64.0	69.0	74.0	79.0	89.0	98.0
		f_p	44.0	49.0	54.0	59.0	64.0	69.0	79.0
		F_{p2}	128.0	167.0	207.0	236.0	266.0	295.0	325.0
		F_r	68.0	83.0	90.0	105.0	120.0	136.0	143.0
		F_i'	148.0	177.0	207.0	236.0	256.0	285.0	305.0
		f_i'	69.0	74.0	74.0	79.0	84.0	89.0	93.0
>2.0 ~3.55	74.0	f_u	64.0	69.0	74.0	79.0	89.0	93.0	108.0
		f_p	49.0	54.0	59.0	64.0	69.0	74.0	84.0
		F_{p2}	157.0	197.0	236.0	275.0	305.0	344.0	374.0
		F_r	83.0	105.0	120.0	136.0	151.0	166.0	181.0
		F_i'	177.0	216.0	246.0	275.0	305.0	334.0	364.0
		f_i'	89.0	89.0	93.0	98.0	98.0	108.0	108.0
>3.55 ~6.0	93.0	f_u	74.0	74.0	79.0	89.0	93.0	98.0	108.0
		f_p	59.0	59.0	64.0	69.0	74.0	84.0	89.0
		F_{p2}	167.0	216.0	256.0	295.0	334.0	374.0	403.0
		F_r	98.0	120.0	136.0	151.0	173.0	188.0	203.0
		F_i'	207.0	246.0	275.0	305.0	344.0	374.0	403.0
		f_i'	108.0	108.0	108.0	118.0	118.0	128.0	128.0
>6.0 ~10	118.0	f_u	84.0	89.0	93.0	98.0	108.0	118.0	128.0
		f_p	69.0	69.0	74.0	79.0	84.0	89.0	98.0
		F_{p2}	177.0	226.0	275.0	315.0	354.0	403.0	433.0
		F_r	113.0	136.0	151.0	173.0	188.0	211.0	226.0
		F_i'	236.0	275.0	315.0	344.0	384.0	413.0	443.0
		f_i'	128.0	128.0	138.0	138.0	138.0	148.0	148.0
>10 ~16	157.0	f_u	108.0	108.0	108.0	118.0	128.0	138.0	148.0
		f_p	84.0	84.0	89.0	93.0	98.0	108.0	118.0
		F_{p2}	187.0	246.0	295.0	334.0	384.0	423.0	472.0
		F_r	128.0	151.0	173.0	196.0	211.0	233.0	256.0
		F_i'	275.0	325.0	364.0	393.0	433.0	472.0	502.0
		f_i'	167.0	167.0	177.0	177.0	177.0	187.0	197.0
>16 ~25	197.0	f_u	128.0	138.0	138.0	148.0	157.0	167.0	167.0
		f_p	108.0	108.0	108.0	118.0	118.0	128.0	138.0
		F_{p2}	207.0	266.0	315.0	364.0	413.0	452.0	502.0
		F_r	151.0	173.0	196.0	218.0	241.0	256.0	279.0
		F_i'	325.0	364.0	403.0	443.0	482.0	521.0	561.0
		f_i'	216.0	216.0	216.0	216.0	216.0	226.0	236.0
>25 ~40	266.0	f_u	177.0	187.0	187.0	197.0	197.0	207.0	216.0
		f_p	138.0	148.0	148.0	157.0	157.0	167.0	167.0
		F_{p2}	216.0	275.0	334.0	384.0	443.0	492.0	531.0
		F_r	173.0	196.0	218.0	241.0	264.0	286.0	309.0
		F_i'	384.0	433.0	482.0	521.0	561.0	600.0	639.0
		f_i'	285.0	285.0	285.0	295.0	295.0	305.0	305.0
偏差 F_{pz}									
测量长度/mm			15	25	45	75	125	200	300
轴向模数 m_x/mm			>0.5 ~2	>2 ~3.55	>3.55 ~6	>6 ~10	>10 ~16	>16 ~25	>25 ~40
蜗杆头数 z_1	1		44.0	54.0	64.0	84.0	108.0	128.0	157.0
	2		49.0	59.0	79.0	98.0	128.0	157.0	187.0
	3 和 4		54.0	69.0	89.0	118.0	148.0	187.0	226.0
	5 和 6		64.0	84.0	108.0	138.0	167.0	216.0	266.0
	>6		84.0	98.0	128.0	157.0	207.0	256.0	305.0

表 12　12 级精度轮齿偏差的允许值

单位为微米

模数 $m(m_t,m_x)$/mm	偏差		分度圆直径 d/mm						
	F_α		>10~50	>50~125	>125~280	>280~560	>560~1 000	>1 000~1 600	>1 600~2 500
>0.5~2.0	87.0	f_u	94.0	102.0	110.0	118.0	126.0	142.0	157.0
		f_p	71.0	79.0	87.0	94.0	102.0	110.0	126.0
		F_{p2}	205.0	267.0	330.0	378.0	425.0	472.0	519.0
		F_r	95.0	116.0	126.0	148.0	169.0	190.0	200.0
		F_i'	236.0	283.0	330.0	378.0	409.0	456.0	488.0
		f_i'	110.0	118.0	118.0	126.0	134.0	142.0	149.0
>2.0~3.55	118.0	f_u	102.0	110.0	118.0	126.0	142.0	149.0	173.0
		f_p	79.0	87.0	94.0	102.0	110.0	118.0	134.0
		F_{p2}	252.0	315.0	378.0	441.0	488.0	551.0	598.0
		F_r	116.0	148.0	169.0	190.0	211.0	232.0	253.0
		F_i'	283.0	346.0	393.0	441.0	488.0	535.0	582.0
		f_i'	142.0	142.0	149.0	157.0	157.0	173.0	173.0
>3.55~6.0	149.0	f_u	118.0	118.0	126.0	142.0	149.0	157.0	173.0
		f_p	94.0	94.0	102.0	110.0	118.0	134.0	142.0
		F_{p2}	267.0	346.0	409.0	472.0	535.0	598.0	645.0
		F_r	137.0	169.0	190.0	211.0	242.0	264.0	285.0
		F_i'	330.0	393.0	441.0	488.0	551.0	598.0	645.0
		f_i'	173.0	173.0	173.0	189.0	189.0	205.0	205.0
>6.0~10	189.0	f_u	134.0	142.0	149.0	157.0	173.0	189.0	205.0
		f_p	110.0	110.0	118.0	126.0	134.0	142.0	157.0
		F_{p2}	283.0	362.0	441.0	504.0	566.0	645.0	692.0
		F_r	158.0	190.0	211.0	242.0	264.0	295.0	316.0
		F_i'	378.0	441.0	504.0	551.0	614.0	661.0	708.0
		f_i'	205.0	205.0	220.0	220.0	220.0	236.0	236.0
>10~16	252.0	f_u	173.0	173.0	173.0	189.0	205.0	220.0	236.0
		f_p	134.0	134.0	142.0	149.0	157.0	173.0	189.0
		F_{p2}	299.0	393.0	472.0	535.0	614.0	677.0	755.0
		F_r	179.0	211.0	242.0	274.0	295.0	327.0	358.0
		F_i'	441.0	519.0	582.0	629.0	692.0	755.0	802.0
		f_i'	267.0	267.0	283.0	283.0	283.0	299.0	315.0
>16~25	315.0	f_u	205.0	220.0	220.0	236.0	252.0	267.0	267.0
		f_p	173.0	173.0	173.0	189.0	189.0	205.0	220.0
		F_{p2}	330.0	425.0	504.0	582.0	661.0	724.0	802.0
		F_r	211.0	242.0	274.0	306.0	337.0	358.0	390.0
		F_i'	519.0	582.0	645.0	708.0	771.0	834.0	897.0
		f_i'	346.0	346.0	346.0	346.0	346.0	362.0	378.0
>25~40	425.0	f_u	283.0	299.0	299.0	315.0	315.0	330.0	346.0
		f_p	220.0	236.0	236.0	252.0	252.0	267.0	267.0
		F_{p2}	346.0	441.0	535.0	614.0	708.0	787.0	850.0
		F_r	242.0	274.0	306.0	337.0	369.0	401.0	432.0
		F_i'	614.0	692.0	771.0	834.0	897.0	960.0	1 023.0
		f_i'	456.0	456.0	456.0	472.0	472.0	488.0	488.0
偏差 F_{pz}									
测量长度/mm			15	25	45	75	125	200	300
轴向模数 m_x/mm			>0.5~2	>2~3.55	>3.55~6	>6~10	>10~16	>16~25	>25~40
蜗杆头数 z_1	1		71.0	87.0	102.0	134.0	173.0	205.0	252.0
	2		79.0	94.0	126.0	157.0	205.0	252.0	299.0
	3 和 4		87.0	110.0	142.0	189.0	236.0	299.0	362.0
	5 和 6		102.0	134.0	173.0	220.0	267.0	346.0	425.0
	>6		134.0	157.0	205.0	252.0	330.0	409.0	488.0

附 录 A
（规范性附录）
蜗杆副的接触斑点要求

蜗杆副的接触斑点主要按其形状、分布位置与面积大小来评定。接触斑点的要求应符合表 A.1 的规定。

表 A.1 蜗杆副接触斑点的要求

<table>
<tr><th rowspan="2">精度等级</th><th colspan="2">接触面积的百分比/%</th><th rowspan="2">接 触 形 状</th><th rowspan="2">接 触 位 置</th></tr>
<tr><th>沿齿高不小于</th><th>沿齿长不小于</th></tr>
<tr><td>1 和 2</td><td>75</td><td>70</td><td rowspan="3">接触斑点在齿高方向无断缺，不允许成带状条纹</td><td rowspan="3">接触斑点痕迹的分布位置趋近齿面中部，允许略偏于啮入端。在齿顶和啮入、啮出端的棱边处不允许接触</td></tr>
<tr><td>3 和 4</td><td>70</td><td>65</td></tr>
<tr><td>5 和 6</td><td>65</td><td>60</td></tr>
<tr><td>7 和 8</td><td>55</td><td>50</td><td rowspan="3">不作要求</td><td rowspan="3">接触斑点痕迹应偏于啮出端，但不允许在齿顶和啮入、啮出端的棱边接触</td></tr>
<tr><td>9 和 10</td><td>45</td><td>40</td></tr>
<tr><td>11 和 12</td><td>30</td><td>30</td></tr>
<tr><td colspan="5">注：采用修形齿面的蜗杆传动，接触斑点的接触形状要求可不受表中规定的限制。</td></tr>
</table>

INTERNATIONAL STANDARD

ISO 21771

First edition
2007-09-01

Gears — Cylindrical involute gears and gear pairs — Concepts and geometry

Engrenages — Roues et engrenages cylindriques à développante — Concepts et géométrie

Reference number
ISO 21771:2007(E)

Contents

Page

Foreword ... iv

1 Scope ... 1

2 Normative references ... 1

3 Symbols, subscripts and units ... 2
3.1 Symbols ... 2
3.2 Subscripts ... 8
3.3 Units ... 9

4 Individual cylindrical gears ... 10
4.1 Concepts for an individual gear ... 10
4.2 Reference surfaces, datum lines and reference quantities ... 12
4.3 Involute helicoids ... 17
4.4 Angular pitch and pitches ... 21
4.5 Diameters of gear teeth ... 24
4.6 Gear tooth height ... 24
4.7 Tooth thickness, space width ... 25

5 Cylindrical gear pairs ... 27
5.1 Concepts for a gear pair ... 27
5.2 Mating quantities ... 28
5.3 Calculation of the sum of the profile shift coefficients ... 31
5.4 Tooth engagement ... 32
5.5 Backlash ... 40
5.6 Sliding conditions at the tooth flanks ... 41

6 Tooth flank modifications ... 44
6.1 Tooth flank modifications which restrict the usable flank ... 44
6.2 Transverse profile modifications ... 45
6.3 Flank line (helix) modifications ... 48
6.4 Flank face modifications ... 49
6.5 Descriptions of modifications by functions ... 51

7 Geometrical limits ... 52
7.1 Counterpart rack tooth profile ... 53
7.2 Machining allowance ... 54
7.3 Deviations in tooth thickness ... 55
7.4 Generating profile shift, generating profile shift coefficient ... 56
7.5 Generated root diameter ... 57
7.6 Usable area of the tooth flank, tip and root form diameter ... 57
7.7 Undercut ... 59
7.8 Overcut ... 59
7.9 Minimum tooth thickness at the tip circle of a gear ... 59

Annex A (informative) **Calculations related to tooth thickness** ... 60

Bibliography ... 83

Foreword

ISO (the International Organization for Standardization) is a worldwide federation of national standards bodies (ISO member bodies). The work of preparing International Standards is normally carried out through ISO technical committees. Each member body interested in a subject for which a technical committee has been established has the right to be represented on that committee. International organizations, governmental and non-governmental, in liaison with ISO, also take part in the work. ISO collaborates closely with the International Electrotechnical Commission (IEC) on all matters of electrotechnical standardization.

International Standards are drafted in accordance with the rules given in the ISO/IEC Directives, Part 2.

The main task of technical committees is to prepare International Standards. Draft International Standards adopted by the technical committees are circulated to the member bodies for voting. Publication as an International Standard requires approval by at least 75 % of the member bodies casting a vote.

Attention is drawn to the possibility that some of the elements of this document may be the subject of patent rights. ISO shall not be held responsible for identifying any or all such patent rights.

ISO 21771 was prepared by Technical Committee ISO/TC 60, *Gears*, Subcommittee SC 1, *Nomenclature and wormgearing*.

This first edition of ISO 21771 cancels and replaces ISO/TR 4467:1982, of which it constitutes a technical revision.

Gears — Cylindrical involute gears and gear pairs — Concepts and geometry

1 Scope

This International Standard specifies the geometric concepts and parameters for cylindrical gears with involute helicoid tooth flanks. Flank modifications are included.

It also covers the concepts and parameters for cylindrical gear pairs with parallel axes and a constant gear ratio, which consist of cylindrical gears according to it. Gear and mating gear in these gear pairs have the same basic rack tooth profile.

The equations given are not restricted to the pressure angle, $\alpha_P = 20°$.

The standard is structured as follows.

— Listing of symbols and nomenclature for a unique description of gears and gear pairs (see Clause 3).

— Equations and explanations of the relevant values for defining a cylindrical gear and its tooth system. The equations for determination of the nominal values for zero-deviation gear description parameters are stated for radial tooth dimensions (gear tooth heights), the distance between flanks of the same hand, the distance between flanks of opposite hand, as well as the tooth flank characterizing parameters (see Clause 4).

— Equations and explanations of the relevant values for defining cylindrical gear pairs. The equations for the essential parameters characterizing the engagement conditions of the unloaded gear pair are listed (see Clause 5).

— Equations and suggestions for desired flank modifications (see Clause 6).

— Concepts and recommendations needed for a unique geometrical definition of the intended results from manufacture (Clause 7).

— Equations for determination of the nominal values or the limiting values for the most used inspection methods for tooth thickness (see Annex A).

2 Normative references

The following referenced documents are indispensable for the application of this document. For dated references, only the edition cited applies. For undated references, the latest edition of the referenced document (including any amendments) applies.

ISO 53:1998, *Cylindrical gears for general and heavy engineering — Standard basic rack tooth profile*

ISO 1328-1:1995, *Cylindrical gears — ISO system of accuracy — Part 1: Definitions and allowable values of deviations relevant to corresponding flanks of gear teeth*

ISO 1328-2:1997, *Cylindrical gears — ISO system of accuracy — Part 2: Definitions and allowable values of deviations relevant to radial composite deviations and runout information*

3 Symbols, subscripts and units

3.1 Symbols

Symbol	Description	Used in
a_w	centre distance of a cylindrical gear pair	5.2.3
a_0	centre distance in the generating gear unit	7.5
a_L	centre distance for tooth flank engagement	A.8
b	facewidth	4.2.8
b_F	usable facewidth	4.2.8
b_M	contact line overlap (for measuring base tangent length)	A.2.1
b_w	active facewidth (the facewidth used)	5.4.7.2
c	tip clearance	5.2.7
c_F	form over dimension	5.4.4
d	reference diameter	4.2.4
d_a	tip diameter	4.5.3
d_{a0}	tip diameter of tool	7.5
d_{aM}	tip diameter of overcut cylindrical gears	A.9
d_b	base diameter	4.3.10
d_{b0}	base diameter of the pinion-type cutter	7.6
d_f	root diameter (nominal dimension)	4.5.4
d_{fE}	root diameter produced	7.5
d_{f0}	root diameter of the pinion-type cutter	A.9
d_v	V-circle diameter	4.5.1
d_w	working pitch diameter	5.2.5
d_y	Y-circle diameter	4.3.3
d_{Fa}	tip form diameter	7.6
d_{Fa0}	tip form diameter of the pinion-type cutter	7.6
d_{Ff}	root form diameter	7.6
d_K	diameter of circle through centre of ball	A.5
d_M	diameter of a measuring circle	A.2.1
d_{Na}	active tip diameter	5.4.1
d_{Nf}	start of active profile diameter (SAP diameter, active root diameter)	5.4.1
e_t	space width on the reference cylinder	4.7.3
e_{yt}	space width on the Y-cylinder	4.7.3

Symbol	Description	Used in
e_P	space width of the standard basic rack tooth profile	4.2.3
g_a	length of addendum path of contact	5.4.5.2
g_f	length of dedendum path of contact	5.4.5.2
g_α	length of path of contact	5.4.5.2
$g_{\alpha y}$	distance of a point Y from pitch point C	5.6.1
g_β	arc of contact	5.4.7.4
h	tooth depth (between tip line and root line)	4.6.1
h_a	addendum	4.6.2
h_{aP}	addendum of the standard basic rack tooth profile	Figure 4
h_{aP0}	addendum of the tool standard basic rack tooth profile	7.5
h_f	dedendum	4.6.2
h_{fP}	dedendum of the standard basic rack tooth profile	Figure 4
h_{fP0}	dedendum of the tool standard basic rack tooth profile	A.9
h_w	working depth of teeth in a gear pair	5.2.6
h_{FfP}	depth of dedendum form of the standard basic rack tooth profile	Figure 4
h_K	radius of the tip corner chamfering or tip corner rounding	6.1.2
h_P	tooth depth of standard basic rack tooth profile	Figure 4
inv	involute function	4.3.9
j_{bn}	contact backlash	5.5
j_r	radial backlash	5.5
j_t	circumferential backlash at the reference circle	5.5.2
j_{wt}	circumferential backlash at the pitch circle	5.5
k	number of teeth, spaces or pitches in a span (e.g. number of teeth spanned)	A.2.1
k	addendum modification coefficient	4.5.2
l_{max}	path of engagement	5.4.8
$\sum l$	sum of path of contact	5.4.8
m_n	normal module	4.2.7
m_t	transverse module	4.2.7
m_x	axial module	4.2.7
n_a	number of revolutions of driving gear (rpm)	5.2.2
n_b	number of revolutions of driven gear (rpm)	5.2.2
p	pitch, pitch on the reference cylinder	Figure 4

Symbol	Description	Used in
p_{bn}	normal pitch on the base cylinder	4.4.5
p_{bt}	transverse pitch on the base cylinder	4.4.5.1
p_{en}	normal base pitch on the path of contact	4.4.5.2
p_{et}	transverse base pitch on the path of contact	4.4.5.1
p_n	normal pitch	4.4.2.2
p_t	transverse pitch	4.4.2.1
p_x	axial pitch	4.4.4
p_{yn}	normal pitch on the Y-cylinder	4.4.3
p_{yt}	transverse pitch on the Y-cylinder	4.4.3
p_z	lead	4.3.2
q	machining allowance on tooth flank	7.2
q_{Fs}	undercut	Figure 24
s_{aK}	residual tooth thickness at tip with tip corner chamfering or tip corner rounding	6.1.2
s_{bn}	normal tooth thickness on the base circle	A.2.2
s_n	normal tooth thickness on the reference circle	4.7.5
s_{ni}	minimum normal tooth thickness on the reference circle	7.3
s_{ns}	maximum normal tooth thickness on the reference circle	7.3
s_t	transverse tooth thickness on the reference circle	4.7.1
s_{yn}	normal tooth thickness on the Y-cylinder	4.7.5
s_{yt}	transverse tooth thickness on the Y-cylinder	4.7.1
s_P	tooth thickness of the standard basic rack tooth profile	4.2.3
u	gear ratio	5.2.1
v_g	sliding speed	5.6.1
v_{ga}	sliding speed at the addendum	5.6.1
v_{gf}	sliding speed at the dedendum	5.6.1
v_n	normal speed	5.6.1
x	profile shift coefficient	4.2.9
x_E	generating profile shift coefficient	7.4
x_{Emin}	generating profile shift coefficient at undercut limit	7.7
x_L	profile shift coefficient of master gear	A.8
z	number of teeth	4.1.5
z_a	number of teeth of driving gear	5.2.2

Symbol	Description	Used in
z_b	number of teeth of driven gear	5.2.2
z_L	number of teeth of master gear	A.8
z_0	number of teeth of pinion-type cutter	7.6
A	starting point of meshing	5.4.3
B	starting point of single tooth contact on driving gear	5.4.5.1
C	pitch point, depth of relief for modifications	5.4.3
C_{ay}	modification of the profile	6.5
$C_{\beta y}$	modification of the flank line	6.5
$C_{\Sigma y}$	modification of the flank surface	6.5
$C_{\alpha a}$	amount of tip relief	6.2.1
$C_{\alpha f}$	amount of root relief	6.2.1
C_{Ea}	tip amount of triangular end relief modification	6.4.2
C_{Ef}	root amount of triangular end relief modification	6.4.2
$C_{i,j}$	amount of modification at point (i,j)	6.4.1
$C_{H\alpha}$	amount of transverse profile slope modification	6.2.2
C_{α}	amount of profile crowning (barrelling)	6.2.3
$C_{\beta I}$, $C_{\beta II}$	amount of end relief	6.3.1
C_{β}	amount of flank line crowning	6.3.3
$C_{H\beta}$	amount of flank line slope modification	6.3.2
D_M	measuring ball or measuring cylinder diameter	A.5
D	end point of single tooth contact point on driving gear	5.4.5.1
E	end point of meshing	5.4.3
E_{sn}	normal tooth thickness deviation limit (or allowance)	A.9
E_{sni}	lower deviation limit for tooth thickness	7.3
E_{sns}	upper deviation limit for tooth thickness	7.3
K_g	sliding factor	5.6.2
K_{ga}	sliding factor at tooth tip	5.6.2
K_{gf}	sliding factor at tooth root	5.6.2
L_{AE}	roll length	6.2
L_{Ca}	tip relief roll length	6.2.1
L_{Cf}	root relief roll length	6.2.1
L_{CI}, L_{CII}	length of end relief	6.3.1
L_{Ea}	tip roll length of triangular end relief modification	6.4.2

Symbol	Description	Used in
L_{Ef}	root roll length of triangular end relief modification	6.4.2
M_{dK}	dimension over balls	A.7
M_{dZ}	dimension over cylinders	A.7.1
M_{rK}	radial single-ball dimension	A.5
M_{rZ}	radial single-cylinder dimension	A.6
N	number of tooth or pitch	4.1.6
O	centre of a circle	Figure 10
S_{α}	twist of the transverse profile	6.4.3
S_{β}	twist of the flank line	6.4.3
T_{sn}	tooth thickness tolerance	Figure 37
T	contact point of tangent (lines of engagement) at base circle	Figure 10
U	involute point of origin	4.3.7
W_{k}	base tangent length over k measured teeth or measured spaces	A.2.1
Y	any point on a tooth flank or involute	4.3.5
α_{n}	normal pressure angle	4.3.6
α_{t}	transverse pressure angle	4.3.5
α_{wt}	working transverse pressure angle of gear pair	5.2.4
α_{wt0}	working transverse pressure angle in the generating gear unit	7.6
α_{yn}	normal pressure angle at the Y-cylinder	4.3.6
α_{yt}	transverse pressure angle at the Y-cylinder	4.3.5
α_{Ff}	pressure angle at root form circle	7.6
α_{K}	pressure angle at circle through centre of ball	A.5
α_{Kt}	transverse pressure angle at a point at circle through centre of ball	A.5
α_{Mt}	transverse pressure angle at a point at measuring circle	A.5
α_{P}	pressure angle of the standard basic rack tooth profile	4.3.6
α_{P0}	pressure angle of the tool basic rack tooth profile	7
α_{L}	working transverse pressure angle for double-flank engagement	A.8
α_{vt}	transverse pressure angle at the V-cylinder	A.5
β	helix angle	4.3.3
β_{b}	base helix angle	4.3.3
β_{y}	helix angle at Y-cylinder	4.3.3
δ_{w}	angle of rocking for span measurement	A.2.1

Symbol	Description	Used in
γ	lead angle at reference cylinder	4.3.3
γ_{y}	lead angle at Y-cylinder	4.3.3
ε_{α}	transverse contact ratio	5.4.7.1
ε_{β}	overlap ratio	5.4.7.3
ε_{γ}	total contact ratio	5.4.7.5
ζ	specific sliding	5.6.3
ζ_{f}	specific sliding at end points of path of contact	5.6.3
η	space width half angle at reference circle	4.7.4
η_{b}	base space width half angle	4.7.4
η_{y}	space width half angle at Y-circle	4.7.4
ξ_{y}	rolling angle of the involute at point Y	4.3.7
ξ_{Fa0}	rolling angle at tip form circle of pinion-type cutter	7.6
ξ_{Ff}	rolling angle at root form circle	7.6
ξ_{Na}	rolling angle at active tip circle	5.4.1
ξ_{Nf}	rolling angle at active root circle	5.4.1
ρ_{fP}	root radius on the standard basic rack tooth profile	Figure 4
ρ_{y}	radius of curvature of the involute at point Y	4.3.8
τ	angular pitch	4.4.2
φ_{j}	backlash angle	5.5.2
φ_{α}	transverse angle of transmission	5.4.7.1
φ_{β}	overlap angle	5.4.7.3
φ_{γ}	total angle of transmission	5.4.7.5
ψ	tooth thickness half angle at reference circle	4.7.2
ψ_{b}	base tooth thickness half angle	4.7.2
ψ_{y}	tooth thickness half angle at Y-circle	4.7.2
ω_{a}	angular velocity of driving gear	5.2.2
ω_{b}	angular velocity of driven gear	5.2.2
$\sum x$	sum of profile shift coefficients	5.3
$\sum x_{\mathrm{E}}$	sum of profile shift coefficient, non-zero backlash	5.3

3.2 Subscripts

Subscript	Description	Used in [b]
—	[a]	
a	for quantities associated with the tip of a tooth or for the driving gear	5.2.2
b	for quantities associated with the base cylinder	4.3.10
b	for quantities associated with the driven gear	5.2.2
e	for quantities associated with the plane of action	
f	for quantities associated with the root	
g	for “sliding”	
i	for the lower limit in the case of deviations	
k	for a number of teeth, spaces, pitches or spans	
l	for “left-hand”	
m	for a mean value	
max	for a maximum value	
min	for a minimum value	
n	for quantities in a normal section	4.2.6.2
r	for “right-hand”	
s	relating to “tooth thickness”, for the upper limit in the case of deviations	
t	for quantities in a transverse section	4.2.6.1
v	for quantities associated with the V-cylinder	4.5.1
w	for quantities associated with the pitch cylinder and working values of a gear pair	
x	for quantities in an axial section	4.2.6.3
y	for values at a point Y (on the Y-cylinder)	
E	relating to “generating” (e.g. quantities generated on the cylindrical gear) or “generator”	
F	for quantities determining form circles and maximum usable flank area	
K	for quantities resulting from corner chamfering or for ball dimensions	
L	for designating a master gear	
L	for designating left flanks	4.1.8.2
M	for designating a measured value	
N	for active circles	
P	for quantities of the standard basic rack tooth profile	
P0	for quantities of the tool standard basic rack tooth profile	
R	for designating right flanks	4.1.8.2
V	for working side, for rough gear cutting	
W	for measuring base tangent length	

Subscript	Description	Used in [b]
Z	for quantities associated with cylinder dimensions	
α	for quantities associated with contact	
β	for quantities associated with a tooth trace	
γ	for total contact ratio	
$\sum$	for "sum"	
0	for quantities associated with the generating tool or the generating gear unit	7
1	for quantities associated with the pinion (smaller gear) of a gear pair	5.1.3
2	for quantities associated with the wheel (larger gear) or internal gear, used for designating a coefficient relating to the module	5.1.3
I	for locating face	4.2.1
II	for the face opposite the locating face	4.2.1

[a] No subscript designates quantities associated with the reference cylinder.

[b] Used with the symbols listed in 3.1 or as additions.

3.3 Units

The quantities dealt with in this International Standard are to be stated in the following units:

— modules, lengths and linear dimensions in millimetres (mm);

— angles which are to be used in equations in radians (rad);

— angles which can be used for entries or to display results in degrees (°);

— angular velocity in radians per second (rad/s).

NOTE The notation $|z|$, denotes the absolute value, which is always positive, e.g. $|-50| = +50$. The expression $\frac{z}{|z|}$ is used to extract the sign of the tooth number and is convenient for programming. In particular, it is used often to determine the appropriate sign for an element of an expression; the result is 1 for external gears and −1 for internal gears.

4 Individual cylindrical gears

In this clause, the geometry of gear teeth is described using a generation process based on zero backlash engagement with a basic rack. The relationships are valid for any basic rack, but the standard basic rack (see ISO 53) is used for illustration. The standard basic rack tooth profile of the tooth system has straight flanks. Its datum line is the straight line on which the nominal dimensions of tooth thickness and space width are defined as equal to half the pitch. The standard basic rack tooth profile has the same pressure angles for the left and right flanks and the addendum plus bottom clearance equal to the dedendum. The helix angles for all the tooth flanks of a gear have the same nominal value.

4.1 Concepts for an individual gear

4.1.1 Gear, cylindrical gear, external gear, internal gear

A gear is a rotationally symmetrical object (gear blank) with a tooth system worked into the rim. A cylindrical gear is a gear with a cylindrical reference surface. A distinction is made between external and internal gears according to the radial arrangement of the teeth in each case. The tips of the teeth point outwards in an external gear and inwards in an internal gear.

4.1.2 Tooth system, external teeth, and internal teeth

The tooth system refers to all the teeth and space widths around the rim of a gear. As in 4.1.1, a distinction is made between internal and external gear teeth.

4.1.3 Tooth and space

A tooth is a geometrical element on the gearwheel body that enables the transmission of force and motion. The form and dimensions of the teeth and the distance between consecutive teeth are defined by the tooth system parameters. The space is the gap between two consecutive teeth.

4.1.4 Tooth system parameters

The nominal dimensions of involute cylindrical gear teeth are uniquely determined by the diameter of the reference cylinder, the associated basic rack and its position in relation to the reference circle. The nominal dimensions are defined by the following parameters, which are independent of each other:

— number of teeth, z;

— standard basic rack tooth profile;

— normal module, m_n;

— helix angle, β, and flank direction;

— profile shift coefficient, x;

— tip diameter, d_a;

— facewidth, b.

4.1.5 Number of teeth and sign of number of teeth

The number of teeth around the rim of the gearwheel is denoted by z.

The number of teeth, z, of an external cylindrical gear must be taken as a positive value in the following equations while the number of teeth, z, in an internal cylindrical gear is to be taken as a negative value.

In the case of segments, the number of teeth, z, used in calculations is the number that there would be on the whole circumference.

4.1.6 Tooth number

When numbering teeth, the designations tooth 1, tooth 2, etc. are to be defined on a transverse surface (datum face) viewed in an agreed direction so that the teeth are numbered in ascending order (moving in a clockwise direction). If the letter N is used to denote a reference tooth, the next tooth in the direction of counting is denoted by $N + 1$ and the previous tooth going in the opposite direction by $N - 1$. Tooth No. z is followed by tooth 1 in the direction of counting, see Figure 1.

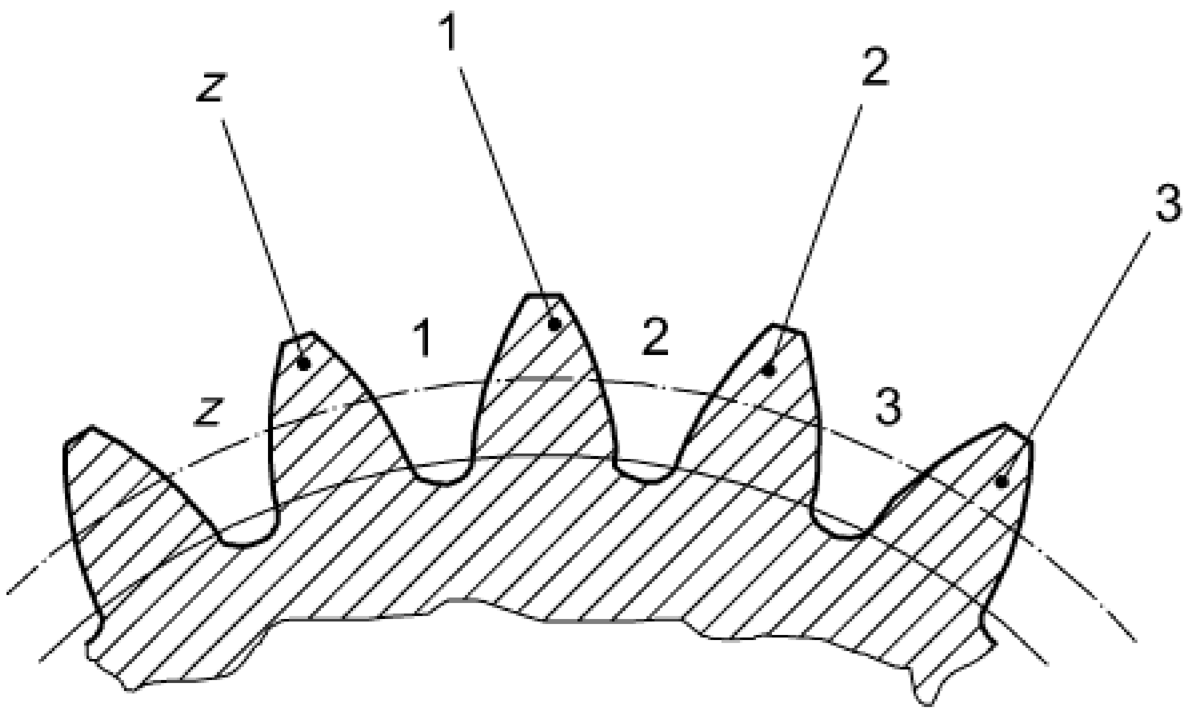

Figure 1 — Numbering of teeth and spaces on datum face

4.1.7 Top land and bottom land

4.1.7.1 Top land

The top land of a tooth is the outermost (innermost in the case of internal gears) periphery of the tooth concentric to the reference cylinder, see Figure 2.

4.1.7.2 Bottom land

The bottom land is the innermost (outermost in the case of internal gears) periphery of the space width concentric to the reference cylinder, see Figure 2.

4.1.8 Tooth flanks and flank sections

4.1.8.1 Tooth flank

Tooth flanks are those parts of the surface of a tooth that are located between the top land and the bottom land, see Figure 2.

4.1.8.2 Right flank, left flank

The right flank (or left flank) is the tooth flank that an observer sees on the right-hand (or left-hand) side when viewing the datum face of a tooth when it is pointing upwards. This definition applies to both external and internal gears, see Figure 2.

Right flank parameters are indicated by the subscript R and left flank parameters by the subscript L.

a) Internal tooth

b) External tooth

Key

1 top land
2 addendum flank
3 reference cylinder
4 dedendum flank
5 bottom land
6 datum face

Figure 2 — Top land, bottom land and tooth flank with division (internal and external teeth)

4.1.8.3 Addendum flank, dedendum flank

The addendum flank (or dedendum flank) is that part of a tooth flank that is located between the reference cylinder and the top land (or the bottom land), see Figure 2.

4.1.8.4 Usable flank

The usable flank is that part of a tooth flank that can be used to engage with a mating flank. On a cylindrical gear, it is part of the involute helicoid including any flank modifications.

4.2 Reference surfaces, datum lines and reference quantities

4.2.1 Reference surface, datum surface, datum face

The reference surface of the teeth is an imaginary surface to which the geometrical parameters relate. In the case of cylindrical gears, the reference surface is termed the *reference cylinder*.

The agreed front of the gear (usually used for text or suitably marked) is used as the datum face. Parameters which relate to the datum face are denoted by the subscript I while parameters which relate to the opposite face are denoted by the subscript II.

4.2.2 Reference rack

The reference rack is the rack that can be produced using the same gear-cutting tool, gear-cutting method and pitch point (pitch axis) as the actual cylindrical gear. It is characterized by its profile, the direction of its teeth in relation to the pitch axis of the generating gear unit, tip plane, root plane and facewidth, see Figure 3.

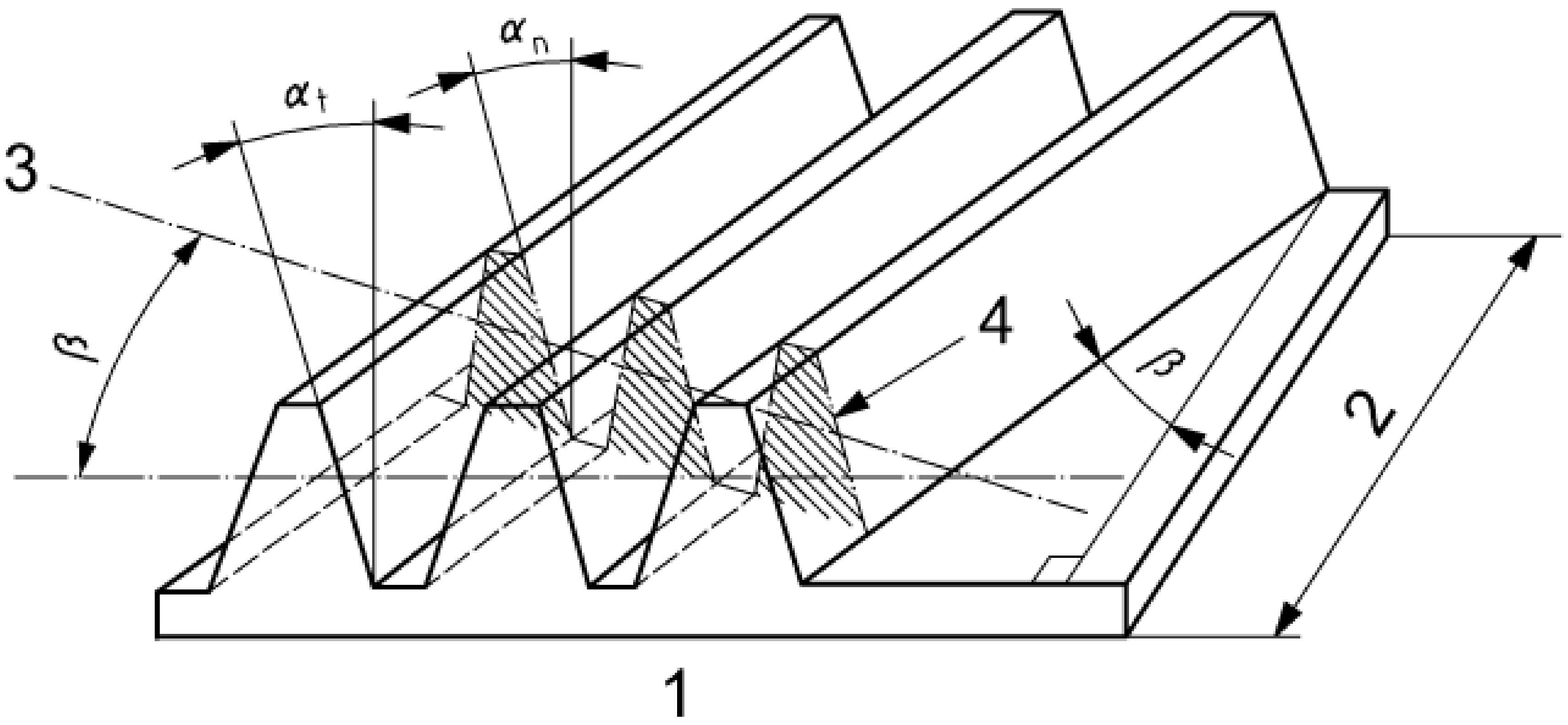

Key

1 transverse section

2 facewidth

3 normal section

4 standard basic rack tooth profile

Figure 3 — Concepts and parameters relating to reference rack

4.2.3 Basic rack tooth profile for involute gear teeth

The basic rack tooth profile is defined in a normal section. The flanks of the basic rack tooth profile of involute teeth are straight lines. Tooth thickness, s_P, and space width, e_P, on the datum line of the basic rack (P-P) in the reference plane are equal, see Figure 4.

The standard basic rack tooth profile for involute teeth is standardized in ISO 53.

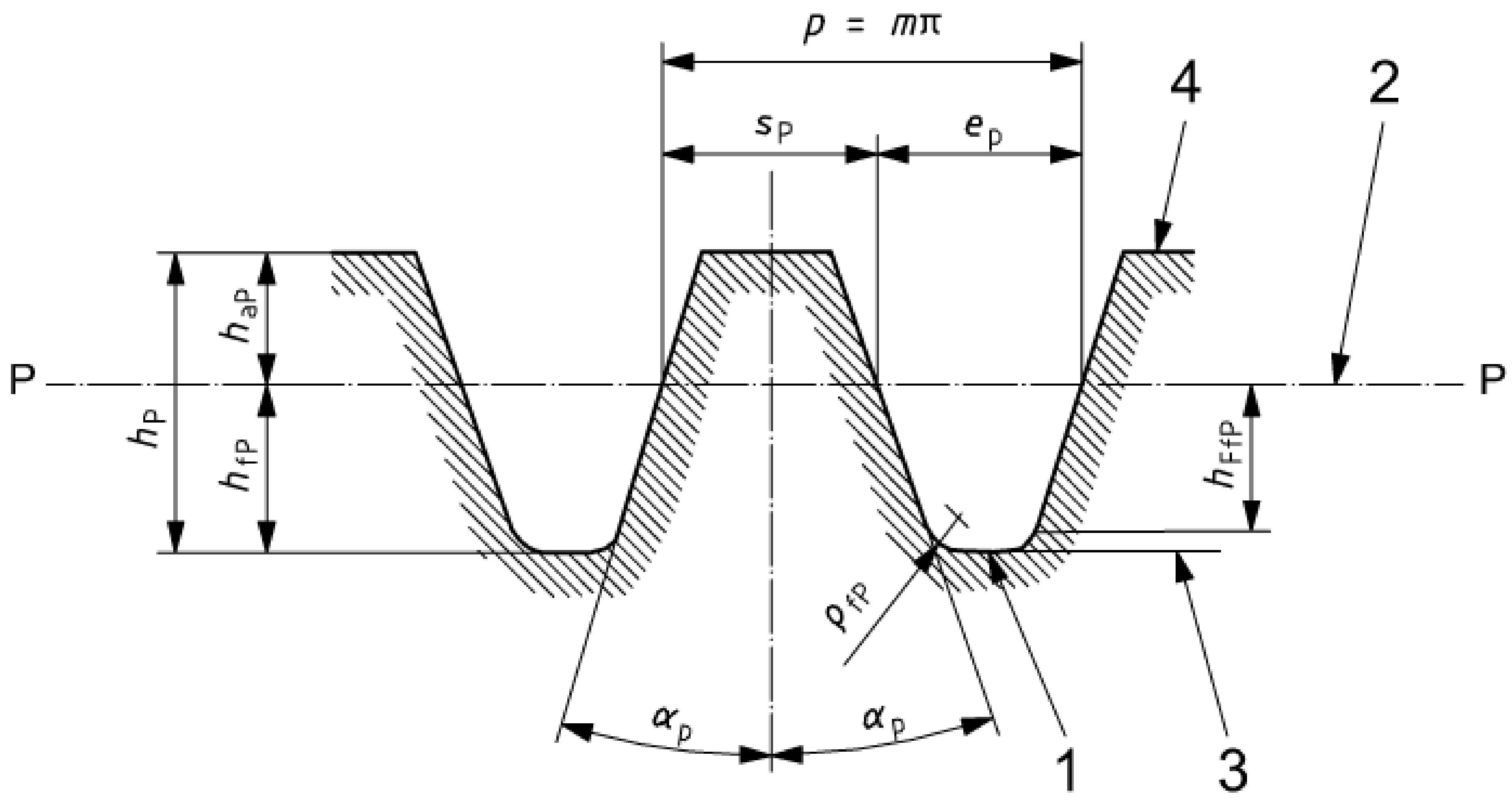

Key

1 basic rack profile

2 datum line

3 root line

4 tip line

Figure 4 — Terms and parameters relating to basic rack tooth profile in normal section

4.2.4 Reference cylinder, reference circle, reference diameter

The reference cylinder is the reference surface for the cylindrical gear teeth. Its axis coincides with the axis of the gear (gear axis). The reference circle is the intersection of the reference cylinder with a transverse plane section. The reference diameter, d, is determined by

$$d = |z|\, m_{\mathrm{t}} = \frac{|z|\, m_{\mathrm{n}}}{\cos\beta} \tag{1}$$

4.2.5 Gear axis

The axis of a gear (gear axis) is the axis that is defined by the geometrical axis of the support surfaces.

4.2.6 Sections through a cylindrical gear

4.2.6.1 Transverse section, transverse profile

The sectioning of cylindrical gear teeth by a plane perpendicular to the gear axis yields a transverse section. For helical gears, quantities in the transverse section are denoted by the subscript t. The intersection of a tooth with a transverse plane is termed the transverse profile.

4.2.6.2 Normal section, normal profile

The sectioning of involute helical gear teeth by a surface perpendicular to the flank lines of the involute helicoid yields a normal surface. The normal surface is curved three-dimensionally.

Quantities on the normal surface are denoted by the subscript n. The intersection of a tooth with a normal surface is termed the normal profile.

4.2.6.3 Axial section, axial profile

The sectioning of cylindrical gear teeth by a plane containing the gear axis yields an axial section.

Quantities in the axial section are denoted by the subscript x. The intersection of a tooth with an axial plane is termed the axial profile.

4.2.6.4 Cylindrical section, flank lines

The flank lines are lines of intersection of the right and left flanks with a cylinder that has an axis which coincides with the gear axis. Hence, right and left flank lines are to be distinguished.

The reference flank line (tooth trace) is the line of intersection of the flank with the reference cylinder. The base flank line is the line of intersection of the involute flank — possibly imagined as extended — with the base cylinder. The base flank line is a helix on the base cylinder. The origin of the involute helicoid is a base flank line. The tip flank line is the line of intersection of the involute flank — possibly imagined as extended — with the tip cylinder.

The flank lines are helices in the case of helical gear teeth and straight lines in the case of spur gear teeth.

4.2.7 Module

The module of a basic rack is found as the pitch of the rack divided by the number π (see Figure 4). The normal module, m_{n}, of the cylindrical gear is found as the module of the standard basic rack tooth profile (module series ISO 54).

For a helical gear, the transverse module, m_t, is found as

$$m_t = \frac{m_n}{\cos\beta} \tag{2}$$

and the axial module, m_x, as

$$m_x = \frac{m_n}{\sin\beta} = \frac{m_n}{\cos\gamma} = \frac{m_t}{\tan\beta} \tag{3}$$

For a spur gear, the module is $m = m_t = m_n$.

4.2.8 Facewidth

The facewidth, b, is the length of the toothed part of the cylindrical gear measured in the axial direction on the V-cylinder. (See 4.5.1.)

The usable facewidth, b_F, is the distance between two transverse sections that contain the fully developed height of the tooth flank. (See Figure 5.)

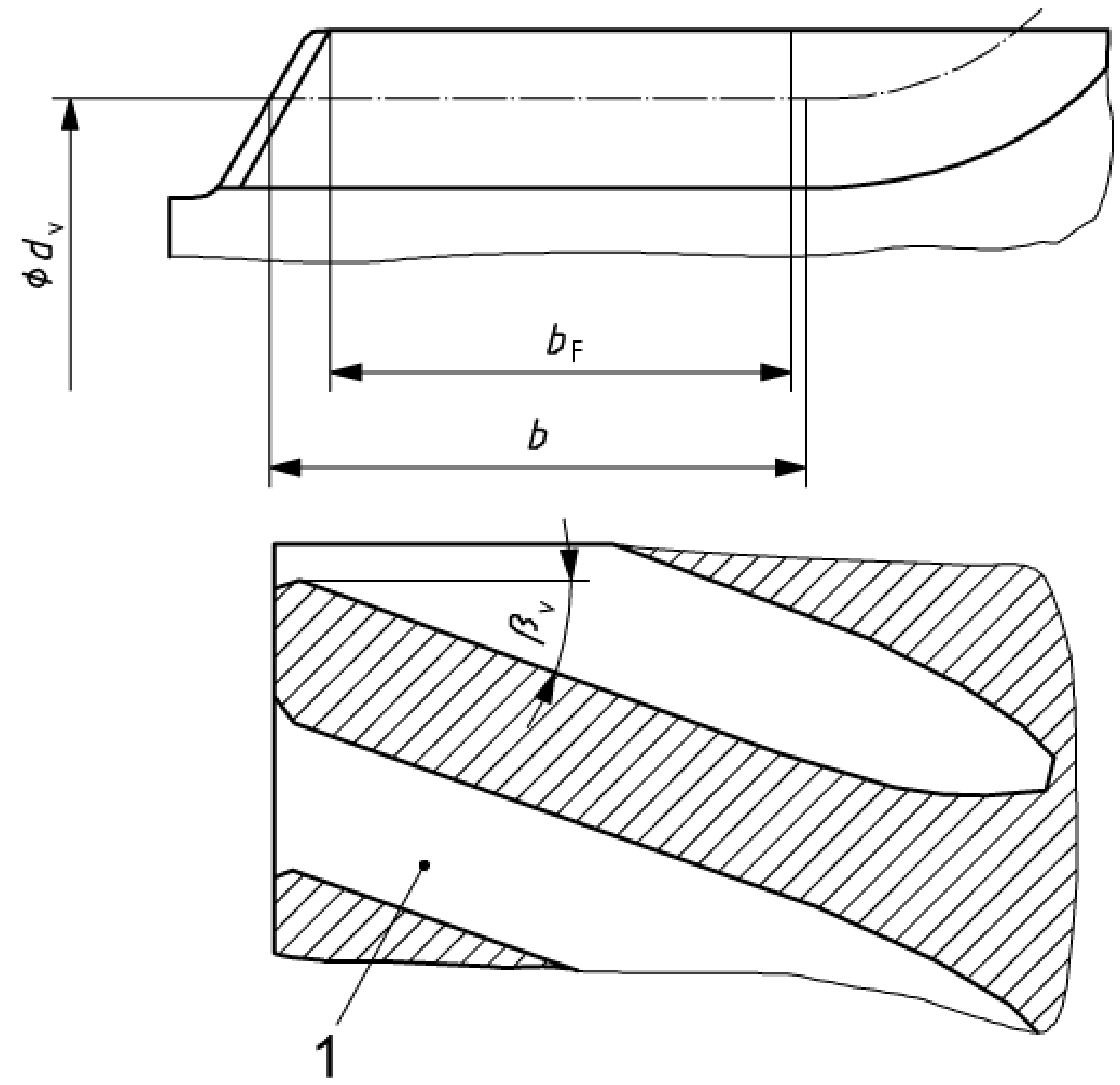

Key

1 developed view of V-cylinder

Figure 5 — Facewidth b, usable facewidth b_F

4.2.9 Profile shift, profile shift coefficient and sign of profile shift

The profile shift, xm_n, for involute gear teeth is the displacement of the basic rack datum line from the reference cylinder. The magnitude of the profile shift can be made non-dimensional by dividing by the normal module, and it is then expressed by the profile shift coefficient, x. Positive profile shift increases the tooth thickness on the reference cylinder. (See Figure 6.)

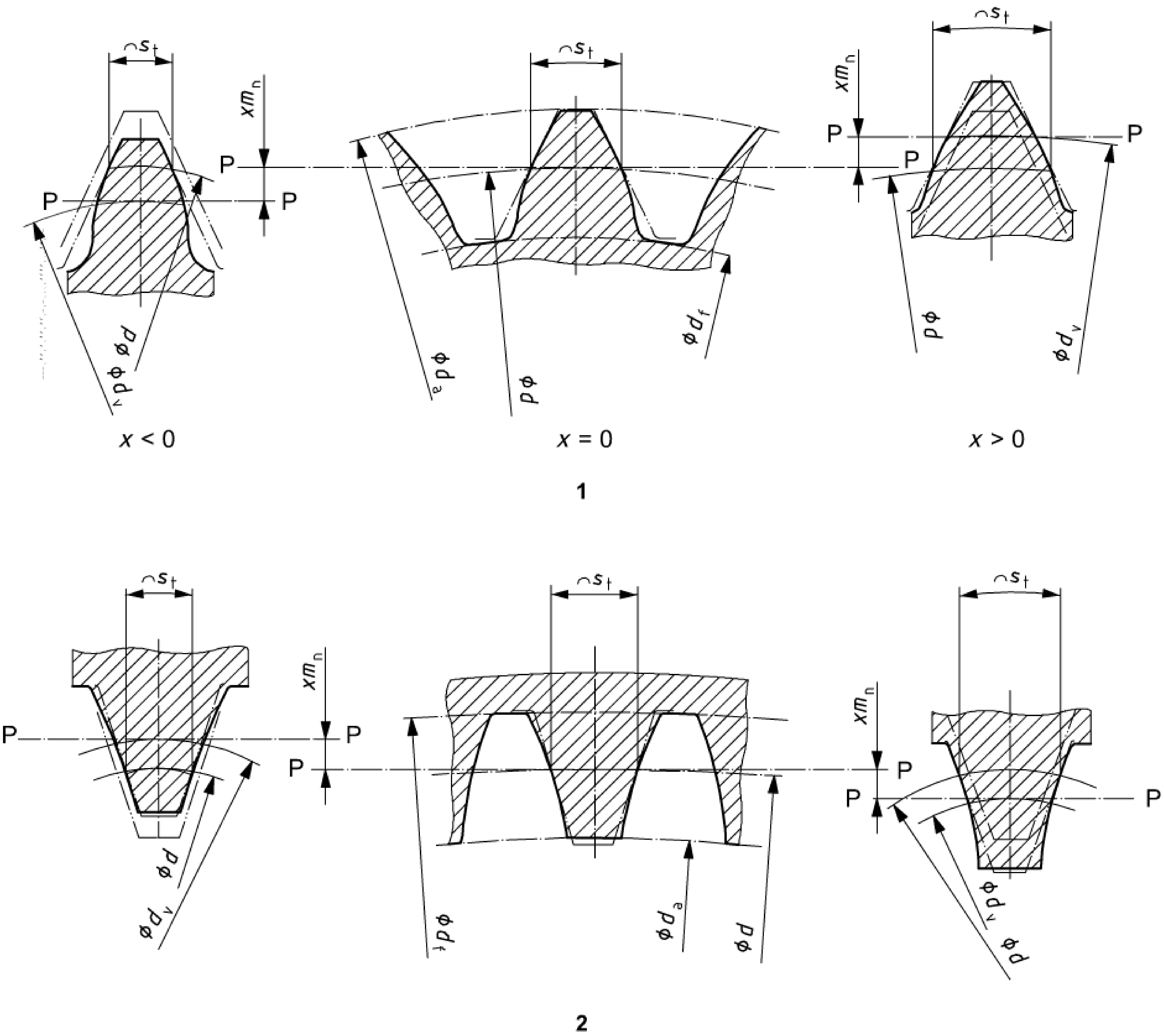

Key

⌒ measurement along an arc

P–P datum line of basic rack

1 external gear

2 internal gear

Figure 6 — Profile shift for external and internal gear teeth

4.3 Involute helicoids

4.3.1 Generator of involute helicoids

In developing the base cylinder surface as a plane, a flank line on the base cylinder describes an involute helicoid. The straight line inclined to the axial line in the developed surface (base cylinder tangential plane) is the generator of the involute helicoid, see Figure 7.

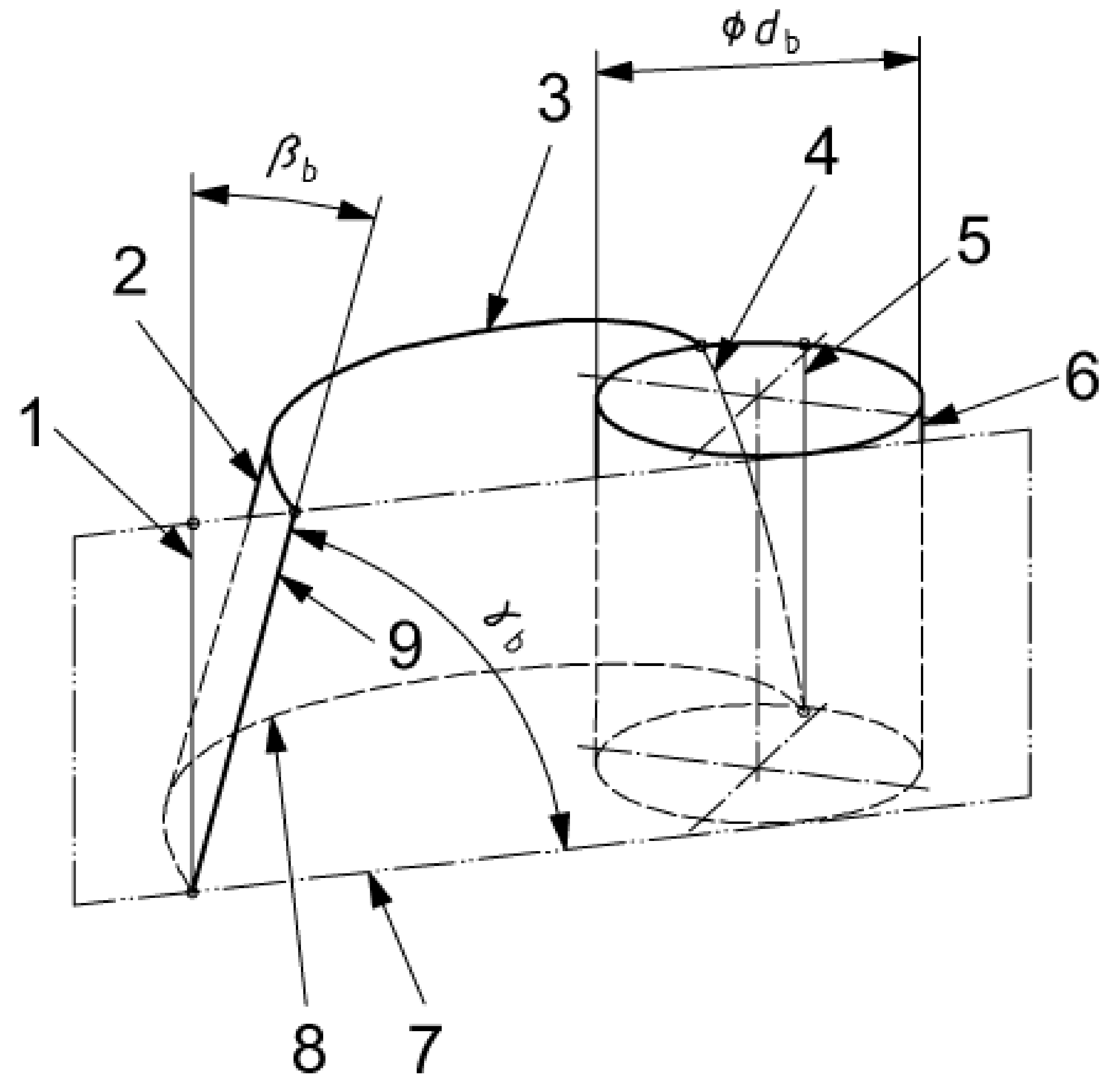

Key

1 developed axial line
2 involute helicoid
3 involute
4 base helix
5 base cylinder axial line
6 base cylinder
7 developed base cylinder envelope
8 involute
9 straight line generator

Figure 7 — Base cylinder with generator and involute helicoids

4.3.2 Lead

The lead, p_z, is the distance between successive intersections of an axial line with the involute helicoid, see Figure 8. The lead is independent of the diameter of the cylinder.

$$p_z = \frac{|z| m_n \pi}{\sin\beta} = \frac{|z| m_t \pi}{\tan\beta} = |z| p_x \tag{4}$$

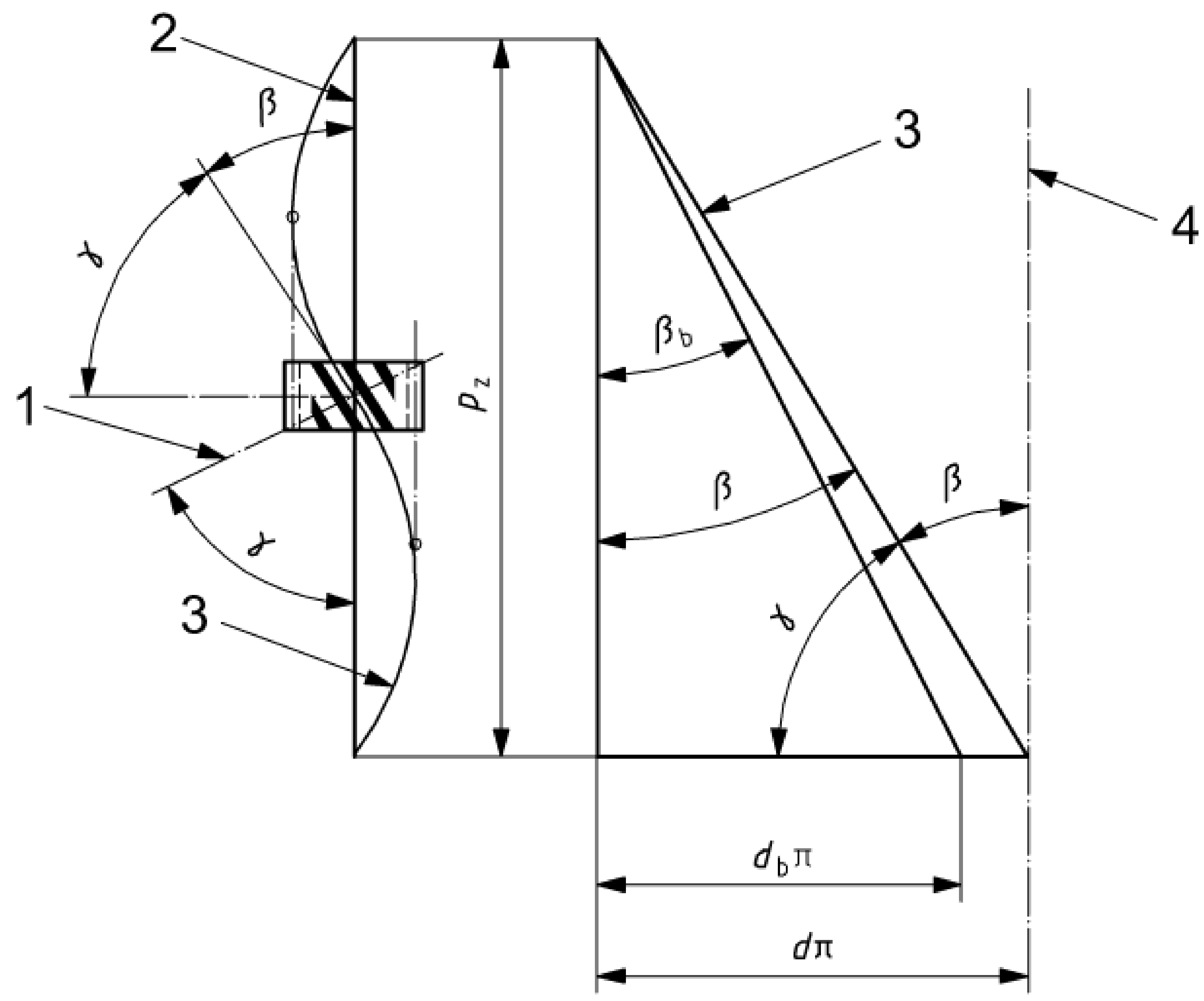

$\beta + \gamma = 90°$

Key

1 normal plane
2 reference cylinder envelope line, gear axis
3 reference trace
4 projection of the gear axis

Figure 8 — Lead triangle, lead, helix angle, lead angle

4.3.3 Helix angle, lead angle

The helix angle, β, is the angle between a tangent to a reference helix and the reference cylinder envelope line through the tangent contact point. In special cases, the helix angle, β_R, of right flanks may differ from the helix angle, β_L, of left flanks; however, all equations are based on equal helix angles.

The relationship between β and the base helix angle, β_b (helix angle on the base cylinder), is found from Equations (5) to (7):

$$\tan\beta_b = \tan\beta \cos\alpha_t \tag{5}$$

$$\sin\beta_b = \sin\beta \cos\alpha_n \tag{6}$$

$$\cos\beta_b = \cos\beta \frac{\cos\alpha_n}{\cos\alpha_t} = \frac{\sin\alpha_n}{\sin\alpha_t} = \frac{\sin\alpha_{yn}}{\sin\alpha_{yt}} = \cos\alpha_n \sqrt{\tan^2\alpha_n + \cos^2\beta} \tag{7}$$

On a cylinder with arbitrary diameter, d_y, the helix angle, β_y, is found from Equations (8) to (10):

$$\tan\beta_y = \tan\beta \frac{d_y}{d} = \tan\beta \frac{\cos\alpha_t}{\cos\alpha_{yt}} = \tan\beta_b \frac{d_y}{d_b} = \frac{\tan\beta_b}{\cos\alpha_{yt}} \tag{8}$$

$$\sin\beta_y = \sin\beta \frac{\cos\alpha_n}{\cos\alpha_{yn}} = \frac{\sin\beta_b}{\cos\alpha_{yn}} \tag{9}$$

$$\cos\beta_y = \frac{\tan\alpha_{yn}}{\tan\alpha_{yt}} = \frac{\cos\alpha_{yt}\cos\beta_b}{\cos\alpha_{yn}} \tag{10}$$

The lead angle, γ, is the angle at which the normal plane crosses the gear axis, see Figure 8. It is also the angle between a tangent to a reference helix (reference flank line) and the transverse section through the tangent contact point:

$$\gamma_y = 90° - \beta_y \tag{11}$$

For spur gears, $\beta = 0°$ and $\gamma = 90°$.

4.3.4 Flank direction

The flank direction is right-handed if the flank line describes a right-hand helix and left-handed if the flank line describes a left-hand helix. (See Figure 9.)

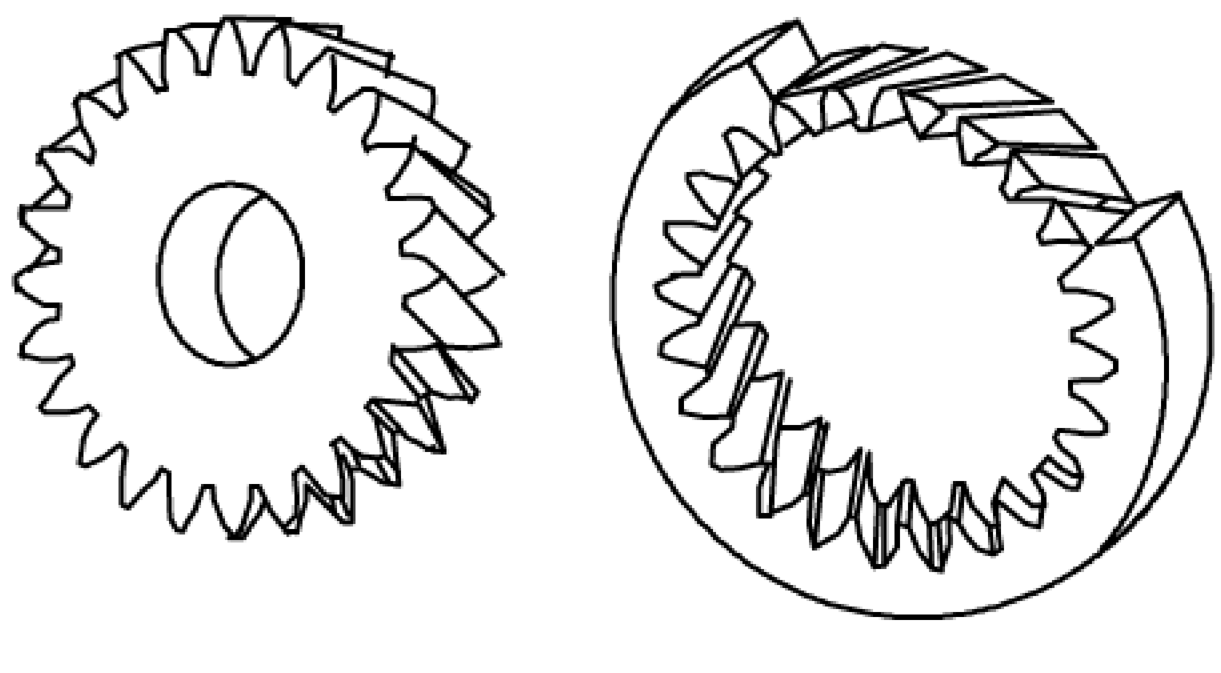

a) Right-hand teeth

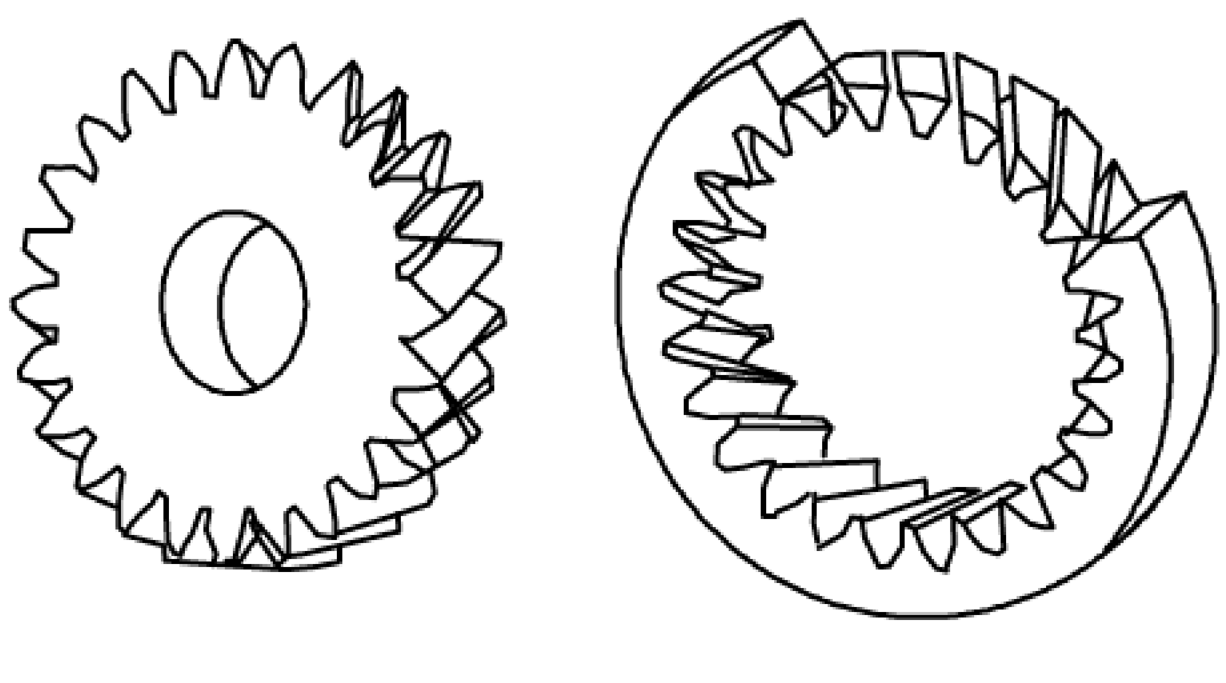

b) Left-hand teeth

Figure 9 — Direction of helix

4.3.5 Transverse pressure angle at a point, transverse pressure angle

In a transverse section, the tangent to the involute at the arbitrary point Y is inclined to the radius to that point by the transverse pressure angle, α_{yt}:

$$\cos\alpha_{yt} = \frac{d_b}{d_y} = \frac{d}{d_y}\cos\alpha_t \tag{12}$$

(See Figure 10.)

The transverse pressure angle, α_t, is the acute angle between the tangent to the involutes at their point of intersection with the reference circle and the radius through this point of intersection. It is expressed by

$$\cos\alpha_t = \frac{d_b}{d} \tag{13}$$

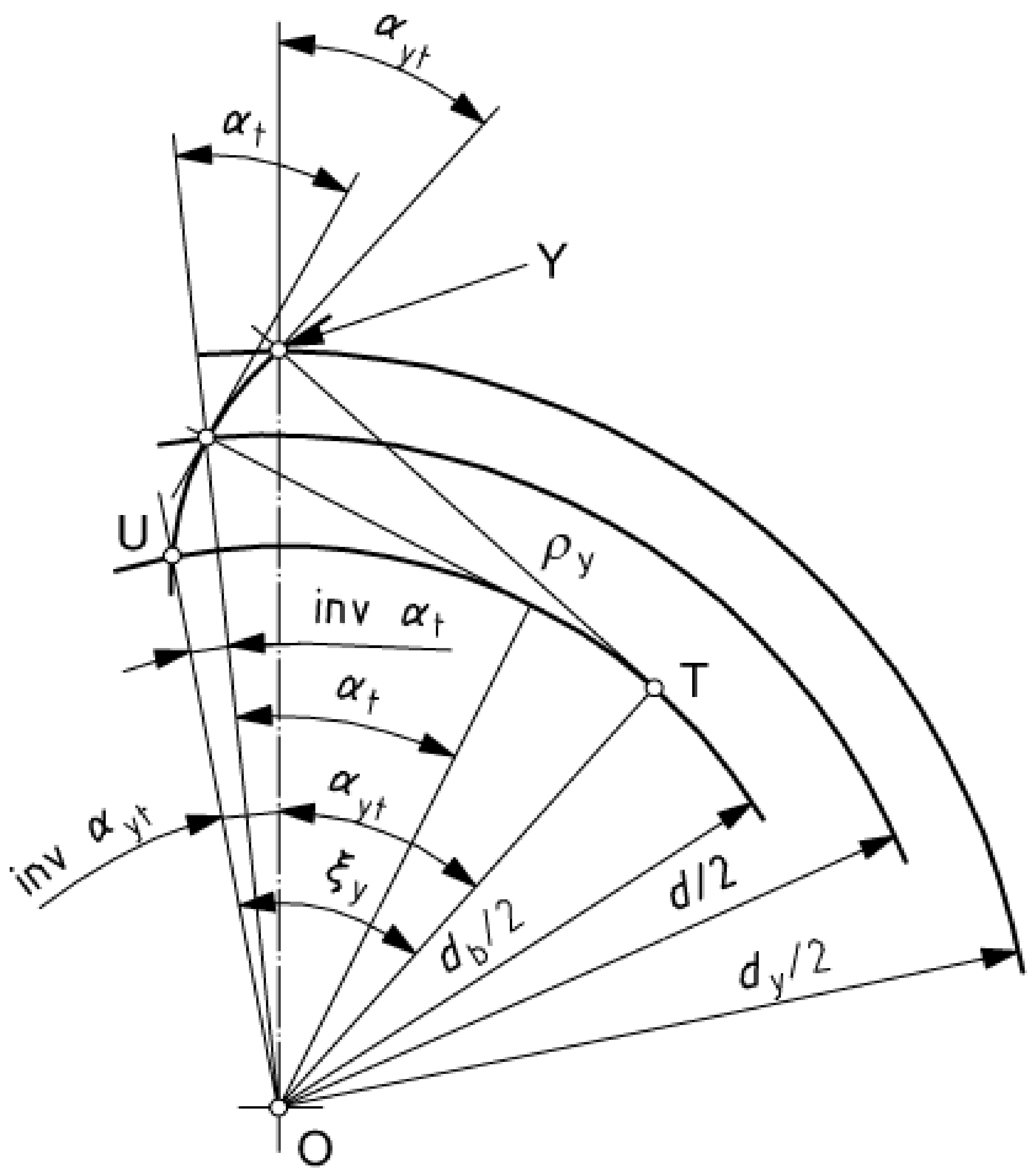

Figure 10 — Parameters relating to involute

4.3.6 Normal pressure angle at a point, normal pressure angle

In the normal section of the involute helicoid, the tangent to this section at an arbitrary point Y is inclined to the radius through Y by the normal pressure angle at that point, α_{yn}. The corresponding angle of inclination at the reference cylinder is the normal pressure angle, α_n; this is equal to the pressure angle, α_P, of the standard basic rack tooth profile.

$$\tan\alpha_n = \tan\alpha_t \cos\beta \tag{14}$$

$$\tan\alpha_{yn} = \tan\alpha_{yt} \cos\beta_y \tag{15}$$

For a spur gear, $\alpha_n = \alpha_t$ and $\alpha_{yn} = \alpha_{yt}$.

4.3.7 Roll angle of the involute

The angle at the centre over the base circle arc from the origin, U, of the involute to the contact point, T, of the tangent from point Y to the base circle is the roll angle, ξ_y, of the involute, see Figure 10. The base circle arc, UT, is equal to the tangent portion, YT, hence

$$\xi_y = \tan\alpha_{yt} \tag{16}$$

4.3.8 Radius of curvature of the involute, length of roll

The tangent portion, YT, is the radius of curvature, ρ_y, of the involute at point Y and at the same time the length of roll, L_y, belonging to point Y, i.e. the developed base circle arc from the involute origin, U. In the triangle OTY it is the side opposite the transverse pressure angle, α_{yt}, at the centre of the circle O:

$$L_y = \rho_y = \frac{z}{|z|}\frac{d_b}{2}\xi_y = \frac{z}{|z|}\frac{d_b}{2}\tan\alpha_{yt} = \frac{z}{|z|}\frac{\sqrt{d_y^2 - d_b^2}}{2} \tag{17}$$

(See Figure 10.)

4.3.9 Involute function

The angular difference, $\xi_y - \alpha_{yt}$, is termed the involute function of angle α_{yt} and is denoted by inv α_{yt} (to be read as “involute α_{yt}”):

$$\mathrm{inv}\,\alpha_{yt} = \xi_y - \alpha_{yt} = \tan\alpha_{yt} - \alpha_{yt} \tag{18}$$

(See Figure 10.)

4.3.10 Base cylinder, base circle, base diameter

The base cylinder is that cylinder coaxial with the gear axis that is determinative for the generation of the involute helicoids, see Figure 10. Quantities associated with the base cylinder are denoted by the subscript b.

The base circle is the intersection of the base cylinder with a plane of transverse section. The involutes from the base circle form the transverse profiles of the gearing. The base diameter, d_b, is given by

$$d_b = d\cos\alpha_t = |z|\,m_t\cos\alpha_t = \frac{|z|\,m_n\cos\alpha_t}{\cos\beta} = \frac{|z|\,m_n}{\sqrt{\tan^2\alpha_n + \cos^2\beta}} \tag{19}$$

$$d_b = |z|\,m_n\frac{\cos\alpha_n}{\cos\beta_b} \tag{20}$$

4.4 Angular pitch and pitches

4.4.1 Angular pitch

The angular pitch, τ, is that angle laying in transverse sections that result from the dividing of the complete periphery of a circle into z equal parts.

$$\tau = \frac{2\pi}{|z|} = \frac{2p_{yt}}{d_y} \text{ in radians} \tag{21}$$

$$\tau = \frac{360}{|z|} \text{ in degrees} \tag{22}$$

4.4.2 Pitches on the reference cylinder

4.4.2.1 Transverse pitch

The (reference cylinder) transverse pitch, p_t, is the length of the reference circle arc between two successive equal-handed tooth flanks (right or left flanks):

$$p_t = \frac{\pi m_n}{\cos \beta} = \frac{d}{2} \tau = \frac{\pi d}{|z|} = \pi m_t \tag{23}$$

(See Figure 11.)

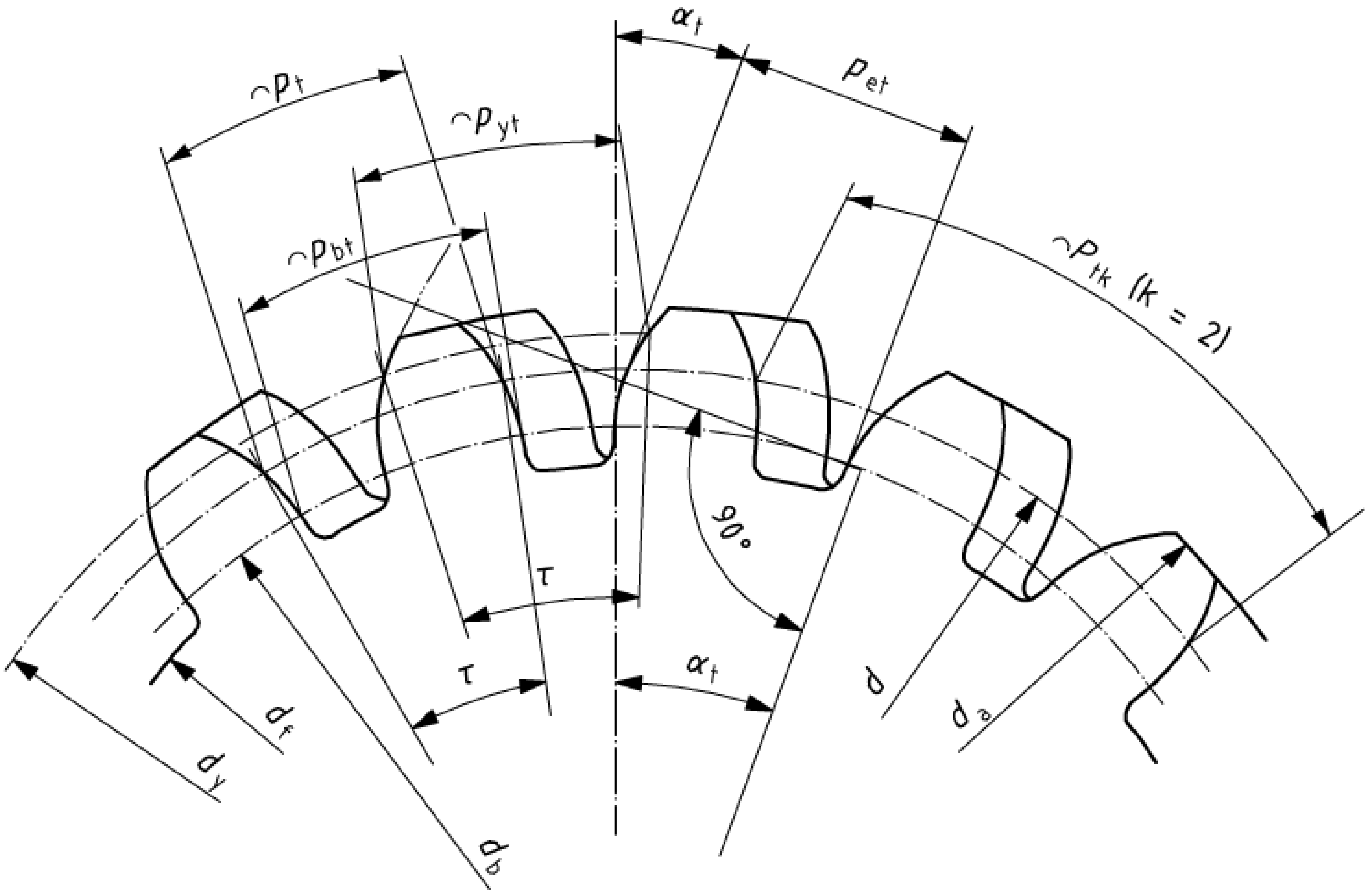

Key

⌒ measurement along an arc

Figure 11 — Diameter, angular pitch, transverse pitches on helical cylindrical gear

4.4.2.2 Normal pitch

The (reference cylinder) normal pitch, p_n, is the length of the helix arc between two successive equal-handed tooth flanks (right or left flanks) on the reference cylinder in the normal section of the gear:

$$p_n = \pi m_n = p_t \cos \beta \tag{24}$$

(See Figure 12.)

4.4.3 Pitches on any cylinder

It is necessary to distinguish between the transverse pitch, p_{yt}, and the normal pitch, p_{yn}, on a cylinder of any diameter, d_y, (Y-cylinder):

$$p_{yt} = \frac{d_y}{2} \tau = \frac{\pi d_y}{|z|} = \frac{d_y}{d} p_t \tag{25}$$

$$p_{yn} = p_{yt} \cos \beta_y \tag{26}$$

4.4.4 Axial pitch

The axial pitch, p_x, of a helical gear is the portion of a generation line of a cylinder concentric with the gear axis between two successive equal-handed tooth flanks (right or left flanks), see Figure 12. The axial pitch is independent of the diameter of the cylinder. Axial pitch does not apply to spur gears. It is expressed by

$$p_x = \frac{\pi m_n}{\sin\beta} = \pi m_x = \frac{p_z}{|z|} = \frac{\pi m_t}{\tan\beta} = \frac{p_{yt}}{\tan\beta_y} = \frac{p_{yn}}{\sin\beta_y} \tag{27}$$

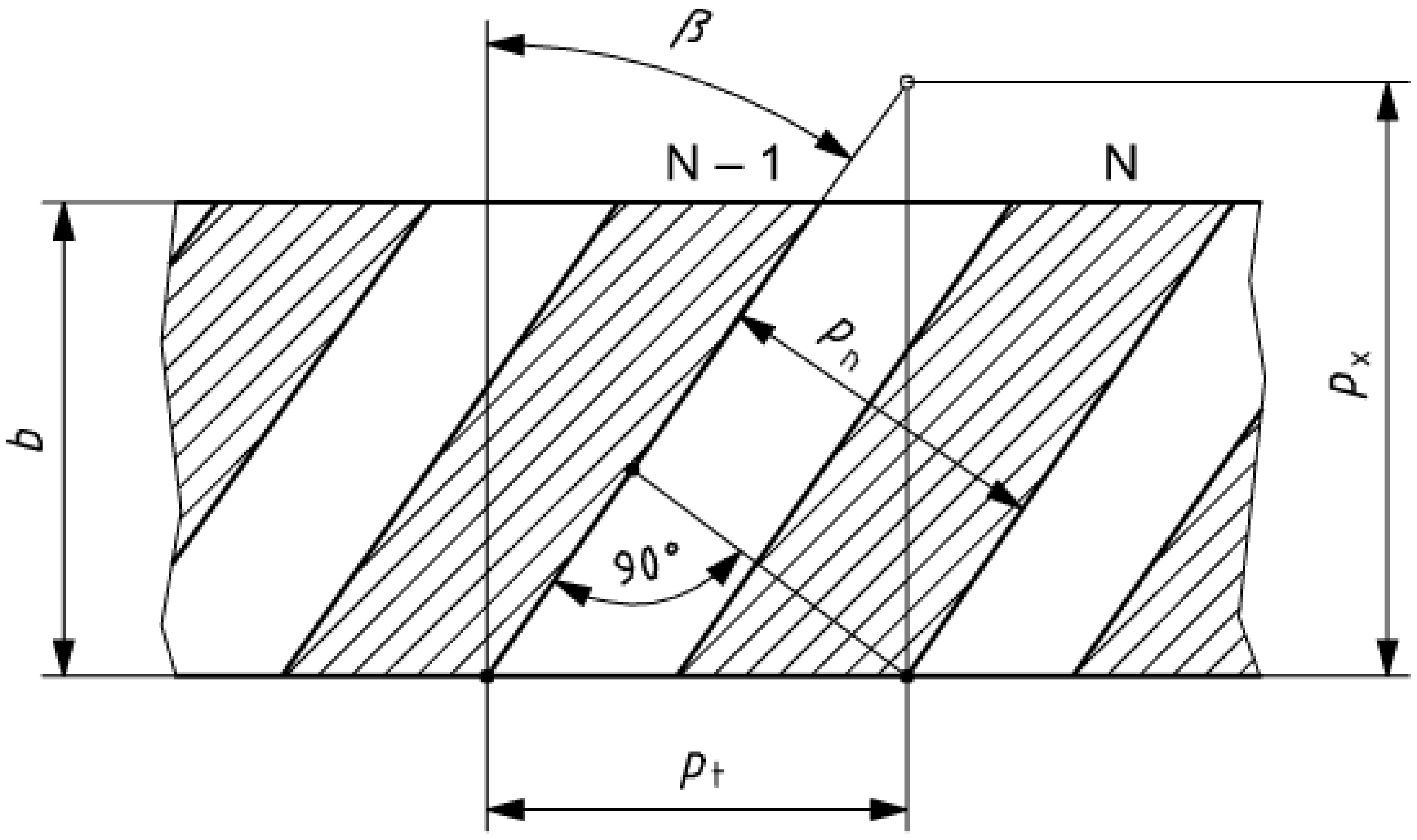

Figure 12 — Geometrical relations between transverse, normal and axial pitch in a developed view of a reference cylinder

4.4.5 Base pitch

The distance between successive equal-handed tooth flanks (right or left flanks) on the developed base cylinder tangential plane is the base pitch.

— Transverse base pitch:

$$p_{bt} = \frac{d_b}{2}\tau = p_t \cos\alpha_t = p_{yt}\cos\alpha_{yt} = \frac{\pi d_b}{|z|} = \frac{d_b}{d} p_t \tag{28}$$

— Normal base pitch:

$$p_{bn} = p_n \cos\alpha_n = p_{bt}\cos\beta_b \tag{29}$$

4.4.5.1 Transverse base pitch on the path of contact

The transverse base pitch on path of contact, p_{et}, is the distance between two parallel tangents in a transverse section which contact two successive equal-handed tooth flanks:

$$p_{et} = p_{bt} \tag{30}$$

(See Figure 11.)

4.4.5.2 Normal base pitch on the plane of contact

The normal base pitch, p_{en}, is the distance between two parallel tangential planes which contact two successive equal-handed tooth flanks:

$$p_{en} = p_{bn} \tag{31}$$

4.5 Diameters of gear teeth

The position of the standard basic rack tooth profile relative to the reference cylinder gives rise to the following cylindrical surfaces and diameters with respect to the gear teeth.

4.5.1 V-cylinder, V-circle diameter

The V-cylinder is the cylinder which is tangent to the reference plane of the basic rack in its generating position (see Figure 6). Its nominal diameter, d_V (V-circle diameter), is

$$d_\mathrm{V} = d + 2\frac{z}{|z|} x m_\mathrm{n} \tag{32}$$

4.5.2 Tip alteration coefficient

A change to the addendum relating to the addendum determined in the standard basic rack tooth profile is expressed by the tip alteration. The tip alteration is made non-dimensional by dividing by the normal module, and it is then expressed as the tip alteration coefficient, k.

The value to be used for k is signed.

A negative value yields a shorter addendum for either external or internal gears.

4.5.3 Tip cylinder, tip circle, tip diameter

The tip cylinder is the cylinder that defines the tips of the gear tooth system. A transverse section yields the tip circle. The nominal dimension of the tip diameter, d_a, is

$$d_\mathrm{a} = d + 2\frac{z}{|z|}(x m_\mathrm{n} + h_\mathrm{aP} + k m_\mathrm{n}) \tag{33}$$

4.5.4 Root cylinder, root circle, root diameter

The root cylinder is the cylindrical envelope surface that forms the bottom of the tooth space. A transverse section yields the root circle. The nominal dimension of the root diameter, d_f, is

$$d_\mathrm{f} = d - 2\frac{z}{|z|}(h_\mathrm{fP} - x m_\mathrm{n}) \tag{34}$$

4.6 Gear tooth height

4.6.1 Tooth depth

The tooth depth, h, of cylindrical gear (or rack) teeth is the difference between tip and root radius:

$$h = \frac{|d_\mathrm{a} - d_\mathrm{f}|}{2} = h_\mathrm{aP} + k m_\mathrm{n} + h_\mathrm{fP} \tag{35}$$

4.6.2 Addendum, dedendum

The addendum, h_a, and the dedendum, h_f, of a cylindrical gear are stated on the basis of the reference circle. Their values are calculated from Equations (36) and (37):

$$h_a = \frac{|d_a - d|}{2} = h_{aP} + x m_n + k m_n \tag{36}$$

$$h_f = \frac{|d - d_f|}{2} = h_{fP} - x m_n \tag{37}$$

4.7 Tooth thickness, space width

The equations in this section yield the tooth thickness and space width and their half angles for any value of x. If x is the nominal profile shift factor then nominal sizes for the tooth thickness and space width and their half angles result. If the generating profile shift factor, x_E, is used, then generated sizes for the tooth thickness and space width and their half angles result.

See Annex A for tooth thickness measuring methods.

4.7.1 Transverse tooth thickness

The transverse tooth thickness, s_{yt}, in the transverse section is the length of the circular arc of diameter, d_y, between the two involute helicoids of a tooth:

$$s_{yt} = d_y \psi_y = d_y \left[\psi + \frac{z}{|z|}(\mathrm{inv}\,\alpha_t - \mathrm{inv}\,\alpha_{yt}) \right] = d_y \left[\frac{\pi + 4x\tan\alpha_n}{2|z|} + \frac{z}{|z|}(\mathrm{inv}\,\alpha_t - \mathrm{inv}\,\alpha_{yt}) \right] \tag{38}$$

(See Figure 13.)

The transverse tooth thickness, s_t, on the reference circle is produced from

$$s_t = d\psi = d\left(\frac{\pi + 4x\tan\alpha_n}{2|z|} \right) = \frac{m_n}{\cos\beta}\left(\frac{\pi}{2} + 2x\tan\alpha_n \right) \tag{39}$$

4.7.2 Tooth thickness half angle

Tooth thickness angles are angles at the centre in a transverse section which are enclosed by the radii bounding a transverse tooth thickness, see Figure 13. The corresponding tooth thickness half angles, ψ_y, for any transverse tooth thickness, s_{yt}, are expressed by

$$\psi_y = \frac{s_{yt}}{d_y} = \psi + \frac{z}{|z|}(\mathrm{inv}\,\alpha_t - \mathrm{inv}\,\alpha_{yt}) \tag{40}$$

The following tooth thickness half angle applies to the reference circle:

$$\psi = \frac{\pi + 4x\tan\alpha_n}{2|z|} \tag{41}$$

In the case of the base circle, the base tooth thickness half angle is produced by

$$\psi_b = \psi + \frac{z}{|z|}\mathrm{inv}\,\alpha_t \tag{42}$$

4.7.3 Space width

The space width, e_{yt}, in the transverse section is the length of a circular arc of diameter, d_y, between the two involute helicoids of a space width:

$$e_{yt} = d_y \eta_y = d_y \left[\eta - \frac{z}{|z|} (\text{inv}\,\alpha_t - \text{inv}\,\alpha_{yt}) \right] = d_y \left[\frac{\pi - 4\,x \tan\alpha_n}{2|z|} - \frac{z}{|z|} (\text{inv}\,\alpha_t - \text{inv}\,\alpha_{yt}) \right] \quad (43)$$

(See Figure 13.)

The space width, e_t, on the reference circle is produced by

$$e_t = d\eta = d \left(\frac{\pi - 4\,x \tan\alpha_n}{2|z|} \right) = \frac{m_n}{\cos\beta} \left(\frac{\pi}{2} - 2\,x \tan\alpha_n \right) \quad (44)$$

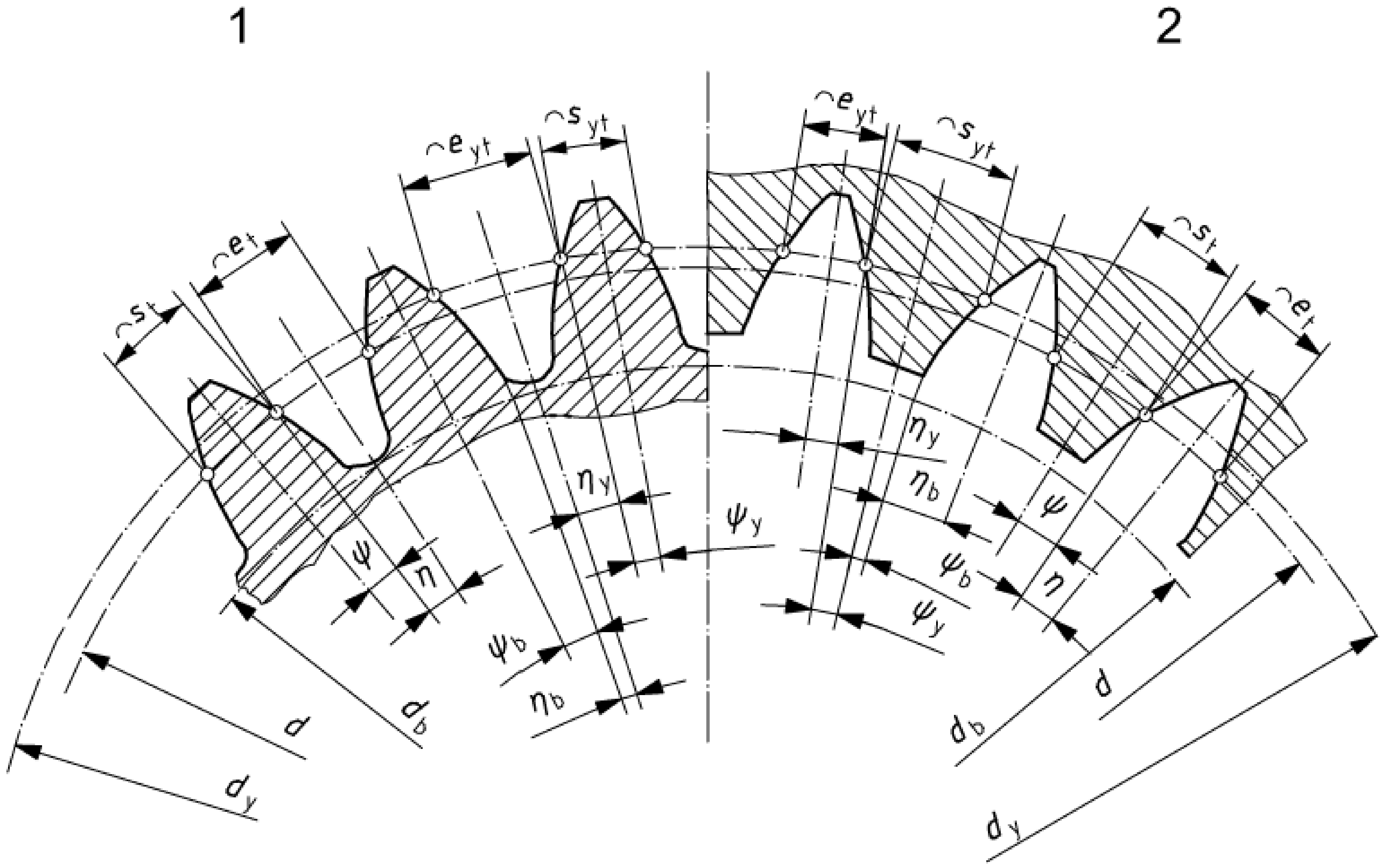

Key

⌒ measurement along an arc

1 external gear

2 internal gear

Figure 13 — Tooth thickness and space width (external and internal gear teeth)

4.7.4 Space width half angle

Space width angles are angles at the centre in a transverse section which are enclosed by the radii bounding a space width, see Figure 13. The corresponding space width half angles, η_y, for any space width, e_{yt}, are produced by

$$\eta_y = \frac{e_{yt}}{d_y} = \eta - \frac{z}{|z|} (\text{inv}\,\alpha_t - \text{inv}\,\alpha_{yt}) \quad (45)$$

The following space width half angle applies to the reference circle:

$$\eta = \frac{\pi - 4\,x \tan\alpha_{\mathrm{n}}}{2|z|} \tag{46}$$

At the base circle, the base space width half angle is produced by

$$\eta_{\mathrm{b}} = \eta - \frac{z}{|z|}\operatorname{inv}\alpha_{\mathrm{t}} \tag{47}$$

4.7.5 Normal tooth thickness

The normal tooth thickness is the tooth thickness in a normal section of the gear teeth. It is the length of the helical arc on the respective cylinder between the two involute helicoids of a tooth. The normal tooth thickness, s_{yn}, for any cylinder is calculated using

$$s_{\mathrm{yn}} = s_{\mathrm{yt}} \cos\beta_{\mathrm{y}} \tag{48}$$

The following normal tooth thickness applies to the reference cylinder:

$$s_{\mathrm{n}} = s_{\mathrm{t}} \cos\beta = m_{\mathrm{n}}\left(\frac{\pi}{2} + 2\,x \tan\alpha_{\mathrm{n}}\right) \tag{49}$$

4.7.6 Normal space width

The normal space width is the space width in a normal section of the gear teeth. It is the length of the helical arc on the respective cylinder between the two involute helicoids of a space width. The normal space width, e_{yn}, for any cylinder is calculated using

$$e_{\mathrm{yn}} = e_{\mathrm{yt}} \cos\beta_{\mathrm{y}} \tag{50}$$

The following normal space width applies to the reference cylinder:

$$e_{\mathrm{n}} = e_{\mathrm{t}} \cos\beta = m_{\mathrm{n}}\left(\frac{\pi}{2} - 2\,x \tan\alpha_{\mathrm{n}}\right) \tag{51}$$

5 Cylindrical gear pairs

The basic prerequisites for meshing of a cylindrical gear pair (or rack and pinion) according to this International Standard are

— identical standard basic rack tooth profiles for gear and mating gear (rack), and

— the same base helix angle with appropriate hands of the helices.

5.1 Concepts for a gear pair

5.1.1 Mating gear, mating flank

The mating gear in a gear pair is the gear which meshes with the other gear in question. The mating flanks for the tooth system of the other gear in question are the contacting tooth flanks of the mating gears.

5.1.2 Working flank, non-working flank

The tooth flank which transmits the torque during meshing is called the working flank. The other flank of this tooth is the non-working flank.

5.1.3 External gear pair

The mating of two external cylindrical gears (external gears) gives an external gear pair. The mating of an external gear with a rack gives a rack and pinion.

In the case of an external gear pair, the subscript 1 is used in equations for the smaller gear (pinion) and the subscript 2 for the larger gear (wheel). When the gears are of the same size, the subscripts can be allocated as desired. In the case of an external gear pair with helical gear teeth, one gear has a left-handed and the other gear (mating gear) a right-handed flank direction.

5.1.4 Internal gear pair

The mating of an external cylindrical gear (external gear) with an internal cylindrical gear (internal gear) gives an internal gear pair.

In the case of an internal gear pair, the subscript 1 is used in equations for the external gear and the subscript 2 for the internal gear. In the case of an internal gear pair with helical gear teeth, both gears have the same flank direction. Both are either right-handed or left-handed.

5.2 Mating quantities

5.2.1 Gear ratio

The gear ratio, u, of a gear pair is the ratio of the number of teeth of the wheel (or internal gear), z_2, to the number of teeth of the pinion, z_1:

$$u = \frac{z_2}{z_1}, \ |u| \geqslant 1 \tag{52}$$

5.2.2 Driving gear, driven gear, transmission ratio

The driving gear introduces rotation to the gear pair and effects the rotation of the driven gear.

The transmission, i, of a gear pair is the ratio of the angular speed (rotational speed) of the driving gear (subscript a) to that of the driven gear (subscript b):

$$i = \frac{\omega_a}{\omega_b} = \frac{n_a}{n_b} = -\frac{z_b}{z_a} \tag{53}$$

In the case of an external gear pair, the two cylindrical gears rotate in opposite directions, i.e. their angular speeds or rotational speeds have opposite signs; the transmission ratio is negative. In the case of an internal gear pair, the two cylindrical gears have the same direction of rotation, i.e. their angular speeds or rotational speeds have the same sign; the transmission ratio is positive. If it is necessary to make a distinction, ratios such that $|i| > 1$ are said to be “speed reducing ratios” while ratios such that $|i| < 1$ are said to be “speed increasing ratios”.

5.2.3 Line of centres, centre distance

In a transverse section of two mating gears, the line which connects the two axes is called the *line of centres*. The centre distance, a_w, is the working distance between the gear axes of the two gears on the line of centres, see Figure 14.

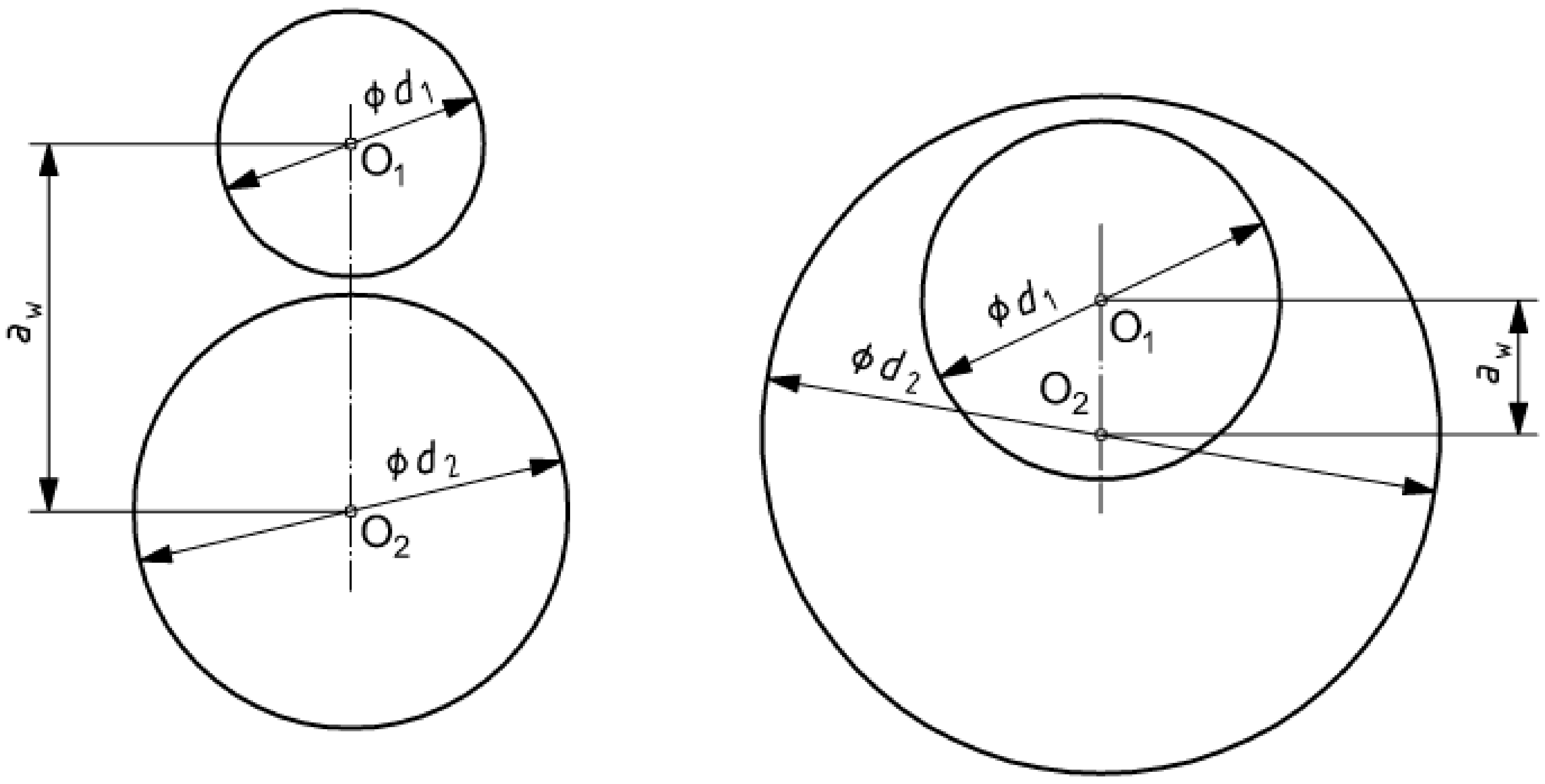

Figure 14 — Line of centres, centre distance

5.2.4 Working transverse pressure angle

The working transverse pressure angle, α_{wt}, is that pressure angle whose vertex lies on the pitch circle (working pitch circle). When a_w is known, α_{wt} is calculated from

$$\alpha_{wt} = \arccos\left[\left|z_1 + z_2\right|\left(\frac{m_n \cos\alpha_t}{2a_w \cos\beta}\right)\right] \tag{54}$$

Alternatively, for the particular case of zero backlash, α_{wt} results from

$$\operatorname{inv}\alpha_{wt} = \operatorname{inv}\alpha_t + \frac{2\tan\alpha_n}{z_1 + z_2}\left(x_1 + x_2\right) \tag{55}$$

5.2.5 Pitch point, pitch cylinders, pitch circles, pitch diameter, pitch axis

The pitch point divides the centre distance in the ratio of the tooth numbers. The pitch cylinders (pitch circles) are those cylinders (circles) which pass through the pitch point. The pitch diameter is the diameter of the pitch circle. The pitch axis is the axis through the pitch point, parallel to the axis of a pitch cylinder.

NOTE During operation, the peripheral velocities on the pitch cylinders are the same.

The pitch circles established during the operation of a cylindrical gear pair (gear pair in a gear unit) are termed *working pitch circles* (d_w). (See Figures 15 and 17.) The pitch circles established by a generating cutter during the generating of a tooth system in a generating gear unit are termed *generating pitch circles*.

The diameters of the working pitch circles are calculated from Equations (56) and (57):

$$d_{w1} = \frac{2a_w}{\frac{z_2}{z_1} + 1} = d_1 \frac{\cos\alpha_t}{\cos\alpha_{wt}} = \frac{d_{b1}}{\cos\alpha_{wt}} \tag{56}$$

$$d_{w2} = \frac{2a_w}{\frac{z_1}{z_2} + 1} = d_2 \frac{\cos\alpha_t}{\cos\alpha_{wt}} = \frac{d_{b2}}{\cos\alpha_{wt}} \tag{57}$$

This gives

$$a_{\mathrm{w}} = \frac{1}{2}\left(d_{\mathrm{w2}} + \frac{z_2}{|z_2|}\, d_{\mathrm{w1}}\right) \tag{58}$$

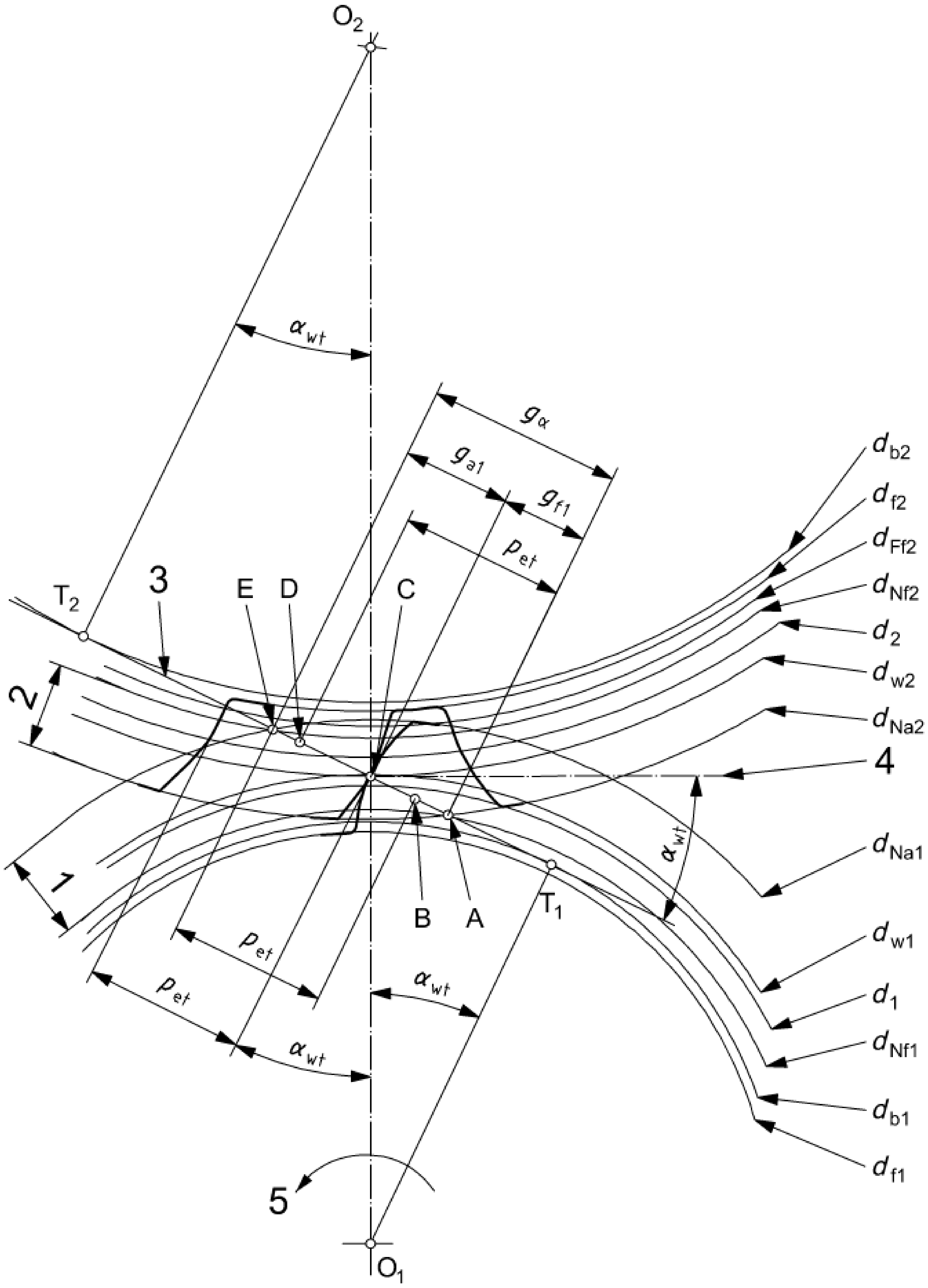

Key

1 radial part of active flank gear 1
2 radial part of active flank gear 2
3 line of action
4 tangent to pitch circles
5 direction of rotation of driving pinion

NOTE See 5.4.5.1 for description of lettered points.

Figure 15 — Meshing conditions and active ranges on working flanks in a transverse section of an external gear pair

5.2.6 Working depth

The working depth, h_w, of a gear pair is the overlap of the tip circles of the two cylindrical gears on the line of centres:

$$h_w = \frac{d_{a1} + \frac{z_2}{|z_2|} d_{a2}}{2} - \frac{z_2}{|z_2|} a_w \tag{59}$$

(See Figure 16.)

5.2.7 Tip clearance

The tip clearance, c, is the distance by which the tip circle of a gear is separated from the root circle of the mating gear, see Figure 16.

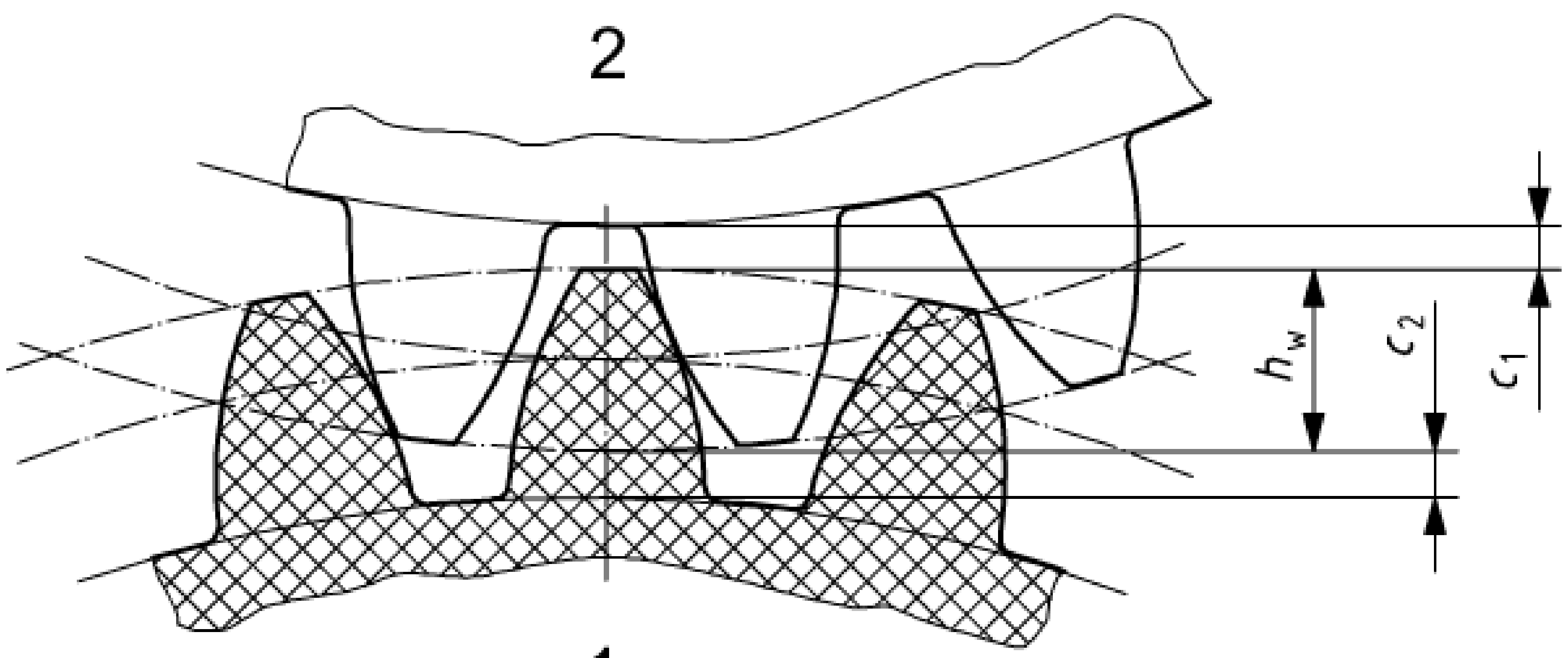

Key

1 pinion

2 gear wheel

Figure 16 — Working depth, h_w, and tip clearances c_1 and c_2 of a gear pair

The actual clearance follows from the centre distance, a_w, the manufactured tip diameter, d_a, and the generated root diameter, d_{fE}. For a pinion it is

$$c_1 = \frac{z_2}{|z_2|}\left(a_w - \frac{d_{fE2}}{2}\right) - \frac{d_{a1}}{2} \tag{60}$$

and for a wheel

$$c_2 = \frac{z_2}{|z_2|}\left(a_w - \frac{d_{a2}}{2}\right) - \frac{d_{fE1}}{2} \tag{61}$$

5.3 Calculation of the sum of the profile shift coefficients

The sum of the profile shift coefficients which corresponds to the zero backlash condition is related to the basic tooth parameters and centre distance by Equation (62), with a_{wt} from Equation (54):

$$\sum x = x_1 + x_2 = \frac{(z_1 + z_2)(\mathrm{inv}\alpha_{wt} - \mathrm{inv}\alpha_t)}{2\tan\alpha_n} \tag{62}$$

In the case of non-zero backlash, the normal backlash, j_{bn} (see 5.5.1), is included in the calculation:

$$\sum x_E = x_{E1} + x_{E2} = \frac{(z_1 + z_2)(\text{inv}\alpha_{wt} - \text{inv}\alpha_t)}{2\tan\alpha_n} - \frac{j_{bn}}{2m_n \sin(\alpha_n)} \tag{63}$$

The way in which $\sum x = x_1 + x_2$ is distributed between the two gears may be decided on the basis of aspects such as permissible stress, sliding velocities or other specified dimensions of the gear teeth such as root diameter.

5.4 Tooth engagement

Tooth engagement refers to the meshing of a gear (or a rack) with its mating gear. The tooth engagement is influenced by the geometry of the gear pair (or rack and pinion), the mutual contact of the tooth flanks and the sliding conditions, see Figures 15 and 17.

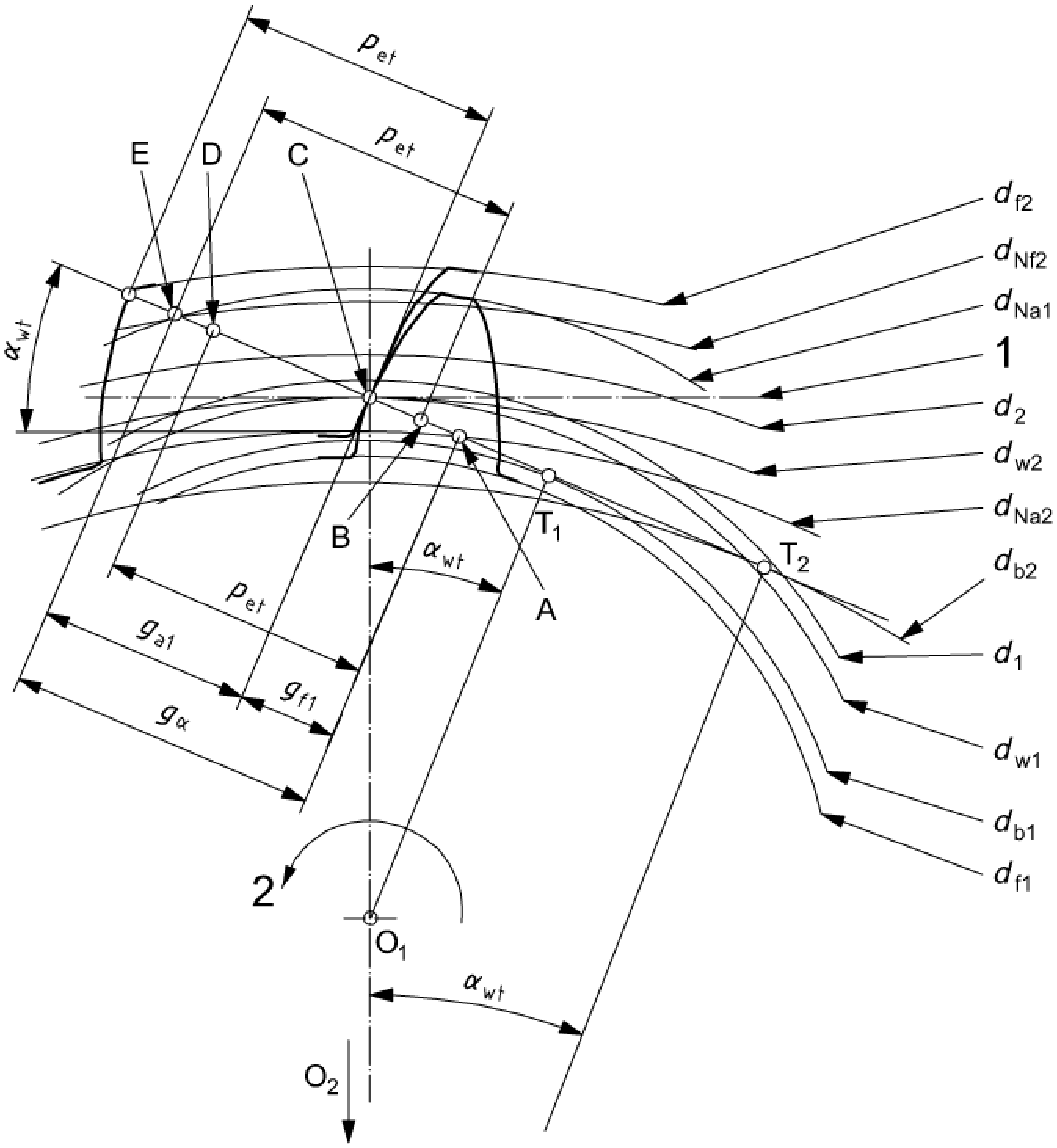

Key

1 tangent to pitch circles

2 direction of rotation of driving pinion

NOTE See 5.4.5.1 for a description of points A, B, C, D and E.

Figure 17 — Meshing conditions and active ranges on working flanks in a transverse section of an internal gear pair

5.4.1 Start of involute, active area of the tooth flanks, start of active profile and active tip diameters

The root form diameter, d_{Ff}, is the start of the involute portion of the profile. For an external gear it is the greatest of the base diameter, d_{b}, or the diameter of the intersection of the flank with the root fillet or trochoid (taking into account undercut if necessary).

In a defined gear pair the active tip diameter, d_{Na}, of a gear may be governed either by its tip form diameter, d_{Fa}, or by the start of involute of its mate (i.e. $d_{\text{Na}} \leqslant d_{\text{Fa}}$). The start of active profile (active root) diameter, d_{Nf}, may be governed either by the diameter of start of involute or by the tip form diameter of its mate. The active area of the flank extends from the active tip diameter to the active root diameter and so is dependent on the characteristics of both gears and the centre distance.

The following applies to a gear pair.

Usually, root contact on both gears is limited by the tip form diameter of the mating gear ($d_{\text{Na}} = d_{\text{Fa}}$). In this case:

$$d_{\text{Nf1}} = \sqrt{\left(2a_{\text{w}} \sin\alpha_{\text{wt}} - \frac{z_2}{|z_2|}\sqrt{d_{\text{Fa2}}^2 - d_{\text{b2}}^2}\right)^2 + d_{\text{b1}}^2} \tag{64}$$

$$d_{\text{Nf2}} = \sqrt{\left(2a_{\text{w}} \sin\alpha_{\text{wt}} - \sqrt{d_{\text{Fa1}}^2 - d_{\text{b1}}^2}\right)^2 + d_{\text{b2}}^2} \tag{65}$$

However, if d_{Ff} is greater than the quantity calculated by the corresponding equation above, then:

$$d_{\text{Nf1}} = d_{\text{Ff1}} \tag{66}$$

$$d_{\text{Nf2}} = d_{\text{Ff2}} \tag{67}$$

(See 7.6 for d_{Ff}.)

If $d_{\text{Nf1}} = d_{\text{Ff1}}$, then

$$d_{\text{Na2}} = \sqrt{\left(2a_{\text{w}} \sin\alpha_{\text{wt}} - \sqrt{d_{\text{Ff1}}^2 - d_{\text{b1}}^2}\right)^2 + d_{\text{b2}}^2} \tag{68}$$

otherwise, $d_{\text{Na2}} = d_{\text{Fa2}}$.

If $d_{\text{Nf2}} = d_{\text{Ff2}}$, then

$$d_{\text{Na1}} = \sqrt{\left(2a_{\text{w}} \sin\alpha_{\text{wt}} - \frac{z_2}{|z_2|}\sqrt{d_{\text{Ff2}}^2 - d_{\text{b2}}^2}\right)^2 + d_{\text{b1}}^2} \tag{69}$$

otherwise, $d_{\text{Na1}} = d_{\text{Fa1}}$.

The roll angle (see 4.3.7), $\xi_{\text{Nf}} = \tan\alpha_{\text{Nf}}$, can be used to obtain the active root diameter of the external gear (z_1) used by the mating gear (z_2) as,

$$d_{\text{Nf1}} = \frac{d_{\text{b1}}}{\cos\alpha_{\text{Nf1}}} \tag{70}$$

with α_{Nf1} from

$$\xi_{\text{Nf1}} = \frac{z_2}{z_1}\left(\xi_{\text{wt}} - \xi_{\text{Na2}}\right) + \xi_{\text{wt}} \tag{71}$$

$$\xi_{\text{Na2}} = \tan\arccos\frac{d_{\text{b2}}}{d_{\text{Na2}}} \tag{72}$$

and the usable root diameter of the internal gear (z_2) used by the pinion (z_1) as

$$d_{\text{Nf2}} = \frac{d_{\text{b2}}}{\cos\alpha_{\text{Nf2}}} \tag{73}$$

with α_{Nf2} from

$$\xi_{\text{Nf2}} = \frac{z_1}{z_2}\left(\xi_{\text{wt}} - \xi_{\text{Na1}}\right) + \xi_{\text{wt}} \tag{74}$$

$$\xi_{\text{Na1}} = \tan\arccos\frac{d_{\text{b1}}}{d_{\text{Na1}}} \tag{75}$$

5.4.2 Plane of action, zone of action, contact line

The plane of action of a cylindrical gear pair is tangent to the base cylinders of the gear and mating gear. In the case of an external gear pair, the plane of action passes between the base cylinders. The intersection of the two planes of action (one for each tooth flank) is parallel to the gear axes, and is the pitch axis (see 5.2.5). The zones of action are the parts of the planes of action which are limited by the usable tip cylinders of the gear and mating gear and by the facewidth and, in the case of external gears, can be further limited by the start of the involute. A zone of action is linked to the flank that is normal to it. Hence, one of the planes of action is linked to the right flanks and the other to the left flanks.

At any instant in time, the intersection of the zone of action with the corresponding tooth flanks of a gear pair is known as the *contact line*. With the rotation of the gears around their axes, the contact lines move through the zone of action. On tooth flanks, the contact lines are identical to the generators of flank and mating flank, see 4.3.1.

5.4.3 Line of action, path of contact, point of contact

Lines of action are where the planes of action intersect transverse sections. According to 5.4.2, it is necessary to distinguish between the right flank line of action and the left flank line of action. A line of action is inclined to the common tangent to the pitch circles at the pitch point (pitch circle tangent) by the working transverse pressure angle, α_{wt} (see Figures 15 and 17), and it contacts the two base circles at the points T_1 and T_2.

A path of contact is that part of the line of action which is within the zone of action. The starting point, A, of the path of contact is at or near the tip circle of the driven gear. The finishing point, E, of the path of contact is at or near the tip circle of the driving gear.

NOTE In Figures 15 and 17, only the line of action of the working flanks is shown in each case.

The lines of action intersect the centre line at pitch point C (see 5.2.5). Pitch point C is also the point at which the two lines of action intersect.

A point of contact is a point where a path of contact intersects the corresponding tooth flanks in a specific working position of the two gears. It is a point on the contact line.

5.4.4 Form over dimension

The form over dimension, c_{F}, is the radial distance between active root diameter and form root diameter.

$$c_{\mathrm{F}} = \frac{1}{2}\frac{z_2}{|z_2|}\left(d_{\mathrm{Nf}} - d_{\mathrm{Ff}}\right) \tag{76}$$

5.4.5 Designations and values relating to the line of action

5.4.5.1 Special points on the line of action

Special points on the line of action (see Figures 15 and 17) are as follows:

- T_1 is the point of contact between the line of action and the base circle of pinion (d_{b1});
- T_2 is the point of contact between the line of action and the base circle of wheel (d_{b2});
- C is the pitch point, the intersection of the line of action with the line of centres.

In Figures 15 and 17 the pinion is the driving gear and ε_α is less than 2. Special points on the path of contact are the following:

- A is the starting point of engagement, the point at which the line of action intersects the active tip diameters, d_{Na}, of the driven gear;
- B is the inner point of single pair contact on the driving gear, outer point of single pair contact on the driven gear; where $\varepsilon_\alpha < 2$, it is the point within the path of contact which is one transverse base pitch away from point E;
- D is the outer point of single pair contact on the driving gear, inner point of single pair contact on the driven gear; where $\varepsilon_\alpha < 2$, it is the point within the path of contact which is one transverse base pitch away from point A;
- E is the end point of engagement, the point at which the line of action intersects the active tip diameter, d_{Na}, of the driving gear.

5.4.5.2 Length of the path of contact

The length, g_α, of the path of contact (length between points A and E on the contact lines, which is also defined as L_{AE} in ISO 1328-1) of two mating cylindrical gears is

$$g_\alpha = \frac{1}{2}\left[\sqrt{d_{\mathrm{Na1}}^2 - d_{\mathrm{b1}}^2} + \frac{z_2}{|z_2|}\left(\sqrt{d_{\mathrm{Na2}}^2 - d_{\mathrm{b2}}^2} - 2a_{\mathrm{w}}\sin\alpha_{\mathrm{wt}}\right)\right] \tag{77}$$

The length of the path of contact when a cylindrical gear (subscript 1) is mated with a rack is

$$g_\alpha = \frac{1}{2}\left(\sqrt{d_{\mathrm{Na1}}^2 - d_{\mathrm{b1}}^2} - d_{\mathrm{b1}}\tan\alpha_{\mathrm{t}}\right) + \frac{h_{\mathrm{aP}} - x_1 m_{\mathrm{n}}}{\sin\alpha_{\mathrm{t}}} \tag{78}$$

The path of contact is divided by pitch point C into the approach path of contact (portion of the path of contact at the root flank of the driving gear between the root circle, d_{Nf1}, and the pitch point) and the recess path of contact (portion of the path of contact at the tip flank of the driving gear between the pitch point and the tip circle, d_{Na1}), see Figures 15 and 17. These portions of the path of contact are sometimes referred to as the tip (addendum) path of contact, g_{a}, and root (dedendum) path of contact, g_{f}, of the gears.

For the case where pinion is the driving gear and wheel the driven gear, the approach path of contact is equal to the dedendum path of contact, g_{f1}, of pinion, which is equal to the addendum path of contact, g_{a2}, of wheel:

$$g_{f1} = \overline{AC} = \frac{1}{2}\frac{z_2}{|z_2|}\left(\sqrt{d_{Na2}^2 - d_{b2}^2} - d_{b2}\tan\alpha_{wt}\right) = g_{a2} \tag{79}$$

The recess path of contact is equal to the addendum path of contact, g_{a1}, of pinion, which is equal to the dedendum path of contact, g_{f2}, of wheel:

$$g_{a1} = \overline{CE} = \frac{1}{2}\left(\sqrt{d_{Na1}^2 - d_{b1}^2} - d_{b1}\tan\alpha_{wt}\right) = g_{f2} \tag{80}$$

For the opposite case (wheel driving, pinion driven), in Equations (79) and (80), g_a and g_f are to be interchanged.

5.4.5.3 Radii of curvature of the tooth flanks

The following segments of the lines of action give rise to the radii of curvature of the tooth flanks in the transverse plane (see Figures 15 and 17):

$$\overline{T_1C} = \rho_{C1} = \frac{1}{2}\sqrt{d_{w1}^2 - d_{b1}^2} = \frac{1}{2}d_{b1}\tan\alpha_{wt} \tag{81}$$

$$\overline{T_2C} = \rho_{C2} = \frac{1}{2}\frac{z_2}{|z_2|}\sqrt{d_{w2}^2 - d_{b2}^2} = \frac{1}{2}\frac{z_2}{|z_2|}d_{b2}\tan\alpha_{wt} \tag{82}$$

$$\overline{T_2A} = \rho_{A2} = \frac{1}{2}\frac{z_2}{|z_2|}\sqrt{d_{Na2}^2 - d_{b2}^2} \tag{83}$$

$$\overline{T_1E} = \rho_{E1} = \frac{1}{2}\sqrt{d_{Na1}^2 - d_{b1}^2} \tag{84}$$

$$\overline{T_1B} = \rho_{B1} = \rho_{E1} - p_{et} \tag{85}$$

$$\overline{T_2D} = \rho_{D2} = \rho_{A2} - p_{et} \tag{86}$$

$$\overline{T_1T_2} = \rho_{C1} + \rho_{C2} = \frac{z_2}{|z_2|}a_w\sin\alpha_{wt} = \rho_{A1} + \rho_{A2} = \rho_{E1} + \rho_{E2} \tag{87}$$

Equations (83) to (86) apply if pinion is the driving gear and wheel the driven gear. In the opposite case, A and E, as well as B and D, are to be interchanged in Figures 15 and 17 and in Equations (83) to (86).

NOTE The values obtained for the curvature radii of an internal gear and for the segment $\overline{T_1T_2}$ of an internal gear pair are negative values.

5.4.6 Tooth interference

Interference conditions occur if parts of the tooth flanks or top lands of a gear come into contact with non-involute flank sections or the root on the mating gear. Additional meshing difficulties can be caused by contacts by a tooth tip with a non-working flank, which is a particular problem with internal gears. Also see 7.8.

NOTE Such complexities are not covered in this International Standard.

5.4.7 Overlaps

5.4.7.1 Transverse angle of transmission, transverse contact ratio

The transverse angle of transmission, φ_α, is the centre angle through which a gear of a gear pair rotates from start to finish of engagement of one active tooth flank transverse profile with its mating profile. The transverse angle of transmission of pinion and gear is given as follows:

$$\varphi_{\alpha 1} = \frac{2 g_\alpha}{d_{b1}} = |u|\, \varphi_{\alpha 2} \tag{88}$$

$$\varphi_{\alpha 2} = \frac{2 g_\alpha}{d_{b2}} = \frac{\varphi_{\alpha 1}}{|u|} \tag{89}$$

The transverse contact ratio, ε_α, is the ratio of the transverse angle of transmission, φ_α, to the angular pitch, τ, or the ratio of the path of contact to the transverse normal base pitch:

$$\varepsilon_\alpha = \frac{\varphi_{\alpha 1}}{\tau_1} = \frac{\varphi_{\alpha 2}}{\tau_2} = \frac{g_\alpha}{p_{et}} = \frac{g_f + g_a}{p_{et}} \tag{90}$$

where $p_{et} = p_{bt}$.

5.4.7.2 Active facewidth

The active facewidth, b_w, is the overlapping section of the usable facewidths of the gear pair, see Figure 18 and Figure 5.

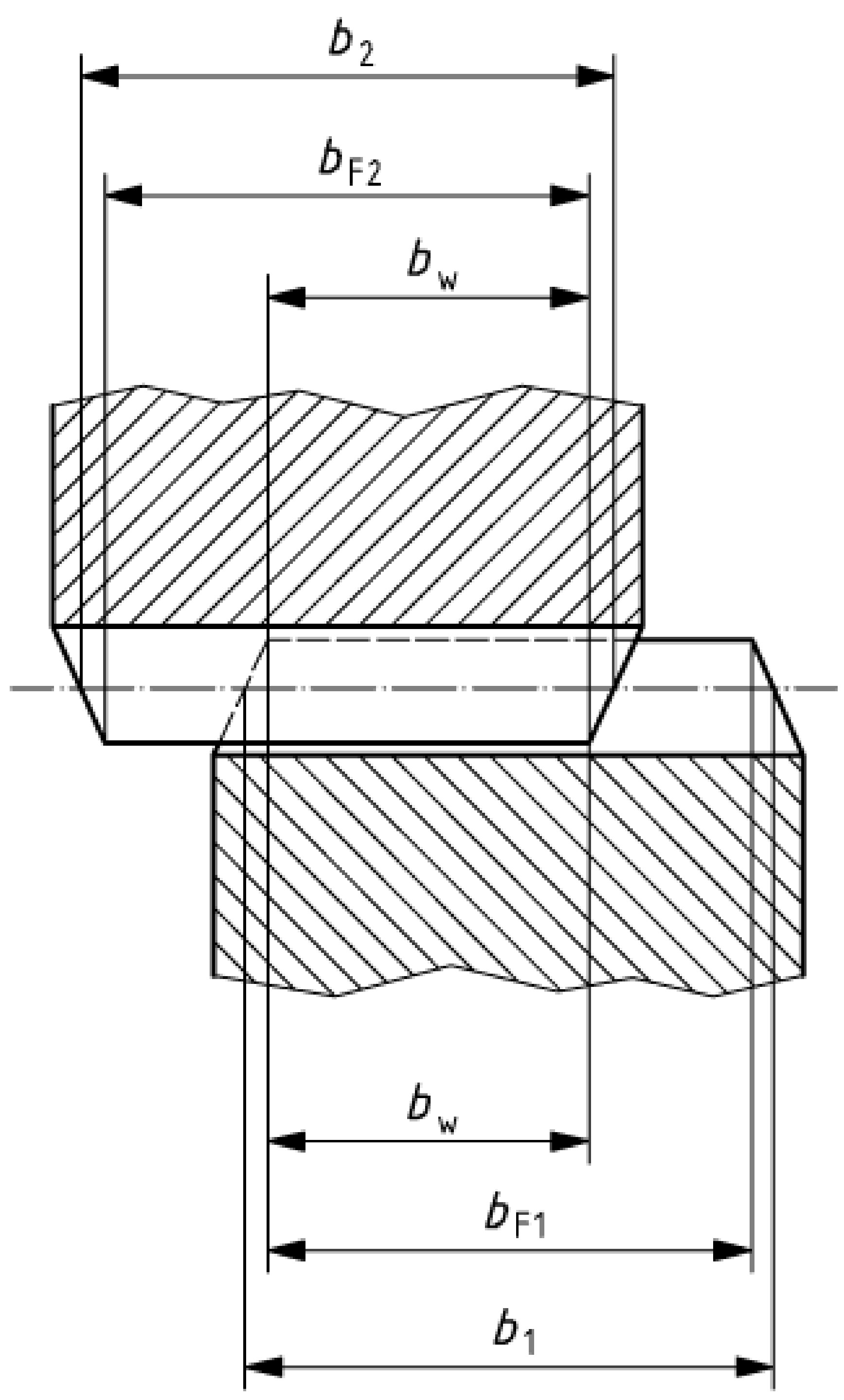

Figure 18 — Active facewidth, b_w

5.4.7.3 Overlap angle, overlap ratio

The overlap angle, φ_β, is the angle between the two axial planes enclosing the end points of a tooth trace of the gear pair:

$$\varphi_{\beta 1} = \frac{2\, b_\mathrm{w}\, \tan\beta}{d_1} = \frac{2\, b_\mathrm{w}\, \sin\beta}{m_\mathrm{n}\, z_1} = |u|\, \varphi_{\beta 2} \tag{91}$$

$$\varphi_{\beta 2} = \frac{2\, b_\mathrm{w}\, \sin\beta}{m_\mathrm{n}\, z_2} = \frac{\varphi_{\beta 1}}{|u|} \tag{92}$$

(See Figure 19.)

The overlap ratio, ε_β, is the ratio of the overlap angle, φ_β, to the angular pitch, τ, or the ratio of the facewidth, b, to the axial pitch, p_x.

$$\varepsilon_\beta = \frac{\varphi_{\beta 1}}{\tau_1} = \frac{\varphi_{\beta 2}}{\tau_2} = \frac{b}{p_\mathrm{x}} = \frac{b\, \sin\beta}{m_\mathrm{n}\, \pi} = \frac{b\, \tan\beta}{p_\mathrm{t}} = \frac{b\, \tan\beta_\mathrm{b}}{p_\mathrm{et}} \tag{93}$$

5.4.7.4 Overlap length

The overlap length, g_β, of a helical gear is the reference circle arc belonging to the overlap angle, φ_β:

$$g_\beta = r\, \varphi_\beta = b_\mathrm{w}\, \tan\beta \tag{94}$$

5.4.7.5 Total angle of transmission, total contact ratio

The total angle of transmission, φ_γ, is the angle at the centre of a gear in a gear pair through which the gear rotates from start to finish of contact of one of its flanks with its mating flank. It is equal to the sum of the transverse angle of transmission and the overlap angle:

$$\varphi_{\gamma 1} = \varphi_{\alpha 1} + \varphi_{\beta 1} = |u|\, \varphi_{\gamma 2} \tag{95}$$

$$\varphi_{\gamma 2} = \varphi_{\alpha 2} + \varphi_{\beta 2} = \frac{\varphi_{\gamma 1}}{|u|} \tag{96}$$

The total contact ratio, ε_γ, is the ratio of the total angle of transmission to the angular pitch. It is equal to the sum of the transverse contact ratio and the overlap ratio:

$$\varepsilon_\gamma = \frac{\varphi_{\gamma 1}}{\tau_1} = \frac{\varphi_{\gamma 2}}{\tau_2} = \varepsilon_\alpha + \varepsilon_\beta \tag{97}$$

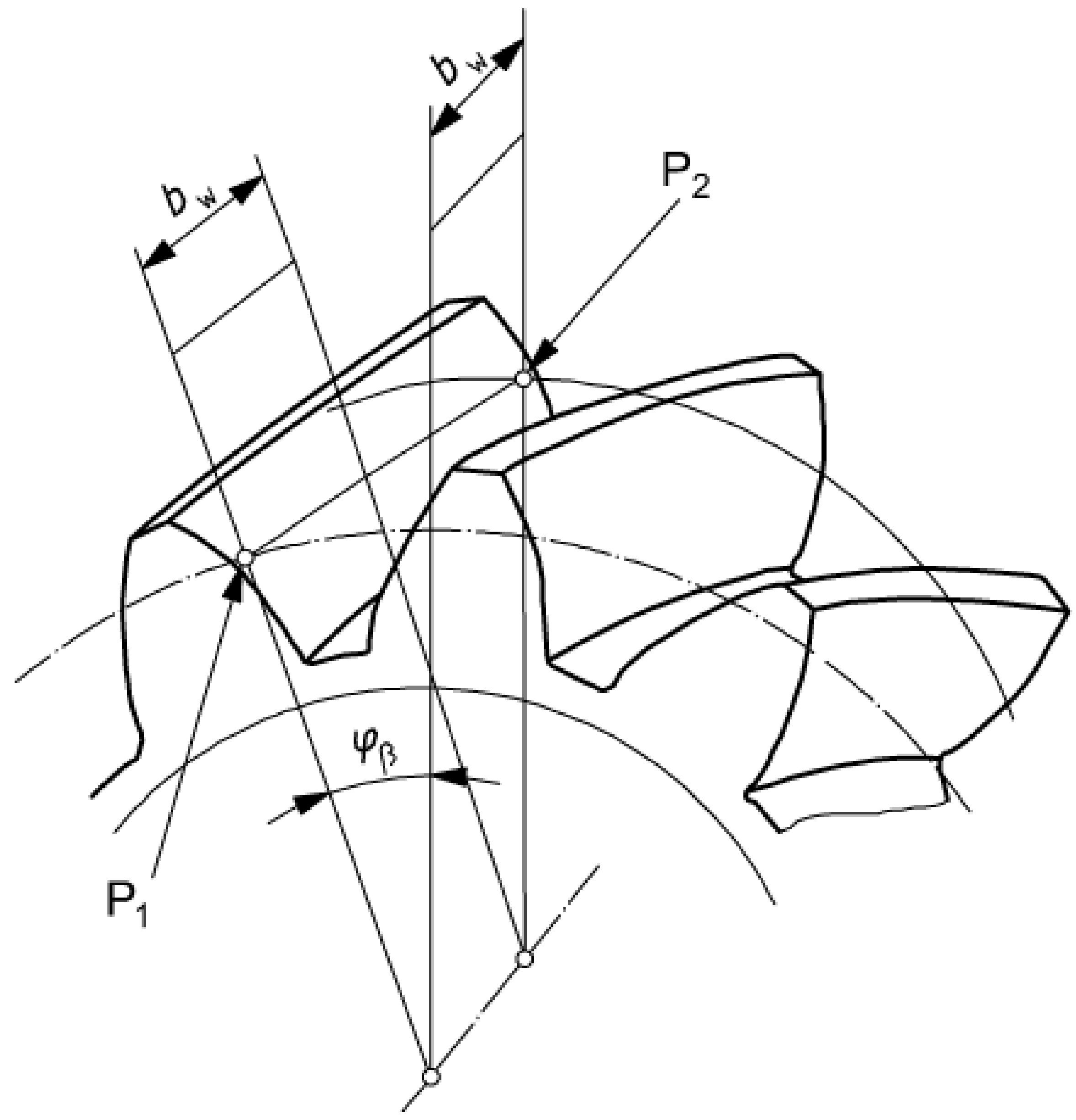

Figure 19 — Overlap angle of gear pair, φ_β

5.4.8 Contact line, sum of the contact line lengths

The contact line is the theoretical line at an instant in time where the flanks of a tooth pair of the gear and mating gear touch; l_{max} is the maximum length of such a contact line of a flank pair.

When spur-toothed gears are in contact, the individual tooth pair contact line length remains constant. When tooth traces are not modified (e.g. by crowning), the value of l_{max} is equal to the facewidth, b_w; see 5.4.7.2.

In the case of helical gears, the contact lines are within the zone of action and are at angle β_b to the pitch axis, see Figure 20. The length of the contact line changes with the rolling of the flank pair. It starts as a point contact at the beginning of engagement, reaches its maximum value, l_{max}, in a working position or in a certain range of rotational angles and is subsequently reduced to the point contact at the end of the engagement of the flank pair.

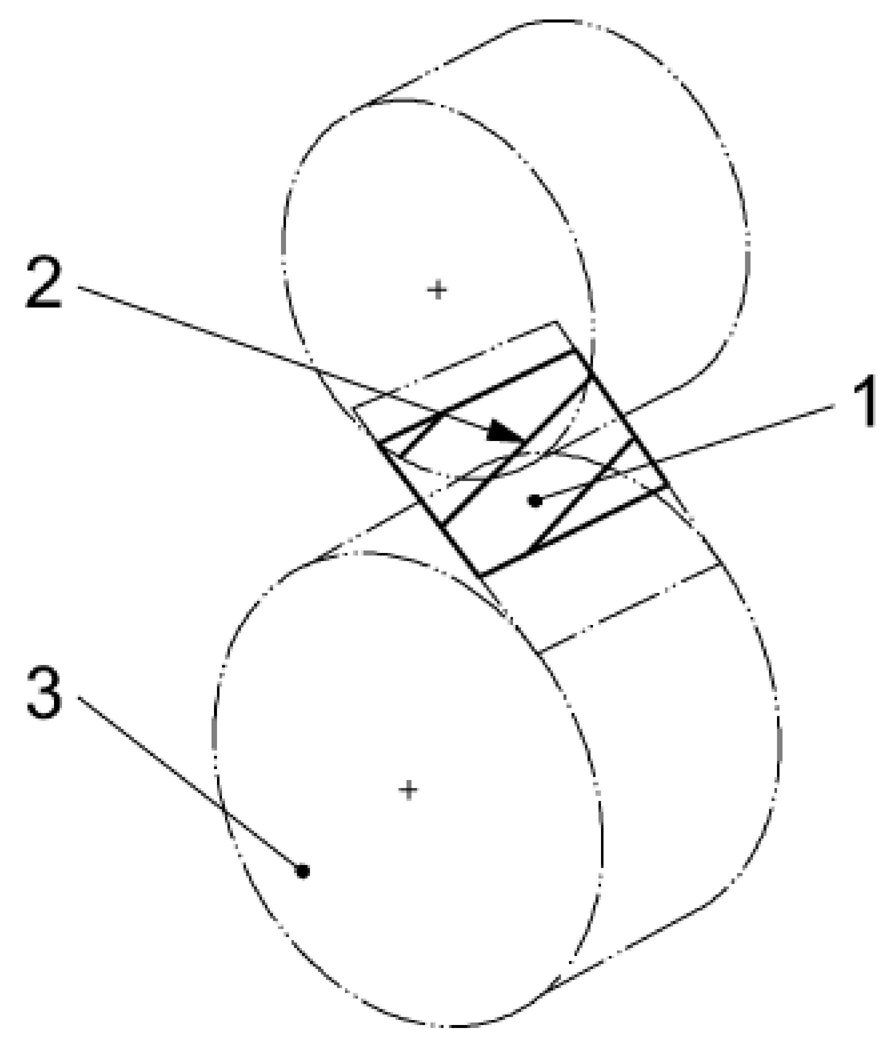

Key

1 zone of action

2 helical contact lines

3 base cylinder

Figure 20 — Zone of action

The maximum length of a contact line, l_{max}, is given by

$$l_{max} = \frac{g_\alpha}{\sin \beta_b} \tag{98}$$

or

$$l_{max} = \frac{b_w}{\cos \beta_b} \tag{99}$$

whichever is less.

NOTE If $\frac{b_w}{\cos\beta_b} > \frac{g_a}{\sin\beta_b}$, then the contact line extends across the whole active range of the transverse profile but not across the whole facewidth; while if it is less, then the contact line extends across the whole facewidth but across only part of the active range of the transverse profile.

The sum of the individual contact lines, $\sum l$, is the total length of all the contact lines which occur at the same time when the gear pair is in an instantaneous working position in the zone of action.

5.5 Backlash

The backlash is the clearance between the non-working flanks of the teeth of a gear pair when the working flanks are in contact.

There is a distinction between the normal backlash, j_{bn}, circumferential backlash, j_{wt}, and radial backlash, j_r; see Figure 21.

5.5.1 Normal backlash

Normal backlash, j_{bn}, is the shortest distance between the non-working flanks of the teeth of a gear pair when the working flanks are in contact with zero force. It is defined in the plane of action of the non-working flanks.

5.5.2 Backlash angle, circumferential backlash

The backlash angle, φ_j, is the angle of rotation through which the gear can be rotated, while the mating gear is stationary, from the point where the right flanks are in contact to the point where the left flanks are in contact; see Figure 21. The backlash angle for each gear is found from the normal backlash, j_{bn}:

$$\varphi_{j1} = \frac{2}{m_n z_1 \cos \alpha_n} j_{bn} \tag{100}$$

$$\varphi_{j2} = \frac{2}{m_n \left| z_2 \right| \cos \alpha_n} j_{bn} \tag{101}$$

The circumferential backlash, j_{wt}, is the length of the pitch circle arc through which each of the two gears can be rotated, whilst the other is held stationary, from the point where the right flanks are in contact to the point where the left flanks are in contact. Its magnitude is given by

$$j_{wt} = \frac{1}{\cos \alpha_{wt} \cos \beta_b} j_{bn} \tag{102}$$

or in relation to the length of the reference circle arc by

$$j_t = \frac{1}{\cos \beta \cos \alpha_n} j_{bn} \tag{103}$$

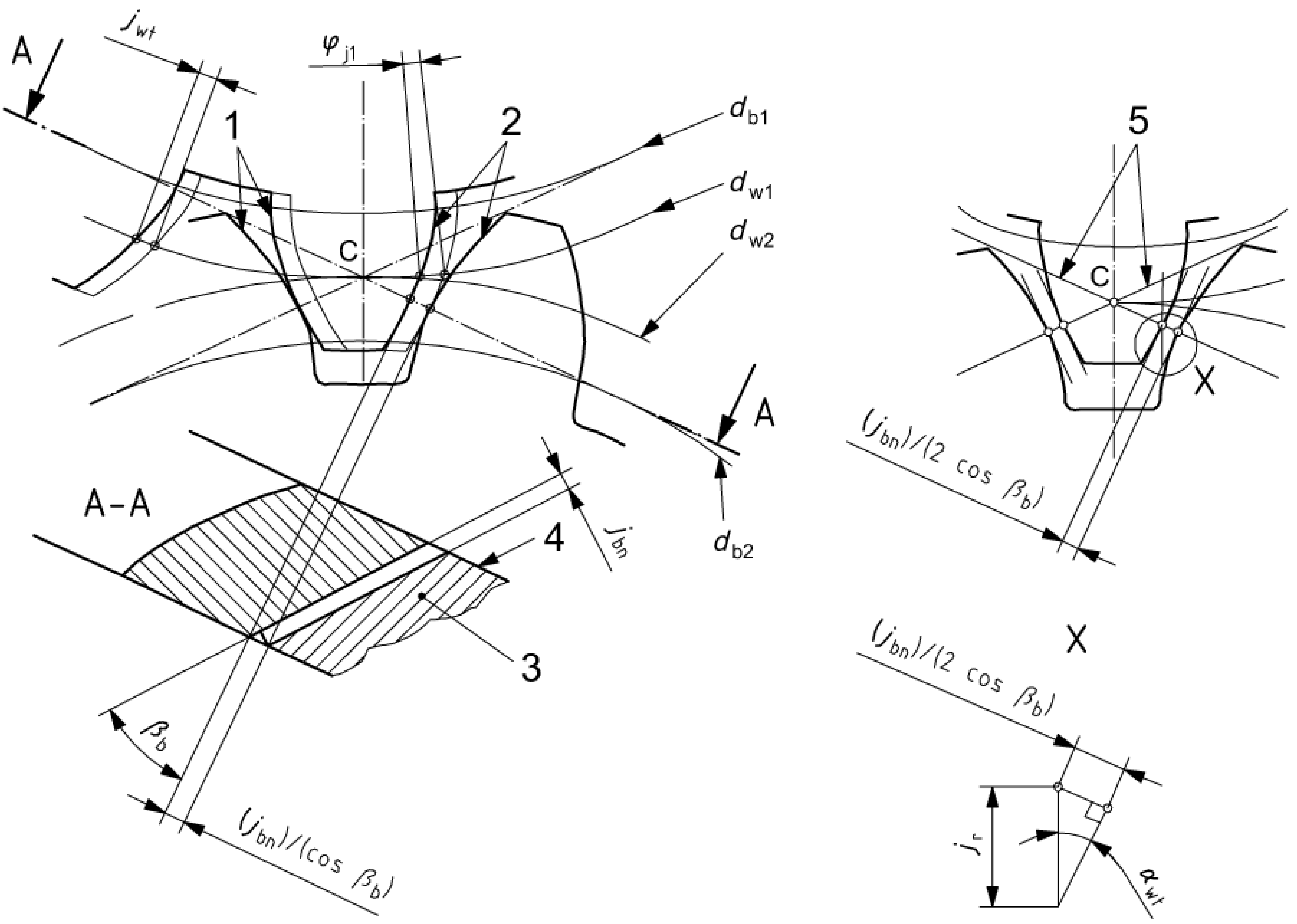

Key

1 working flanks
2 non-working flanks
3 plane of action non-working flanks
4 end face
5 plane of action

Figure 21 — Diagram showing backlash when working flanks are in contact (left-hand side) and with symmetrical positioning of tooth in space of mating gear (right-hand side)

5.5.3 Radial backlash

The radial backlash, j_r, is the difference in the centre distance in the working condition of the gear pair and the centre distance produced if one of the gears is moved towards the centre line until zero-backlash engagement of the flank pairs occurs; see Figure 21 (right-hand side).

The relation between circumferential backlash, j_{wt}, and radial backlash, j_r, is as follows:

$$j_r = \frac{1}{2 \tan\alpha_{wt}} j_{wt} \tag{104}$$

5.6 Sliding conditions at the tooth flanks

5.6.1 Sliding speed

At a point of contact of two tooth flanks in engagement, the sliding speed, v_g, is the difference of the speeds of the two transverse profiles in the direction of the common tangent.

At the point of contact Y, see Figures 22 and 23, the two transverse profiles have the normal speed:

$$v_n = \frac{1}{2}\,\omega_1\,d_{b1} \tag{105}$$

This yields the sliding speed:

$$v_g = \pm\,\omega_1\left(\frac{\rho_{y2}}{u} - \rho_{y1}\right) \tag{106}$$

where the curvature radii, ρ_{y1} and ρ_{y2}, are to be determined using equation (17).

The distance, $g_{\alpha y}$, between Y and C is

$$g_{\alpha y} = \left|\rho_{c1} - \rho_{y1}\right| = \left|\rho_{c2} - \rho_{y2}\right| \tag{107}$$

where |~| denotes absolute value.

Hence

$$v_g = \left|\omega_1\, g_{\alpha y}\left(1 + \frac{1}{u}\right)\right| \tag{108}$$

NOTE $g_{\alpha y}$ is always positive. Since u is positive for an external gear pair and negative for an internal gear pair, it usually follows that the sliding speed is greater for external gear teeth than for internal gear teeth.

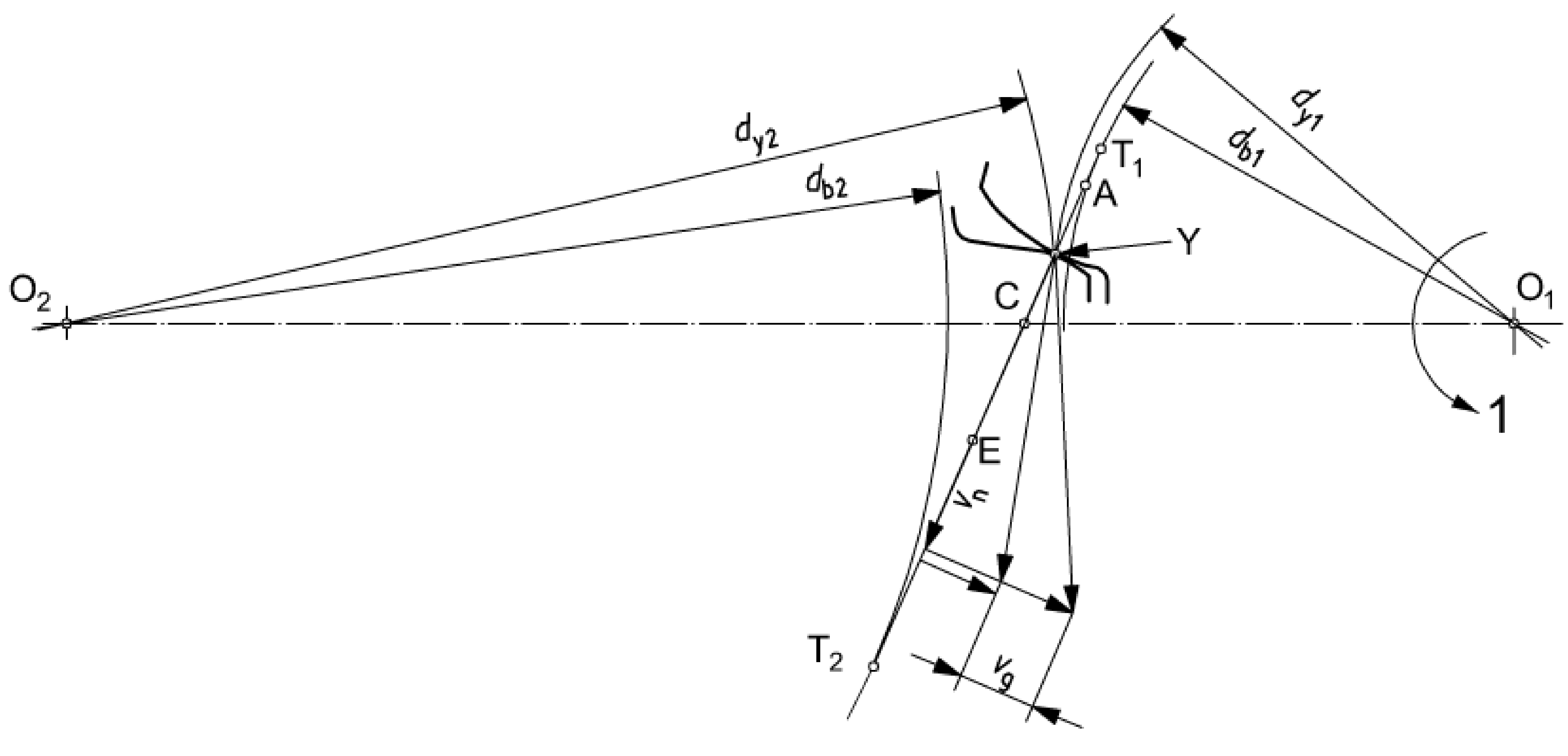

Key

1 direction of rotation of driving pinion

Figure 22 — Sliding speed, v_g, at point of contact Y on external gear pair

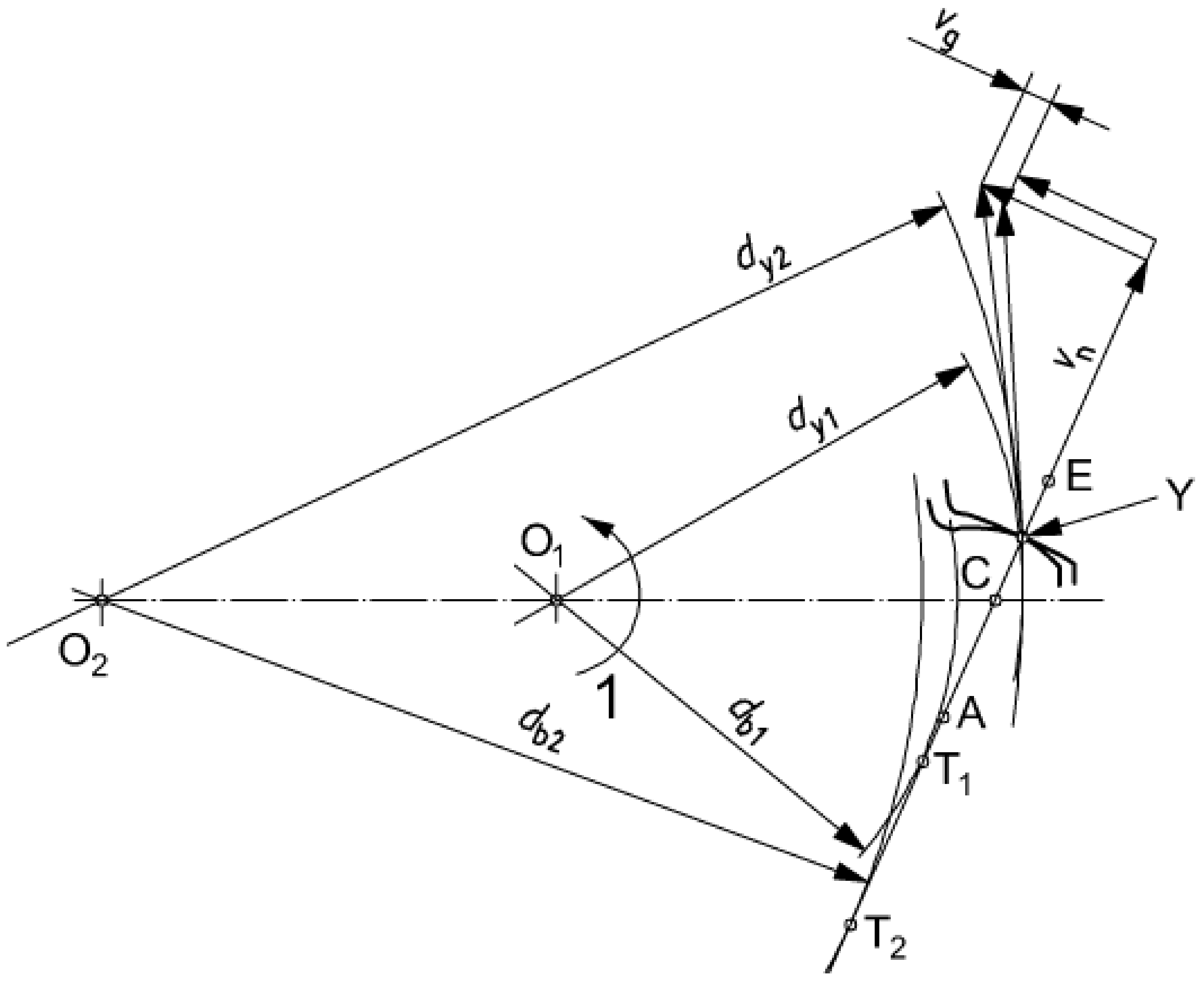

Key

1 direction of rotation of driving pinion

Figure 23 — Sliding speed, v_g, at point of contact Y on internal gear pair

The sliding speed is proportional to distance $g_{\alpha y}$ and equal to zero at the pitch point. It reaches its maximum values at the end points A and E of the path of contact:

$$v_{gf} = \left| \omega_1 \; g_f \left(1 + \frac{1}{u} \right) \right| \tag{109}$$

$$v_{ga} = \left| \omega_1 \; g_a \left(1 + \frac{1}{u} \right) \right| \tag{110}$$

with g_f and g_a according to Equations (79) and (80).

5.6.2 Sliding factor

The sliding factor, K_g, is the ratio of sliding speed, v_g, to the velocity, v_t, of the pitch circles:

$$K_g = \frac{v_g}{v_t} = \frac{2 \, g_{\alpha y}}{d_{w1}} \left(1 + \frac{1}{u} \right) \tag{111}$$

The maximum values for K_g are attained at end points A and E of the path of contact:

— at A:

$$K_{gf} = \frac{2 \, g_f}{d_{w1}} \left(1 + \frac{1}{u} \right) \tag{112}$$

— at E:

$$K_{ga} = \frac{2 \, g_a}{d_{w1}} \left(1 + \frac{1}{u} \right) \tag{113}$$

5.6.3 Specific sliding

The specific sliding, ζ, is the ratio of the sliding speed to the speed of a transverse profile in the direction of the tangent to the profile. The tangential velocity is equal to $\rho_y\omega$. Equation (106) yields:

$$\zeta_1 = 1 - \frac{\rho_{y2}}{u\ \rho_{y1}} \tag{114}$$

$$\zeta_2 = 1 - \frac{u\ \rho_{y1}}{\rho_{y2}} \tag{115}$$

The maximum values of ζ are reached at end points A and E of the path of contact:

— at A:

$$\zeta_{f1} = 1 - \frac{\rho_{A2}}{u\ \rho_{A1}} \tag{116}$$

— at E:

$$\zeta_{f2} = 1 - \frac{u\ \rho_{E1}}{\rho_{E2}} \tag{117}$$

using the curvature radii, ρ_A and ρ_E, according to 4.3.8 and 5.4.5.3.

6 Tooth flank modifications

Tooth flank modifications are desired alterations to the tooth flank face compared with the main geometry described in 4.3. Superimposing the nominal modifications on the main geometry produces the nominal tooth flank. The modifications can be defined in characteristic profiles of the tooth flank or in relation to the flank face. Modification depths are always given in the transverse section and normal to the involute of the main geometry.

6.1 Tooth flank modifications which restrict the usable flank

6.1.1 Pre-finish flank undercut

Pre-finish (root) relief is a planned, generated, undercut (e.g. using a protuberance tool) of the transverse profile of a tooth flank in the area of the root. The magnitude of the relief, q_{FS}, is the greatest distance between the root rounding and the involute imagined as extended to the base circle, see Figure 24. Below this, the datum is a line from the involute origin to the gear centre.

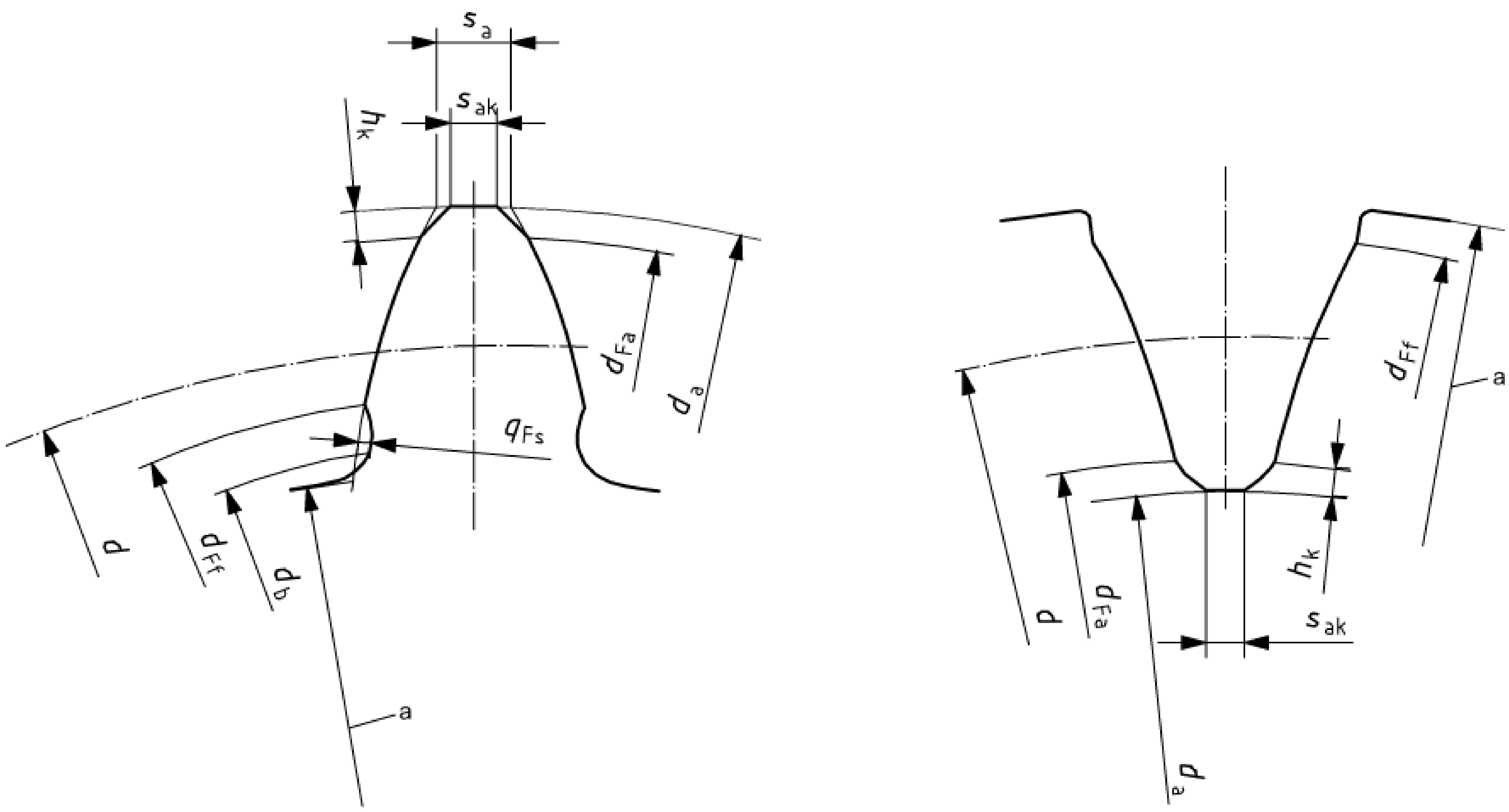

[a] d_f or d_{fE}.

Figure 24 — Spur cylindrical gear with undercut and tip corner chamfering

6.1.2 Tip corner chamfering, tip corner rounding

Tip corner chamfering and tip corner rounding are reliefs of the transverse profile which restrict the usable area of the tooth flank. Tip corner chamfering is the chamfer arising through removal of the tip corner. In the case of tip corner rounding, this corner is radiused in the normal plane. The radial height, h_K, and the residual tooth thickness at the tip, s_{aK}, are given as the dimensions of this modification, see Figure 24, and are different for chamfering and rounding.

6.2 Transverse profile modifications

In the following, L_{AE} is used to define the roll length for compatibility with ISO 1328-1. L_{AE} is equivalent to length of path of contact, g_α.

6.2.1 Tip and root relief

Tip and root reliefs are the continuously increasing reliefs of the transverse profile of the main geometry from defined points in each case (diameter, length of roll, roll angle) in the direction of the tip or root (mostly involute). See Figure 25.

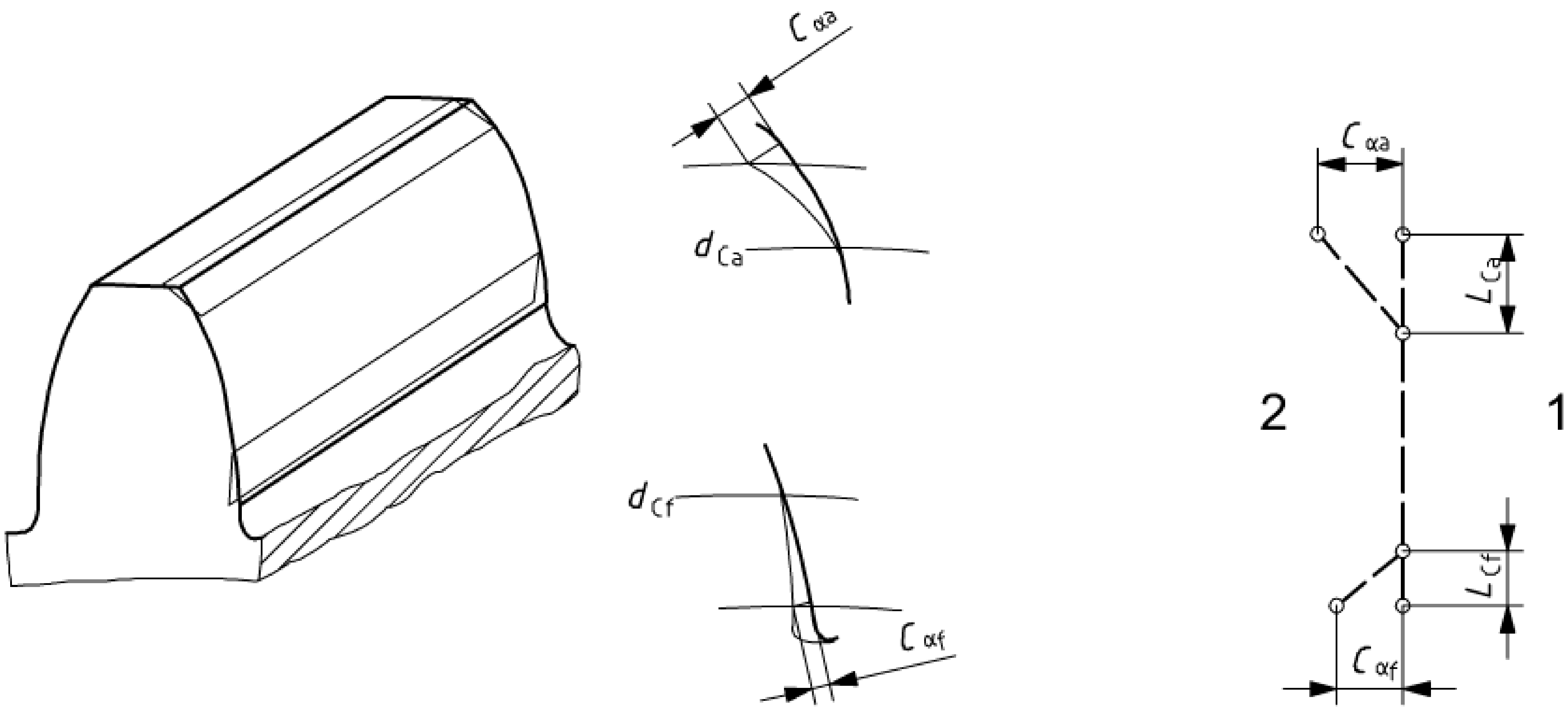

Key

d_{Ca} tip relief datum diameter

L_{Ca} tip relief roll length

$C_{\alpha\mathrm{a}}$ amount of tip relief

d_{Cf} root relief datum diameter

L_{Cf} root relief roll length

$C_{\alpha\mathrm{f}}$ amount of root relief

1 space

2 tooth

Figure 25 — Tip and root relief

6.2.2 Transverse profile slope modification, $C_{\mathrm{H}\alpha}$

This is similarly defined as for tip or root relief, except that $C_{\mathrm{H}\alpha}$ extends over the whole width of the face. See Figure 26.

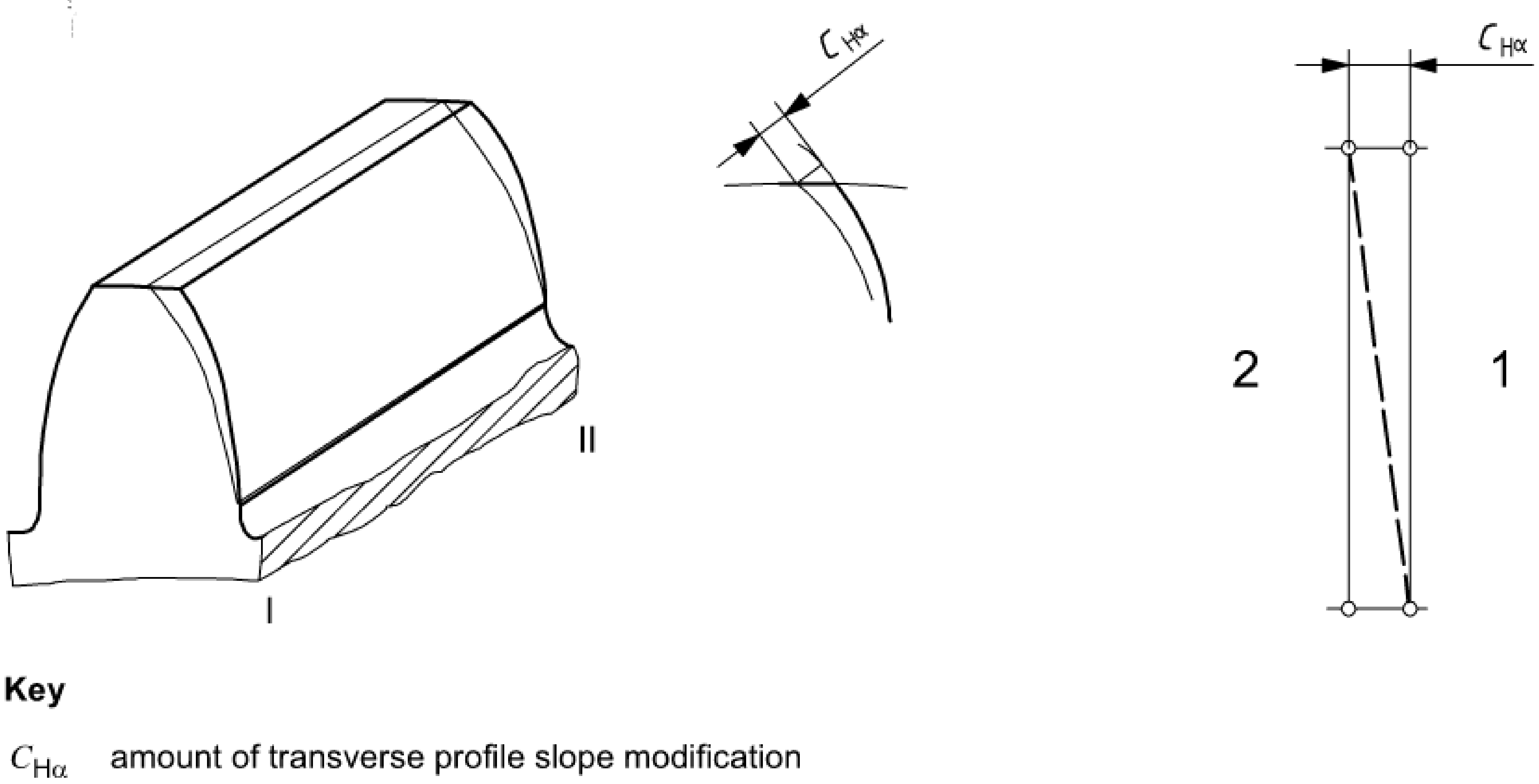

Key

$C_{\mathrm{H}\alpha}$ amount of transverse profile slope modification

1 space

2 tooth

Figure 26 — Transverse profile slope modification

6.2.3 Profile crowning (barrelling), C_α

Profile crowning is the continuously increasing relief of the transverse profile from a common defined point of the main geometry (diameter, length of roll, roll angle) in the direction of the tip and root of the gear teeth. See Figure 27.

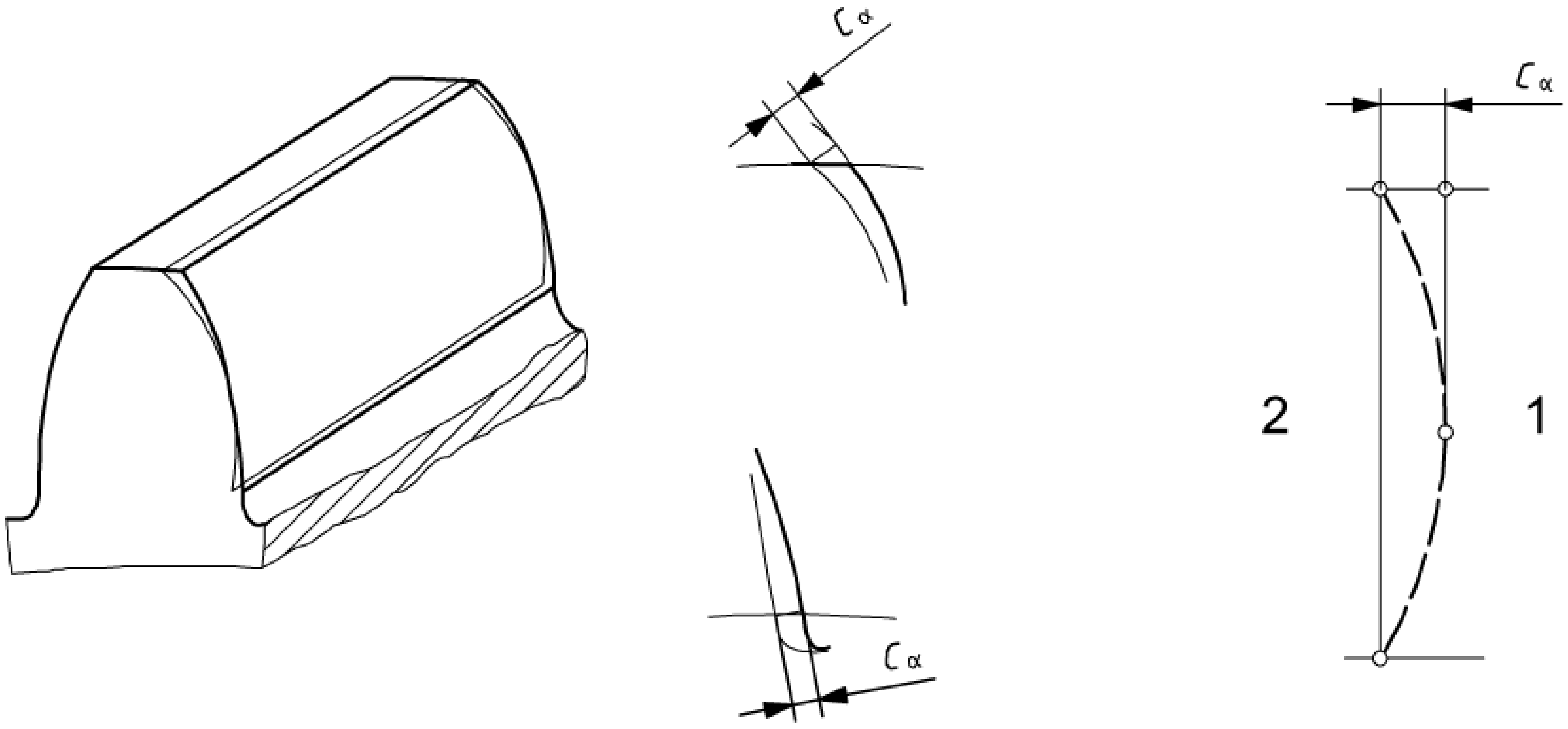

Key

C_α amount of profile crowning

1 space

2 tooth

Figure 27 — Profile crowning

Profile crowning is generally defined with respect to the centre of the length of roll of the usable flank and has a parabolic form passing though the points defined by C_α.

6.3 Flank line (helix) modifications

6.3.1 Flank line end relief

Flank line end reliefs are continuously increasing reliefs of the flank line from defined points of the main geometry in each case in the direction of the datum faces (linear or parabolic). See Figure 28.

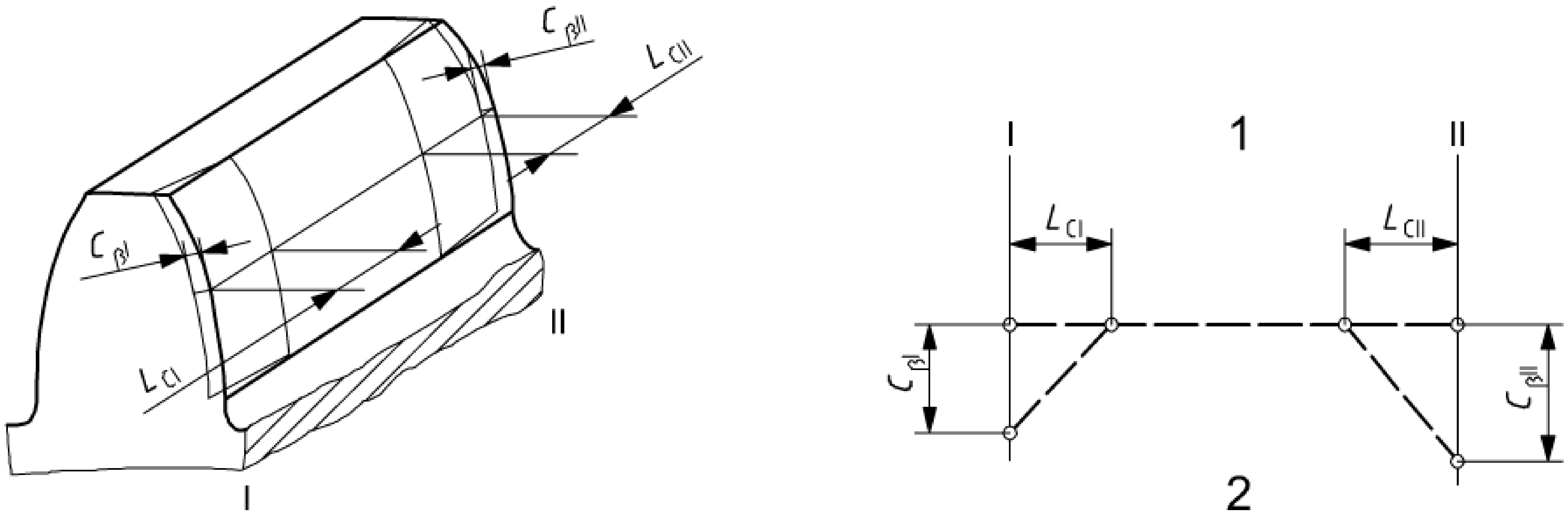

Key

L_{CI} length (datum face)

$C_{\beta I}$ amount of end relief (datum face)

L_{CII} length (non-datum face)

$C_{\beta II}$ amount of end relief (non-datum face)

1 space

2 tooth

Figure 28 — Flank line end relief

6.3.2 Flank line (helix) slope modification, $C_{H\beta}$

This is similarly defined as for end relief, but L_{CI} or L_{CII} extends across the whole facewidth. It is not necessarily linear. See Figure 29.

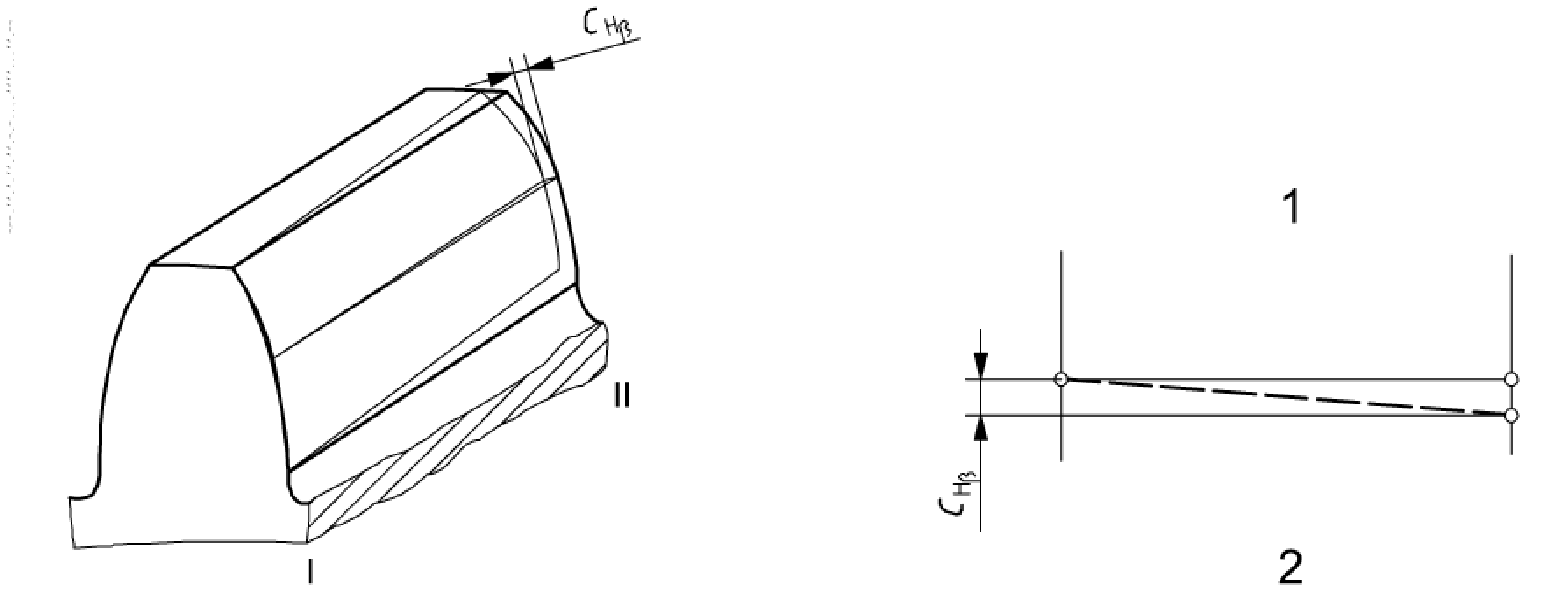

Key

$C_{H\beta}$ amount of flank line slope modification

1 space

2 tooth

Figure 29 — Flank line slope modification

6.3.3 Flank line (helix) crowning, C_β

Flank line crowning is the continuously increasing relief of the flank line from a common defined point of the main geometry, symmetrically in the direction of both ends of the tooth (arc-shaped or parabolic). See Figure 30.

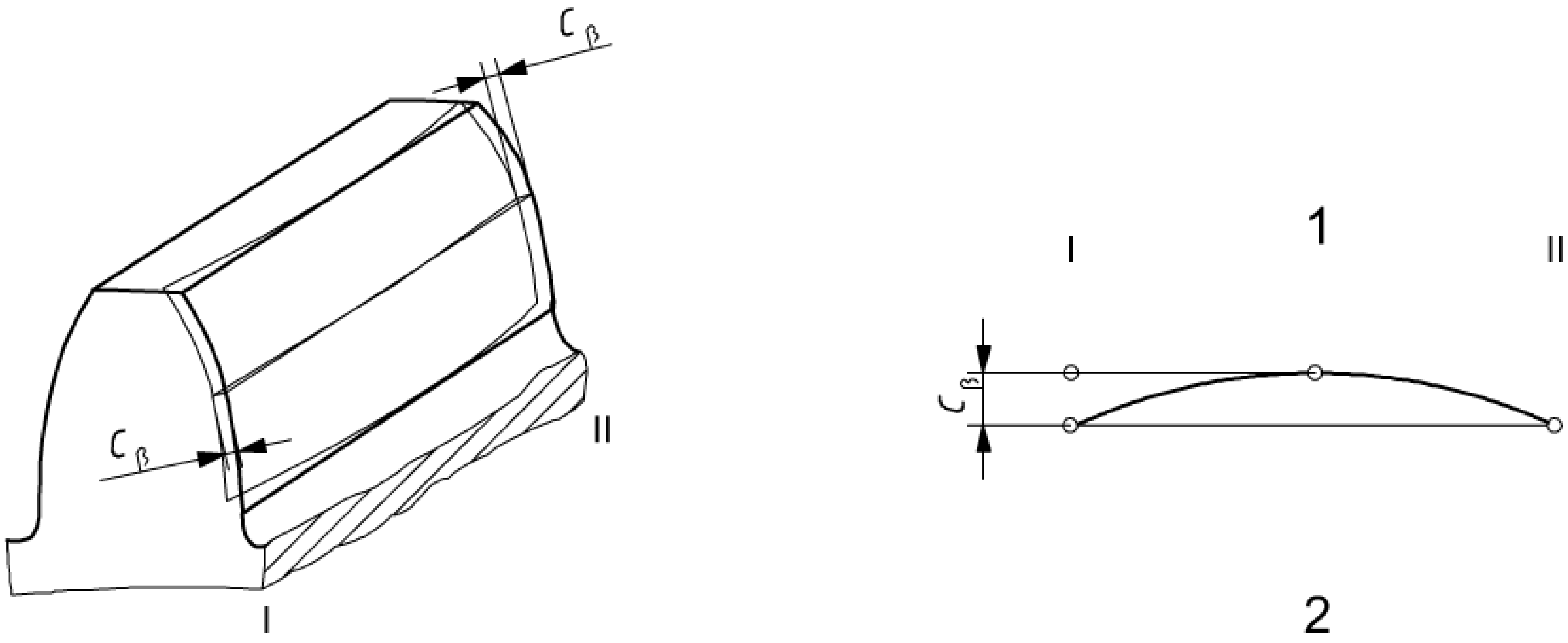

Key

C_β amount of the flank line crowning

1 space

2 tooth

Figure 30 — Flank line crowning

6.4 Flank face modifications

6.4.1 Topographical modifications

The desired deviation from the unmodified involute helicoid is determined in relation to each point of intersection on a grid laid over the tooth flank of the main geometry. See Figure 31.

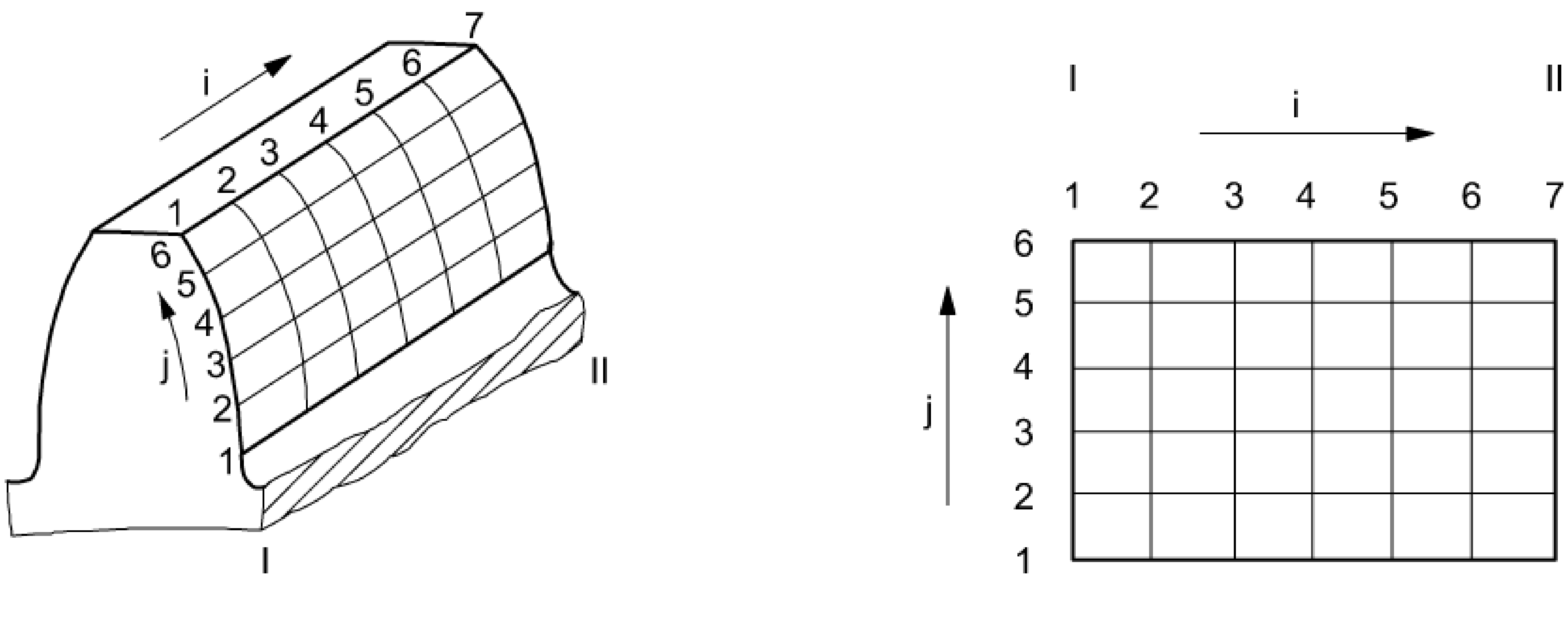

Key

$C_{i,j}$ amount of modification on point (i,j)[a]

[a] Transverse section i; flank line j. If necessary, interpolated points between the defined points (i,j) of a grid can be generated.

Figure 31 — Topographical modification

6.4.2 Triangular end relief

Triangular end reliefs are continuously increasing reliefs of the tooth flanks generally perpendicular to the generators of the main geometry (along the lines of contact) from a defined roll angle in the direction of the start or end of roll on the tooth flank. See Figure 32.

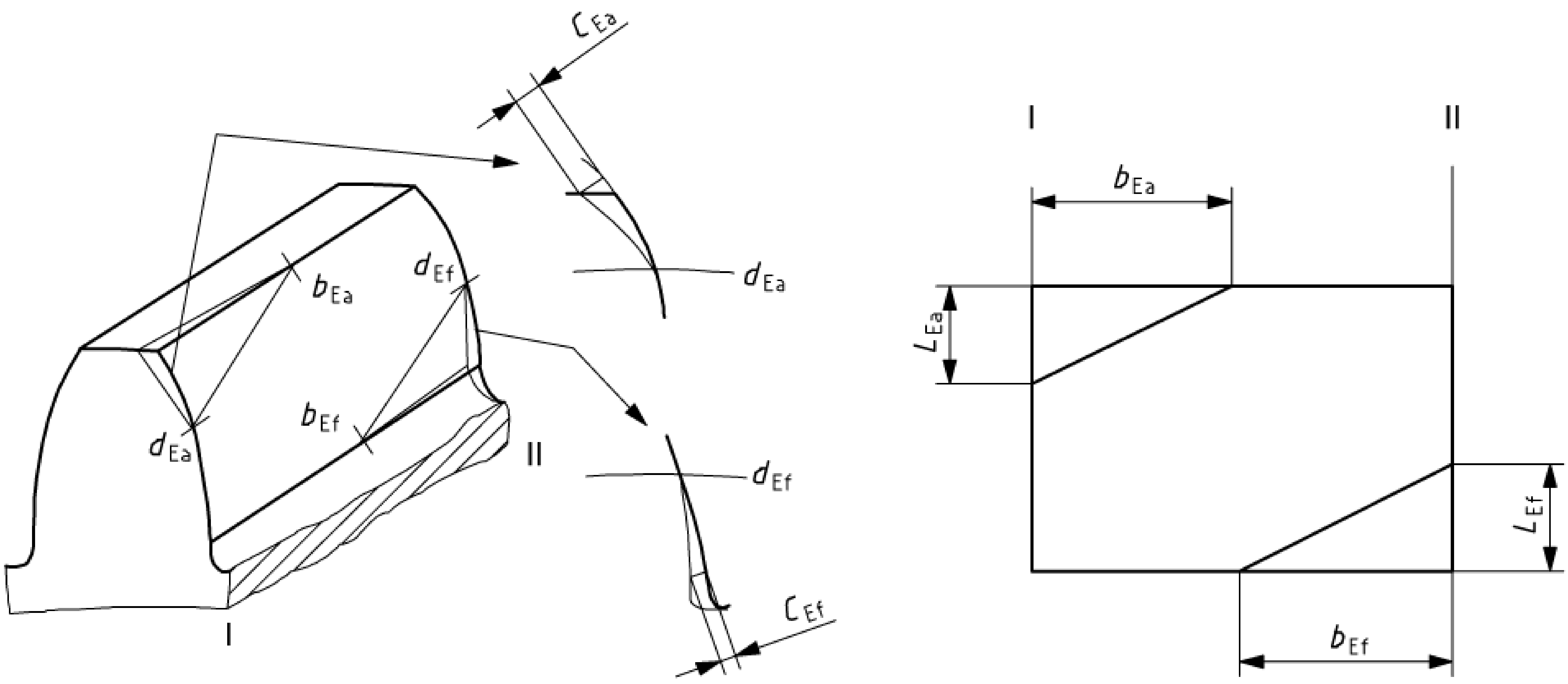

Key

C_{Ea} amount of modification (tip)

d_{Ea} datum diameter (tip)

L_{Ea} roll length (tip)

b_{Ea} length of relief (tip)

C_{Ef} amount of modification (root)

d_{Ef} datum diameter (root)

L_{Ef} roll length (root)

b_{Ef} length of relief (root)

Figure 32 — Triangular end relief

6.4.3 Flank twist

Twist is an effect on a flank described as a rotation of the transverse profile along a helix. There is a distinction between twist of the transverse profile, S_α, and of the flank line, S_β. If not otherwise defined, it changes linearly from the beginning to the end of the useable flank. The sign of the flank twist is very important, but is not defined here. See Figure 33.

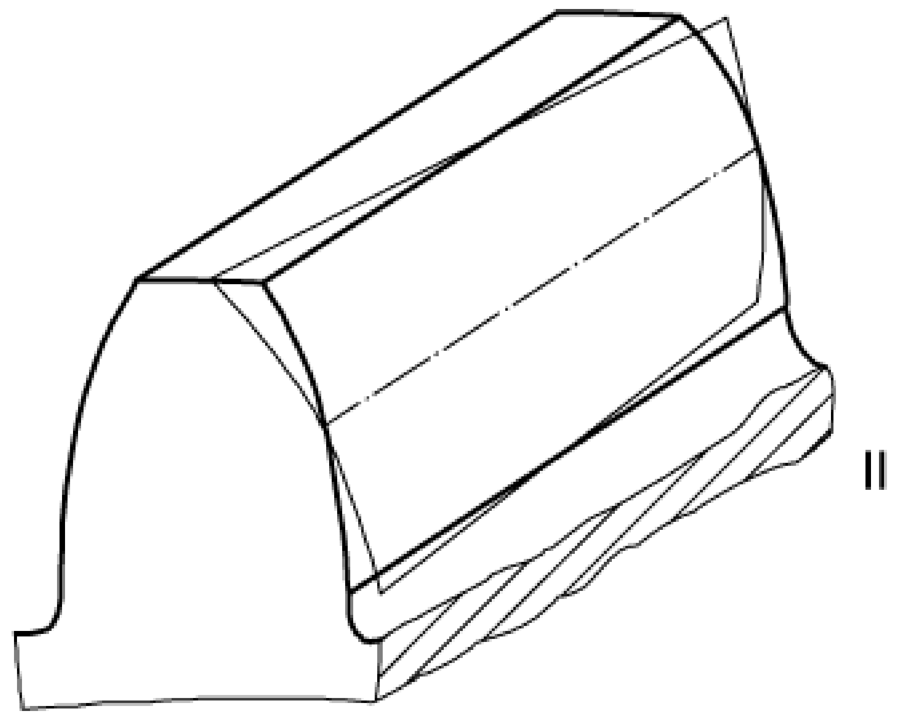

Twist of transverse profile, S_α:

$$\left|S_\alpha\right| = \left|C_{\mathrm{H\alpha I}} - C_{\mathrm{H\alpha II}}\right| \text{ with } C_{\mathrm{H\alpha I}} = -C_{\mathrm{H\alpha II}}$$

See 6.2.2.

Twist of flank profile, S_β:

$$\left|S_\beta\right| = \left|C_{\mathrm{H\beta Na}} - C_{\mathrm{H\beta Nf}}\right| \text{ with } C_{\mathrm{H\beta Na}} = -C_{\mathrm{H\beta Nf}}$$

See 6.3.2.

Figure 33 — Flank twist

6.5 Descriptions of modifications by functions

Modifications of the profile can be given as functions of the diameter, d_{y}, or the corresponding roll distances or angles, and modifications of the flank lines as functions of the axial distance from the start of the usable facewidth in the direction of the non-datum face. The combination of both functional relationships describes the modification of the whole flank surface.

— Modification of the profile: $C_{\mathrm{ay}} = f\left(d_{\mathrm{y}}\right)$; alternatively, $C_{\mathrm{ay}} = f\left(L_{\mathrm{y}}\right)$ or $C_{\mathrm{ay}} = f\left(\xi_{\mathrm{y}}\right)$.

— Modification of the flank line: $C_{\mathrm{\beta y}} = f\left(b_{\mathrm{Fy}}\right)$.

— Modification of the flank surface: $C_{\Sigma\mathrm{y}} = f\left(d_{\mathrm{y}}, b_{\mathrm{Fy}}\right)$; alternatively, $C_{\Sigma\mathrm{y}} = f\left(L_{\mathrm{y}}, b_{\mathrm{Fy}}\right)$ or $C_{\Sigma\mathrm{y}} = f\left(\xi_{\mathrm{y}}, b_{\mathrm{Fy}}\right)$.

— Definition of tooth flank modification by tolerance fields.

Graphically, it is usual to show tooth surface modifications as deviations from the exact involute helicoid with respect to roll length for radial deviations (as in Figure 25) and position across the tooth width for axial deviations (as in Figure 28). For intentional deviations which vary in the radial/axial direction from the exact involute geometry in any defined transverse plane, these deviations can be defined by tolerance fields, generally called "K" diagrams, which show the range of acceptable measured values, see Figure 34. Such diagrams are not necessarily bounded by straight lines.

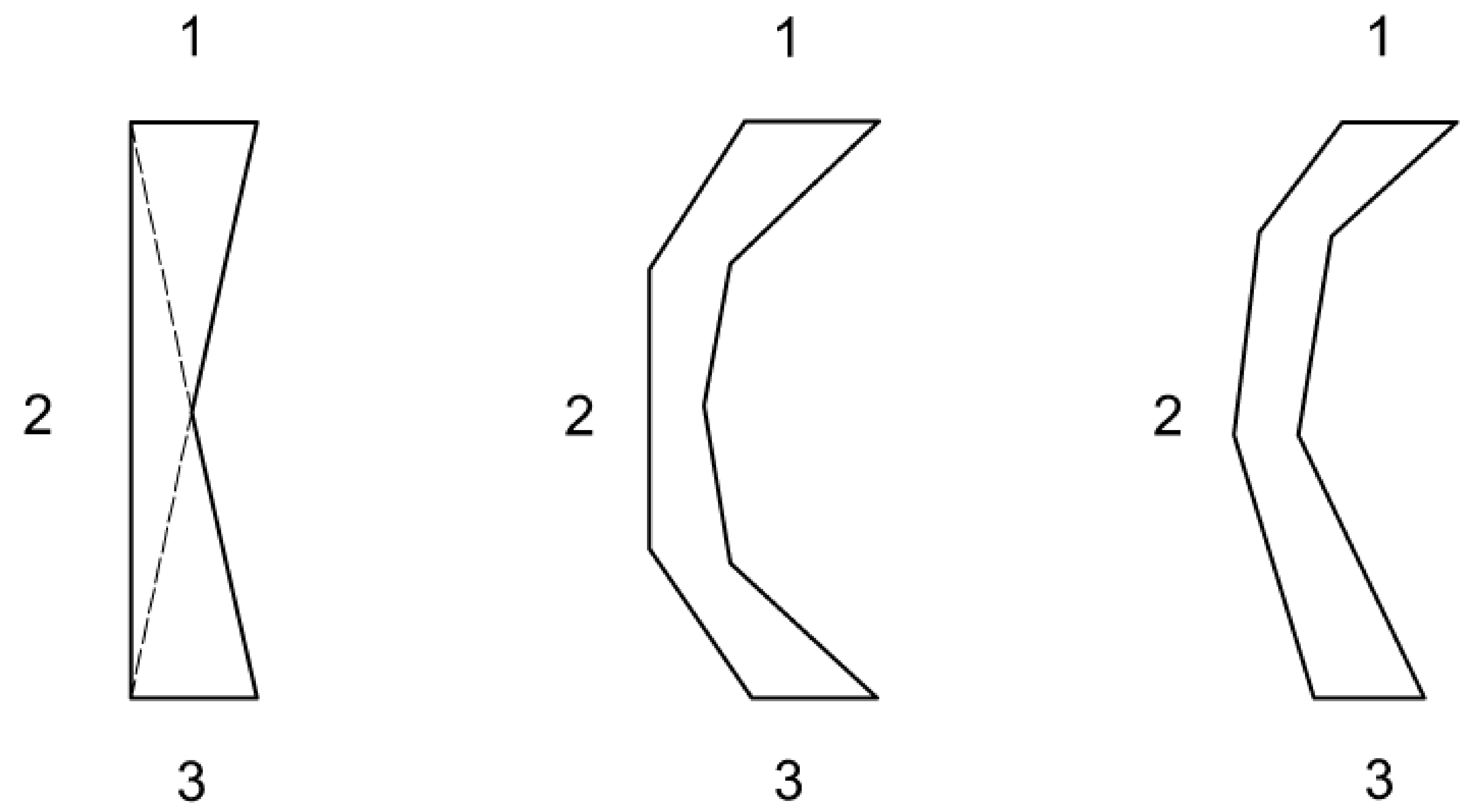

Key

1 tip or datum face

2 non-material side

3 root or non-datum face

Figure 34 — K-diagram (examples)

7 Geometrical limits

In this clause, the finished state at the conclusion of all manufacturing operations is examined. The basic concepts presented in Clause 4 are expanded to include the effect of such items as tooth thinning for backlash and manufacturing tolerances. The effects of manufacturing tolerances are both direct, such as tooth thickness tolerance, and indirect, such as the change in functional tooth thickness as a result of runout or profile slope deviation. The classification of tolerances is not covered in this International Standard (for this, see ISO 1328).

In manufacturing a cylindrical gear with involute teeth using generating methods, the tool (e.g. hob, pinion-type cutter, rack-shaped cutter, grinding wheel, grinding worm) and the gear form a generating process. The same concepts and the corresponding equations which apply to a cylindrical gear pair shall apply to the paired work piece and generating tool (if $\alpha_{P0} = \alpha_P$, see Clause 5). When producing a cylindrical gear with involute teeth by means of forming (non-generating) methods, the enveloping surface produced by the geometry of the tool and its motions are mapped directly onto the work piece.

If bottom land, root rounding and involute helicoid are machine-finished using the same tool, only the working cycle using this tool is of importance for the dimensions of the tooth parameters. Otherwise, the teeth produced (and their reference rack) are the sum of separate processes which produce the final dimensions of root circle, root rounding and usable flank surface including modifications in each case. The total result of the working cycles can be represented by a single hypothetical tool, the counterpart rack (see Figure 36).

7.1 Counterpart rack tooth profile

The counterpart rack tooth profile is the complement to the standard basic rack tooth profile enclosing the bottom land, see Figures 35 and 36.

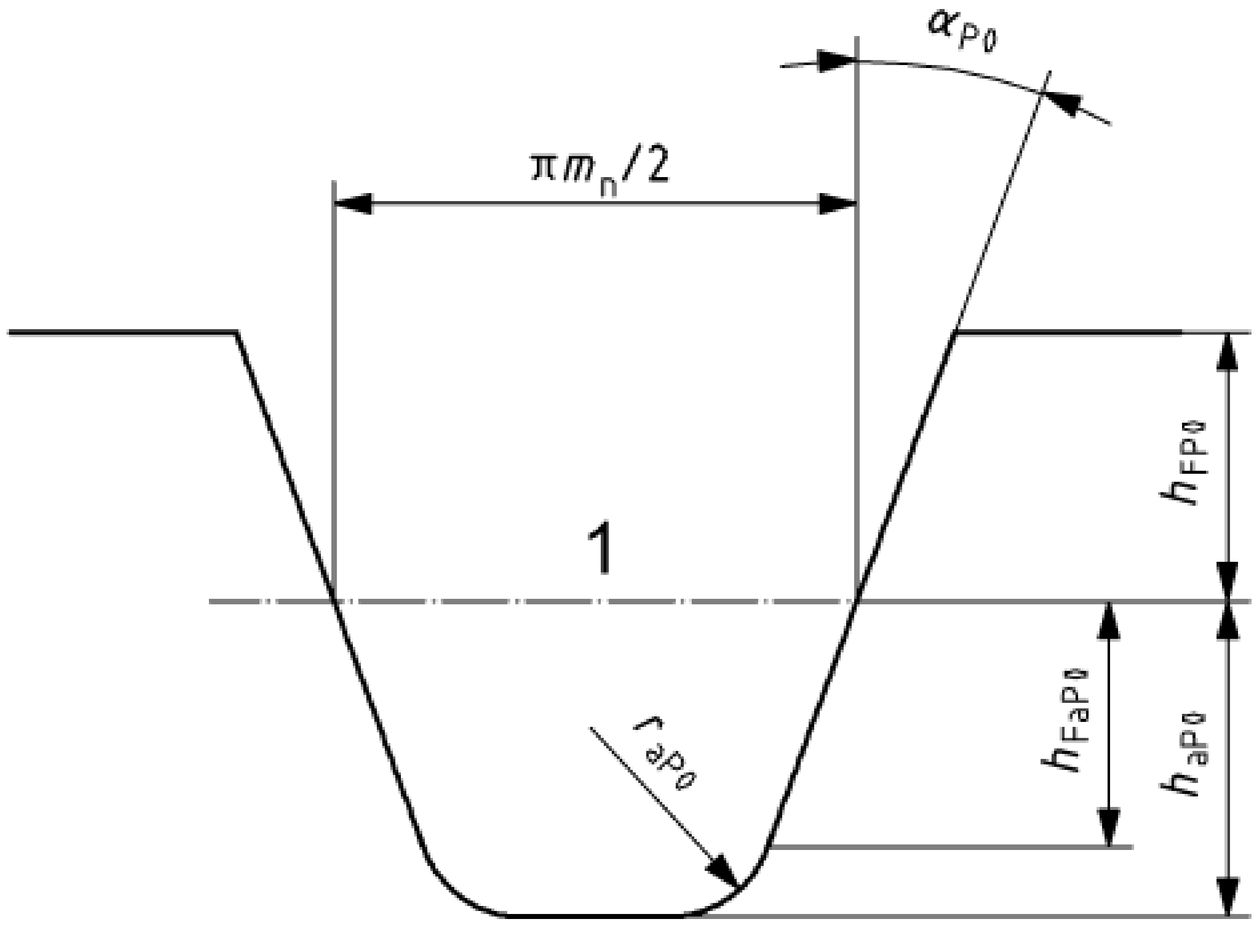

Key

1 datum line of tool

Figure 35 — Counterpart rack tooth profile

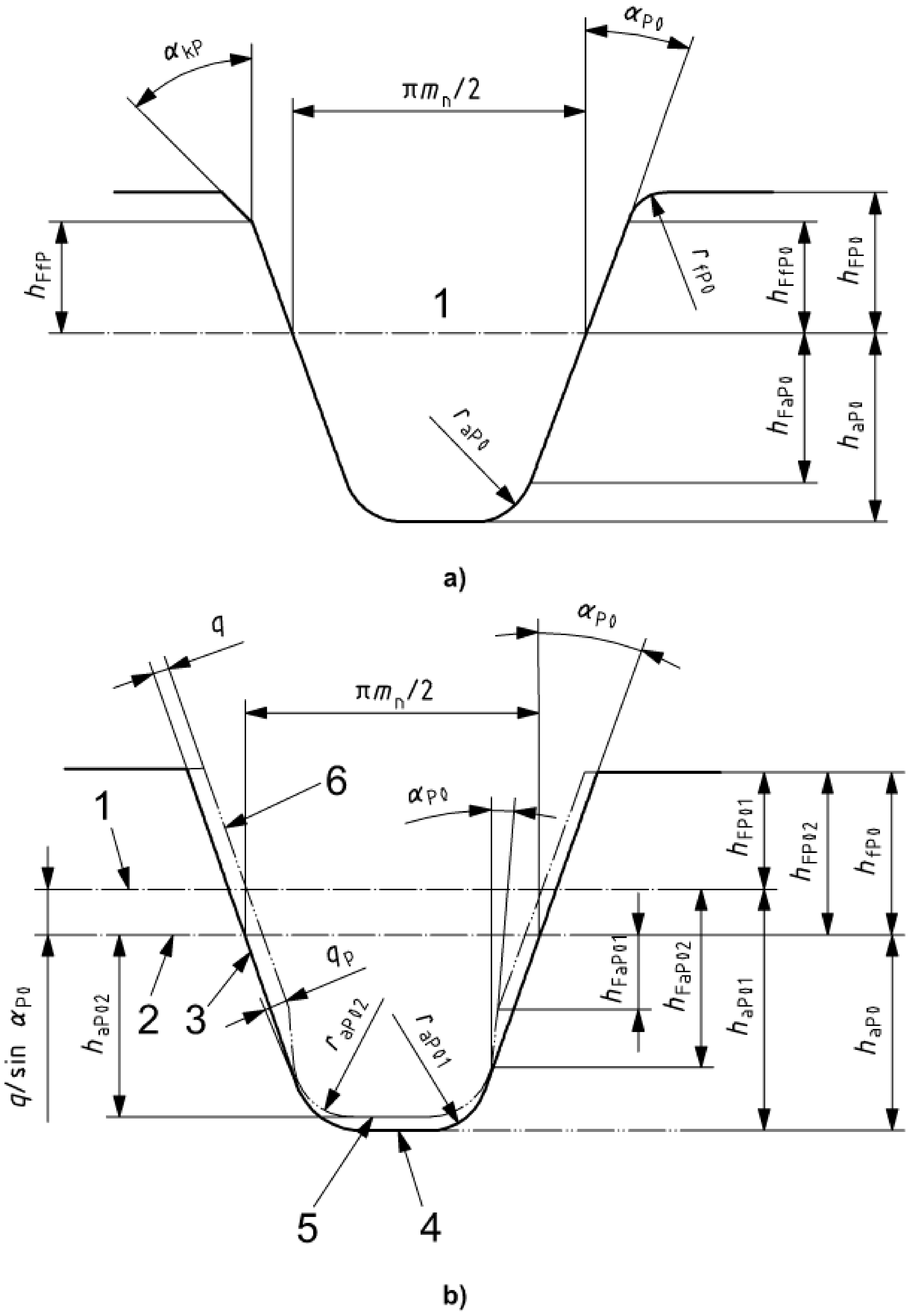

Key

1 datum line of roughing tool

2 datum line of finishing tool

3 finishing tool rack

4 tip of roughing tool

5 tip of finishing tool

6 roughing tool rack

NOTE Items 3 and 4 together make up the hypothetical tool.

Figure 36 — Modified counterpart rack tooth profiles

7.2 Machining allowance

A roughing gear-cutting tool leaves the machining allowance, q, for the subsequent finish gear cutting on the flank of the cylindrical gear. The machining allowance is defined normal to the tooth surface. The tooth thickness produced by the roughing gear-cutting tool on the cylindrical gear is thus $2q/\cos\alpha_n$ greater than the tooth thickness, s_n, produced by the finish gear-cutting tool. In practice, the machining allowance ranges from q_{min} to q_{max}. See Figure 37.

7.3 Deviations in tooth thickness

The corresponding maximum and minimum limits of tooth thickness (s_{ns} and s_{ni}) to be required on the generated teeth are obtained by determining (upper and lower) tooth thickness allowances (E_{sns} and E_{sni}).

$$s_{ns} = s_n + E_{sns} \tag{118}$$

$$s_{ni} = s_n + E_{sni} \tag{119}$$

A negative tooth thickness allowance reduces the tooth thickness and increases the space width compared to the nominal dimensions, determining the contribution of the tooth thickness to the backlash, j_{bn} (see 5.5).

In addition to the finish machining tolerances, the backlash is also affected by elemental tolerances such as profile, helix and runout. The elemental tolerances will increase the tolerance band of functional tooth thickness; this will reduce the minimum backlash and increase the maximum backlash. (See Figure 37.) Therefore, a complete analysis of the tooth thickness for the purpose of determining the backlash must include all the elemental tolerances that affect the functional tooth thickness. The relative importance of the different tolerances depends not only on those tolerances but also on the measuring methods used. See Annex A, ISO/TR 10064-2, AGMA 2002 and DIN 3967 for additional information.

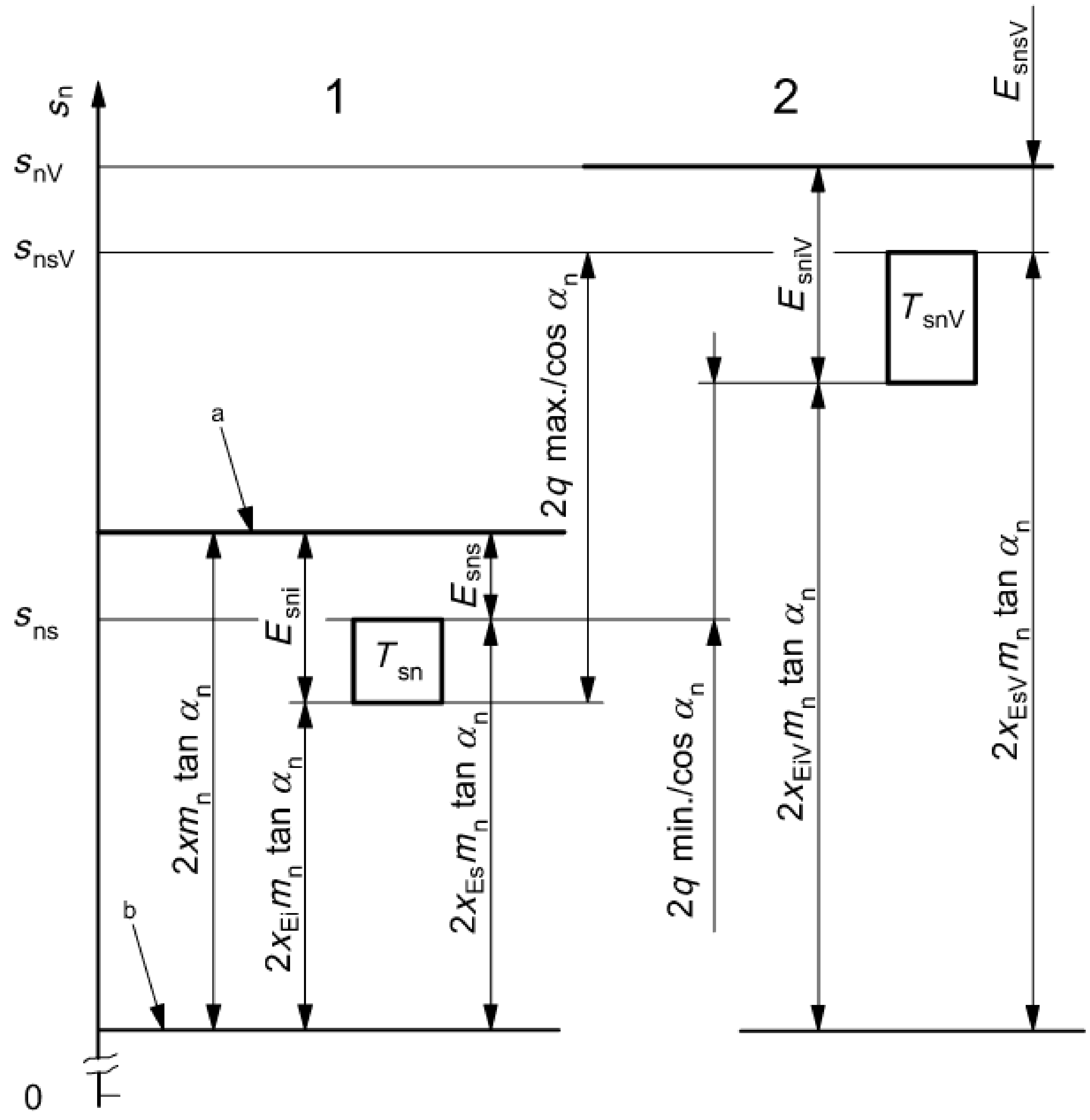

Key

1 finishing

2 pre-finish

a s_n where $x > 0$ and $j_{bn} = 0$.

b s_n where $x = 0$.

Figure 37 — Diagram of dimensioning of tooth thickness with positive profile shift

7.4 Generating profile shift, generating profile shift coefficient

The generating profile shift, $x_E m_n$, of a gear with involute teeth is the distance between the datum line of the counterpart rack tooth profile and the reference cylinder of the gear; see Figure 38.

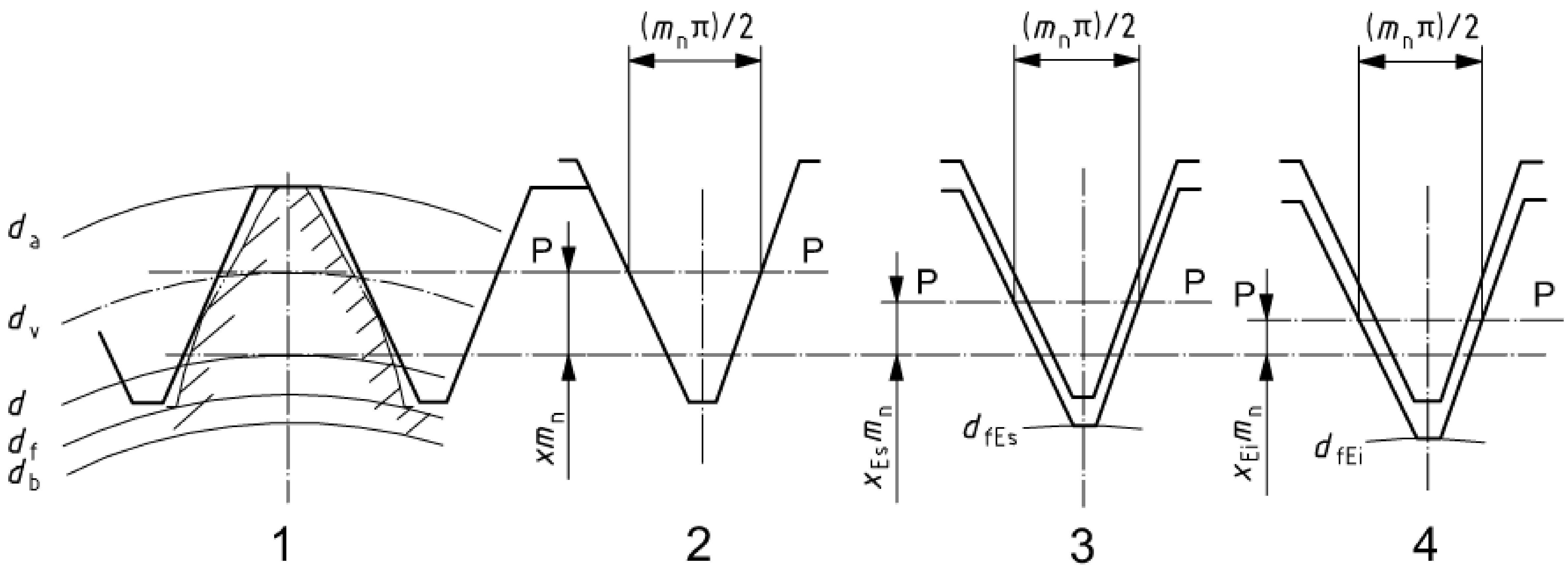

Key

P-P datum line of basic rack
1 reference rack
2 counterpart rack
3 counterpart rack at upper allowance
4 counterpart rack at lower allowance

Figure 38 — Generating profile shift, $x_E m_n$ — Example: external gear, $x > 0$

The generating profile shift takes account of the predetermined upper and lower tooth thickness allowances, E_{sns} and E_{sni} (see 7.3) and, if necessary, the machining allowances, q_{max} and q_{min}, provided for the finish-machining of a gear are included.

The values of x_E are determined with Equations (120) and (121). The permissible maximum and minimum tooth thickness inspection dimensions can be determined by calculation using x_E in the equations in Annex A. The cases of application are to be identified by corresponding additional subscripts.

Taking account of the relations shown in Figure 38, it follows for roughing with tooth thickness allowances (E_{snsV} and E_{sniV}) and a machining allowance, q, that:

$$x_{EsV} m_n = x_{Ei} m_n + \frac{q_{max}}{\sin \alpha_n} \tag{120}$$

$$x_{EiV} m_n = x_{Es} m_n + \frac{q_{min}}{\sin \alpha_n} \tag{121}$$

$$q_{max} = q_{min} + \left(T_{sn} + T_{snv}\right) \frac{\cos \alpha_n}{2} \tag{122}$$

The following applies to finish gear cutting (q = 0):

$$x_{Es} m_n = x m_n + \frac{E_{sns}}{2 \tan \alpha_n} \tag{123}$$

$$x_{Ei} m_n = x m_n + \frac{E_{sni}}{2 \tan \alpha_n} \tag{124}$$

7.5 Generated root diameter

The root diameter generated by a rack gear cutter (e.g. hob, rack-shaped cutter or grinding wheel) with the addendum h_{aP0} is

$$d_{\mathrm{fE}} = d + 2x_{\mathrm{E}}m_{\mathrm{n}} - 2h_{\mathrm{aP0}} \tag{125}$$

The root diameter produced by a pinion-type cutter is

$$d_{\mathrm{fE}} = 2a_0 - \frac{z}{|z|}d_{\mathrm{a0}} \tag{126}$$

For x_{E}, h_{aP0}, a_0 and d_{a0}, it is necessary to use the values for the process that produces the finished tooth.

7.6 Usable area of the tooth flank, tip and root form diameter

The maximum usable area of the tooth flank of a cylindrical gear is enclosed by the tip form circle (diameter d_{Fa}) and the root form circle (diameter d_{Ff}), see Figure 24. These circles arise during the generation of the cylindrical gear. They are determined by the starting point A_{E} and the finishing point E_{E} of the generating path of contact (see Figure 39) and limit the involute section of the tooth profile. With direct transition between the nominal involute helicoid and the top land of the tooth, the tip form diameter is equal to the tip diameter ($d_{\mathrm{Fa}} = d_{\mathrm{a}}$). In the case of tip radiusing or tip chamfering, tip form diameter and tip diameter differ by double the radius h_{K}:

$$d_{\mathrm{Fa}} = d_{\mathrm{a}} - 2\frac{z}{|z|}h_{\mathrm{K}} \tag{127}$$

(See Figure 24.)

The root form diameter, d_{Ff}, follows from the relevant working cycle during gear cutting.

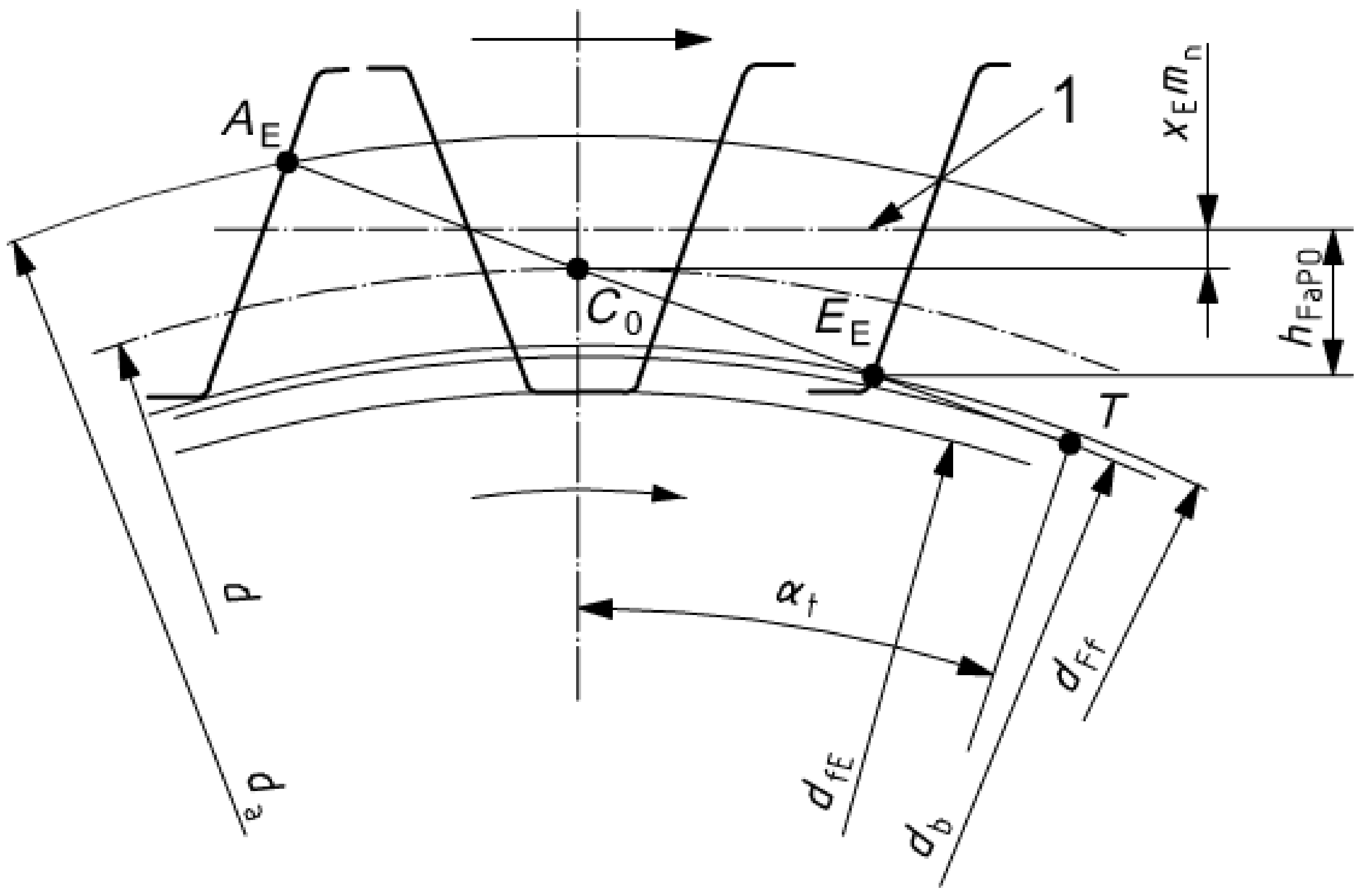

$\alpha_{\mathrm{P0}} = \alpha_{\mathrm{P}}$

Key

C_0	pitch point of the generating gear	T	contact point between generating line of action and base circle of gear
A_{E}	starting point of meshing	h_{FaP0}	straight part of tip flank of tool-generating profile
E_{E}	end point of meshing	1	datum line of basic rack

NOTE Figure 39 also covers the possible case of different pressure angles α_{P0} and α_{P} at the tool and the cylindrical gear standard basic rack tooth profile — for example, with single-tooth and single-flank tools (e.g. part generating grinding). The generating gear then has the normal pressure angle, α_{wt0}, and the generating pitch circle diameter $d_{\mathrm{wE}} = d_{\mathrm{b}} / \cos\alpha_{\mathrm{wt0}}$ instead of α_{t} and d in the case of $\alpha_{\mathrm{P0}} = \alpha_{\mathrm{P}}$.

Figure 39 — Meshing of involute transverse profile of left flank of cylindrical gear during generation with straight flank part of tooth flank of basic generating profile

In the case of tooth systems which are finish-machined using the generating method and tools whose cutter tips lie parallel to the datum line (hob, rack-shaped cutter) and have no undercut or pre-finish root relief, the following applies to an external gear:

$$d_{\mathrm{Ff}} = \sqrt{\left\{ d \sin\alpha_{\mathrm{t}} - \frac{2\left[h_{\mathrm{aP0}} - x_{\mathrm{E}} m_{\mathrm{n}} - \rho_{\mathrm{aP0}}\left(1-\sin\alpha_{\mathrm{t}}\right)\right]}{\sin\alpha_{\mathrm{t}}} \right\}^2 + d_{\mathrm{b}}{}^2}$$
$$= \sqrt{\left\{ d - 2\left[h_{\mathrm{aP0}} - x_{\mathrm{E}} m_{\mathrm{n}} - \rho_{\mathrm{aP0}}\left(1-\sin\alpha_{\mathrm{t}}\right)\right]\right\}^2 + 4\left[h_{\mathrm{aP0}} - x_{\mathrm{E}} m_{\mathrm{n}} - \rho_{\mathrm{aP0}}\left(1-\sin\alpha_{\mathrm{t}}\right)\right]^2 \cot^2\alpha_{\mathrm{t}}} \quad (128)$$

or, using the roll angle $\tan\alpha_{\mathrm{Ff}} = \xi_{\mathrm{Ff}}$, the following is produced:

$$d_{\mathrm{Ff}} = \frac{d_{\mathrm{b}}}{\cos\alpha_{\mathrm{Ff}}} \quad (129)$$

where α_{Ff} follows from

$$\tan\alpha_{\mathrm{Ff}} = \xi_{\mathrm{Ff}} = \xi_{\mathrm{t}} - \frac{4\left[h_{\mathrm{aP0}} - \rho_{\mathrm{aP0}}\left(1-\sin\alpha_{\mathrm{t}}\right)/m_{\mathrm{n}} - x_{\mathrm{E}}\right]\cos\beta}{z\sin 2\alpha_{\mathrm{t}}} \quad (130)$$

In the case of external and internal gears, which are generated by means of the generating method using a pinion-type cutter (number of teeth z_0, base diameter d_{b0}, tip form diameter d_{Fa0}, generating centre distance a_0, and generating working transverse pressure angle α_{wt0}) and have no undercut or pre-finish root relief, the following applies:

$$d_{\mathrm{Ff}} = \sqrt{\left(2a_0 \sin\alpha_{\mathrm{wt0}} - \frac{z}{|z|}\sqrt{d_{\mathrm{Fa0}}^2 - d_{\mathrm{b0}}^2}\right)^2 + d_{\mathrm{b}}^2} \quad (131)$$

or, using the roll angle $\tan\alpha_{\mathrm{Ff}} = \xi_{\mathrm{Ff}}$:

$$d_{\mathrm{Ff}} = \frac{d_{\mathrm{b}}}{\cos\alpha_{\mathrm{Ff}}} \quad (132)$$

with

$$\xi_{\mathrm{Ff}} = \frac{z_0}{z}\left(\xi_{\mathrm{wt0}} - \xi_{\mathrm{Fa0}}\right) + \xi_{\mathrm{wt0}} \quad (133)$$

$$\xi_{\mathrm{Fa0}} = \tan\left(\arccos\frac{d_{\mathrm{b0}}}{d_{\mathrm{Fa0}}}\right) \quad (134)$$

In the case of gears with undercut, the root form diameter arises from the intersection between the involute part of the tooth flank and the root curve.

7.7 Undercut

Undercut is the removal of material in the dedendum flank on external cylindrical gears. Undercutting occurs when the relative path of the tool tip corner rounding cuts into the involute portion of the tooth flank during the rolling action in the generating gear unit. This undercutting can be avoided or minimized by positive profile shift.

For a cylindrical gear produced using a non-protuberance rack-shaped cutter or hob, the minimum value of the generating profile shift coefficient for zero-undercut teeth arises from

$$x_{\mathrm{E\,min}} = \frac{h_{\mathrm{Fa}P0}}{m_{\mathrm{n}}} - \frac{z \sin^2 \alpha_{\mathrm{t}}}{2 \cos \beta} \tag{135}$$

When using a pinion-type cutter, $x_{\mathrm{E\,min}}$ arises from the mating conditions of the generating gear unit.

7.8 Overcut

Overcut is the removal of material from the flank of an internal gear. Overcutting occurs when the relative path of the tool tip corner rounding cuts into the involute portion of the tooth flank near the tooth tip during the rolling action in the generating gear unit.

Overcutting will not occur if the radius of curvature of the flank of an involute cutter at the tip is less than the radius of curvature of the flank of the internal gear at the tip.

7.9 Minimum tooth thickness at the tip circle of a gear

In calculating minimum tooth thickness at the tip circle, the upper limit (not theoretical) tip diameter must be used, and tip chamfering should be accounted for. Minimum tooth thickness should be limited based on material, its heat treatment and the application.

Equation (38) may be used to calculate the tooth thickness at the tip.

The minimum tooth thickness, as well as the undercut, sets a lower limit on the number of teeth that it is practicable to cut in an external gear.

Annex A
(informative)

Calculations related to tooth thickness

A.1 Purpose

Tooth thickness is defined as a circular or helical arc, and is difficult to measure directly. Therefore, indirect measuring methods, such as measurements over balls, span measurement, and chordal measurement, are used. This annex presents two systems for calculating the values related to tooth thickness and the corresponding backlash of a gear set. They are known as the *nominal tooth thickness system* and the *functional tooth thickness system*. Information specific to coordinate-measuring methods is not included, although such methods are becoming quite common.

A.1.1 Symbols

The following symbols are used in this annex.

$d_{\mathrm{y+F}}$	diameter at which the maximum acceptable chordal tooth thickness is calculated
$d_{\mathrm{y-F}}$	diameter at which the minimum acceptable chordal tooth thickness is calculated
F_{rc}	runout tolerance correction to Y-cylinder diameter to account for manufacturing tolerances
h_{cy}	height above the chord to the outside diameter
h_{ccy}	height above the chord to the outside diameter, used for both maximum and minimum chordal tooth thickness measurements (chordal addendum)
s_{ny}	tooth thickness, normal, on the Y-cylinder
s_{c}	tooth thickness, chordal
s_{cy}	tooth thickness, chordal, at Y-cylinder
$s_{\mathrm{(y+F)n\,max}}$	tooth thickness, normal, maximum effective, at Y + F cylinder,
$s_{\mathrm{(y-F)n\,min}}$	tooth thickness, normal, minimum effective, at Y − F cylinder,
$\beta_{\mathrm{y+F}}$	helix angle at Y + F cylinder
$\beta_{\mathrm{y-F}}$	helix angle at Y − F cylinder
Δs	correction for the difference in arc heights of the maximum and minimum chords

A.1.2 Tooth thickness relationships

The relationship between measured tooth thickness and the operating backlash depends on both the tooth thickness measuring method and the accuracy grade. This is because the effective (functional) tooth thickness of a gear will be different to the measured tooth thickness by an amount equal to the combined effects of deviations in the mounting of the gear and all the tooth element deviations. In the nominal system, this difference is applied to the backlash. In the functional system, this difference is accounted for in the allowable measured tooth thickness. Both systems have been used with equal success.

The nominal system uses a direct calculation to go from the specified tooth thickness tolerance to the allowable range of measured tooth thickness (planned test dimensions). The range of predicted backlash for the gear pair is then calculated based on the tolerances of the operating centre distance, the tooth thickness test dimensions for each of the gears, the measuring methods used and the elemental tolerances of the gears. The predicted backlash range must be verified for suitability and, if necessary, changes made to the nominal tooth thickness tolerance, the measuring method, the centre distance or the accuracy grade (the elemental tolerances, also known as the allowable elemental deviations, are a function of the specified accuracy grade). This annex includes the technique for calculation of the tooth thickness test dimensions using the nominal system, but does not include calculations for the predicted backlash range. See DIN 3967 for such calculations.

In the functional system there is a direct correlation between the specified functional tooth thickness and the backlash. The tooth thickness test dimensions are calculated as a function of both the measuring method used and the allowable values of the elemental deviations (tolerances) of the gears. The resulting allowable measured tooth thickness range must be verified for suitability and, if necessary, changes must be made to the functional tooth thickness tolerance, the measuring method, the centre distance or the accuracy grade.

Within the nominal tooth thickness system, the equations in 4.7.1 to 4.7.5 produce the nominal test dimensions if the nominal (zero-backlash) profile shift coefficient x is used in these and in the equations for the tooth thickness half angle ψ (4.7.2) or space width half angle η (4.7.4). The planned test dimensions (the permissible maximum and minimum dimensions or their arithmetic means) for the finish or rough gear cutting can be determined if, instead of x, the generating profile shift coefficient, x_E, is used according to Equations (120) and (121) for $q \geqslant 0$ and for the half angles.

Within the functional tooth thickness system, the generating profile shift coefficient x_E is always used.

A.2 Span measurement

The span measurement, W_k, is the distance measured between two parallel planes normal to the base tangent plane which contact a left and right flank over k teeth on an external helical or spur gear, or measured over k tooth spaces in an internal spur gear. The contact points lie in a base tangent plane. Internal helical gears cannot be measured with this technique. The two parallel planes must contact a right flank and a left flank respectively in the involute portion of those tooth flanks. (See Figure A.1.) For internal spur gears, measuring cylinders or measuring balls must be used instead of flat measuring surfaces. See ISO/TR 10064-2 for additional information.

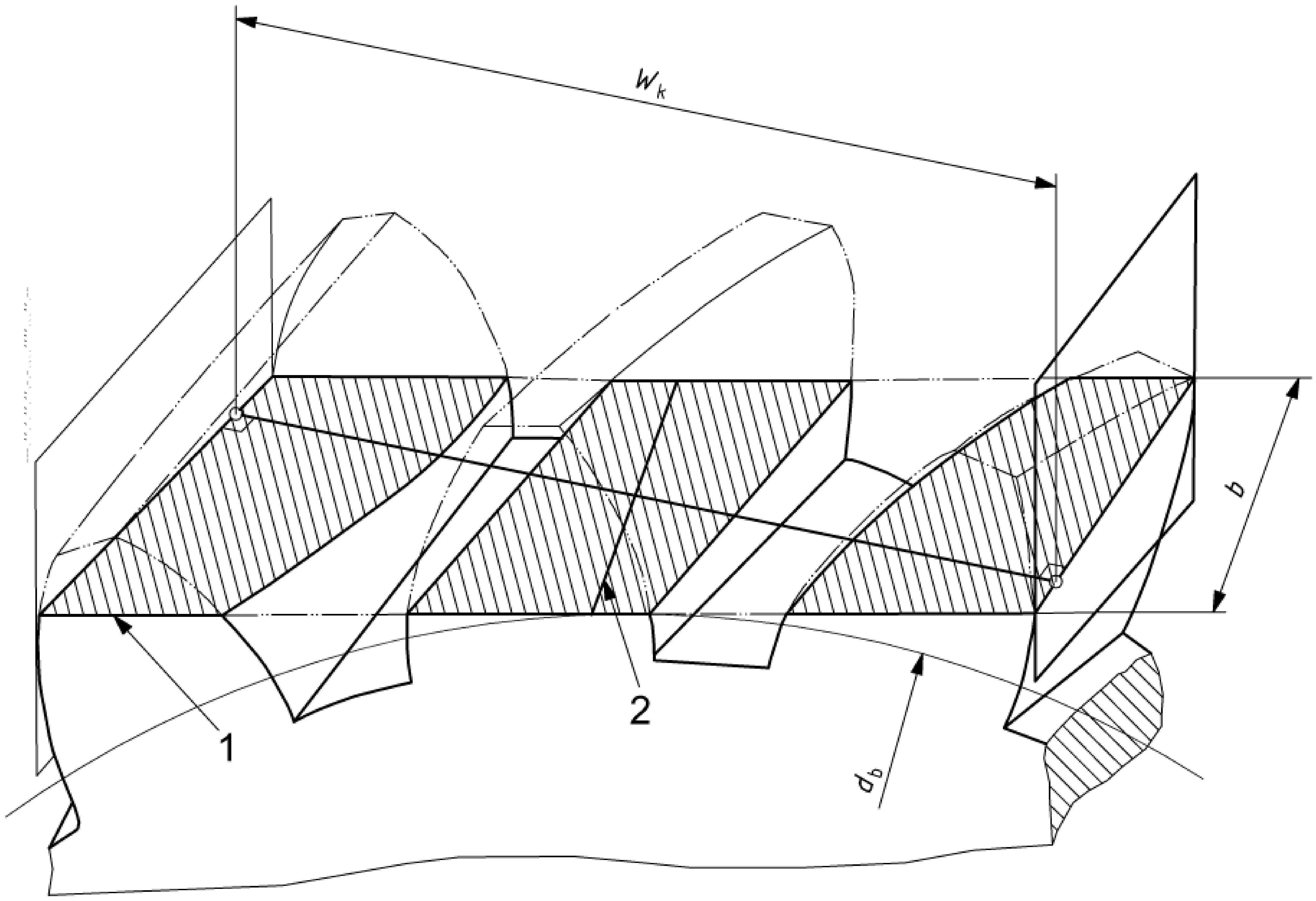

Key

1 base cylinder tangential plan

2 projection of the gear axis

Figure A.1 — Span measurement, W_k, on helical cylindrical gear

The span measurement is a flank-related measurement quantity and therefore independent of (not a function of) deviations of position between the gear axis and the axis of the teeth.

In many cases, on the same gear, span can be measured over several different numbers of teeth (or tooth spaces). Flank modifications, undercut, tip diameter variations and changed parameters of the standard basic rack tooth profile (e.g. alignment teeth with involute tooth profile according to ISO 4156) can lead to the reduction of the usable area of the tooth flank for measuring the span. This restricts the possible number of teeth spanned (measured number of tooth spaces), k. In some cases, particularly for helical gears with a low face to diameter ratio, span measurement cannot be used.

In the following equations, the integer function (INT) signifies that k is the closest whole number less than or equal to the decimal number of the value in brackets.

A.2.1 External gears, number of teeth spanned

The number of teeth spanned (measured number of tooth spaces) may be chosen from either:

$$k = \mathrm{INT}\left[\frac{z}{\pi}\left(\frac{\tan\alpha_{\mathrm{vt}}}{\cos^2\beta_{\mathrm{b}}} - \mathrm{inv}\alpha_{\mathrm{t}} - \frac{2x}{z}\tan\alpha_{\mathrm{n}}\right) + 1\right] \quad \text{(A.1)}$$

or, alternatively,

$$k = \mathrm{INT}\left(\frac{\dfrac{\sqrt{{d_\mathrm{v}}^2 - d_\mathrm{b}^2}}{\cos\beta_\mathrm{b}} - s_\mathrm{bn}}{p_\mathrm{bn}} + 1 \right) \tag{A.2}$$

or by means of an approximation, which is sufficient in many cases as

$$k = \mathrm{INT}\left(z \frac{\mathrm{inv}\alpha_\mathrm{t}}{\mathrm{inv}\alpha_\mathrm{n}} \frac{\alpha_\mathrm{vn}}{\pi} + 1 \right) \tag{A.3}$$

α_vn may be calculated according to Equation (15) on the V circle.

The usable range of number of teeth spanned (measured number of tooth spaces), k, on flanks without modification as limited by the diameter of the root form circle, d_Ff, and the tip form circle, d_Fa, can be obtained from

$$k_\mathrm{min} = \mathrm{INT}\left[\frac{z}{\pi} \left(\frac{\tan\alpha_\mathrm{Ff}}{\cos^2\beta_\mathrm{b}} - \mathrm{inv}\alpha_\mathrm{t} - \frac{2x}{z}\tan\alpha_\mathrm{n} \right) + 1{,}5 \right] = \mathrm{INT}\left(\frac{\dfrac{\sqrt{d_\mathrm{Ff}^2 - d_\mathrm{b}^2}}{\cos\beta_\mathrm{b}} - s_\mathrm{bn}}{p_\mathrm{bn}} + 1{,}5 \right) \tag{A.4}$$

$$k_\mathrm{max} = \mathrm{INT}\left[\frac{z}{\pi} \left(\frac{\tan\alpha_\mathrm{Fa}}{\cos^2\beta_\mathrm{b}} - \mathrm{inv}\alpha_\mathrm{t} - \frac{2x}{z}\tan\alpha_\mathrm{n} \right) + 0{,}5 \right] = \mathrm{INT}\left(\frac{\dfrac{\sqrt{d_\mathrm{Fa}^2 - d_\mathrm{b}^2}}{\cos\beta_\mathrm{b}} - s_\mathrm{bn}}{p_\mathrm{bn}} + 0{,}5 \right) \tag{A.5}$$

If the flanks are modified, use the unmodified flank limit diameters instead of the root and tip form diameters. With the user-chosen integer value for k ($k_\mathrm{min} \leqslant k \leqslant k_\mathrm{max}$) the base tangent length is given by:

$$\begin{aligned} W_\mathrm{k} &= m_\mathrm{n} \cos\alpha_\mathrm{n} \left[\pi(k-1) + z\,\mathrm{inv}\alpha_\mathrm{t} + z\psi \right] \\ &= m_\mathrm{n} \cos\alpha_\mathrm{n} \left[\pi(k-0{,}5) + z\,\mathrm{inv}\alpha_\mathrm{t} \right] + 2xm_\mathrm{n} \sin\alpha_\mathrm{n} \\ &= (k-1)\,p_\mathrm{bn} + s_\mathrm{bn} \end{aligned} \tag{A.6}$$

where tooth thickness half angle ψ is determined using Equation (41) with the generating profile shift coefficient.

In the case of external helical gears, it is always necessary to check the practicality of the span measurement for the calculated or selected number, k, of teeth to be spanned. In order to ensure a sufficiently reliable measurement of W_k for a gear with usable facewidth b_F (b reduced by the chamfers or curves at the tooth ends, see 4.2.8), b_F must equal or exceed a minimum value of $b_\mathrm{F\,min}$, which is required to ensure that the straight contact lines between the measuring surfaces and the two tooth flanks (involute helicoids) are satisfactorily long. Thereby, a secure measuring surface contact is guaranteed and the imaginary axis of the measuring device (shown by the points on the straight contact lines indicated by dimension W_k in Figures A.1 to A.3) is positioned perpendicular to the flank generators. Usable facewidth b_F (see Figure A.2) should not be less than value $b_\mathrm{F\,min}$ determined using:

$$b_{\mathrm{F}} \geqslant b_{\mathrm{Fmin}} = W_{\mathrm{k}} \sin \beta_{\mathrm{b}} + b_{\mathrm{M}} \cos \beta_{\mathrm{b}} \tag{A.7}$$

with

$$b_{\mathrm{M}} = 1{,}2 + 0{,}018 W_{\mathrm{k}} \tag{A.8}$$

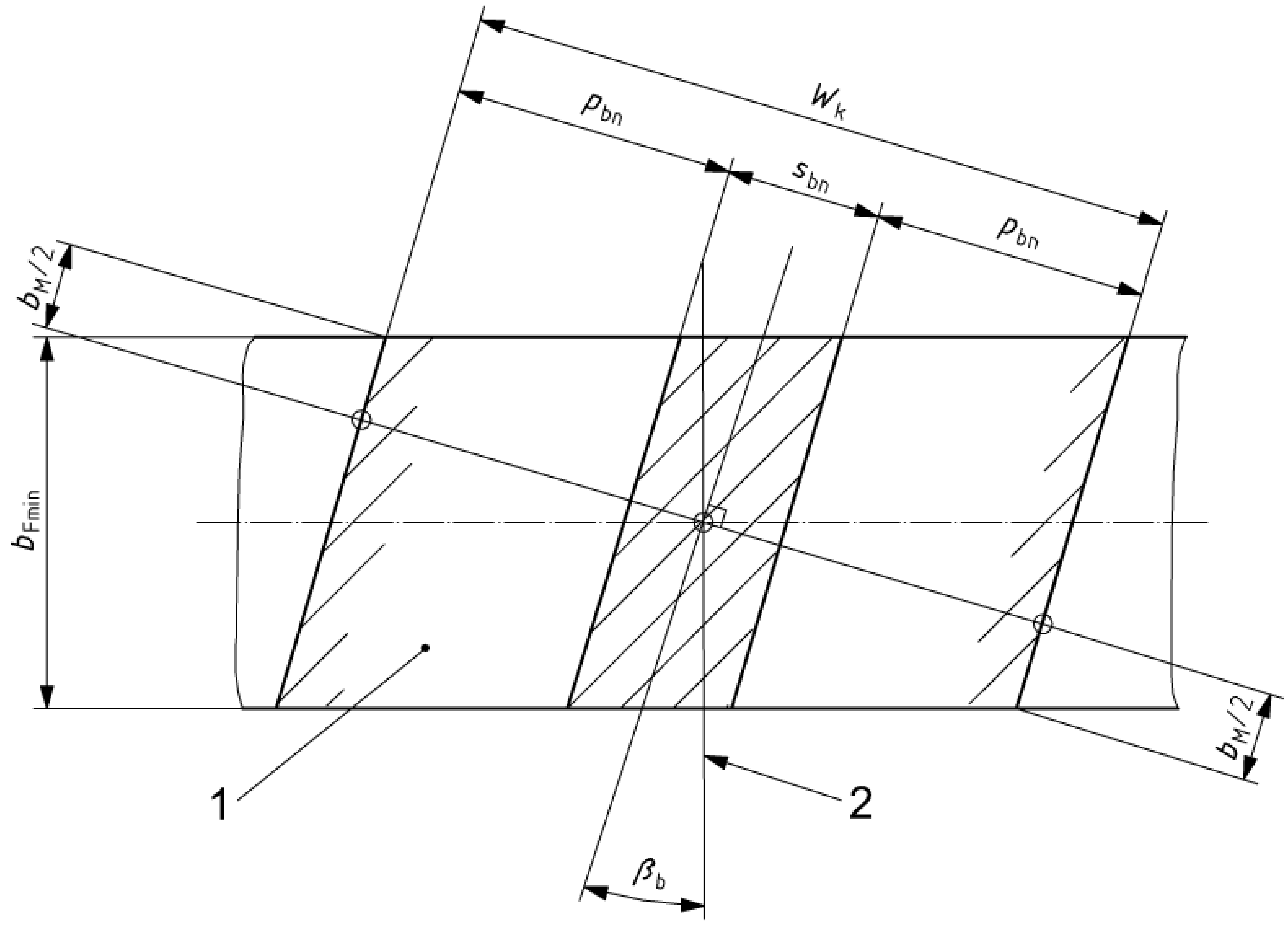

Key

1 base cylinder tangential plane

2 projection of the gear axis

Figure A.2 — Diagram showing facewidth required to permit adequate span measurement

In the case of spur gears, with the chosen integer number of teeth spanned (measured number of tooth spaces) k, the measuring planes will contact the tooth flanks (with symmetrical positioning of the measuring planes, see Figure A.3) at the measuring circle diameter d_{M}:

$$d_{\mathrm{M}} = \sqrt{d_{\mathrm{b}}^2 + W_{\mathrm{k}}^2} \tag{A.9}$$

The possibilities for rocking the measuring device in relation to the symmetrical positioning of the measuring surfaces (angle of rock, δ_{W}) within the tooth flank surface limited by tip form diameter d_{Fa} and root form diameter d_{Ff} are determined by the tooth parameters.

Where $W_{\mathrm{k}} - \frac{d_{\mathrm{b}}}{2} \tan \alpha_{\mathrm{Fa}} > \frac{d_{\mathrm{b}}}{2} \tan \alpha_{\mathrm{Ff}}$, it follows that

$$\delta_{\mathrm{W}} = 2\left(\tan \alpha_{\mathrm{Fa}} - \frac{W_{\mathrm{k}}}{d_{\mathrm{b}}} \right) \tag{A.10}$$

Where $W_k - \frac{d_b}{2}\tan\alpha_{Fa} \leqslant \frac{d_b}{2}\tan\alpha_{Ff}$ (see Figure A.3), it follows that

$$\delta_w = 2\left(\frac{W_k}{d_b} - \tan\alpha_{Ff}\right) \tag{A.11}$$

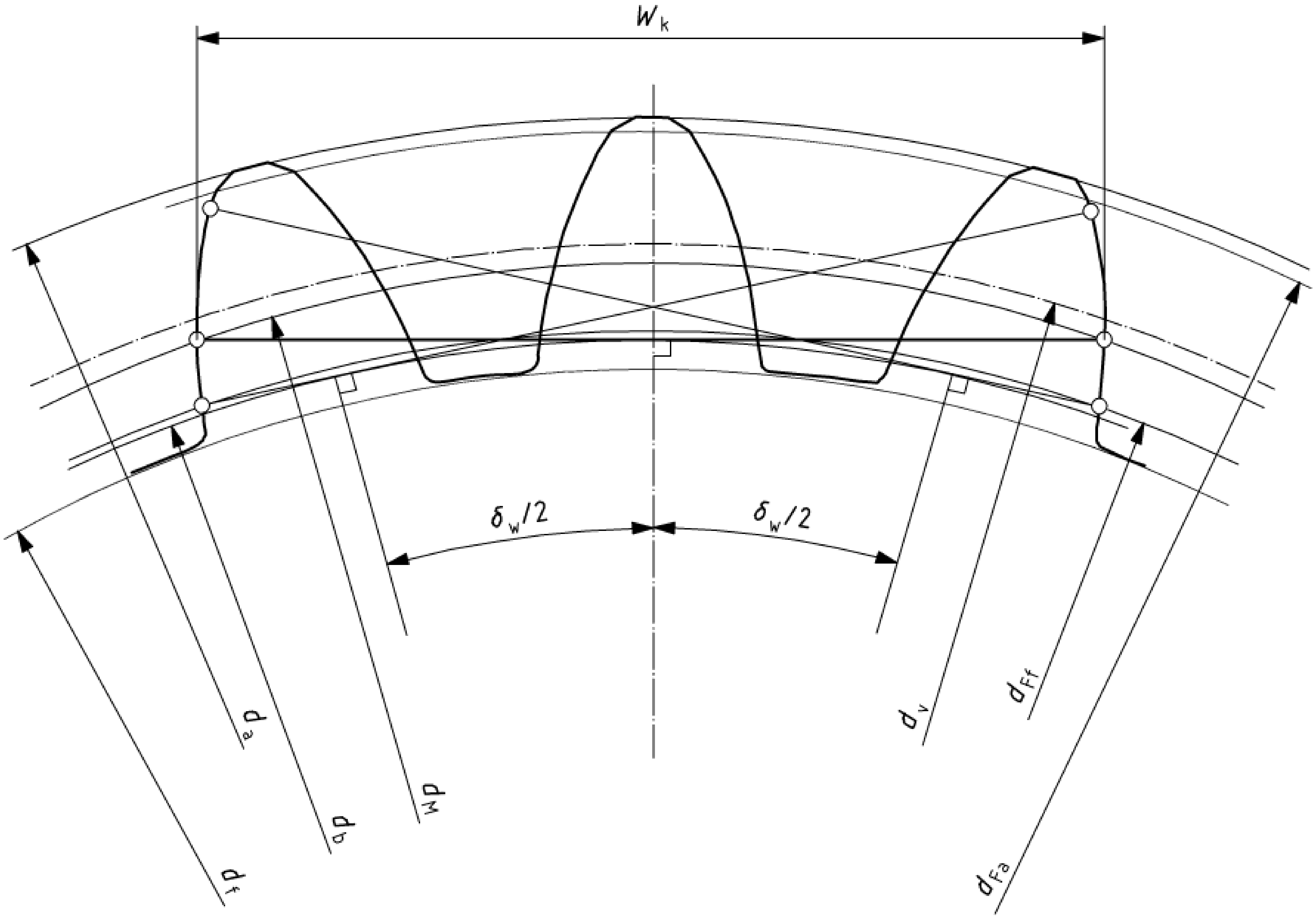

Figure A.3 — Diagram of portion of transverse section available for span measurement on external spur gear with number of teeth spanned k = 3 for a secure measuring surface contact

A.2.2 Internal spur gears, number of tooth spaces spanned

Number of tooth spaces spanned, k, may be chosen from

$$k = \text{INT}\left[\frac{|z|}{\pi}\left(\tan\alpha_{\text{v}} - \text{inv}\alpha - \frac{2x}{z}\cdot\tan\alpha_{\text{n}}\right) - 1\right] \tag{A.12}$$

or, alternatively,

$$k = \text{INT}\left(\frac{\sqrt{d_{\text{v}}{}^2 - d_{\text{b}}^2} + s_{\text{b}}}{p_{\text{b}}} - 1\right) \tag{A.13}$$

or by means of approximation, which is sufficient in many cases as

$$k = \text{INT}\left(|z|\frac{\alpha_{\text{v}}}{\pi} - 1\right) \tag{A.14}$$

α_{vn} may be calculated according to Equation (16) on the V, circle.

The root form diameter limits the maximum number of tooth spaces that can be spanned, while the internal tooth tip diameter limits the minimum number of tooth spaces that can be spanned:

$$k_{\max} = \text{INT}\left(\frac{\sqrt{d_{\text{Ff}}^2 - d_{\text{b}}^2} + s_{\text{bn}}}{p_{\text{bn}}} - 0{,}5\right) \tag{A.15}$$

$$k_{\min} = \text{INT}\left(\frac{\sqrt{d_{\text{a}}{}^2 - d_{\text{b}}^2} + s_{\text{bn}}}{p_{\text{bn}}} + 0{,}5\right) \tag{A.16}$$

If the flanks are modified, use the unmodified flank limit diameters instead of the root and tip form diameters.

With the user-chosen integer value for k $\left(k_{\min} \leqslant k \leqslant k_{\max}\right)$, the base tangent length is given by

$$\begin{aligned} W_{\text{k}} &= m_{\text{n}}\cos\alpha_{\text{n}}\left(\pi k + |z|\text{inv}\alpha_{\text{t}} + z\psi\right) \\ &= m_{\text{n}}\cos\alpha_{\text{n}}\left[\pi\left(k - 0{,}5\right) + |z|\text{inv}\alpha_{\text{t}}\right] - 2xm_{\text{n}}\sin\alpha_{\text{n}} \\ &= k\,p_{\text{bn}} - s_{\text{bn}} \end{aligned} \tag{A.17}$$

where tooth thickness half angle ψ is determined using Equation (41) with the generating profile shift coefficient.

A.2.3 Functional system — Span adjustment for allowable tolerances

The number of teeth to be spanned in the functional system is the same as that in the nominal system (see A.2.1).

The span measurement gives the tooth thickness in relation to the base cylinder. Deviations in base pitch, accumulated pitch over k teeth, tooth profile, and lead can all affect the span measurement, and runout (between the base cylinder and the bearing journals) can affect the functional tooth thickness. The allowable span measurement must therefore be adjusted if the functional tooth thickness is to be limited.

The adjustment is made by decreasing the maximum base tooth thickness when calculating the maximum span measurement and increasing the minimum base tooth thickness when calculating the minimum span measurement. The effects of lead and profile deviations can usually be ignored since they are usually much smaller than the runout and pitch deviations:

$$s_{\mathrm{bn.amax}} = s_{\mathrm{bn.max}} - \cos\beta_{\mathrm{b}} \left(F_{\mathrm{r}} \tan\alpha_{\mathrm{tM}} + F_{\mathrm{pk}} \cos\alpha_{\mathrm{tM}} \right) \tag{A.18}$$

$$s_{\mathrm{bn.amin}} = s_{\mathrm{bn.min}} + \cos\beta_{\mathrm{b}} \left(F_{\mathrm{r}} \tan\alpha_{\mathrm{tM}} + F_{\mathrm{pk}} \cos\alpha_{\mathrm{tM}} \right) \tag{A.19}$$

The deviations F_{r} and F_{pk} are found in ISO 1328.

The transverse pressure angle at the measuring diameter may be calculated at the diameter found from Equation (A.9).

Thus the allowable range of span measurement for external gears is

$$W_{\mathrm{k.amax}} = (k-1)\, p_{\mathrm{bn}} + s_{\mathrm{bn.amax}} \tag{A.20}$$

$$W_{\mathrm{k.amin}} = (k-1)\, p_{\mathrm{bn}} + s_{\mathrm{bn.amin}} \tag{A.21}$$

The allowable range of span measurement for internal gears is

$$W_{\mathrm{k.amax}} = k\, p_{\mathrm{bn}} + s_{\mathrm{bn.amax}} \tag{A.22}$$

$$W_{\mathrm{k.amin}} = k\, p_{\mathrm{bn}} + s_{\mathrm{bn.amin}} \tag{A.23}$$

A.3 Normal chordal tooth thicknesses and heights above the chords

A.3.1 General

The normal chordal tooth thickness, s_{cy}, is the shortest straight-line distance between tooth traces of a tooth on any pitch cylinder (Y-cylinder). (See Figure A.4.) In calculating and measuring the chordal tooth thickness, $d_a - 2m_n$ is often used as the Y-cylinder diameter.

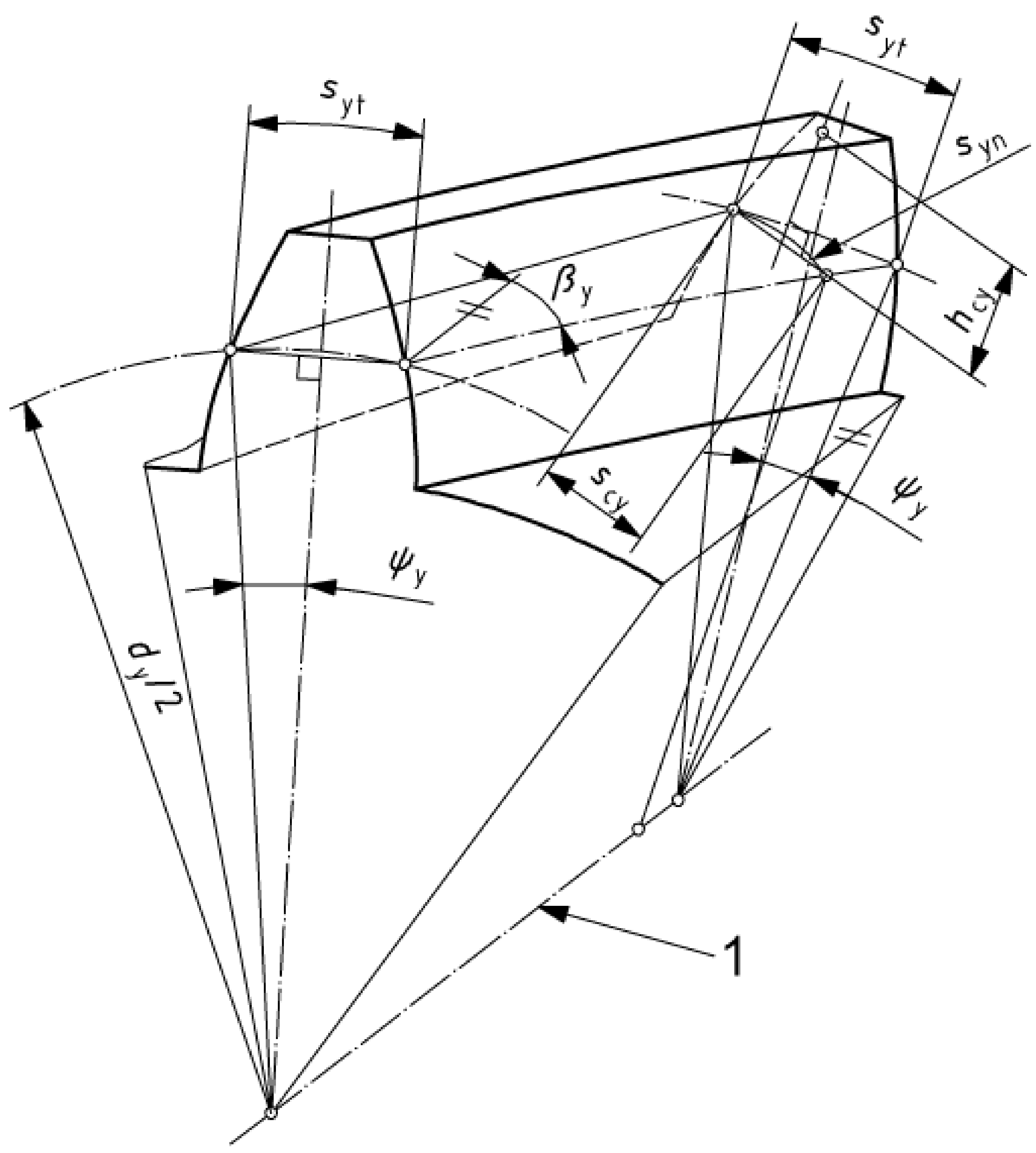

Key

1 gear axis

Figure A.4 — Tooth thicknesses, normal chordal tooth thicknesses and height above normal chordal tooth thickness on tooth at Y-cylinder of right-hand helical cylindrical gear

On the Y-cylinder, the following applies:

$$s_{cy} = d_y \sqrt{\left(\psi_y \cos\beta_y \sin\beta_y\right)^2 + \sin^2\left(\psi_y \cos^2\beta_y\right)} \quad \text{(A.24)}$$

or

$$s_{cy} = \sqrt{\left(s_{yn} \sin\beta_y\right)^2 + \left[d_y \sin\left(\frac{s_{yn}\cos\beta_y}{d_y}\right)\right]^2} \quad \text{(A.25)}$$

The normal chordal tooth thickness on the reference cylinder is

$$s_c = d\sqrt{\left(\psi \cos\beta \sin\beta\right)^2 + \sin^2\left(\psi \cos^2\beta\right)} \quad \text{(A.26)}$$

or

$$s_{\mathrm{c}} = \sqrt{\left(s_{\mathrm{n}} \sin\beta\right)^2 + \left(d \sin\left(\frac{s_{\mathrm{n}} \cos\beta}{d}\right)\right)^2} \tag{A.27}$$

The height, h_{cy}, above the chord, s_{cy}, to outside diameter d_{a} is

$$h_{\mathrm{cy}} = \left| \frac{d_{\mathrm{a}}}{2} - \frac{d_{\mathrm{y}}}{2} \cos\left(\frac{s_{\mathrm{yn}} \cos\beta_{\mathrm{y}}}{d_{\mathrm{y}}}\right) \right| \tag{A.28}$$

NOTE h_{cy} is also known as the chordal addendum. It is calculated in the transverse plane. The absolute value is used for internal gears.

For the reference chordal addendum, h_{c}, above the reference chordal measurement, s_{c}:

$$h_{\mathrm{c}} = \left| \frac{d_{\mathrm{a}}}{2} - \frac{d}{2} \cos\left(\frac{s_{\mathrm{n}} \cos\beta}{d}\right) \right| \tag{A.29}$$

A.3.2 Functional tooth thickness system — Chordal tooth thickness

The effective tooth thickness is influenced by runout. Therefore, runout should be included in the specified (manufacturing or measured) chordal tooth thickness tolerance calculation. Although large amounts of involute and helix form and slope deviations can affect the chordal thickness measurement, they can normally be neglected. To adjust the maximum effective tooth thickness, one half of the runout tolerance is added to the radius at which calculations are made. However, the calculation of the addendum bar (height slide) setting is made based on diameter d_{y}. Thus the maximum effective tooth thickness will be acceptable when, due to runout, that point on the tooth is effectively at a larger diameter than d_{y}. Therefore, the diameter to be used in calculating the maximum allowable chordal tooth thickness is

$$d_{\mathrm{y+F}} = d_{\mathrm{y}} + F_{\mathrm{rc}} \tag{A.30}$$

where F_{rc} is the correction made to the chordal addendum to account for manufacturing tolerances.

The value used for this runout allowance should be a combination of the outside diameter runout and the gear tooth runout. If the actual outside diameter and its runout at the point of measurement are known, they should be used. If the outside diameter runout is not known, it can be assumed to be equal to the allowable runout of the gear teeth. The runout of the gear teeth can be assumed to be 80 % of the total cumulative pitch deviation. [See ISO 1328-2:1997, Equation (B.1).]

The corrected values for maximum measured tooth thickness thus become:

$$s_{\mathrm{cy.max}} = \sqrt{\left(s_{\mathrm{(y+F)n.max}} \sin(\beta_{\mathrm{y+F}})\right)^2 + \left\{d_{\mathrm{y+F}} \sin\left[\frac{s_{\mathrm{(y+F)n.max}} \cos\left(\beta_{\mathrm{y+F}}\right)}{d_{\mathrm{y+F}}}\right]\right\}^2} \tag{A.31}$$

$$h_{\mathrm{ccy}} = \frac{\left| d_{\mathrm{a.max}} - d_{\mathrm{y+F}} \cos\left(\frac{s_{\mathrm{(y+F)n.max}} \cos(\beta_{\mathrm{y+F}})}{d_{\mathrm{y+F}}}\right) \right| + F_{\mathrm{rc}}}{2} \tag{A.32}$$

Thus $s_{\mathrm{cy.max}}$ is based on diameter $d_{\mathrm{y+F}}$, but the runout corrected chordal addendum, h_{ccy}, is essentially set at diameter d_{y}, since although it starts with $d_{\mathrm{y+F}}$, it is corrected not only for the difference in height between the arc and the chord, but also corrected by F_{rc}.

If the backlash is to be tightly controlled, then the minimum tooth thickness is important. In this case, the effective runout must be subtracted from diameter d_y. In addition, the measurement should be referenced to the minimum tip diameter. Thus the diameter for calculation becomes:

$$d_{y-F} = d_y - F_{rc} - \left(d_{a.max} - d_{a.min}\right) \tag{A.33}$$

To allow the same chordal addendum to be used for the acceptable minimum measured chordal tooth thickness, the equation for $s_{cy.min}$ also contains the term Δs to correct for the difference in arc heights of the maximum and minimum chords. Thus the corrected value for minimum measured chordal tooth thickness is

$$s_{cy.min} = \sqrt{\left(s_{(y-F)n.min} \sin(\beta_{y-F})\right)^2 + \left\{d_{y-F} \sin\left[\frac{s_{(y-F)n.min} \cos\left(\beta_{y-F}\right)}{d_{y-F}}\right]\right\}^2} - \Delta s \tag{A.34}$$

$$\Delta s \approx 2\left(\Delta h_{min} - \Delta h_{max}\right)\tan\alpha_{yn} \quad \Delta h = \frac{d_y}{2}\left[1-\cos\left(\frac{s_{yn}\cos\beta_y}{d_y}\right)\right]$$

$$\Delta s \approx \left\{d_{y-F}\left[1-\cos\left(\frac{s_{(y-F)nmin}\cos\beta_{y-F}}{d_{y-F}}\right)\right] - d_{y+F}\left[1-\cos\left(\frac{s_{(y+F)nmax}\cos\beta_{y+F}}{d_{y+F}}\right)\right]\right\}\tan\alpha_{yn} \tag{A.35}$$

The measured chordal tooth thickness can then be specified with the limits $s_{cy.max}$ and $s_{cy.min}$, both measured at h_{ccy}. As can be seen in Figure A.5, the allowable variation in measured tooth thickness is less than the variation in effective tooth thickness due to manufacturing tolerances. In Figure A.5, the curvature of the arcs is highly exaggerated so they can be easily seen, and the runout is exaggerated so that the arcs are well separated. What is not exaggerated is the fact that the effective tooth thickness can be significantly larger or smaller than the apparent measured tooth thickness.

See Figures A.6 and A.7 for the maximum and minimum allowable chordal tooth thickness measurement corrections, respectively.

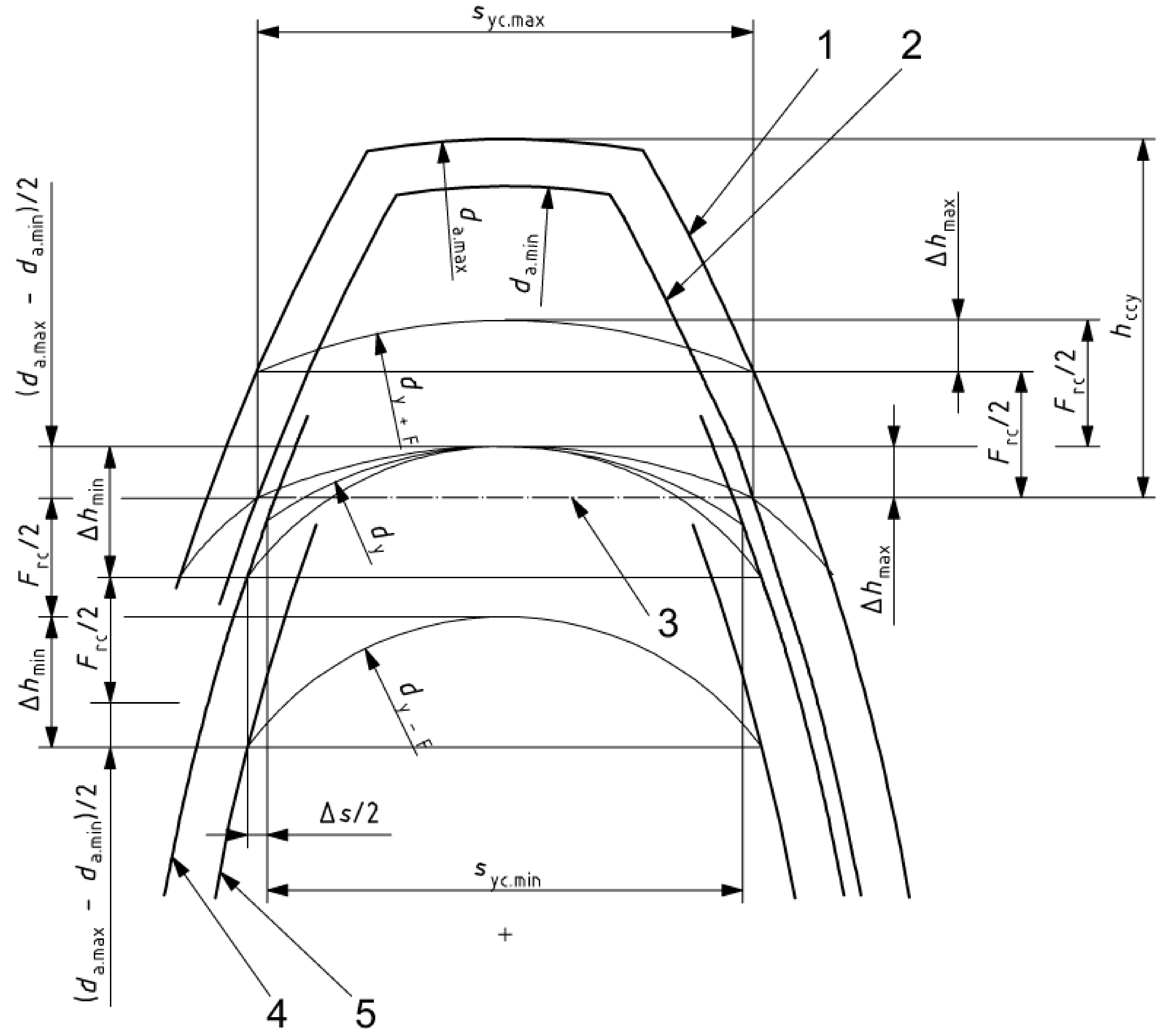

a

Key

1 maximum tooth thickness, effective

2 maximum tooth thickness, manufacturing (measured)

3 measurement line

4 minimum tooth thickness, manufacturing (measured)

5 minimum tooth thickness, effective

[a] Transverse plane.

Figure A.5 — Correction of allowable chordal tooth thickness measurement to account for runout and outside diameter deviations

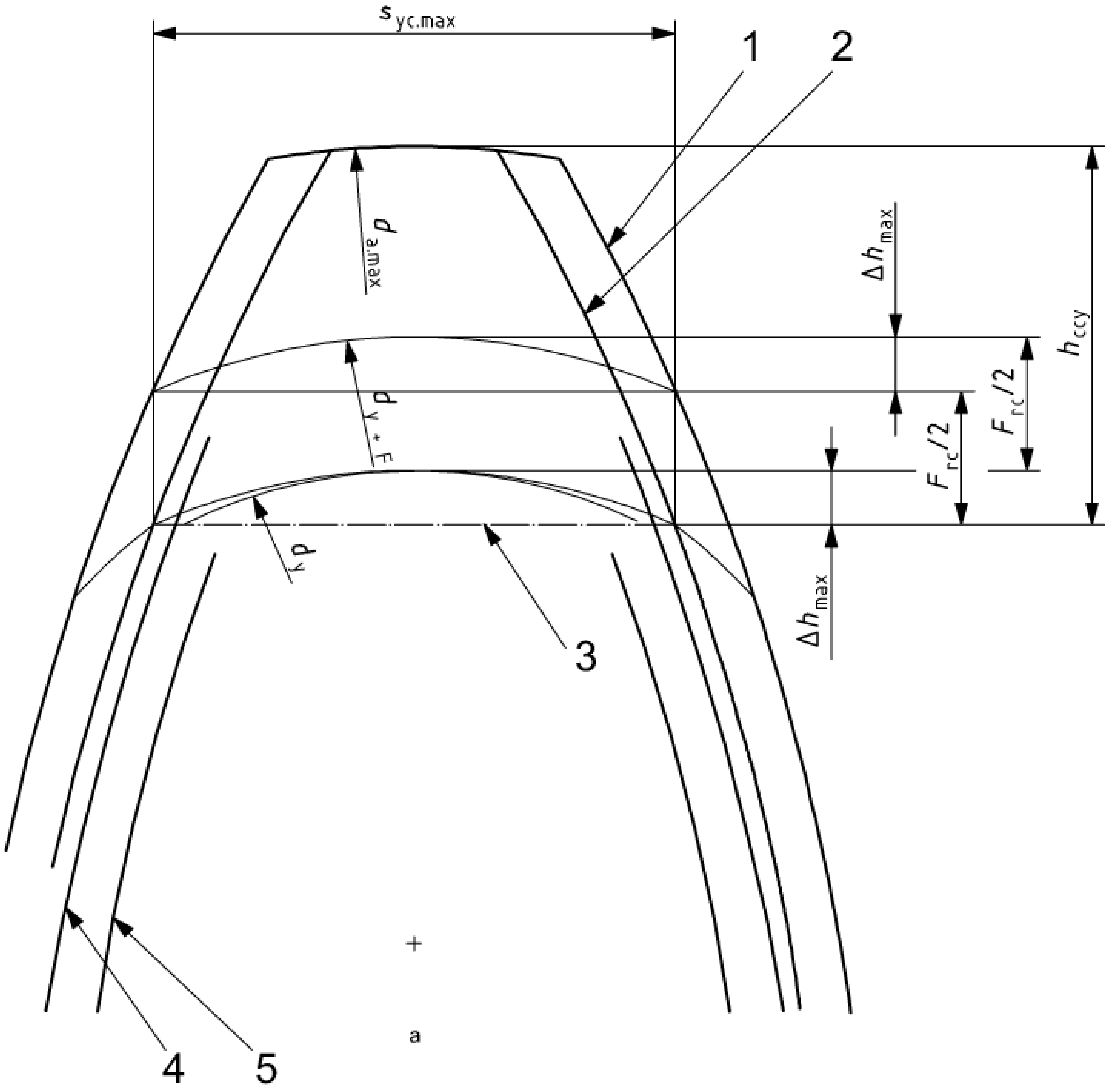

Key

1 maximum tooth thickness, effective

2 maximum tooth thickness, manufacturing (measured)

3 measurement line

4 minimum tooth thickness, manufacturing (measured)

5 minimum tooth thickness, effective

a Transverse plane.

Figure A.6 — Correction of maximum allowable chordal tooth thickness measurement to account for runout

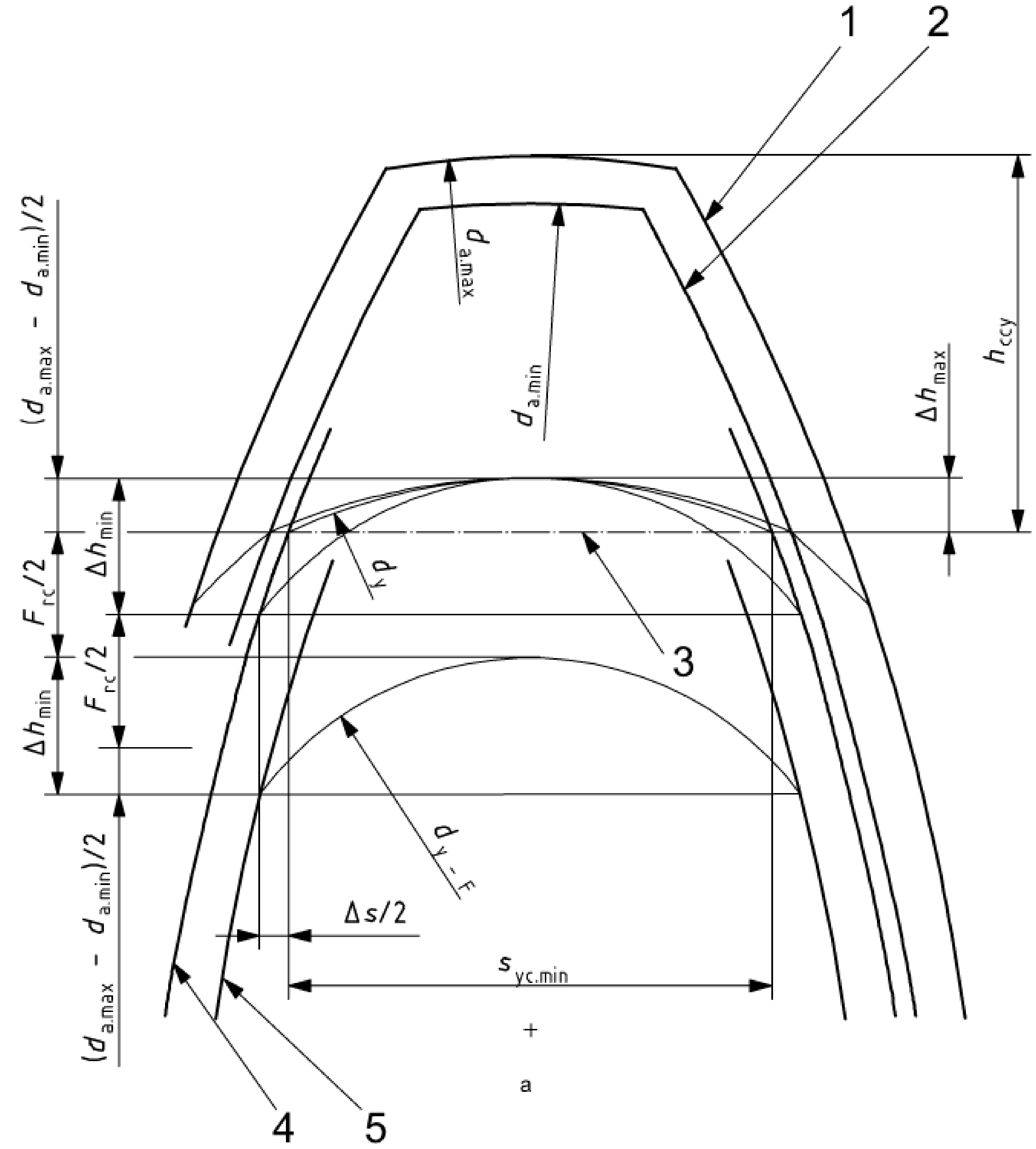

Key

1 maximum tooth thickness, effective
2 maximum tooth thickness, manufacturing (measured)
3 measurement line
4 minimum tooth thickness, manufacturing (measured)
5 minimum tooth thickness, effective

[a] Transverse plane.

Figure A.7 — Correction of minimum allowable chordal tooth thickness measurement to account for runout and outside diameter deviations

A.4 Constant chord

The constant chordal tooth thickness, s_{cc}, is the length of the straight lines produced between the flank points when two tangents forming an apex angle of $2\alpha_t$ at both profiles of a tooth in the transverse section are positioned symmetrically, see Figure A.8.

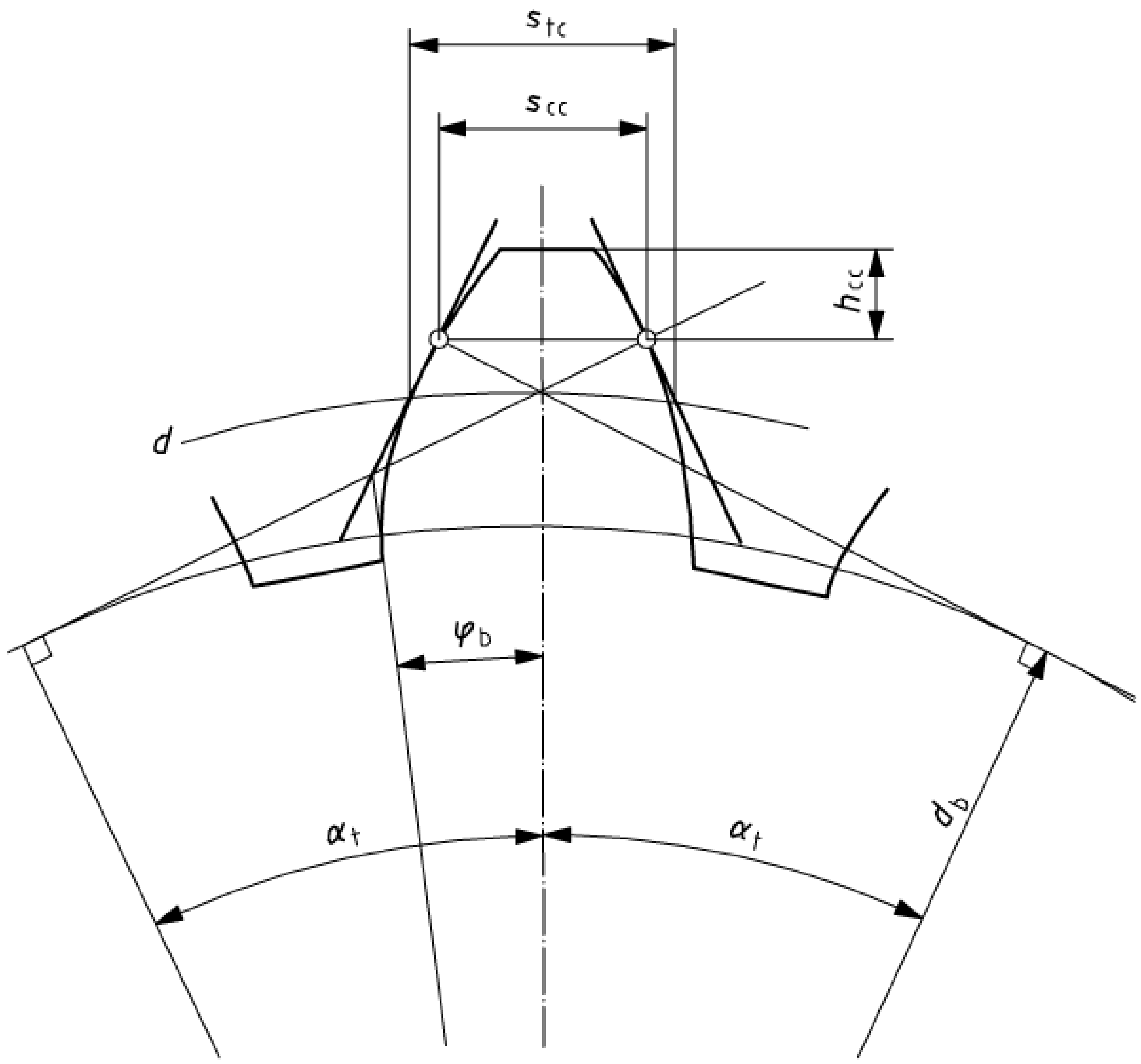

Figure A.8 — Constant chord s_{cc} and height h_{cc} above constant chord in transverse section of external helical gear

Constant tooth thickness chord s_{cc} and height h_{cc} above the constant chord are expressed as

$$s_{cc} = s_n \frac{\cos^2 \alpha_t}{\cos \beta} = m_n \left(\frac{\pi}{2} + 2x \tan \alpha_n \right) \frac{\cos^2 \alpha_t}{\cos \beta} \tag{A.36}$$

$$h_{cc} = h_a - \frac{s_t}{2} \sin \alpha_t \cos \alpha_t = h_a - \frac{m_n}{2} \left(\frac{\pi}{2} + 2x \tan \alpha_n \right) \frac{\sin \alpha_t \cos \alpha_t}{\cos \beta} \tag{A.37}$$

Spur-toothed cylindrical gears of the same standard basic rack tooth profile and with the same profile shift have the same (constant) chordal tooth thickness, s_{cc}, independent of the number of teeth. For this reason, s_{cc} is termed the *constant chord*.

A.5 Radial single-ball test dimension

The radial single-ball dimension, M_{rK}, is the distance between the gear axis and

— in the case of an external gear, the outermost point, and

— in the case of an internal gear, the innermost point

of a measuring ball of diameter, D_M, which lies in a tooth space on both tooth flanks; see Figures A.9 and A.10.

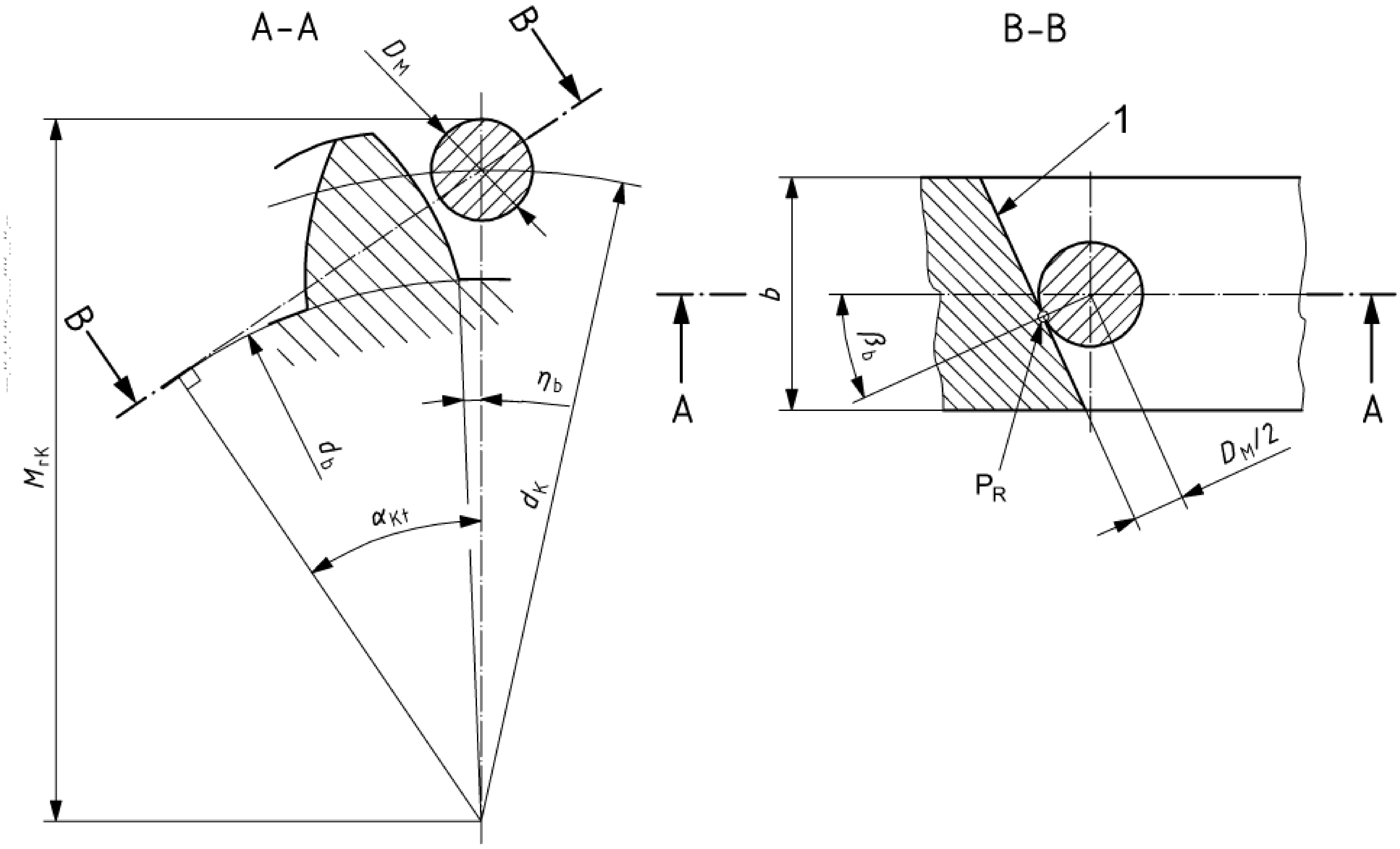

Key

A-A transverse section through the centre of the measuring ball

B-B section of base cylinder tangential plane of the right flank on a left-hand cylindrical gear

P_R contact point of the measuring ball on the right flank

1 generator

Figure A.9 — Radial single-ball dimension, M_{rK}, on external helical gear

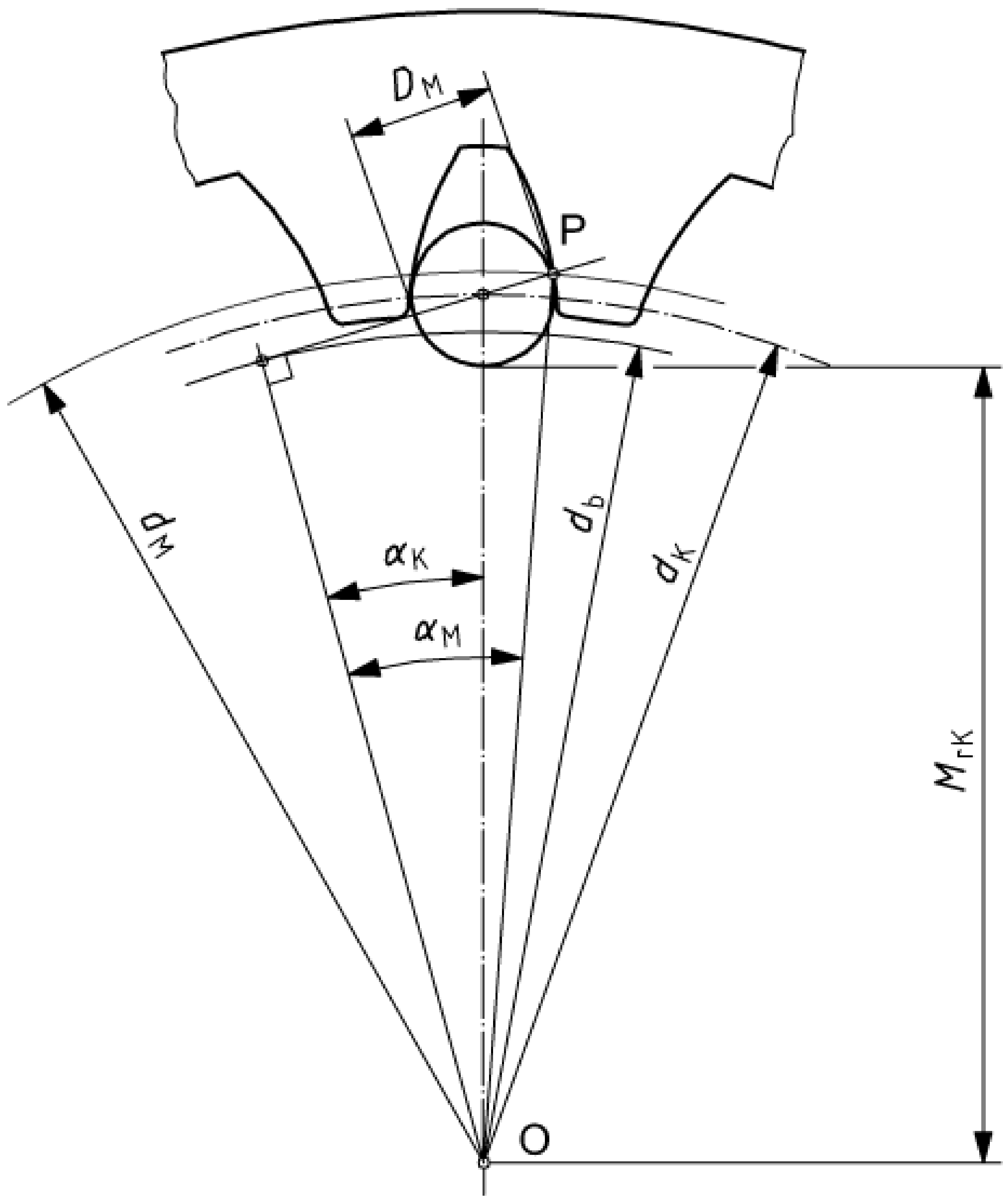

Figure A.10 — Radial single-ball dimension M_{rK} in transverse section of internal spur gear

The contact points, P_R and P_L, between the measuring ball and the right and left flank shall lie on or near to the V-cylinder. In order for the contact points to lie on the V-cylinder, D_M must have the following value in the case of helical cylindrical gears:

$$D_M = |z| m_n \cos\alpha_n \frac{\tan\alpha_{Kt} - \tan\alpha_{vt}}{\cos^2\beta_b} \tag{A.38}$$

with α_{vt} according to 4.3.5 and α_{Kt} according to Equation (A.39), which is not explicitly resolvable:

$$\alpha_{Kt} + \text{inv}\alpha_{Kt} \sin^2\beta_b = \tan\alpha_{vt} + \frac{z}{|z|}\eta_b \cos^2\beta_b \tag{A.39}$$

With sufficient approximation, for tooth systems with $\alpha_n = 20°$, the measuring ball diameter D_M required for the contact on a V-cylinder can also be determined using the nomogram shown in Figure A.11. The measuring ball diameter is calculated from the coefficient $D_M{}^*$:

$$D_M = m_n D_M{}^* \tag{A.40}$$

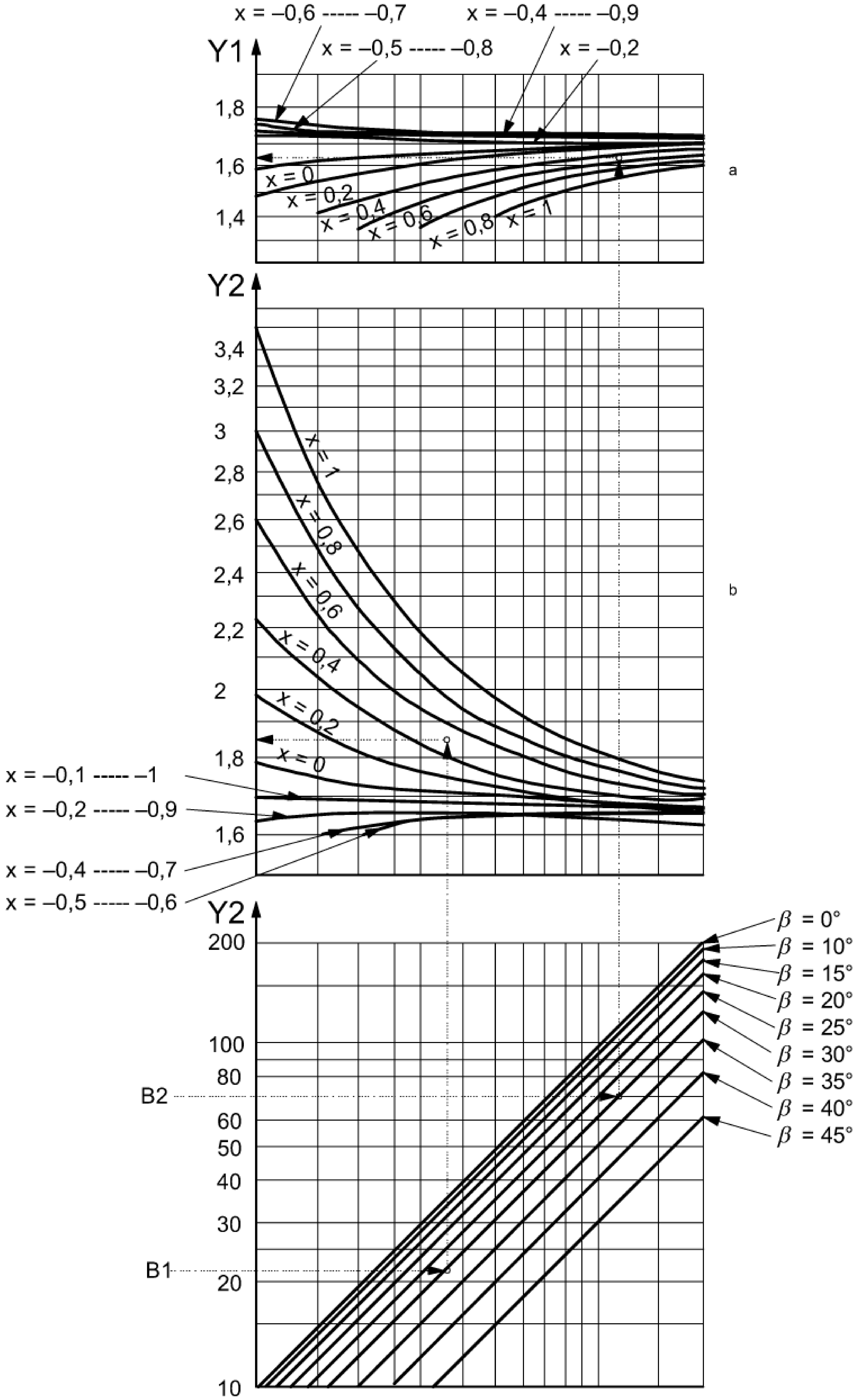

Key

Y1 measuring ball diameter coefficient, D_m

Y2 amount of teeth, z

[a] Internal gear.

[b] External gear.

In the case of cylindrical gears with manufactured or actual tooth thickness dimensions then use x_E instead of x; example B1 (external gear): z = 22; β = 30°; x = 0,5; example B2 (internal gear): z = 70; β = 30°; x = 0,5.

Figure A.11 — Nomogram for determining measuring ball diameter coefficient D_M for radial single-ball dimension or dimension over balls for $\alpha_n = 20°$

In the case of spur-type cylindrical gears, α_K can be calculated exactly from the explicit equation of calculation:

$$\alpha_K = \tan\alpha_v + \eta_b \tag{A.41}$$

D_M is to be calculated according to Equation (A.38). As the measuring balls only need to contact the tooth flanks in the vicinity of the V-cylinder, measuring balls having diameters slightly different from the calculated values may be used.

If measuring ball diameter D_M is known, then the pressure angle at a point, α_{Kt}, in the transverse section on the circle through the centre of the ball is found from

$$\operatorname{inv}\alpha_{Kt} = \frac{D_M}{z m_n \cos\alpha_n} - \frac{z}{|z|}\eta + \operatorname{inv}\alpha_t = \frac{D_M}{d_b \cos\beta_b} - \frac{z}{|z|}\eta_b \tag{A.42}$$

Diameter d_K of the circle on which the centre of the measuring ball lies is found as

$$d_K = d\frac{\cos\alpha_t}{\cos\alpha_{Kt}} = \frac{d_b}{\cos\alpha_{Kt}} \tag{A.43}$$

The radial single-ball dimension is

$$M_{rK} = \frac{1}{2}\left(d_K + \frac{z}{|z|}D_M\right) \tag{A.44}$$

When calculating the test dimensions and determining d_M in order to check whether measuring balls or measuring cylinders contact the tooths flanks in the usable area, the actual values for the selected measuring ball and measuring cylinder diameters are to be used. Diameter d_M of the cylinder on which contact points P_L and P_R between the measuring ball and the two tooth flanks lie is given as

$$d_M = \frac{d_b}{\cos\alpha_{Mt}} = \frac{z m_n \cos\alpha_t}{\cos\beta\cos\alpha_{Mt}} \tag{A.45}$$

where the pressure angle at a point, α_{Mt}, on the circle of diameter d_M is produced by

$$\tan\alpha_{Mt} = \tan\alpha_{Kt} - \frac{D_M}{d_b}\cos\beta_b \tag{A.46}$$

A.6 Radial single-cylinder dimension

In the case of external gears and internal spur gears, measuring cylinders of diameter D_M can also be used instead of measuring balls. Equations (A.38) to (A.46) also apply to the radial single-cylinder dimension, M_{rZ}.

A.7 Diametral test dimension over balls

In the case of an external gear, the dimension over balls, M_{dK}, is the largest external dimension over two balls; while in the case of an internal gear it is the smallest internal dimension between two balls of diameter D_M and in contact with the flanks in two tooth spaces at the maximum possible separation from each other on the gear. The centres of the two measuring balls must be located in the same transverse section of the gear. For selection and calculation of measuring ball diameter D_M and diameter d_K of the ball centre circle, see A.5.

For an even number of teeth, see Figure A.12; test dimension M_{dK} is calculated using

$$M_{dK} = d_K + \frac{z}{|z|} D_M \tag{A.47}$$

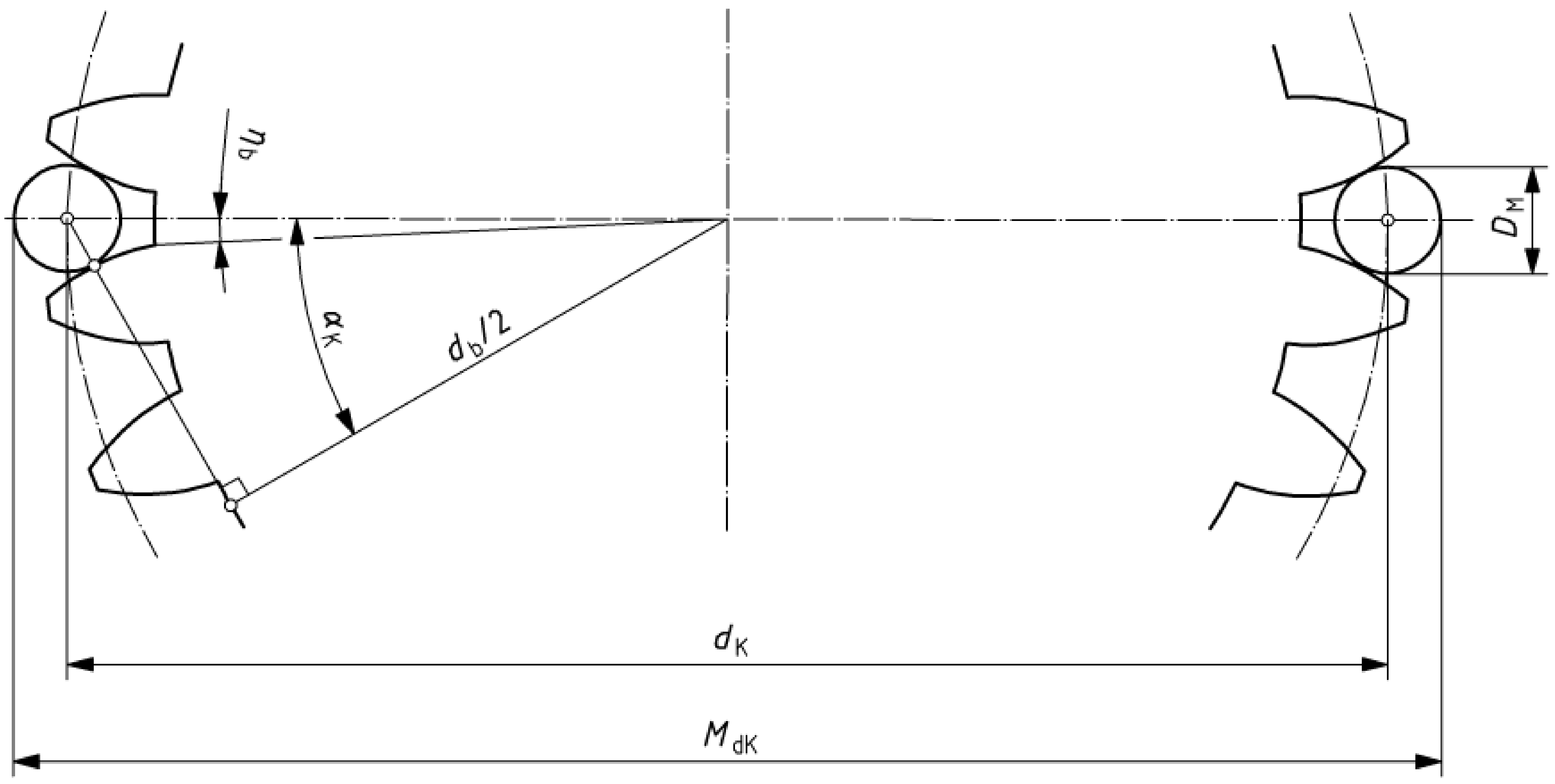

Figure A.12 — Dimension over balls M_{dK} in the case of external spur gear with even number of teeth

For an odd number of teeth, see Figures A.13 and A.14; test dimension M_{dK} is calculated using

$$M_{\mathrm{dK}} = d_{\mathrm{K}} \cos\frac{\pi}{2 * z} + \frac{z}{|z|} D_{\mathrm{M}} \tag{A.48}$$

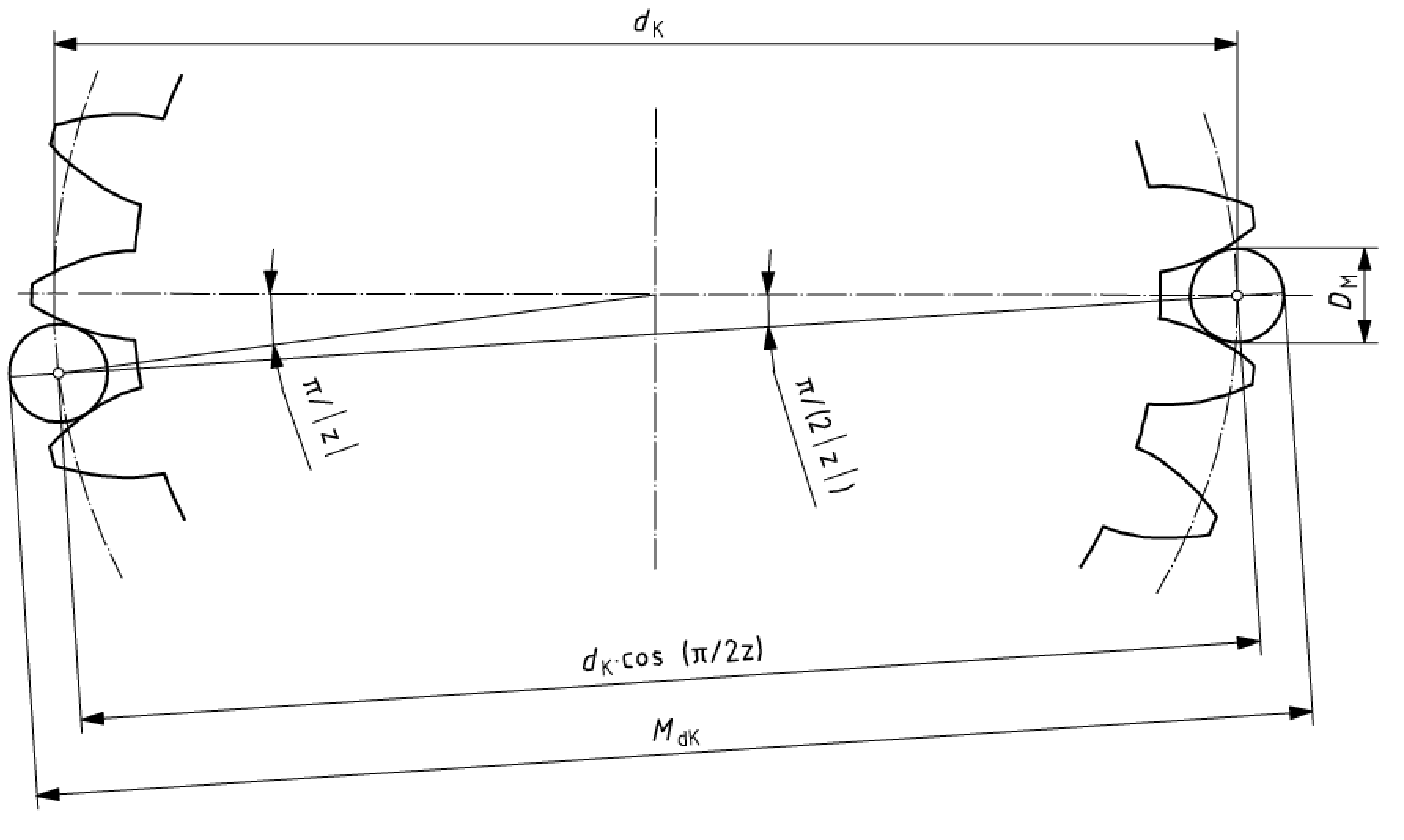

Figure A.13 — Dimension over balls M_{dK} in the case of external spur gear with odd number of teeth

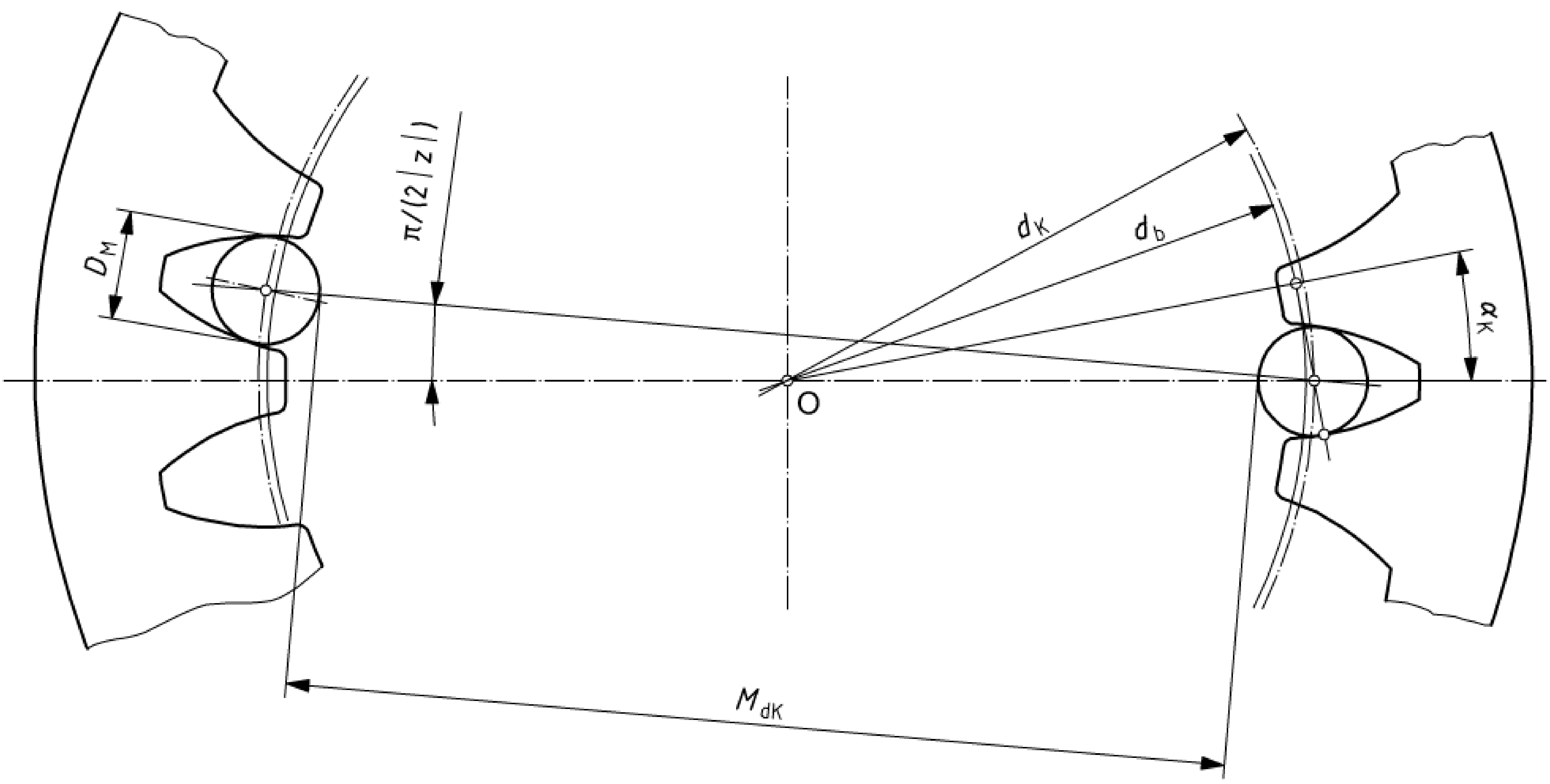

Figure A.14 — Dimension over balls M_{dK} in the case of internal spur gear with odd number of teeth

A.7.1 Dimension over cylinders

In the case of external gears and internal spur gears, measuring cylinders of diameter D_M can also be used instead of measuring balls. Equations (A.38) to (A.48) can be used when calculating the test dimension M_{dZ} for the dimension over cylinders in the case of an even number of teeth or in the case of spur gears. For helical gears with an odd number of teeth, special calculations are necessary.

A.7.2 Functional tooth thickness system — Measurement over balls — Correction for tooth deviations (adjustment for allowable tolerances)

If the pins or balls make contact near the mid-point of the active profile, the influence of flank deviations is minimized. The effect of allowable pitch deviation is usually much smaller than allowable runout, so it can be ignored except for gears with low numbers of teeth or other unusual cases.

If measurements are made from a ball or pin to the mounting diameter, the effect of runout is included and no correction is necessary. If the measurement is made over balls or pins on opposite sides of the gear, then the effect of runout should be calculated and the allowable measurements adjusted. This adjustment will decrease the allowable range of the measurement.

$$M_{\text{dk.amax}} = M_{\text{dk.max}} - \frac{F_r}{2} \tag{A.49}$$

$$M_{\text{dk.amin}} = M_{\text{dk.min}} + \frac{F_r}{2} \tag{A.50}$$

A.8 Double-flank centre distance

The double-flank centre distance, a_L, is the centre distance with zero-backlash mating of the cylindrical gear under test with a master gear. It can be used as a test dimension when checking the tooth thickness of the test object. For a test pair consisting of a gear with number of teeth z and a master gear with number of teeth z_L, profile shift coefficient x_L and known actual tooth thickness deviation E_{snL}, the values for the relevant test dimensions can be calculated using

$$a_L = \left(|z| + \frac{z}{|z|} z_L \right) \frac{m_n \cos \alpha_t}{2 \cos \beta \cos \alpha_L} \tag{A.51}$$

where the working transverse pressure angle a_L is found from

$$\operatorname{inv} \alpha_L = \operatorname{inv} \alpha_t + \frac{z}{|z|} \frac{2 \tan \alpha_n}{|z| + \frac{z}{|z|} z_L} \left(x + x_L + \frac{E_{snL}}{2 m_n \tan \alpha_n} \right) \tag{A.52}$$

A.9 Tooth thickness test dimensions relating to the tip circle

When producing external cylindrical gears using generating methods, if specially designed hobs and pinion-type cutters (topping gear-cutting tools) are used, it is possible to produce the bottom land, tooth flank and top land of the gear during the same working cycle. Nominally defined tip diameter d_a (see 4.5.3) will only be produced if its diameter is smaller than the pre-machined diameter and it happens to correspond to the tip diameter produced by the tool (root or edge chamfering). The diameter, d_{aM}, of the overcut tip cylinder is determined by the dedendum of tool rack tooth profile h_{fP0}. When using a hob, with x_{Es} according to Equations (120) and (121), d_{aM} is found as

$$d_{aM} = d + 2 x_{Es} m_n + 2 h_{fP0} \tag{A.53}$$

When using a pinion-type cutter, d_{aM} is determined by cutter root diameter d_{f0} as

$$d_{aM} = 2a_0 - d_{f0} \tag{A.54}$$

With these production variations, there is a relation between the dimension of overcut tip diameter d_{aM} and tooth thickness s_n. The deviation of overcut tip diameter E_{daM} can be converted to the actual tooth thickness deviation, E_{sn}:

$$E_{sn} = E_{daM} \tan\alpha_n \tag{A.55}$$

Bibliography

[1] ISO 54, *Cylindrical gears for general engineering and for heavy engineering — Modules*

[2] ISO 701:1998, *International gear notation — Symbols for geometrical data*

[3] ISO 1122-1:1998, *Vocabulary of gear terms — Part 1: Definitions related to geometry*

[4] ISO 4156, *Straight cylindrical involute splines — Metric module, side fit — Part 1: Generalities*

[5] ISO/TR 10064-1:1992, *Code of inspection practice — Part 1: Inspection of corresponding flanks of gear teeth*

[6] ISO/TR 10064-2:1996, *Code of inspection practice — Part 2: Inspection related to radial composite deviations, runout, tooth thickness and backlash*

[7] ISO/TR 10064-3:1996, *Code of inspection practice — Part 3: Recommendations relative to gear blanks, shaft centre distance and parallelism of axes*

[8] DIN 867:1986, *Basic rack tooth profiles for involute teeth of cylindrical gears for general engineering and heavy engineering*

[9] DIN 868:1976, *General definitions and specification factors for gears, gear pairs and gear trains*

[10] DIN 3967, *System of gear fits — Backlash, tooth thickness allowances, tooth thickness tolerances — Principles*

[11] ANSI/AGMA 2002-B88, *Tooth thickness specification and measurement*

ICS 21.200

Price based on 83 pages